

**Can wastewater treatment plants
cope with future nanoparticle
loading scenarios?**

Valerio Cappadona

Thesis submitted to the Department of Civil
and Environmental Engineering, University of
Strathclyde, Glasgow, in fulfilment of the
requirements for the degree of:

Doctor of Philosophy

In

Civil and Environmental Engineering

Declaration of authenticity and author's right

This thesis is the result of the author's original research. It has been composed by the author and has not been previously submitted for examination, which has led to the award of a degree.

The copyright of this thesis belongs to the author under the terms of the United Kingdom Copyright Acts as qualified by University of Strathclyde Regulation 3.50.

Due acknowledgement must always be made of the use of any material contained in, or derived from, this thesis.

Signed:

Date: November 2020

Acknowledgements

I would like to thank my supervisor Prof Vernon Phoenix. I have always felt appreciated, supported, guided and helped throughout this path together. We both started in a completely new setting at Strathclyde and we managed to get through it. You thought me a lot and you were always there for me with your open door. Thank you Vern!

A big thank to Dr Charles Knapp for his insightful advices, lab tips and prolific discussions during the whole period.

Dr Rebecca Skuce, thank you Rebecca. You were always available to review my work. Your PhD thesis has constantly been an example to follow and aspire to. Without you I would have never discovered the world of water and wastewater industry. You managed to arrange me an industrial placement at Scottish Water which was one of the most interesting, entertaining and satisfying periods of my life.

A big thank to the best lab manager and lab technician, respectively Mara Knapp and Dr Tanya Peshkur. Your help during my PhD is literally invaluable, I will never thank you enough. Together we extinguished a fire (which we did not start) and we run what I think to be the highest number of ICP samples for a single PhD project! Thank you girls!

A huge thanks to the whole Hydro Nation Scholars Programme (HNSP) for believing in me and giving me this amazing opportunity. HNSP has always been a family. Thank you Barry Craig, Bob Ferrier, John Rowan, Nikki Dodd, Laura Logie and of course all my fellow scholars.

A big thanks to all the Scottish Water folks I had the pleasure to meet and work with. In particular Jamie Dolan, Gordon, Rusty Russell, Frankie, Susan, Dave, Roy, Willy, Mark, Gerry, Graham, Colin, Stuart and Chris!

A special thank goes to Andrea and Carla (in alphabetic order) for the great time we had together. I met a lot of amazing people, thanks to all of them as well, but the two of you will always be in my loop even if you make fun of me when I very often come back with empty hands after endless fishing sessions.

Last but not least, a huge thanks to my family. My parents have always been my greatest supporters. You always encouraged me to pursue what I like and you always believed in me, especially when I did not. Thanks Mum and Dad!

A huge thanks to my sister: Ilaria, you have simply been a model for me.

To my family

Abstract

The increased production and utilization of nanomaterials has brought significant advantages and developments in many sectors. The application of nanoparticles (NPs), however, comes with the challenge of their growing release into wastewater streams which could eventually enter the natural environment. Exposure to NPs can lead to a wide range of chronic and acute toxic effects on living organisms. These may vary from DNA damages, impairment of metabolic functions, organ injuries and ultimately death. Furthermore, NPs can also interact with other chemical substances. This has the potential to affect their behaviour and, in some cases, increase the toxicity of the generated NPs – chemicals mixtures.

The presence and toxicology of NPs in conventional wastewater treatment plants has received increasing attention, attempting to understand their transport through, and impact on, wastewater treatments systems. While these efforts have largely focused on single NP types and concentrations equal to or below the predicted environmental concentrations, few attempts have investigated NP mixture scenarios as well extremely high NP concentrations. Further investigation into high concentration scenarios are needed due to the likely increase in NP use and therefore release into wastewater in the future. Moreover, further examination of NP removal in mixed NP systems is needed as most wastewaters will contain a mixture of NPs. In addition, the time dependent removal profile of NPs in wastewater secondary treatments has largely been ignored, with most studies focussing on the single endpoint of NP bulk removal. These current gaps indicate that we are poorly prepared to deal with nanoparticle pollution. Extreme NP release events can occur in case of accidents, unregulated discharge, and these spike events are of great concern for water and wastewater companies.

The main aim of this PhD was to assess whether conventional and emerging secondary biological treatments can remove single and NP mixtures from wastewater and hence prevent their release into receiving water bodies.

Firstly, a range of protocols for processing and analysing NPs were examined to determine the most effective. From this, NP determination was achieved via development and validation of a single analytical method based on microwave assisted acid digestion followed by inductively coupled plasma optical emission spectroscopy (IPC-OES). The results demonstrated the robustness of the method to quantify single

and, most importantly, NP mixtures in aqueous solutions. The removal of NPs was studied as a function of NP type, concentration, time and bacteria nature. Activated (aerobic) and granular (anaerobic) sludge microorganisms were used to treat wastewater spiked with nano sized copper oxide (CuO), titanium dioxide (TiO₂) and zinc oxide (ZnO). NPs – bacteria experiments prove that wastewater biological treatments can reduce NP release into the environment. Overall, activated sludge had greater efficiency than anaerobic granules. Activated sludge yielded NP removal greater than 90% in most of the experimental conditions tested within 180 minutes. However, the treatment efficacy was reduced at high NP mixture concentration. The presence of anaerobic granules could remove up to 70% of the NPs present in wastewater. However, these microorganisms did not seem to suffer reduction of removal performances in a NP concentration dependent manner. The effects of natural secondary wastewater liquor on NP behaviour were also assessed. Results show that primary treated wastewater liquor has the potential to stabilize NPs and hence reduce their removal due to aggregation driven sedimentation.

The research presented here highlights the importance of the presence of biologically mediated secondary treatments to cope with the increasing occurrence of NPs in wastewater. The results indicate that microorganisms are an effective tool to remove NPs from sewage and therefore protect the natural aquatic environment. These findings hold implications for the fate and transport of nanoparticles through environmental systems and wastewater treatment plants.

Table of Contents

1 Introduction.....	1
1.1 Nanotechnology and nanoparticles.....	1
1.2 Metal oxide nanoparticles.....	3
1.2.1 Copper oxide.....	4
1.2.2 Titanium dioxide.....	5
1.2.3 Zinc oxide.....	6
1.3 Techniques used for nanoparticle characterization.....	6
1.4 How much NPs are already in the environment?	8
1.5 Nanoparticle behaviour in the environment.....	11
1.5.1 pH.....	13
1.5.2 Cations.....	14
1.5.3 Natural organic matter.....	15
1.5.4 Nanoparticle dissolution and sulphidation.....	15
1.6 Nanoparticle toxicity – the challenge and state of the art.....	16
1.7 Bacteria.....	21
1.8 Biofilm.....	22
1.9 Wastewater treatment and the role of biofilm.....	24
1.10 Biofilm – nanoparticle interactions and toxicity.....	27
1.11 Research objectives.....	34
1.12 Bibliography.....	37
2 Materials and Methods.....	53
2.1 Introduction.....	53
2.2 Biological experiments.....	54
2.2.1 Activated sludge collection and storage.....	54
2.2.2 anaerobic granular sludge collection and storage.....	54
2.2.3 Samples characterization.....	55
2.2.4 Biological experiments execution.....	55
2.2.5 Nanoparticle removal by activated sludge experiments.....	56
2.2.6 Nanoparticle removal by anaerobic granular sludge biomass...	56
2.2.7 Experimental differences.....	57
2.3 Biomass-free liquor NP removal experiments.....	58
2.4 Nanomaterials.....	60
2.5 Nanoparticle suspensions preparation.....	60
2.6 Nanoparticle characterization.....	60
2.6.1 Transmission electron microscopy.....	60
2.6.2 Dynamic light scattering.....	63
2.6.3 Inductively coupled plasma – optical emission spectrometry...	65
2.6.4 Ultrafiltration.....	66
2.7 Cleaning and sterilization.....	67
2.8 Bibliography.....	68
3 Assessment of the suitability of sample processing methods for quantification of NPs in wastewater samples.....	70
3.1 Summary.....	71
3.2 Introduction.....	72
3.3 Materials and Methods.....	76
3.3.1 Preliminary investigations	76

3.3.2 Instrumentations and analytical procedure.....	78
3.3.3 Calibration and linear correlation.....	79
3.3.4 Method detection limit (<i>MDL</i>) and Method Quantification limit (<i>MQL</i>).....	80
3.3.5 Precision and trueness evaluation.....	82
3.4 Results and discussion.....	83
3.4.1 Linearity and linear range.....	83
3.4.2 Limit of detection and limit of quantification evaluation.....	85
3.4.3 Acid mixture and NP digestion protocol identification.....	89
3.4.4 Determination and evaluation of analytical trueness and Precision.....	93
3.5 Conclusions, advantages and limitations of the analytical method...	104
3.6 Bibliography.....	106
4 Insights into the removal mechanisms of nanoparticles and nanoparticle mixtures by activated sludge biomass.....	109
4.1 Summary.....	110
4.2 Introduction.....	111
4.3 Materials and Methods.....	114
4.3.1 Activated sludge collection and biomass free liquor preparation.....	114
4.3.2 Nanoparticle removal by activated sludge biomass and in biomass-free liquor.....	114
4.3.3 Nanoparticle quantification.....	115
4.3.4 Nanoparticle characterization, dissolution and stability in ultrapure water and biomass free liquor.....	115
4.3.5 Analytical methods.....	117
4.4 Results and discussion.....	118
4.4.1 Nanoparticles characterization.....	118
4.4.2 Removal of singularly spiked CuO, TiO ₂ and ZnO by activated sludge biomass.....	121
4.4.3 Removal and behaviour of singularly spiked CuO, TiO ₂ and ZnO in biomass-free liquor.....	126
4.4.4 Removal of CuO, TiO ₂ and ZnO mixtures by activated sludge biomass.....	132
4.4.5 Removal and behaviour of CuO, TiO ₂ and ZnO mixtures in biomass-free liquor.....	135
4.5 Conclusions.....	140
4.6 Bibliography.....	141
5 CuO, TiO ₂ , ZnO nanoparticle removal by anaerobic granules sludge.....	146
5.1 Summary.....	147
5.2 Introduction.....	148
5.3 Materials and methods.....	151
5.3.1 Biomass collection and storage.....	151
5.3.2 Nanoparticle preparation.....	151
5.3.3 Nanoparticle quantification.....	152
5.3.4 Nanoparticle removal by anaerobic granular sludge biomass...	152
5.3.5 Analytical methods.....	153
5.4 Results and discussion.....	154

5.4.1 Removal of singularly spiked CuO, TiO ₂ and ZnO by anaerobic granules sludge.....	154
5.4.2 Removal of CuO, TiO ₂ and ZnO nanoparticle mixtures by anaerobic granules sludge.....	160
5.4.3 Removal of CuO, TiO ₂ and ZnO nanoparticle mixtures in synthetic wastewater (without anaerobic granules).....	168
5.5 Conclusions.....	179
5.6 Bibliography.....	180
6 Conclusions.....	185
6.1 Summary.....	185
6.2 Assessment of the suitability of sample processing methods and analytical method for NP quantification in wastewater samples.....	186
6.3 Nanoparticle removal by activated sludge biomass.....	188
6.4 Nanoparticle removal by anaerobic granular sludge.....	190
6.5 Comparison between activated and anaerobic granular sludge performances.....	191
6.5 Future work.....	204

List of figures

Chapter 1	
Figure 1.1	Re-arranged nanomaterials classification (Peralta-Videa et al. 2011)..... 2
Figure 1.2	High angle annular dark field scanning transmission electron microscopy images of CuO, ZnO and TiO ₂ nanoparticles used in this research project (see section 4.4.1)..... 4
Figure 1.3	Resume of modeled and analytical concentrations of engineered nanomaterials (ENM) in waste water treatment plant effluents. The green boxes show the range (and the arithmetic mean on the log scale) of modeled results, the yellow boxes measured equivalents and the orange box combines measurements and modeling. Picture taken from (Gottschalk et al. 2013)..... 10
Figure 1.4	Representation of a negatively charged (nano)particle in solution. Adsorbed ions are in the Stern layer while more loosely ions are in the diffuse layer. Stern and diffuse layer together compose the electric double layer (EDL). Picture taken from Hartmann et al. (2014)..... 11
Figure 1.5	Transformations of NPs in the environment. These include physically, chemically and biologically mediated transformations. The physicochemical properties of NPs, together with environmental factors, determine the type of transformation processes. Picture taken from Zhang et al. (2018)..... 13
Figure 1.6	a) pH dependent Zeta-potential of a nanoparticle. The green areas ($-30 \text{ mV} < z\text{-potential} > +30 \text{ mV}$) show stability regions. The blue area, where NP distribution is unstable due to ($-30 \text{ mV} > z\text{-potential} < +30 \text{ mV}$) falls between a pH range of 5.5 ± 2 around the pH of isoelectric point ($z\text{-potential} = 0$). (Malvern Panalytical, Isoelectric points of nanomaterials, https://www.materials-talks.com/blog/2017/07/27/isoelectric-points-of-nanomaterials-qa/ , March 27 th , 2020). b) Effect of pH on z-potential and size distribution of TiO ₂ . The isoelectric point is around 6, and the unstable zone ($z\text{-potential}$ between -30 and $+30 \text{ mV}$) extends from 5.5 to 7.5. Within this region, the lower electrostatic repulsions causes the formation of larger TiO ₂ aggregates (Loosli et al. 2014)..... 14
Figure 1.7	Schematic way of biofilm formation, maturation and escape modes. Picture taken from Petrova and Sauer (2016)..... 24
Figure 1.8	Schematic view of a conventional wastewater treatment plant including, preliminary, primary and activated sludge based secondary treatment..... 25

Figure 1.9	Resume of NP, biofilm and environmental factors governing NP – biofilm interactions. Picture taken from Joo and Aggarwal (2018).	28
Figure 1.10	Resume of physical mechanisms involved in the NP - biofilm interactions. Picture taken from Huangfu et al. (2019).....	29
Figure 1.11	Resume of chemical mechanisms involved in the NP - biofilm interactions. Picture taken from Huangfu et al. (2019).....	30
Figure 1.12	Resume of biological mechanisms involved in the NP - biofilm interactions. Picture taken from (Ikuma et al. 2015)	31
Chapter 2		
Figure 2.1	Representation of a transmission electron microscopy (TEM) (Tanaka 2017).....	62
Figure 2.2	Illustration of the electrical double layer (EDL) of a negatively charged nanoparticle. The EDL includes the stern layer as well the diffuse layer. The graph shows the Z-potentials (vertical axis) relative to the two layers and slipping planes as a function of the distance from the particle surface. Picture taken from (Williams 2016).....	63
Chapter 3		
Figure 3.1	Linear range of signal intensity and analytes' concentration for Cu ²⁺ , Ti ⁴⁺ and Zn ²⁺ in 4% HNO ₃ and 4% H ₂ SO ₄ . Results are shown as average ± standard deviation (n=3). All standard deviations smaller than the marker size (6), highest standard deviation value was 0.11 counts/second.....	83
Figure 3.2	Ti ⁴⁺ recovery from suspensions of TiO ₂ (100 mg/L) digested with different procedures and acid mixtures. The green lines (90 and 110 %) show the accepted value for metal recovery evaluation with ICP-OES (U.S. Environmental Protection Agency 1987). Results are shown as average ± standard deviation (n=5).....	89
Figure 3.3	Metal recovery from suspensions of single CuO, TiO ₂ and ZnO (100 mg/L) digested in HNO ₃ - H ₂ SO ₄ through microwave assisted reaction system and ICP-OES analysis. The green lines (90 and 110 %) show the accepted value for metal recovery evaluation with ICP-OES (U.S. Environmental Protection Agency 1987). Results are shown as average ± standard deviation (n=5).....	90
Figure 3.4	Measured versus nominal concentrations of Cu ²⁺ , Ti ⁴⁺ and Zn ²⁺ determined after acid digestion procedure. Panel a and b refer to Cu ²⁺ , c and d to Ti ⁴⁺ while Zn ²⁺ is shown in panels e and f . Every point is shown as average ± standard deviation (n=3). Error bars only visible for Zn ²⁺ tests. In panels a,b,c and d , standard deviations are covered by the markers (size used is 5) and did not exceed the value of 0.77 mg/l for Cu ²⁺ and 0.59 mg/L for Ti ⁴⁺	92

Figure 3.5	Measured concentration of Cu^{2+} determined with ICP-OES after $\text{HNO}_3 - \text{H}_2\text{SO}_4$ digestion of samples containing CuO , TiO_2 and ZnO . Cu^{2+} quantification happened simultaneously to Ti^{4+} and Zn^{2+} determination (results shown in Fig. 2.6 and Fig. 2.7) Panel a refers to suspensions prepared in water and commercial TiO_2 . Panel b refers to suspensions prepared in synthetic wastewater and commercial TiO_2 . Panel c refers to suspensions prepared in water and certified reference material for TiO_2 . Panel d refers to certified reference TiO_2 suspensions prepared in synthetic wastewater. Every point is shown as average \pm standard deviation ($n=5$). Where not visible, standard deviations covered by markers (size 6).....	101
Figure 3.6	Measured versus nominal concentration of Ti^{4+} determined with ICP-OES after $\text{HNO}_3 - \text{H}_2\text{SO}_4$ digestion of samples containing CuO , TiO_2 and ZnO . Ti^{4+} quantification happened simultaneously to Cu^{2+} and Zn^{2+} determination (results shown in Fig. 2.5 and Fig. 2.7) Panel a refers to suspensions prepared in water and commercial TiO_2 . Panel b refers to suspensions prepared in synthetic wastewater and commercial TiO_2 . Panel c refers to suspensions prepared in water and certified reference material for TiO_2 . Panel d refers to certified reference TiO_2 suspensions prepared in synthetic wastewater. Every point is shown as average \pm standard deviation ($n=5$). Where not visible, standard deviations covered by markers (size 6).....	102
Figure 3.7	Measured versus nominal concentration of Zn^{2+} determined with ICP-OES after $\text{HNO}_3 - \text{H}_2\text{SO}_4$ digestion of samples containing CuO , TiO_2 and ZnO . Zn^{2+} quantification happened simultaneously to Cu^{2+} and Ti^{4+} determination (results shown in Fig. 2.5 and Fig. 2.6) Panel a refers to suspensions prepared in water and commercial TiO_2 . Panel b refers to suspensions prepared in synthetic wastewater and commercial TiO_2 . Panel c refers to suspensions prepared in water and certified reference material for TiO_2 . Panel d refers to certified reference TiO_2 suspensions prepared in synthetic wastewater. Every point is shown as average \pm standard deviation ($n=5$). Where not visible, standard deviations covered by markers (size 6).....	103
 Chapter 4		
Figure 4.1	High angle annular dark field scanning transmission electron microscopy images of the CuO , ZnO and TiO_2 nanoparticles, together with representative EELS spectra for each type of nanoparticle, with comparisons to standards for CuO (Ngantcha et al. 2005) and anatase TiO_2 (Bertoni et al. 2006), both in pale grey below the experimental spectrum...	118

Figure 4.2	Removal profile ($n=3 \pm$ standard deviation) of singularly spiked CuO, TiO ₂ and ZnO reported as removal percent. Nanomaterials were spiked in presence of activated sludge biomass at concentrations of 9 mg/L (a), 90 mg/L (b) and 180 (c). Where not visible, standard deviations covered by markers (size 9).....	123
Figure 4.3	Concentration of released Cu ²⁺ and Zn ²⁺ in single CuO and ZnO dissolution experiments in biomass-free liquor ($n=3 \pm$ standard deviation). Where not visible, standard deviations covered by markers (size 9).....	125
Figure 4.4	Removal profile ($n=3 \pm$ standard deviation) of singularly spiked CuO, TiO ₂ and ZnO reported as removal percent. Nanomaterials were spiked in biomass-free liquor at concentrations of 9 mg/L (a) and (b) and 180 mg/L. Where not visible, standard deviations covered by markers (size 9).	127
Figure 4.5	Zeta potential (a) and Z-average diameter (b) of 100 mg/L CuO suspension as function of pH in ultrapure water and biomass-free liquor. The grey area ($pzc \pm 2$ unit) shows pH range where aggregation is expected to happen due to low zeta potential. Where not visible, standard deviations covered by markers (size 8).....	129
Figure 4.6	Zeta potential (a) and Z-average diameter (b) of 100 mg/L TiO ₂ suspension as function of pH in ultrapure water and biomass-free liquor. The grey area ($pzc \pm 2$ unit) shows pH range where aggregation is expected to happen due to low zeta potential. Where not visible, standard deviations covered by markers (size 8).....	130
Figure 4.7	Zeta potential (a) and Z-average diameter (b) of 100 mg/L ZnO suspension as function of pH in ultrapure water and biomass-free liquor. The grey area ($pzc \pm 2$ unit) shows pH range where aggregation is expected to happen due to low zeta potential. Where not visible, standard deviations covered by markers (size 8).....	131
Figure 4.8	Removal profile ($n=3 \pm$ standard deviation) of CuO, TiO ₂ and ZnO mixtures reported as relative removal percent. Panels a,b,c , each nanoparticle type was spiked in presence of activated sludge biomass at concentrations of 9 mg/L (a), 90 mg/L (b) and 180 (c) for a final concentration of 27, 270 and 540 mg of NP/L. Where not visible, standard deviations covered by markers (size 9).....	133
Figure 4.9	Removal profile ($n=3 \pm$ standard deviation) of CuO, TiO ₂ and ZnO mixtures reported as relative removal percent. Panels a,b,c , each nanoparticle type was spiked in biomass-free liquor at concentrations of 9 mg/L (a), 90 mg/L (b) and 180 (c) for a final concentration of 27, 270 and 540 mg of NP/L. Where not visible, standard deviations covered by markers (size 9).....	136

Figure 4.10	Concentration of dissolved Cu^{2+} and Zn^{2+} in mixtures CuO, TiO_2 and ZnO dissolution experiments in biomass-free liquor ($n=3 \pm$ standard deviation). Where not visible, standard deviations covered by markers (size 9).....	138
Chapter 5		
Figure 5.1	Removal profile ($n=3 \pm$ standard deviation) of singularly spiked CuO, TiO_2 and ZnO reported as removal percent. Nanomaterials were spiked in presence of anaerobic granular sludge (AGS) at concentrations of 9 mg/L (a), 90 mg/L (b) and 180 mg/L(c).....	155
Figure 5.2	Removal profile ($n=3 \pm$ standard deviation) of CuO (a), TiO_2 (b), ZnO (c) mixtures and cumulative (d) reported as relative removal percent. Each nanoparticle type was spiked in presence of anaerobic granular sludge (AGS) at concentration of 9 mg/L for a final concentration of 27 mg of NP/L. Removal of each NP type was reported in a separate panel for visual clarity.....	162
Figure 5.3	Removal profile ($n=3 \pm$ standard deviation) of CuO (a), TiO_2 (b), ZnO (c) mixtures and cumulative (d) reported as relative removal percent. Each nanoparticle type was spiked in presence of anaerobic granular sludge (AGS) at concentration of 90 mg/L for a final concentration of 270 mg of NP/L. Removal of each NP type was reported in a separate panel for visual clarity.....	163
Figure 5.4	Removal profile ($n=3 \pm$ standard deviation) of CuO (a), TiO_2 (b), ZnO (c) mixtures and cumulative (d) reported as relative removal percent. Each nanoparticle type was spiked in presence of anaerobic granular sludge (AGS) at concentration of 180 mg/L for a final concentration of 540 mg of NP/L. Removal of each NP type was reported in a separate panel for visual clarity.....	164
Figure 5.5	Removal profile ($n=3 \pm$ standard deviation) of CuO (a), TiO_2 (b), ZnO (c) mixtures and cumulative (d) reported as relative removal percent. Each nanoparticle type was spiked in synthetic wastewater at concentration of 9 mg/L for a final concentration of 27 mg of NP/L. Removal of each NP type was reported in a separate panel for visual clarity.....	169
Figure 5.6	Removal profile ($n=3 \pm$ standard deviation) of CuO (a), TiO_2 (b), ZnO (c) mixtures and cumulative (d) reported as relative removal percent. Each nanoparticle type was spiked in synthetic wastewater at concentration of 90 mg/L for a final concentration of 270 mg of NP/L. Removal of each NP type was reported in a separate panel for visual clarity.....	170
Figure 5.7	Removal profile ($n=3 \pm$ standard deviation) of CuO (a), TiO_2 (b), ZnO (c) mixtures and cumulative (d) reported as relative removal percent. Each nanoparticle type was spiked in synthetic wastewater at concentration of 180 mg/L for a final concentration of 540 mg of NP/L. Removal of each NP type	

was reported in a separate panel for visual clarity..... 171

Chapter 6

Figure 6.1 Assessment of the amount of CuO, TiO₂ and ZnO and their mixture (in mg/L) removed by aggregation driven sedimentation when no biomass was added as function of the spiking concentration. Note that mixture experiments are reported as cumulative concentration (27 mg/L, 270 and 540 mg/L)..... 197

List of tables

Chapter 1

Table 1.1	Re-arrangement of the table of (Fabrega 2009) containing the Predicted concentrations of NMs in the environment released from consumer products. Data were obtained from (Mueller and Nowack 2008) and (Boxall et al. 2008) (in bold) and (Gottschalk et al. 2009) for Europe (underlined)..	9
-----------	--	---

Chapter 3

Table 3.1	TiO ₂ microwave and hotplate assisted acid digestion procedures. Our method (first column) was developed based on the instrument properties. The same protocol was used for comparison with the reverse aqua regia digestion (second column). Third column shows 3030 G standard method for Titanium (APHA/AWWA/WEF 2012) used by Kiser et al. (2009) and the fourth column shows the comparison hotplate digestion with reverse aqua regia.....	78
Table 3.2	ICP-OES method parameters.....	79
Table 3.3	F tabulated and calculated to evaluate linearity of the signal intensity vs analytes concentration.....	84
Table 3.4	Method Detection Limit (MDL) and Method Quantification Limit (MQL), reported in mg/L, for ICP-OES analysis of Cu ²⁺ , Ti ⁴⁺ and Zn ²⁺	86
Table 3.5	Confirmation and evaluation of ICP-OES analysis precision (RSD %) and trueness (bias %) of MDL with Cu ²⁺ , Ti ⁴⁺ and Zn ²⁺ standards in 4% H ₂ SO ₄ and 4% HNO ₃	87
Table 3.6	Summary of the analytical method trueness (metal recovery) and precision (RSD %) for Cu ²⁺ , Ti ⁴⁺ and Zn ²⁺ in ultrapure water (n=5). All nanoparticles purchased from Sigma Aldrich.....	94
Table 3.7	Summary of the analytical method trueness (metal recovery) and precision (RSD %) for Cu ²⁺ , Ti ⁴⁺ and Zn ²⁺ in synthetic wastewater (n=5). All nanoparticles purchased from Sigma Aldrich.....	95
Table 3.8	Summary of the analytical method trueness (metal recovery) and precision (RSD %) for Cu ²⁺ , Ti ⁴⁺ and Zn ²⁺ in ultrapure water (n=5). TiO ₂ certified reference material purchased from NIST. CuO and ZnO purchased from Sigma Aldrich...	96
Table 3.9	Summary of the analytical method trueness (metal recovery) and precision (RSD %) for Cu ²⁺ , Ti ⁴⁺ and Zn ²⁺ in synthetic wastewater (n=5). TiO ₂ certified reference material purchased from NIST. CuO and ZnO purchased from Sigma Aldrich.....	97

Chapter 4	
Table 4.1	T Nanoparticle characterization in ultrapure water and biomass-free liquor. Primary size determined via transmission electron microscopy (TEM), hydrodynamic dimeter and Z-potential via dynamic light scattering (DLS). 119
Table 4.2	Activated sludge and biomass-free liquor characteristics.... 122
Chapter 5	
Table 5.1	Resume of concentration and the relative removal efficiency (n=3 ± standard deviation) of CuO, TiO ₂ and ZnO removed by anaerobic granular sludge (AGS) in the single NP systems..... 157
Table 5.2	Resume of concentration and the relative removal efficiency (n=3 ± standard deviation) of CuO, TiO ₂ and ZnO removed by anaerobic granular sludge (AGS) in mixture experiments. Concentration 1 (9 mg/L * NP type equal to total concentration of 27 mg/L), concentration 2 (90 mg/L * NP type equal to total concentration of 270 mg/L), concentration 3 (180 mg/L * NP type equal to total concentration of 540 mg/L)..... 166
Table 5.3	Resume of concentration and the relative removal efficiency (n=3 ± standard deviation) of CuO, TiO ₂ and ZnO mixtures removed in synthetic wastewater experiments. Concentration 1 (9 mg/L * NP type equal to total concentration of 27 mg/L), concentration 2 (90 mg/L * NP type equal to total concentration of 270 mg/L), concentration 3 (180 mg/L * NP type equal to total concentration of 540 mg/L)..... 173
Table 5.4	Comparison of synthetic wastewater and biomass-free liquor characteristics and the respective cumulative removal of CuO, TiO ₂ and ZnO mixtures. Concentration 1 (9 mg/L * NP type equal to total concentration of 27 mg/L), concentration 2 (90 mg/L * NP type equal to total concentration of 270 mg/L), concentration 3 (180 mg/L * NP type equal to total concentration of 540 mg/L)..... 175
Chapter 6	
Table 6.1	Resume of all the CuO, TiO ₂ and ZnO removal experiments. Activated sludge and biomass free-liquor experiments duration was 180 min. Anaerobic granular sludge (AGS) and synthetic wastewater tests were run for 360 min. All the results are reported as (n=3 ± standard deviation). (-) Experiments not run..... 193

Table 6.2	Comparison of synthetic wastewater and biomass-free liquor. Table reported from chapter 5 (Table 5.4).....	199
Table 6.3	Nanoparticle characterization in ultrapure water and biomass-free liquor. Primary size determined via transmission electron microscopy (TEM), hydrodynamic diameter and Z-potential via dynamic light scattering (DLS)..	201

List of acronyms

AAS	Atomic absorption spectrometry
AFM	Atomic force microscopy
AGS	Anaerobic granular sludge
AnWT	Anaerobic wastewater treatment
BSA	Bovine serum albumin
CAS	Chemical Abstracts Service
CHP	Combined heat and power (engine)
CIT	Citrate
CNT	Carbon nanotubes
COD	Chemical oxygen demand
CRM	Certified reference material
DLS	Dynamic Light Scattering
DLVO	Derjaguin, Landau, Verwey and Overbeek (theory)
DNA	Deoxyribonucleic acid
DOM	Dissolved organic matter
EDL	Electric double layer
EDX	Energy dispersive X-ray
EELS	Electron energy-loss spectroscopy
ENM	Engineered nanomaterial
EPS	Extracellular polymeric substances
FFF	Field flow fractionation
HF	Hydrofluoric acid
HRT	Hydraulic retention time
ICP-AES	Inductively coupled plasma atomic emission spectroscopy
ICP-MS	Inductively coupled plasma – mass spectrometry
ICP-OES	Inductively coupled plasma – optical emission spectroscopy
IONP	Iron oxide nanoparticle
IS	Internal standard
LC	Liquid Chromatography
LDH	Lactate dehydrogenase

LoD	Limit of detection
LoF	Lack of Fit (test)
LoQ	Limit of quantification
MDL	Method detection limit
MeO-NPs	Metal oxide nanoparticles
MLSS	Mixed liquor suspended solids
MQL	Method quantification limit
MSS _{err}	Mean sum of squares of random error
MSSLOF	Mean sum of squares due to lack of fit
MWCNT	Multi walled carbon nanotubes
NIST	National Institute of Standards and Technology
NOM	Natural organic matter
NP	Nanoparticle
NTA	Nanoparticles tracking analysis
OECD	Organization for Economic Co-operation and Development
PCP	Personal care products
PdI	Polydispersity index
PEC	Predicted environmental concentration
PVA	Polyvinyl alcohol
PVP	Polyvinylpyrrolidone
pzc	Point of zero charges
QC	Quality control
RNA	Ribonucleic acid
ROS	Reactive oxygen species
RSD	Relative standard deviation
SBR	Sequencing batch reactor
SEM	Scanning electron microscopy
sp-ICP-MS	Single - particle Inductively coupled plasma – mass spectrometry
sp-ICP-TOFMS	Single-particle inductively coupled plasma time-of-flight mass spectrometry
SWCNT	Single walled carbon nanotubes
TDS	Total dissolved solids

TEM	Transmission electron microscopy
TOC	Total organic carbon
TSS	Total suspended solids
USEPA	United States Environmental Protection Agency
UV	Ultraviolet
WWTP	Wastewater treatment plant

1 Introduction

1.1 Nanotechnology and nanoparticles

In 2013, The European Commission has defined nanotechnology as “the invisible giant tackling Europe’s future challenges” (Directorate-General for Research and Innovation 2013) through the project FP7-NMP - Specific Programme "Cooperation": Nanosciences, Nanotechnologies, Materials and new Production Technologies (FP7-NMP - Specific Programme "Cooperation": Nanosciences, Nanotechnologies, Materials and new Production Technologies, <https://cordis.europa.eu/programme/id/FP7-NMP>, February 19th, 2020). Nanotechnology is the term given to those areas of science and engineering where phenomena that take place at dimensions in the nanometer scale are utilized in the design, characterization, production and application of materials, structures, devices and systems (Scientific Committee on Emerging and Newly Identified Health Risks (SCENIHR), https://ec.europa.eu/health/scientific_committees/opinions_layman/en/nanotechnologies/index.htm#i11, February 19th, 2020). At the end of 2014, 1833 products containing nanomaterials were recorded in the Nanotechnology Consumer Products Inventory <http://www.nanotechproject.org/cpi/products/?sort=-datestamp>, February 19th, 2020) and over 3000 products are currently registered in the Nanodatabase (The Nanodatabase, <http://nanodb.dk/en/>, March 24th 2019). Nanotechnology was predicted to reach a Global Market Value of 125.7 billion US dollars by 2024 (Global Industry Analysts 2019, <https://www.strategyr.com/MarketResearch/market-report-infographic-nanotechnology-forecasts-global-industry-analysts-inc.asp>, February 19th, 2020).

A unique formal definition of nanomaterials has not yet been agreed, however nanoparticles (NPs) are described as material with at least one dimension between about 1 nm and 100 nm (Roco 2003; Salata 2004; Moore 2006). Nanoparticles can originate from either natural sources/processes such as volcanic and biological processes as well as from anthropogenic production (Nowack and Bucheli 2007; Handy et al. 2008; Peralta-Videa et al. 2011). Engineered nanomaterials (ENMs) are usually categorized by their chemical composition (Fig 1.1).

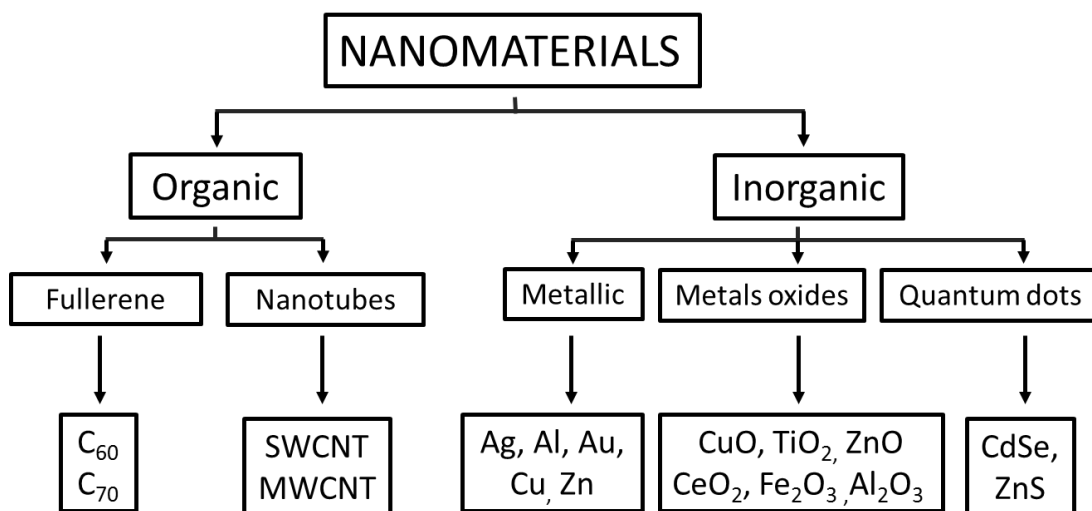


Fig. 1.1 Nanomaterials classification (Peralta-Videa et al. 2011).

However, such relatively simple classification may not necessarily reflect their properties. Indeed, size and shape (i.e. rod-shapes, prisms, tubes, and spheres), as well as crystal structure are all factors that influence their physical and chemical properties. Furthermore, NPs are often modified via addition of coatings, capping agents and functional groups to alter their physio-chemical properties. As result of this, NPs with the same chemical composition but with different size, shape, coating or structure may have different physical and chemical properties (Borm et al. 2006; Balbus et al. 2007; Adlakha-Hutcheon et al. 2009; Savolainen et al. 2010).

Hence, NPs are generally divided into two major families: organic and inorganic (Fig. 1.1). Organic NPs are made of carbon and include the family of fullerenes (C_{60} and C_{70}) which can be arranged in hollow spherical, ellipsoid, spherical and other shapes. Carbon nanotubes (CNT) can be either single walled (SWCNT) or multi-walled (MWCNT). They commonly have a diameter between 1 to 10 nm and a length of few millimeters with a cylindrical shape. These carbon based NPs have found wide application in the medical and electrical fields due to their properties (Srivastava et al. 2015).

Inorganic NPs cover a broad range of nanomaterials. Metallic NPs such as silver (AgNPs), gold (AuNPs) and zinc (ZnNPs) among others are made of pure metal elements. Metal oxide nanoparticles (MeO-NPs) feature instead metal – oxygen bond such as copper oxide (CuO), titanium dioxide (TiO_2), zinc oxide (ZnO), cerium

dioxide (CeO_2) and iron oxides NPs (Fe_2O_3). Quantum dots are fluorescent nanomaterials usually smaller than 10 nm with semiconductor properties, usually of spherical shape and <10 nm. The most commonly studied quantum dots are composed of a cadmium selenide (CdSe) core surrounded by a zinc sulfide (ZnS) shell, and are commercially available (Suri et al. 2013).

1.2 Metal oxide nanoparticles

Metal oxides nanoparticles (MO-NPs) are a branch of nanoparticles among the most widely exploited in nanotechnology applications.

Metal elements are able to form a large diversity of oxide compounds. The reaction mechanisms and, therefore, the functionality of nanostructured MO-NPs depend on their composition, crystallographic structure, morphology, surface stoichiometry and geometry, interactions of the phases, etc. Specifically, oxide nanoparticles can exhibit unique physical and chemical properties due to their limited size and a high density of corner or edge surface sites. Hence, NP high surface/volume ratio provides MO-NPs with three key important groups of basic properties in any material: i) Size-induced structural and mechanical stability, (Ayyub et al. 1995; Mchale et al. 1997; Samsonov et al. 2006) ii) electronic properties (Pacchionia et al. 1996); Casarin et al. 1997; Moriarty 2001), iii) conductivity and chemical reactivity (Rodriguez et al. 1998; Rodriguez 2002).

CuO , TiO_2 and ZnO (Fig. 1.2), among others, are a good example of MO-NPs which can be extensively found in consumer products or used in industrial processes. These three MO-NPs have been chosen as the target of this research work because of their relevance in wastewater. In particular TiO_2 and ZnO are widely present in personal consumer products (PCP) such as toothpaste, sunscreen and cosmetics. Products falling within these categories are used in great quantity on a daily basis by millions of people worldwide. As result of this, NPs are introduced into the sewer networks which ultimately will bring NPs to enter a wastewater treatment plant. CuO instead has found less applications in PCPs in comparison to TiO_2 and ZnO . However, due to its physical properties, CuO has found various applications in the electrical industry. In addition, CuO is used in the biomedical manufacturing industry due to its

antimicrobial properties. Such applications due to antimicrobial properties are highly exploited for ZnO as well.

CuO, TiO₂ and ZnO as well as many other NPs have become more and more abundant in daily used products that we all come in contact every day. However, this is not the sole range of processes and products in which NPs are exploited, as CuO, TiO₂ and ZnO are utilized in variety of industries and large scale processes and less common products where it is hard to realize the presence of NPs. As a result of their presence in the final products and the incorporation of NPs in processes used to assemble and produce such goods, the presence of CuO, TiO₂ and ZnO in sewage has now attracted the attention of the scientific world in order to assess the fate and effects of NPs in wastewater treatment plants and their potential release in environment.

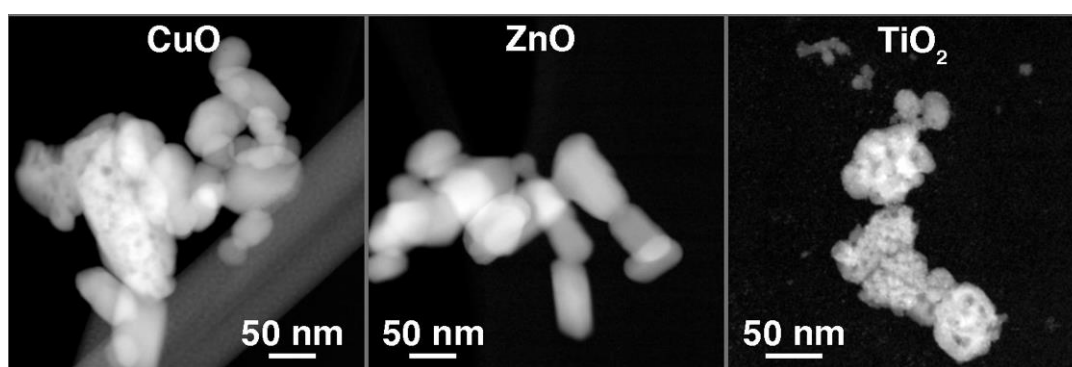


Fig. 1.2 High angle annular dark field scanning transmission electron microscopy images of CuO, ZnO and TiO₂ nanoparticles used in this research project (see section 4.4.1).

1.2.1 Copper oxide

Copper oxide (CuO, cupric oxide or copper (II) oxide, CAS number 1317-38-0) appears as black powder. It has a density of 6.31 g/cm³, molar mass of 79.55 g/mol, melting point of 1026 °C and boiling point equal to 1326 °C (National Center for Biotechnology Information, PubChem Database, https://pubchem.ncbi.nlm.nih.gov/compound/Cu_II_-oxide, March 19th, 2020).

CuO is a semiconducting compound which has attracted particular attention due to a range of useful physical properties such as high temperature superconductivity, electron correlation effects, and spin dynamics (Jadhav et al. 2011; Ahamed et al. 2014).

The numerous cases in which CuO has found applications vary from renewable energy technologies (CuO embedded in fluids can increase thermal conductivity in photovoltaic equipment), to gas sensors, reaction catalysts, batteries and superconductors (Ren et al. 2009).

Biomedical applications of CuO have also gained more attention due the biocidal and antimicrobial properties (Grigore et al. 2016). CuO is allegedly considered to have a broad spectrum bioactivity due to its reported effects on gram-positive and gram-negative bacteria (Schrand et al. 2010; Theron et al. 2008) and antimicrobial activity against *E. coli*, *Micrococcus luteus*, *S. aureus* and *Klebsiella pneumoniae* (Ramyadevi et al. 2011). Nevertheless, CuO is considered a broad spectrum bioactive compound as it is also attributed antimycotic activity (Cioffi et al. 2005), antiviral activity (Fujimori et al. 2012), antialgal activity (Anyagou et al. 2008), antiparasitic activity (Ramyadevi et al. 2011) as well as anticancerous activity (Jose et al. 2011).

1.2.2 Titanium dioxide

Titanium dioxide (TiO₂, Titanium (IV) oxide, CAS numbers 1317-70-0, 1317-80-2, 13463-67-7 and 98084-96-9) is the natural occurring oxide of titanium and it appears as white odourless powder. It can be found under different mineral forms, each: anatase, rutile and brookite. Each of them possesses a different crystalline structure, hence different properties and hereafter usage (Boccaccini et al. 2004), however, anatase and rutile are the most widely used forms. It has a molar mass of 79.866 g/mol and it is also known as E171 as food colouring additive (National Center for Biotechnology Information. PubChem Database. Titanium dioxide, <https://pubchem.ncbi.nlm.nih.gov/compound/Titanium-dioxide>, March 19th, 2020).

TiO₂ is a highly stable, insoluble, light resistant, UV blocking material and excellent photocatalyst (Gottschalk et al. 2010). This nanomaterial has been utilized in a wide range of applications which vary from coatings, plastic, paint, ink, paper to pharmaceutical and cosmetic industries as well as textile and food industries, environmental remediation and renewable energy (Gázquez et al. 2014).

TiO₂ is used in a remarkably high number of daily products readily accessible on the market exemplified in personal care products (PCP) such as toothpaste, sunscreen,

cosmetics (Weir et al. 2012). TiO₂ can be commonly found in clothes (Windler et al. 2012) and foods (Lomer et al. 2000) too.

1.2.3 Zinc oxide

Zinc oxide (ZnO, zinc white, zinc (II) oxide, CAS numbers 1314-13-2) is an inorganic compound in form of white powder which has a wurtzite crystal structure. ZnO has a density of 5.6 g/cm³, molar mass of 81.4 g/mol, it is slightly soluble in water and with melting point of 1974 °C and boiling point equal to 2360 °C (National Center for Biotechnology Information. PubChem Database. Zinc oxide, CID=14806, https://pubchem.ncbi.nlm.nih.gov/compound/zinc_oxide, March 19th, 2020).

ZnO is a semiconductor and exhibits near UV emission, transparent conductivity (providing for clear coatings on transparent surfaces), and piezoelectricity, which make it particularly attractive for electronic sensor, solar voltaic, and transducer applications (Wang 2004).

ZnO nanopowder is currently used in products including plastics, ceramics, glass, cement, rubber, lubricants, paints, pigments, foods (source of Zn nutrient) batteries, fire retardants, etc. In addition, ZnO NPs are common constituents of personal care products including cosmetics and sunscreens due to their excellent UV absorption and reflective properties (Ma et al. 2013a).

1.3 Techniques used for nanoparticle characterisation

Assessing the behaviour (transport, persistence, fate, chemical transformation) of NPs in natural systems is essential to the accurate prediction of exposure, and thus understanding subsequent bioaccumulation, depuration and biological effects (Moore 2006). With regards to this, the prediction of NP environmental behaviour in aqueous and more complex matrices requires the assessment of an array of physio-chemical parameters (Loosli et al. 2015b).

The aim of NP characterization is to provide qualitative and quantitative information regarding studied nanomaterial. Nanomaterials are considered as a revolutionary new type of analytes, involving both chemical (composition, mass and number concentration) and physical information (e.g. size, shape, aggregation), this poses a significant analytical challenge (Lin et al. 2014). To this purpose, a series of

different techniques and methods have been applied in a complex variety of scenarios such as i) Analysis of industrial and consumer products containing NPs, ii) Laboratory experiments involving the release of ENMs from consumer products, as well as their fate, in different test media iii) Ecotoxicological and toxicological studies, iiiii) Monitoring the occurrence and fate of ENMs along their life cycle in the environment and organisms, including humans (Laborda et al. 2016).

In order to provide precise and accurate analytical determination of NPs, sample preparation is often a key step (Chen et al. 2016) aimed to separate the nanomaterial(s) of interest from other background particles. This is commonly achieved via (sequential) filtration and ultracentrifugation (Windler et al. 2012) or field flow fractionation (FFF) (Cascio et al. 2015). These techniques provide NP size fractioning which can include a broad-spectrum size distribution as well as dissolved fraction. nanoparticles tracking analysis (NTA), first commercialized in 2006, is one of the most recently developed techniques capable of providing sizing of NPs in solution (Filipe et al. 2010). Other techniques commonly used for analysis of size distribution are dynamic light scattering (DLS), transmission electron microscopy (TEM) (Bootz et al. 2004), scanning electron microscopy (SEM) (Benn and Westerhoff 2008), atomic force microscopy (AFM) (Mavrocordatos et al. 2004) and Raman Scattering (Joseph et al. 2012). NP chemical identity can be retrieved via energy dispersive x-ray (EDX) or electron energy-loss spectroscopy (EELS) analysis paired with microscopy (Mourdikoudis et al. 2018).

Parallel to the physio-chemical characterization, analytical NP quantification is the other key parameter that needs determination. However, this is hardly or not at all achievable through the methods mentioned above. For quantification purposes, spectrometry-based techniques are generally used. Atomic absorption spectrometry (AAS), inductively coupled plasma – optical emission spectroscopy (ICP-OES) and inductively coupled plasma - mass spectrometry (ICP-MS) are often paired with acid digestion and used to determine NP concentration (Costa-fernández et al. 2016). In recent years ICP-MS based techniques have seen a sharp improvement thanks to the advent of the single particle mode (sp-ICP-MS) (Lamsal et al. 2018). Similarly, ICP-MS can be combined with NP separation techniques such as FFF, liquid chromatography (LC) and electrophoretic techniques. These set-ups enable NP

quantification as well as determination of size distribution and dissolved fraction, however with the limitation of one NP type per analysis (Costa-Fernández et al. 2016). It has only recently been reported that single-particle inductively coupled plasma time-of-flight mass spectrometry (sp-ICP-TOFMS) has the potential to quantify and determine the size distribution of multiple NPs of different types simultaneously (Mehrabi et al. 2019).

The analytical techniques and methodologies for simultaneous physio-chemical characterization and analytical quantification of multiple NP types are experiencing a rapid growth and sharp development. However standardization and widespread utilization of such methods is still in the early stages and significant effort is needed to ensure accurate and precise NP characterization. However, qualitative and quantitative assessment of multiple NPs can be obtained with the use of a multi-technique approach which involves TEM-EDS or EELS, DLS and sequential filtration and ultrafiltration. Through the blend of analytical techniques, determination of the chemical signature, particle distribution and isolation of the dissolved fraction from the colloidal can be achieved in real environmental samples containing multiple NP types, whilst quantification is provided with spectrometry based methods (Polesel et al. 2018).

1.4 How much NPs are already in the environment?

The presence of a variety of nano-enabled products as well as the usage of NPs in industrial processes is a well-established reality nowadays (Santos et al. 2015; Stark et al. 2015). This is causing the release of NPs in environmental compartments all along the material value chain through accidental spills, use and application of NP – containing products as well as waste processing at product end of life. Result of this is leading to an accumulation of NPs in the environment (Lead and Wilkinson 2006; Wiesner et al. 2006).

The technical – analytical development of measurement instruments for NP determination in real samples, despite not yet standardized, is on its way to providing the capacity to quantify NP. However, the lack of online and in-situ monitoring systems as well as a coordinated effort among regions and research and environmental authorities has led to the unavailability of a single database on environmental NP

concentrations (Zhang et al. 2019). This adds up to the innate difficulties of measuring NPs, which are: i) Very low environmental concentrations, ii) High presence of natural nanomaterials which can shadow and interfere with the determination of the NPs of interest, iii) Paucity of suitable sample preservation methods (Montaño et al. 2014; (Wagner et al. 2014; Nowack 2017)

Modelling approaches have also been used and implemented in recent years, however, these also have similar issues of unconformity and hence hard or impossible to apply to different area or scenarios or environmental compartments. For example Mueller and Nowack 2008, used a life cycle perspective to model the release of NPs into the environment in the Swiss context. Predicted environmental concentrations (PEC) of certain nanomaterials have been computationally estimated for UK as well (Boxall et al. 2008). A comparison of the results of these works are reported in table 1.1.

Table 1.1 Re-arrangement of the table of (Fabrega 2009) containing the predicted concentrations of NMs in the environment released from consumer products. Data were obtained from (Mueller and Nowack 2008) and (Boxall et al. 2008) (in bold) and (Gottschalk et al. 2009) for Europe (underlined).

	Air $\mu\text{g}/\text{m}^3$	Water $\mu\text{g}/\text{L}$	Soil $\mu\text{g}/\text{Kg}$
AgNP	1.7×10^{-3}	0.03/ 0.01 / <u>0.000764</u>	0.02/ 0.43
AlO ₃		0.0002	0.01
AuNP		0.14	5.99
CeO ₂		< 0.0001	<0.01
CNT	1.5×10^{-3}	0.0005 / <u>0.000004</u>	0.01
Fullerenes		0.31 / <u>0.000017</u>	13.1
Hydroxyapatite		10.1	422
Latex		103	4307
Organo-silica		0.0005	0.02
SiO ₂		0.0007	0.03
TiO ₂	1.5×10^{-3}	0.7/ 24.5 / <u>0.0015</u>	0.4/ 1030
ZnO		76 / <u>0.010</u>	3194

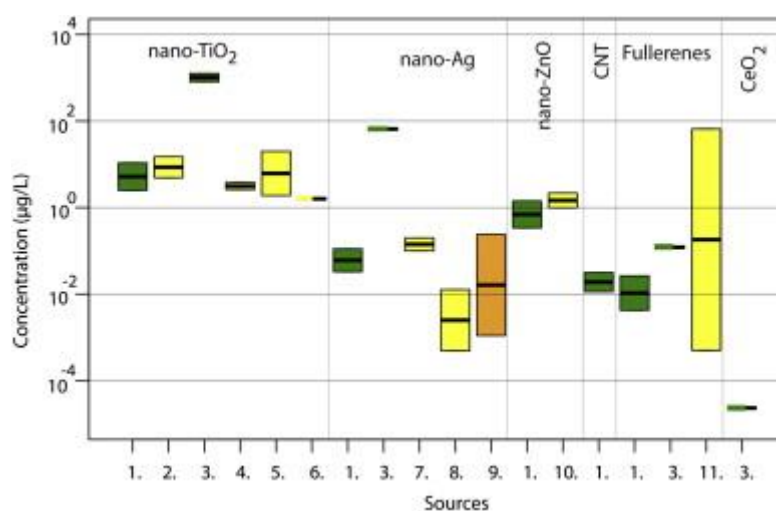


Fig. 1.3 Resume of modeled and analytical concentrations of engineered nanomaterials (ENM) in waste water treatment plant effluents. The green boxes show the range (and the arithmetic mean on the log scale) of modeled results, the yellow boxes measured equivalents and the orange box combines measurements and modeling. Picture taken from (Gottschalk et al. 2013).

Environmentally relevant concentration of CuO in freshwater aquatic compartments are expected to be around 10 µg/L (Black et al. 2017).

Analytical verification of these estimation is only partially available due to the measurement limitations afore mentioned. Nevertheless, some attempts have been reported. It was found that the concentration of titanium in untreated sewage, prior to entering 10 different wastewater treatment plants (WWTPs) in the USA, ranged from 181 to 1233 µg/L (median of 26 samples was 321 µg/L), whereas titanium in the effluent (released in the environment) varied from 0.2 to 16 µg/L (Westerhoff et al. 2011). These data are in agreement with the average titanium concentration entering a different WWTP in the USA equal to 185 µg/L (Kiser et al. 2009). The presence of nano AgNP, CeO₂ and TiO₂ in Dutch surface water has also been confirmed. The respective concentration ranges were 0.3 to 2.5 ng/L for AgNPs, 0.4 to 5.2 ng/L for CeO₂ and 0.2 to 8.1 µg/L for TiO₂ (Peters et al. 2018). In another study assessing the occurrence of AgNPs and TiO₂ in two Norwegian WWTPs serving the city of Trondheim, titanium concentrations were up to 290 µg/L while silver varied from 0.15 to 2.1 µg/L (Polesel et al. 2018).

One of the main routes of nano-waste introduction into the environment occurs through waste management sites such as municipal and industrial wastewater treatment plants as well as landfills and thermal-treatment factories (Musee 2011).

The global production of NPs is still on the rise with the development of new nanomaterials as well as innovative utilization of existing ones. Such widespread and expanding production and use of NPs increases the potential for their release to the environment, with environmental levels expected to rise in the years to come (Ma et al. 2013a).

1.5 Nanoparticle behaviour in the environment

(Nano)particles remain dispersed in suspension as single unit if there is a mechanism that hinders their collision and hence attachment. If this does not happen, (nano)particles tend to aggregate with other identical (nano)particles (homoaggregation) or with (nano)particles of different nature (heteroaggregation) (Burd and Jackson 2009). The classical Derjaguin, Landau, Verwey and Overbeek (DLVO) theory describes the stability and behaviour of charged surfaces in solution. In such a system (Fig. 1.3), two main forces are involved: an electrostatic double layer repulsion that prevents agglomeration/aggregation and van der Waals force that binds particles together (Hartmann et al. 2014).

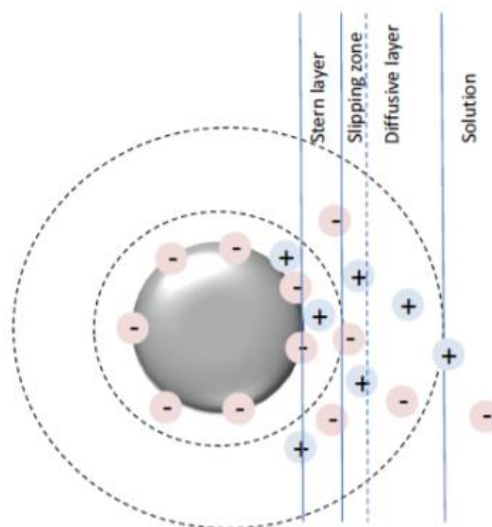


Fig. 1.4 Representation of a negatively charged (nano)particle in solution. Adsorbed ions are in the Stern layer while more loosely ions are in the diffuse layer. Stern and diffuse layer together compose the electric double layer (EDL). Picture taken from Hartmann et al. (2014).

Zeta potential is a measure of the electric potential at the share plane which separates the stern and diffuse layer. At this point the electric potential begins to

decrease exponentially away from the NP surface, controlling particle mobility and thus influence zeta potential of the particle (Vidojkovic et al. 2011).

In complex solutions unlike ultrapure water, other water quality parameters such as presence of cations, pH and organic matter also influence NP interactions and transformation. Indeed, the behaviour of nanomaterials is not only dependent on their properties as it can be affected and altered by the environmental conditions NPs are exposed to as shown in Fig. 1.4.

Results for AgNP, TiO₂, ZnO, and CNTs dispersed in five different surface natural waters that varied from pristine state to highly polluted and brackish water show a variety of behaviour, fate and algal toxicity. Aggregation peaked in salty water where the nanomaterials had lowest zeta-potential and greatest hydrodynamic diameter due to the NP destabilization via compression of the electrical double layer. On the contrary, in water with abundant DOM coating the nanomaterials, the electrosteric repulsion hindered aggregation, diminishing the size distribution which further led to reduced sedimentation. Hence NPs remained dispersed in suspension for a longer time and could exert greater toxicity to algal cells (Zhang et al. 2016). Similar results were reported when assessing the effects of eight different water types on CuO stability. Aggregation and stability were negatively impacted by ionic strength while increased DOM stabilized the NPs. CuO dissolution correlated with pH, however in salt water, the released Copper ions formed insoluble complexes (Conway et al. 2015).

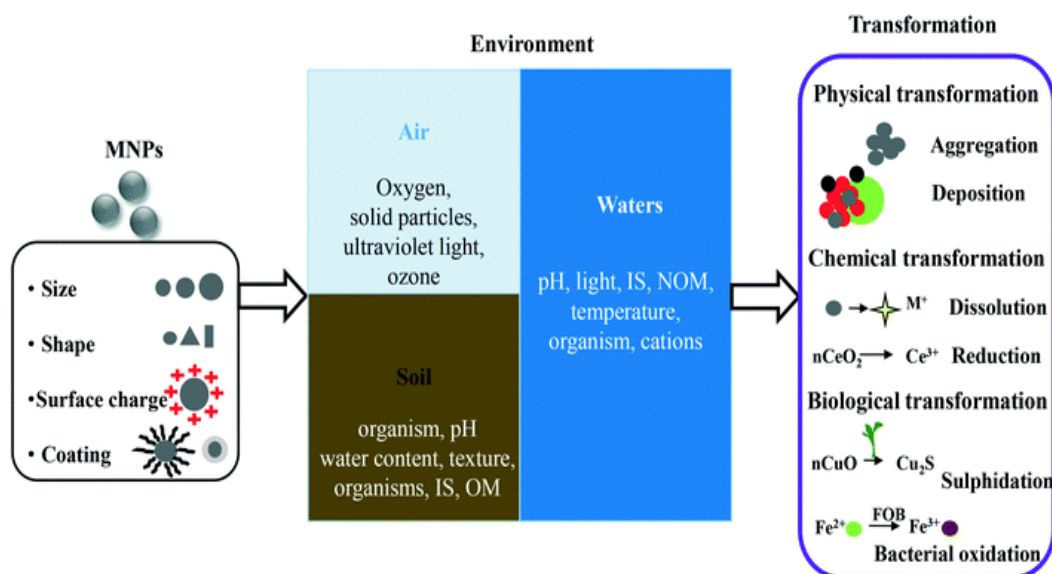


Fig. 1.5 Transformations of NPs in the environment. These include physically, chemically and biologically mediated transformations. The physicochemical properties of NPs, together with environmental factors, determine the type of transformation processes. Picture taken from Zhang et al. (2018).

The main environmental factors affecting NP behaviour and transformation in the water compartment are discussed below.

1.5.1 pH

Under low pH (excess of H^+) NPs result in a positively charged surface, whereas excess of OH^- (high pH) yields a negatively charged surface. The pH at which the H^+ and OH^- concentration causes suspended NPs to have a neutral charge is called point of zero charge (pzc). As pH achieves this point, the electrostatic double layer (EDL) repulsion decreases and aggregation of NMs is promoted.

The variation of pH in which NPs are dispersed can significantly impact the surface charge (z-potential) of the nanomaterials. Under low pH (excess of H^+) NPs result in a positively charged surface, whereas excess of OH^- (high pH) yields a negatively charged surface. Key to understand (nano)particles behaviour in solution is the point of zero charges (pzc) or isoelectric point, defined as the pH value at which the global surface of (nano)particle is neutral (López-Moreno et al. 2018). Near the pH of pzc, the surface charge of the (nano)particle is low, but at pH values far from it, the z-potential increases and (nano)particles are considered stable with zeta potentials either more negative than -30 or more positive than +30 (Fig. 1.3a). As pH achieves the pzc,

the electrostatic double layer (EDL) repulsion decreases and aggregation of NMs is promoted. In the stable regions, (nano)particles are equally charged (and have a significant zeta potential), which induces electrostatic repulsion which hinders aggregation. In the pH regions around the pzc, the z-potential is not strong enough to provide sufficient repulsions between (nano)particles. Hence collisions between (nano)particles will be only partially limited, or not at all, which causes aggregation and increased size (Fig. 1.3b).

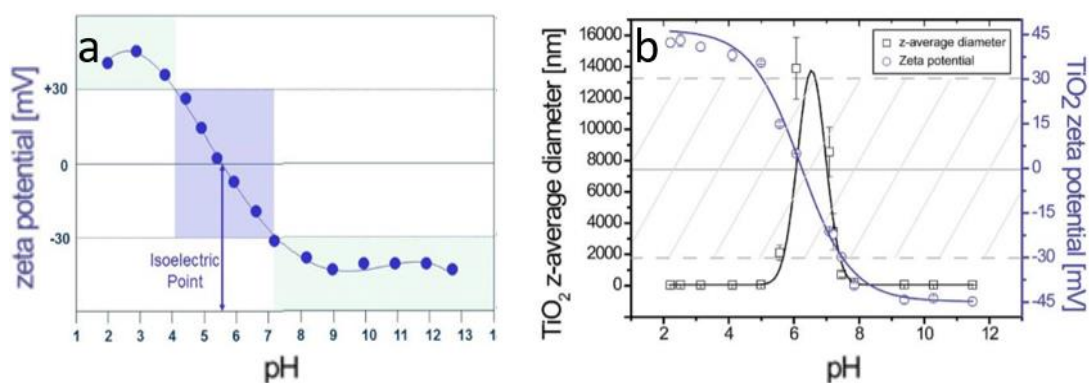


Fig. 1.6 a) pH dependent Zeta-potential of a nanoparticle. The green areas ($-30 \text{ mV} < z\text{-potential} > +30 \text{ mV}$) show stability regions. The blue area, where NP distribution is unstable due to ($-30 \text{ mV} > z\text{-potential} < +30 \text{ mV}$) falls between a pH range of 5.5 ± 2 around the pH of isoelectric point (z-potential = 0). (Malvern Panalytical, Isoelectric points of nanomaterials, <https://www.materials-talks.com/blog/2017/07/27/isoelectric-points-of-nanomaterials-qa/>, March 27th, 2020). **b)** Effect of pH on z-potential and size distribution of TiO₂. The isoelectric point is around 6, and the unstable zone (z-potential between -30 and +30 mV) extends from 5.5 to 7.5. Within this region, the lower electrostatic repulsions causes the formation of larger TiO₂ aggregates (Loosli et al. 2014).

1.5.2 Cations

The presence of monovalent and divalent cations such as Na⁺, K⁺ and Ca²⁺ in suspension lead to the adsorption of such ions onto the NP stern layer causing a net reduction of the surface charge. This reduces the electrostatic repulsion between NPs, hence increasing the number of NP-NP collisions which impacts the suspension stability and lead to increase in NP size due to aggregation (Mostowtt et al. 2019).

1.5.3 Natural organic matter

Natural organic matter (NOM) is a complex matrix that include a hydrophobic (non-humic) fraction and a hydrophilic portion (humic substances, HS) (Grillo et al. 2015a). The presence of (NOM) in aqueous solution has the potential to modify NP behaviour by interacting with their surface. When this happens NOM can create a coating (corona) around the nanomaterial (Pino et al. 2014). The coating mechanism can involve a complex combination of electrostatic forces, van der Waal forces, and steric effects between the NOM and the surfaces of the NPs (Grillo et al. 2015). The organic corona can then provide NPs with an electro-steric barrier that can prevent homo and hetero aggregation (Loosli et al. 2015a; Metreveli et al. 2015) and influence NP toxicity and fate in solution (Docter et al. 2015).

1.5.4 Nanoparticle dissolution and sulphidation

NPs in aqueous solutions and environmental matrices are known to undergo physio-chemical transformation such as reduction, dissolution and sulphidation. These phenomena have the potential to greatly impact and change NP fate, biological reactivity, bioavailability, uptake and toxicity (Lowry et al. 2012).

Light induced reactions (photooxidation and photoreduction) may trigger transformation of the NP coating and especially induce the production of reactive oxygen species (ROS) which can weaken and degrade the NP electro steric barrier. Many bare nanomaterials can also directly produce ROS when exposed to light given their photocatalytic properties (TiO_2 , ZnO , CeO_2 and CNTs).

Dissolution and sulphidation are two tightly connected processes that affect NP surfaces. The occurrence of dissolution and sulphidation is dependent on the NP nature. Class B soft metal cation (Ag, Zn and Cu) based nanomaterials are highly susceptible to such transformations due to the partially soluble nature of their metal-oxide forms. Furthermore, these metal-oxides have great affinity for inorganic and organic sulfide ligands (Lowry et al. 2012). However this does not happen for all metal-oxide NPs. For example, commercially available TiO_2 (anatase) is insoluble in water and can only be degraded in strong concentrated acids. However, other types of TiO_2 have been shown to undergo dissolution depending on factors such as water

quality and temperature, NP size, synthesis method and purity (Schmidt and Vogelsberger 2006).

Dissolution is a dynamic process through which ions of the dissolving NPs pass from the nanomaterial surface to solution. Higher degrees of dissolution occurs at lower pH where the presence of protons triggers ion release (López-Moreno et al. 2018). In addition, NP dissolution rate has been shown to enhance as particle size decreases. This is due to the greater surface area in smaller NPs which provides higher reactivity (Misra et al. 2012).

The released free ions can further undergo sulphidation reacting with inorganic Sulphur species (Misra et al. 2012). The Sulphur-NP compound (i.e. Ag₂S, CuS, ZnS) develops through a mechanism of dissolution and reprecipitation. The newly generated Sulphur-NPs are less soluble, less reactive and more prone to aggregation and sedimentation in comparison to the original unaltered NPs (Ma et al. 2013b). These changes imply that dissolution and sulphidation have great potential to alter NP behaviour and toxicity in the environment.

1.6 Nanoparticle toxicity – the challenge and state of the art

In recent years, the assessment of nanoparticle toxicity has drawn bigger attention from the scientific community. NP environmental concentrations are predicted to increase, and extremely high concentrations are likely in certain areas (e.g. in the vicinity of the production facility) or in contaminated sites where NPs are intentionally released for remediation purposes. Illegal dumping of NPs falls under “intentional release” of nanomaterials in the environment and can cause localized conditions with extremely high NP concentration.

The wide range of environmental concentrations are a common factor between “regular” pollutants and NPs. However, nanomaterials have features that are unique and distinctive of this class of chemicals. Such properties pose a new challenge in comparison to the toxicological assessment of “regular” contaminants. NPs are suspended in water, not dissolved like most chemicals (organic and inorganic compounds). NPs can undergo a variety of physio-chemical transformations such as dissolution, sulphidation, presence of capping agents, adsorption of DOM, aggregation and photo-activation. All these processes have great potential to modify NP toxicity.

NPs have also the capacity to react with other chemicals present in the environment (Sun et al. 2007). This interaction can influence the NP behaviour as well as that of the “absorbed” chemicals (Naasz et al. 2018). The association with other compounds can lead to increased or reduced toxicity, which is a common phenomenon when encountering contaminant mixtures (Naasz et al. 2018). When NPs are present in mixtures with other chemicals however, a “trojan horse effect” can happen, where NPs often play a key role in determining the toxicity of the newly generated NP-chemical compound (Hsiao et al. 2015). NPs have access to biological regions where larger particles would be inhibited (Dhawan and Sharma 2010). NPs can act as a carrier and transport mechanism for contaminants in biological compartments which would otherwise be inaccessible (Naasz et al. 2018). On the other hand, NPs can sequester pollutants making them less or not bioavailable, hence preventing them from exerting their bioactivity (Hsiao et al. 2015). This affects the fate and toxicity of the chemicals that react with NPs (Dhawan and Sharma 2010). In other cases, such as with TiO₂, NPs can trigger photo-oxidation hence photo-remediation of attached compounds or provide sequestration like in the case of heavy metals (Naasz et al. 2018).

NPs can not only generate mixtures with other types of contaminants, indeed NPs can be present as mixtures of different NP types. Research on environmental fate and behavior of NP mixtures has attracted far less attention than it should, given the fact that the most realistic condition under which NPs would be present in natural environment is as mixtures rather than a single NP type pollution. NP mixtures effects have focused on ecotoxicological studies including on single-strain bacteria (Yu et al. 2016), microbial community (Tong et al. 2015), microalgae (Liu et al. 2018), plants (Joško et al. 2017), invertebrates (Lu et al. 2017) and vertebrates (Hua et al. 2016). In contrast, there is a paucity in environmental research on NP mixture transport and fate in environmental and relevant engineered systems. However, the co-occurrence of different NPs is the most likely scenario due to the widespread array of nano-based products currently available (Yu et al. 2016). There is uncertainty regarding the possible interactions that the simultaneous presence of more NP types in WWTP would cause (Eduok et al. 2015). In light of this, the assessment of whether the available technologies can cope with current and future NP loading scenarios still requires elucidation, especially with regards to NP mixtures. To date, few have studied

the interactions between different classes of NPs in WWTP. This relatively new field of NP research has so far focused on ecotoxicological assessment and bulk removal amounts. WWTPs embody the ultimate point where NP mixtures are likely to be found at concentrations that can pose a threat for the environment. WWTPs receive urban and industrial sewage that is likely to contain different NP types simultaneously as the result of the increasing and widespread use and application of nanomaterials. This makes the environmental assessment of NP mixtures in WWTPs an actual gap of great relevance and interest that, up to date, the scientific community has only barely started to cast eye on.

A further complication in the toxicological assessment of NPs occurs due to the physical properties of nanomaterials. NPs of the same family may display different toxicity due to their size, shape, synthesis method, crystalline structure and purity. This variety of possible different scenarios and transformations make NP ecotoxicological test hard to standardize and extremely complex with the sake to provide an all-round evaluation of the nanomaterial toxicity (Handy et al. 2008a). In addition NPs act in a different way from the bulk material. Overtime though, their behaviour hence toxicity can become a combination of mechanisms. Certain metal-based NPs dissolve in aqueous solution. Through the process of dissolution, NPs can release heavy metals in the vicinity or inside cells where they can be a source of damage to the exposed organism (Handy et al. 2008a).

NPs can exert their toxicity through a variety of pathways and mechanisms which begin with biological membrane interactions (Handy et al. 2008a). These are influenced by properties such as polarity, temperature, viscosity, NP type, surface charge, shape and membrane composition, elasticity as well as thickness (Contini et al. 2018). Once in contact with the membranes, NPs can provoke generation of reactive oxygen species (ROS) which results in oxidative stress (Djurišić et al. 2015). This direct interaction can lead to disruption of the cell membrane with loss of homeostasis and even cell lysis (Chang et al. 2012). However, the induction of oxidative stress is not the only interaction that can occur at membrane level. NPs can adhere to the membrane and then internalized into the intracellular space through endocytosis with the use of vesicles (Francia et al. 2020). Furthermore, NPs in environmental matrices are surrounded by a “corona” of organic matter. This is what cells really “see” when

they encounter NPs rather than their pristine surface and this can lead to binding to the cell receptors (Francia et al. 2020) followed by active uptake (Behzadi et al. 2017). If small enough, NPs can autonomously diffuse through the membrane and enter the cells.

Once inside the cells NPs can interact with cells organelles as well as biomolecules with the potential to disrupt a variety of biological processes that can harm the cell. This further disruption can occur via oxidative stress with increased generation of intracellular ROS which can damage and unbalance the regular cell function. NP intracellular interactions can affect biomolecules, largely impairing their functions in maintaining regular physiological processes which further result in toxicity. NPs can directly react and cause disruption to proteins such as enzymes as well as with nucleic acids (DNA and RNA) provoking genotoxicity (Sabella et al. 2014).

Testing aquatic organisms for NP toxicity is essential as the water sphere is considered the main compartment in which contaminants are released and retained (Peralta-Videa et al. 2011). It has been shown that the presence of waterborne NPs can have negative effects on aquatic organisms, from bacteria, to plants, invertebrates and vertebrates. Some examples of the many are reported below.

The photo induced toxicity of TiO₂ and AuNPs have been found on *Escherichia coli* (Vimbela et al. 2017). Toxicity towards *Nitrosomonas europaea* was found upon exposure to ZnO. However ZnO was also effective against pathogens such as *Streptococcus agalactiae* and *Staphylococcus aureus* (Huang et al. 2008). TiO₂ and AgNPs were also found (more) toxic to planktonic and in a reduced manner to some biofilm forms of a natural microbial aquatic community from surface water (Jahan et al. 2017).

CuO induced toxic effects to the macrophyte algae cells of *Nitellopsis obtuse* and to cells of the green algae *Chlorella* (Manusadžianas et al. 2012). CuO were found internalized by the green alga *Chlamydomonas reinhardtii* which caused Oxidative stress, reduced growth rate and metabolism at 0.1 mg/L (Melegari et al. 2013). TiO₂ produced oxidative stress and cell wall damage to the marine phytoplankton *Phaeodactylum tricornutum* (Wang et al. 2016b). The microalgae *Dunaliella tertiolecta* suffered cell growth inhibition when exposed to ZnO at respectively 2 and 5 mg/L (Schiavo et al. 2016). AgNP were internalized and accumulated by the

freshwater alga *Ochromonas danica* which led to oxidative stress and cell growth inhibition (Miao et al. 2010).

Algae are the primary source of food for many small fresh water and marine invertebrates. Among these, the water flea *Daphnia magna* is probably the most widely used model organism. Accumulation and toxicity of many NPs such as AgNP, AuNP, CuO, TiO₂, ZnO and carbon based nanomaterials to this freshwater crustacean have been extensively reported (Tao et al. 2009) (Jo et al. 2012) (Liu et al. 2014) (Xiao et al. 2015) (Adam et al. 2015) (Xiao et al. 2015). It has been shown that the uptake of TiO₂ and ZnO by *Daphnia magna* occurred in both feeding and starvation regimes. However the amount of NPs accumulated by the organisms were roughly three times higher in the presence of algae. This means that NP uptake can happen directly but indirect adsorption of NPs through food can occur too and even increase the overall NP uptake (Renzi and Blašković 2019).

AgNP and AuNP were taken up by Zebra fish (*Dario rerio*) embryos, with the first exerting greater mortality (almost 100%) in comparison to the 3% mortality caused by AuNPs (Jiang et al. 2009). AgNP and CuO NPs were found cytotoxic to rainbow trout (*Oncorhynchus mykiss*) hepatocytes where both NPs were accumulated in the liver causing oxidative stress induced apoptosis (Ostaszewska et al. 2018). Toxicity upon exposures to AgNP (Lee et al. 2012), CuO (Zhao et al. 2011), TiO₂ (Linhua et al. 2009) and ZnO (Hao et al. 2013) were observed as oxidative stress and NP accumulation in juvenile common carp (*Cyprinus carpio*).

These are just few examples, focused on aquatic species, of the many cases of documented toxic effects caused to biota by exposure to NPs. It is very interesting and concerning how NPs can impact all the levels of a trophic net from primary producers (plants and bacteria) to apical predators which feed on herbivores occupying an intermediate level of the food net. In an experiment carried out in estuarine mesocosms containing sea water, sediment, sea grass, microbes, biofilms, snails, clams, shrimp and fish, AuNPs were single dosed in the water column (Ferry et al. 2009). After 12 days, the authors found that most of the NPs were accumulated by biofilm and clams (filter feeders). This proves that AuNPs can rapidly pass from the water column to the trophic web, and overtime be bioconcentrated in the higher levels such as fish, birds and mammals including humans. A similar pathway was observed

for AgNPs released from a consumer product immersed in an estuarine mesocosm for 60 days (Cleveland et al. 2012). Over 80 % of the total AgNPs leaked into the water column and then mostly accumulated in the sediment in the early stages of the test period. Subsequently, the authors found significant amount of silver accumulated in other organisms of higher trophic levels such as clams, grass shrimp and mud snails. Tropic transfer of TiO₂ was observed in simplified freshwater mesocosms containing water fleas (*Daphnia magna*) and Zebra fish (*Dario rerio*) through dietary exposure hence highlighting the potential of food chain transfer (Zhu et al. 2010).

The variety of NP types, shapes, size distribution, synthesis and other processes such as surface modifications and the impact of environmental factors make NP toxicological characterisation a very difficult task, as seen with the vast number of differing results obtained from same Ag NPs, many of them contradictory. Still, the mode of action of most NPs is not yet understood and controversial. Moreover, the lack of standardised testing procedures increases the difficulty of interpreting results and predicting fate and toxicity of groups of particles.

1.7 Bacteria

Bacteria are a large domain of prokaryotic microorganisms capable of adapting and living in the most widespread and diverse environmental conditions on Earth. These include some considered as the most extreme and most harsh to live in such as deserts (A. Belov et al. 2018), Polar zones (Harding et al. 2011) and acid lakes (Merino et al. 2019).

Bacteria are unicellular organisms which display a huge variety of cell shapes such as spherical, filamentous, rod-like and spiral. Their external surface is equipped with a cell-wall that provide structural integrity and protection. Based on the morphology of the cell-wall, bacteria can be classified as gram-positive (thick peptidoglycan layer) and gram-negative (thin peptidoglycan layer plus lipopolysaccharide layer). This can be determined via the Gram-stain assay which is based on the capacity of the bacteria cells to retain or not crystal violet. In the outer part of the cells bacteria can present flagella(s) and pilus. The first have motility purpose while pilus are generally used to adhere to surfaces and other organisms. The main feature of the intracellular space is

the lack of a nucleus. Prokaryotes' genetic material resides in the cytoplasm. In addition, bacteria are equipped with independent pieces of DNA called plasmids.

Thanks to their functional plasticity, Bacteria have been widely exploited by humans in many applications. Engineered Bacteria have been used to produce bio-fuel from waste and crops (Dien M A Cotta T W Jeffries 2003), mitigation of environmental pollution (Liu et al. 2019), biomedical applications (Piñero-Lambea et al. 2015) and resources recovery (Park et al. 2017) to name a few.

1.8 Biofilm

Bacteria can live both as planktonic (free-living cells or aggregates called flocs) and adherent or sessile colonial forms. A microbial community is called a biofilm. These generate from the seeding of individual or aggregated planktonic cells that attach to a surface and develop and mature into a complex and self-sustaining community of microorganisms' overtime.

The structure of a biofilm comprises a variety of microbial cells of different species embedded in a non-cellular extracellular polymeric substances (EPS) matrix. The main components in it are extracellular polysaccharides, proteins and DNA. Besides, this matrix is equipped with channels that enable air, water and nutrients to move throughout the structure (Rabin et al. 2015).

When we talk about the driving force behind biofilm formation, we are asking the question “How does the biofilm mode of growth promote survival and propagation of the cell?”. In natural environments, Bacteria often encounter less-than-ideal conditions to live in. Thereby, living in a biofilm architecture provides them with advantages that improve fitness and survival (Jefferson 2004). The main feature of this lifestyle could be summarized with the general concept of a greater capacity to withstand greater environmental stress. These include resistance to physical forces, resistance to variation of environmental conditions (pH, lack of nutrient, temperature, oxygen, drought), as well as capacity to tolerate and survive the presence of chemicals such as antibiotics, biocides, disinfectant and environmental pollution. On the other side, when encountering favorable environmental conditions, the formation of biofilms provides a way to colonize and settle in a niche where the microbial community can thrive (Jefferson 2004).

These properties make biofilms both interesting and concerning. Indeed biofilms are clinically relevant since they can develop in human cavities as well as on clinical devices such as central venous catheters, central venous catheter, needleless connector, endotracheal tubes, intrauterine devices, mechanical heart valves, pacemakers and peritoneal dialysis catheters among others (Donlan 2001). Cells within biofilms monitor the microenvironment within and outside the physical boundaries to evade host immune responses or utilize the host machinery to propagate (Kumar et al. 2017). The severity of biofilm led infections is amplified by their i) easily transferable resistance to antimicrobial agents, ii) persistent source of infection, iii) pathogens can live in the microbial community, iiiii) escape and expansions mechanisms (Donlan 2001). Biofilm resistance is not just associated with plasmids, transposons and mutations that confer innate resistance to individual bacterial cells. These mechanisms are implemented with multicellular strategies that go beyond conventional notions of single cell scenarios (Tang et al. 2018). These include slower penetration of chemicals, development of resistant phenotypes and altered microenvironment within the biofilm. These community based mechanisms have the possibility to reduce the effectiveness of certain antibiotics (Stewart and Costerton 2001; Saleh et al. 2015) thanks to the complex heterogeneous structure of the EPS matrix which has been shown highly resistant to penetration of small molecules (Wang et al. 2016a)

Despite their sessile lifestyle, biofilm forming bacteria still retain great ability to move, spread and expand the colonized area. This happens as response to changing environmental conditions that can be a threat to biofilm survival. Stressful conditions trigger biofilm expansion through cell desorption, detachment, and dispersion (Fig. 1.6) which will lead to colonization of a more suitable area (Petrova and Sauer 2016).

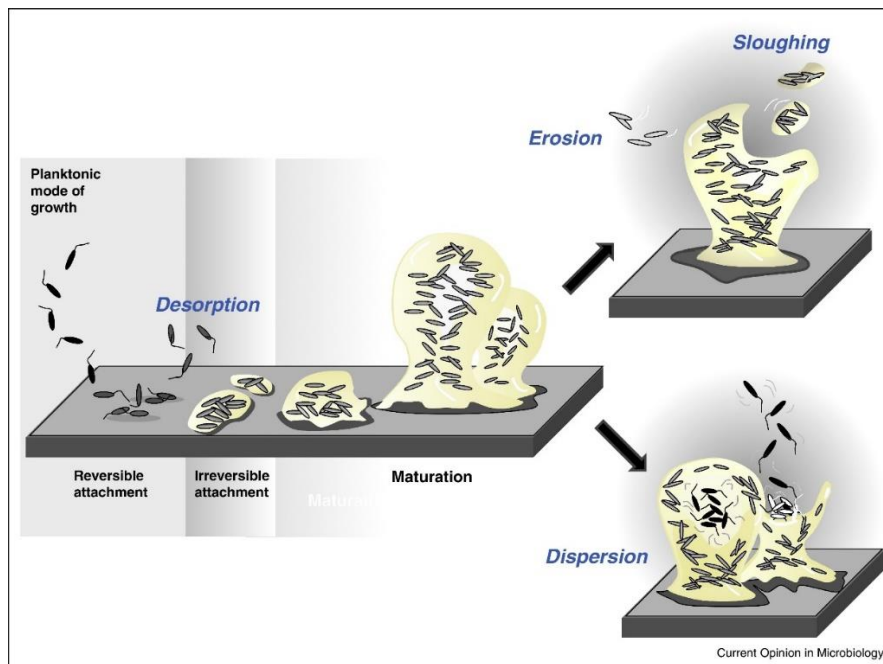


Fig. 1.7 Schematic of biofilm formation, maturation and escape modes. Picture taken from Petrova and Sauer (2016).

Although the severity of biofilm mediated infections in clinical cases, biofilm has found a variety of applications of great benefits for human purposes. Engineered biofilms are used in food and hydrogen production, oil degradation (Roeselers et al. 2008), biocatalysis (Tsoligkas et al. 2011) among others. Certainly, the application of biofilm in environmental pollution decontamination has been one of the fields which has seen the greatest success. Microbial communities have been used to remove contaminants ranging from heavy metals, petroleum, explosives and pesticides. Biofilm-based bioremediation is also used to decontaminate polluted soil and groundwater (Mitra and Mukhopadhyay 2016). One biofilm application in specific has been successfully adopted worldwide for decades now: wastewater treatment.

1.9 Wastewater treatment and the role of biofilm

Wastewater treatment is a series of physical, chemical and biological processes operated to remove contaminants from sewage and achieve an effluent quality such that no harm is done to the receiving water body.

A conventional wastewater treatment plant (WWTP) is composed of three operational stages: preliminary, primary and secondary treatments (Fig. 1.7).

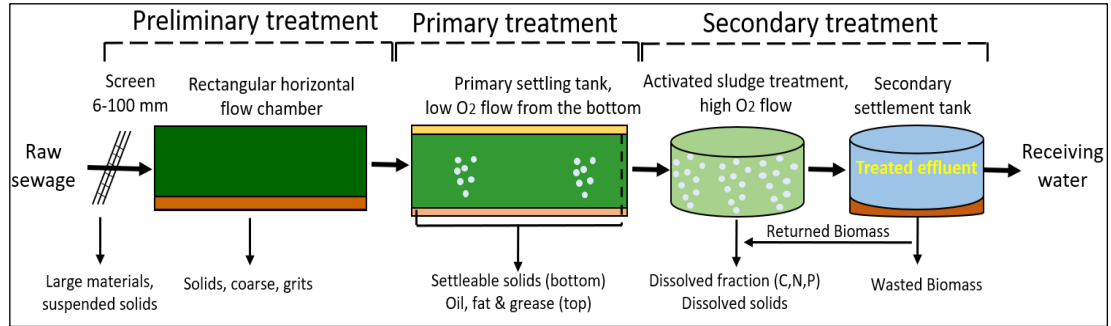


Fig. 1.8 Schematic view of a conventional wastewater treatment plant including, preliminary, primary and activated sludge based secondary treatment.

- *Preliminary treatment:* the incoming sewage goes through bar screens to remove large materials. This is followed by horizontal slow flow channels/chambers where solids, grit and other coarse materials are removed via settling. Chemicals (flocculant) may be added to improve sedimentation of wastewater particles during the following treatment stages.
- *Primary treatment:* Preliminary treated sewage enters circular or rectangular primary sedimentation tanks where the majority of settleable solids are physically removed via gravity and then scraped away. Gentle up flow aeration is also applied to separate oil, fat and grease onto the upper part and then skimmed away.
- *Secondary treatment:* Primary treated sewage reaches the secondary treatment stage where the dissolved organic and solid fractions (Carbon, Nitrogen and Phosphorus species) are removed by microorganisms. Dissolved nutrients are biodegraded and converted into biomass and carbon dioxide. Suspended and non-settleable colloidal solids are also captured and removed by microorganisms. After agitation and aeration, the mixed liquor suspended solids (MLSS, primary treated sewage + biomass) is transferred into secondary sedimentation tanks where the biomass is allowed to settle and separate from the liquid phase. The liquid phase (treated effluent) can be re-introduced into the environment.

In some cases (although infrequently) a further tertiary treatment is necessary. This is called “effluent polishing” and is used in specific cases of more stringent

consents due to the discharge of the effluent in water bodies with special conditions such as recreational or drinking water use, rivers with low flow and water flowing into protected areas. Tertiary treatments include further nitrogen and phosphorus removal to prevent eutrophication and algal blooms that could reduce water quality. Chemicals (aluminium, ferric and calcium ions) can be dosed in as well to enhance phosphorus removal. Another step is disinfection, to prevent emission of pathogens, coliform and faecal coliform. Sanitation can be carried out via UV-treatment, ozonation and chlorination (followed by dichlorination).

Secondary treatment is a microbially led process which relies on biofilms. A variety of designs have been applied. A brief overview is presented below.

- *Activated sludge - suspended biofilm*: This secondary aerobic treatment relies on a suspended biofilm (flocs) community of a microbial community of heterotroph bacteria. Supplied with oxygen, such bacteria can oxidize organic matter and convert it into carbon dioxide and new biomass. Nitrifying bacteria instead convert ammonia and either assimilate it into the floc or convert it into nitrogen gas through oxidation of ammonia to nitrite followed by the oxidation of the nitrite to nitrate (nitrification). Nitrate is then converted into nitrogen gas (denitrification). After agitation and aeration, the biomass and the liquor are separated in sedimentation tanks and a fraction of the settled biomass is returned ahead of the aeration stage. The remaining part is wasted and generally sent to a treatment centre where it is used for energy and fertilizer production.
- *Aerobic granules – suspended granules*: Extremely similar to activated sludge systems. However, biofilms are engineered in granules rather than flocs, which provides economic advantages in terms of time and space. Granules settle faster than flocs and final sedimentation tanks are not required. In addition, very little or no sludge needs to be wasted, which reduces operational costs and carbon footprint. However, this type of plant requires longer preparation time to have mature granules.
- *Filter beds (oxidising beds) – biofilm attached to a substrate*: Generally called trickling filter beds, are widely used in small and medium size WWTPs. This secondary treatment relies on a microbial community that develops and

matures attached to a substrate like coke limestone chips or specially fabricated plastic media. The liquor sprinkles from the upper part and trickles through the bed bringing oxygen in solution so that the microorganisms can utilize it to reduce the organic content. This system is cost effective for sites that need to handle low volumes with relatively low organic load. It does not require aeration and maintenance costs are low.

- *Anaerobic granules – suspended granules*: Opposite to all the systems above, anaerobic granules treatment does not rely on oxygen to degrade the organic content. Each granule is a functional independent unit that consist of a mixture of anaerobic microorganisms. This microbial community greatly differs from the aerobic ones. Anaerobic granules are composed of acidogenic bacteria (degrade organic molecules in volatile fatty acids), acetogenic bacteria (convert volatile fatty acids into acetic acids, carbon dioxide and hydrogen) and methanogens that produce biogas (methane and carbon dioxide) from acetic acid. Biogas can be used as fuel in combined heat and power (CHP) stations to produce energy and heat, reducing the carbon footprint of this type of treatment.

1.10 Biofilm – nanoparticle interactions and toxicity

Biofilms are considered a main sites of NP accumulation in aquatic systems. Bacteria – NP interactions hold implications for the transport of NPs within environmental systems which have great potential to impact NP environmental fate. Despite several mechanisms have been proposed, the understanding of NP – Biofilm interactions is still considered an evolving field due to its complexity.

It is well known that NP – biofilm interactions are governed by nanomaterial characteristics, biofilm properties and environmental factors (Joo and Aggarwal 2018) which are resumed in Fig. 1.9.

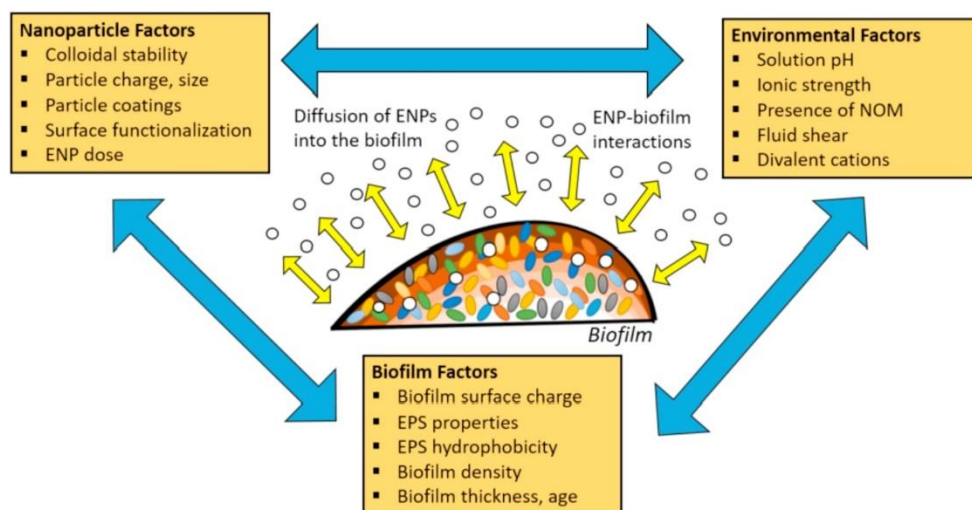


Fig. 1.9 Summary of NP, biofilm and environmental factors governing NP – biofilm interactions. Picture taken from Joo and Aggarwal (2018).

For example, attachment of model nanoparticles (AgNPs, dextran and fluorescent microspheres) to *Pseudomonas fluorescens* biofilms was observed regardless of the NP characteristics (Peulen and Wilkinson 2011). However, NP mobility and fate were found dependent of NP size and biofilm structure. Only NPs with size smaller than 50 nm could penetrate the biofilm. Bigger NPs were observed to accumulate on the external membrane of the biofilm, with the pore size playing a key factor in the occurrence and magnitude of NP diffusion in biofilms (Peulen and Wilkinson 2011).

NP interactions are greatly influenced by their physio-chemical properties. Capping agents such as polyvinylpyrrolidone (PVP), citrate (CIT) and polyvinyl alcohol (PVA) can enhance the colloidal stability of nanomaterials and hence influence interactions with biofilms. In comparison to bare NPs, coated nanomaterials have different attachment efficiency in biofilm-laden porous media experiments. The presence of bovine serum albumin (BSA), alginate and citrate enhanced the portion of NPs retained, while PVP coated NPs were more stable and experienced low attachment efficiency (Xiao and Wiesner 2013). NP coatings have a great potential to impact NP behaviour as discussed in paragraph 1.5.3. The acquisition of a biological corona around NPs is a highly likely process to occur in natural waters. The adsorption of natural organic molecules (NOM) onto NPs can govern the fate of nanomaterials and association with biofilm as this is what cells really “see” when they encounter NPs rather than their pristine surface (Francia et al. 2020).

The NP – biofilm association is described as a three steps interaction which include: i) transport of NPs to the vicinity of the biofilm, ii) initial deposition of NPs onto the biofilm surface, iii) migration into deeper areas of the biofilm (Ikuma et al. 2015). The NP – biofilm association can occur via a series of interactions which can be divided in physical, chemical and biological (Huangfu et al. 2019).

- *Physical mechanisms* (Fig. 1.9) include electrostatic and van der Waals forces which are highly dependent on the NP type and the properties of the liquid. Steric interactions between NPs and other organic molecules can change NP stability, hence reduce aggregation, but can also enhance the association with microbial constituents. Polymer bridging interactions happen when NPs coated with DOM leading to the occurrence of short-range attractive polymeric interactions between NPs.

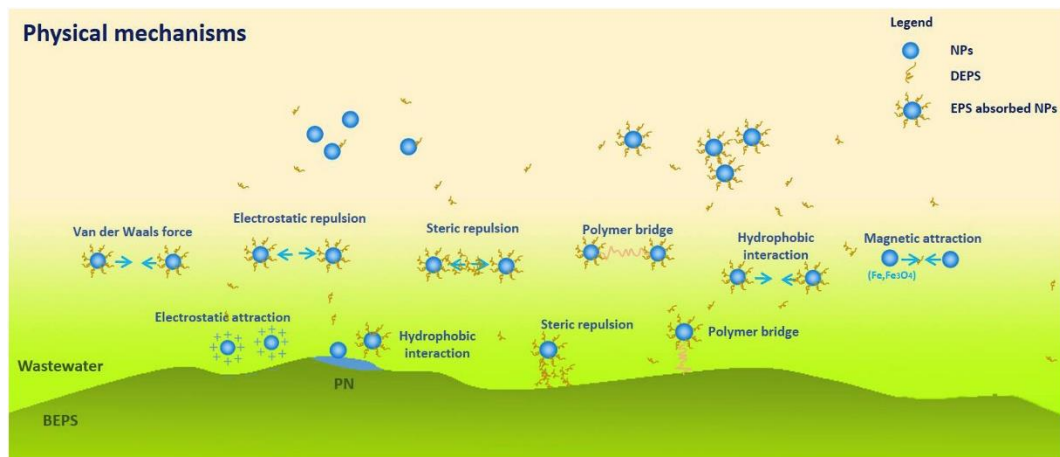


Fig. 1.10 Resume of physical mechanisms involved in the NP - biofilm interactions. Picture taken from Huangfu et al. (2019)

- *Chemical mechanisms* (Fig. 1.10): Among these redox and photocatalytic reactions can lead to NP dissolution which can also generate ROS, hence induce oxidative stress. Dissolved ions can further react with inorganic sulphur and experience precipitation. NPs and the released ions, can interact with functional groups,

including carboxyl, hydroxyl, ether, amine and sulfhydryl groups present in the EPS matrix. The presence of ions, (Ca^{2+} and Mg^{2+} are cations commonly found in wastewater) can trigger the association between NPs and EPS via cation bridging.

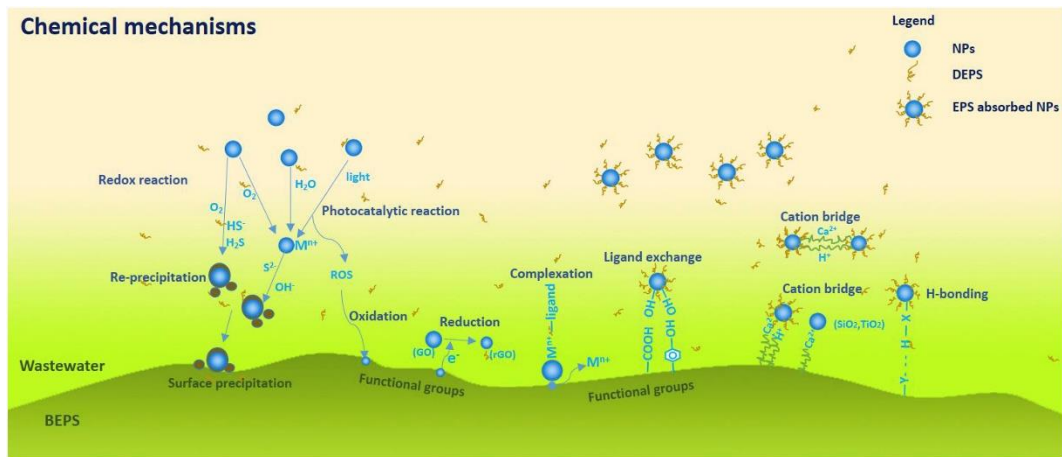


Fig. 1.11 Resume of chemical mechanisms involved in the NP - biofilm interactions. Picture taken from Huangfu et al. (2019)

- *Biological mechanisms* (Fig. 1.11) are thought to happen more rarely than mechanical and chemical mechanisms. It occurs when NPs bind to external

receptors via the presence of a DOM corona around them. Once attached to the receptor, NPs can then be actively uptaken via endocytosis or phagocytosis.

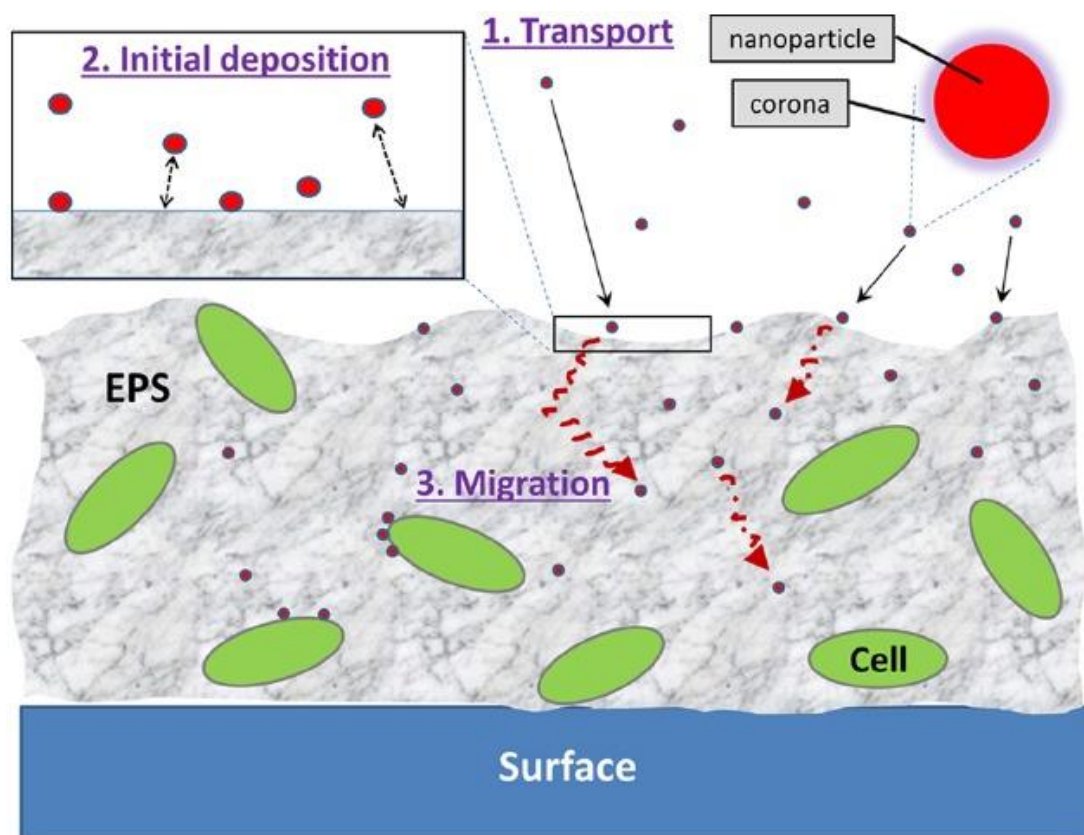


Fig. 1.12 Resume of biological mechanisms involved in the NP - biofilm interactions. Picture taken from (Ikuma et al. 2015)

It is important to remind and highlight that a biofilm is a community of different species embedded into an extracellular polymeric substances (EPS) matrix which makes every biofilm different from another. Coupled with the variety of NP types and their properties and bearing in mind how severely these can be influenced by environmental conditions, NP – biofilm association is an intricate process not yet totally understood.

As a direct result of interaction with biofilm, NPs have the potential to exert toxicity to microorganism used in wastewater treatment plants. Such topic has received great attention in recent years. There is now a growing body of evidences that suggest that NPs can cause minimal negative impact towards microorganism in biofilm form such as activated and anaerobic granular sludge (Durenkamp et al. 2016). Furthermore,

these findings suggest that within these microbial communities, NPs can produce a negative impact mainly towards nitrifying bacteria (Clar et al. 2016; Hou et al. 2016; (Siripattanakul-Ratpukdi et al. 2014). This is the results of the biology of such bacteria. Nitrifiers are generally known for being more susceptible to environmental changes and harsh conditions. In addition, in comparison to carbon-based metabolism heterotrophs bacteria, nitrifiers have slower growth rate and are more affected by stressors such as contaminants. This is the reason why wastewater companies apply a sludge age of around 8 days. This allow the nitrifiers bacteria to develop and reach a fully mature state that provide adequate ammonia removal. In addition, during cold periods, when water temperature falls below 5 °C, the validity of consent for ammonia environmental discharge in treated effluent ceases. This does not apply to COD consent because carbon-based metabolism heterotrophs bacteria are not so badly affected in comparison to nitrifiers.

A similar pattern has been observed in research context following wastewater biofilm exposure to CuO (Hou et al. 2016) where a reduction in ammonia was only observed after 50 days at a concentration of 500 mg/L, but no effect was detected regarding COD removal. Analogous results with no effect on organic matter removal and minimal depletion in nitrification were also reported. These experiments had activated sludge exposed to an initial higher concentration of AgNPs (1 mg/L) followed by a 20 days period with AgNP level of 0.1 mg/L (Liang et al. 2010). Interestingly the fall in ammonia removal were detected after the higher-level spike but where quickly recovered during the chronic phase of the test. In agreement with these evidences were also the data from Yang et al. (2015). The authors demonstrated that a continuously operated activated-sludge sequencing batch reactor (SBR) could remove over the 95% of the added nC60, but the addition of AgNP (2 mg/L) led to SBR disruption and caused short-term fall in nC60 and COD removal efficiency; the system recovered to its performances prior to AgNP “pulse” in 4 days. Although the overall bioreactors functionality was stable for the majority of the duration of the experiments, the authors recognized that the NP removal could be greatly impacted by short-term, “pulse” inputs from different. Very interestingly, also Eduok et al. (2015) found that activated sludge retained its ability to nitrify and degrade organic matter upon exposure to a mixture of AgNPs, TiO₂ and ZnO over a period of 60 days. During

this work the authors suggest of a possible selective inhibitory effect as indicated by a temporal shift in the microbial community structure and diversity where some species could not cope with the nanomaterial burden whereas others, such as *Acidovorax*, *Rhodoferrax*, *Comamonas* and *Methanosarcina* proliferated.

The reason behind these findings is mainly attributed to extracellular polymeric substances (EPS) matrix and functional redundancy. The EPS “shell” provides the cells embedded in it with greater resistance and endurance to environmental stressors such as predation, sudden changes, and adverse environmental conditions. Exposure to contaminants, such as NPs falls within this category. Under stress conditions biofilm forming bacteria can enhance their EPS production (Redmile-Gordon and Chen 2017). This would thicken and expand the physical barrier between the microbial cells and the stressor providing extra protection. Biofilms than have the potential to directly or indirectly release portion of EPS matrix through detachment or exudation of organic molecules from the EPS matrix. Indeed, the occurrence of thick foam formation in wastewater is an early indicator of stressed activated sludge. In addition, wastewater treating bacteria are also known to own functional redundancy where different species with diverse biological features can perform the same function. In this case, the degradation of organic matter and ammonia. As result of exposure to NPs, it is suggested that wastewater biofilm may be subject to stress and even to partial and temporary reduction in performances, especially in high concentration pulse events. However, overtime, it has been shown that biofilm can successfully and fully recover optimal performances.

Such features have always been key for the great success in the application of microbial communities in wastewater treatment plants as well as in many other sectors. This applies to a variety of difficult, harsh and extreme conditions biofilm forming organisms can cope with and carry out their functions in both natural and engineered scenarios.

1.11 Research objectives

This PhD research examines nanoparticle behaviour in sewage and investigates the extent to which secondary biological processes in wastewater treatment can prevent NP release in receiving water bodies.

Nanotechnology's impact on our lifestyles is rapidly increasing and the amount of nanoparticles produced, used and released into the environment is also increasing. The washout of nanoparticles into the sewage network is one the prominent routes through which NPs can reach natural water bodies. This can result in increased exposure to nanoparticles in the natural environment as well as humans. To this extent, wastewater treatment plants are the last barrier between polluted sewage stream and the receiving water bodies. Wastewater treatment plants hence have the potential to prevent the spread of NPs through the environment. This thesis looks to explore NP features and behaviour in sewage and assess the capacity of biofilm employed in wastewater treatment to prevent the emission of NPs.

NP use, and thus their abundance in wastewater, is likely to continue to increase and thus we expect to see higher NP concentrations in wastewater in the future. Due to this, this thesis examines how current and emerging biological sewage treatment systems cope with much higher concentrations of NPs than we typically find today. Moreover, research currently published does not explore these higher concentrations, and thus this thesis helps to fill an important knowledge gap in our understanding of NP behavior in wastewater treatment systems and how they may cope in the future.

Moreover, the effect that the wastewater liquor fraction (the liquid the activated sludge biofilms are suspended in) has on NP removal is currently not understood, and thus its relative contribution to NP removal compared to the biomass is not known. As a result, NP removal by the liquor fraction was also examined as well as by activated sludge.

Prior to exploring the behavior of NPs in wastewater, this thesis assesses and develops the optimal methods for analyzing NP concentrations in wastewater systems. This was done because it was recognized that there was no standardized method for determining concentrations of NP mixtures in wastewater under controlled conditions. Furthermore some of the methods used by the research community may not be suitable for the purpose of this work. This is due to the requirement for HF digestion in ICP-

MS methods. Other techniques, such as field flow fractionation and single-particle inductively coupled plasma time-of-flight mass spectrometry, have the potential to carry out such analysis. However, research on this topic has only recently developed and we have identified what could be a major gap affecting the accuracy of such methods, which is the lack of details on preservation methods and sample stability time. NPs are highly reactive materials, hence it is highly likely that the size distribution of the nanomaterials would quickly change during the time from sample collection to analysis. In addition, the presence of NPs as mixtures adds uncertainty on the robustness of such methods to discern different NP types when heterogeneous aggregates. Our methods offers a safer alternative capable of quantifying multiple NPs types in a single technique under laboratory conditions.

This research effort we present addressed both single NP scenarios as well as the widely less investigated but more environmentally relevant condition of NPs being present as mixtures of different NP types.

The research chapters discussed in this thesis appear in the following order:

- *Chapter 3* – Investigates the suitability of different processing and analysis methods for quantifying single and triple mixtures of CuO, TiO₂ and ZnO nanoparticles in wastewater. This work was undertaken as there are no standard defined methods, and therefore it was currently not known which methods were the most suitable and reliable.
- *Chapter 4* – investigates CuO, TiO₂ and ZnO removal behavior in real activated sludge collected from a municipal wastewater treatment plant. The chapter first presents NP characterization. Zeta – potential, size distribution and dissolution are key factors governing NP partitioning in aqueous solution and were assessed in pure water as well as wastewater liquor to help understand how these factors influence NP removal in wastewater. Activated sludge efficiency in removing single and triple NP mixtures was then assessed. In addition, NP removal by liquor only scenarios (no biomass) was also assessed to reveal NP removal mechanisms not due to biomass (e.g. aggregation and sedimentation).

- *Chapter 5* – builds up on chapter 3 with the difference that anaerobic granular sludge biomass, one of the emerging technologies in secondary wastewater treatment, is employed. The removal efficiency towards single and triple NP mixtures was the main endpoint evaluated in this chapter. The removal of NP mixtures via aggregation driven sedimentation was also assessed.
- *Chapter 6* – Provides a resume of the findings, comparisons between the different treatments and implications of this work. In addition a series of recommendations for further investigations based on the findings of the study are offered, plus suggestions are made on routes to expand this work onto adjacent subjects.

1.12 Bibliography

- A. Belov A, S. Cheptsov V, A. Vorobyova E (2018) Soil bacterial communities of Sahara and Gibson deserts: Physiological and taxonomical characteristics. *AIMS Microbiol* 4:685–710. <https://doi.org/10.3934/microbiol.2018.4.685>
- Adam N, Vakurov A, Knapen D, Blust R (2015) The chronic toxicity of CuO nanoparticles and copper salt to *Daphnia magna*. *J Hazard Mater* 283:416–422. <https://doi.org/10.1016/j.jhazmat.2014.09.037>
- Adlakha-Hutcheon G, Khaydarov R, Korenstein R, et al (2009) *Nanomaterials, Nanotechnology*. pp 195–207
- Ahamed M, Alhadlaq HA, Khan MAM, et al (2014) Synthesis, characterization, and antimicrobial activity of copper oxide nanoparticles. *J Nanomater* 2014:.. <https://doi.org/10.1155/2014/637858>
- Anyaogu KC, Fedorov A V., Neckers DC (2008) Synthesis, characterization, and antifouling potential of functionalized copper nanoparticles. *Langmuir* 24:4340–4346. <https://doi.org/10.1021/la800102f>
- Ayyub P, Palkar VR, Chattopadhyay S, Multani M (1995) Effect of crystal size reduction on lattice symmetry and cooperative properties. *Phys Rev B* 51:6135–6138. <https://doi.org/10.1103/PhysRevB.51.6135>
- Balbus JM, Maynard AD, Colvin VL, et al (2007) Meeting report: Hazard assessment for nanoparticles-report from an interdisciplinary workshop. *Environ Health Perspect* 115:1654–1659. <https://doi.org/10.1289/ehp.10327>
- Behzadi S, Serpooshan V, Tao W, et al (2017) Cellular uptake of nanoparticles: Journey inside the cell. *Chem. Soc. Rev.* 46:4218–4244
- Benn TM, Westerhoff P (2008) Nanoparticle Silver Released into Water from Commercially Available Sock Fabrics. 4133–4139. <https://doi.org/10.1021/es7032718>
- Black MN, Henry EF, Adams OA, et al (2017) Environmentally relevant concentrations of amine-functionalized copper nanoparticles exhibit different mechanisms of bioactivity in *Fundulus Heteroclitus* in fresh and brackish water. *Nanotoxicology* 11:1070–1085. <https://doi.org/10.1080/17435390.2017.1395097>
- Boccaccini AR, Karapappas P, Marijuan JM, Kaya C (2004) TiO₂ coatings on

- silicon carbide and carbon fibre substrates by electrophoretic deposition. In: *Journal of Materials Science*. Springer, pp 851–859
- Bootz A, Vogel V, Schubert D, Kreuter J (2004) Comparison of scanning electron microscopy, dynamic light scattering and analytical ultracentrifugation for the sizing of poly(butyl cyanoacrylate) nanoparticles. *Eur J Pharm Biopharm*. [https://doi.org/10.1016/S0939-6411\(03\)00193-0](https://doi.org/10.1016/S0939-6411(03)00193-0)
- Borm PJA, Robbins D, Haubold S, et al (2006) The potential risks of nanomaterials: A review carried out for ECETOC. Part. *Fibre Toxicol*. 3
- Boxall A., Chaudhry Q., Jones A. JB& WC (2008) Current and Future Predicted Environmental Exposure To Engineered Nanoparticles. Defra Rep 89
- Casarin M, Maccato C, Vittadini A (1997) An LCAO-LDF study of the chemisorption of H₂O and H₂S on ZnO(0001) and ZnO(1010). *Surf Sci* 377–379:587–591. [https://doi.org/10.1016/S0039-6028\(96\)01452-5](https://doi.org/10.1016/S0039-6028(96)01452-5)
- Cascio C, Geiss O, Franchini F, et al (2015) Detection, quantification and derivation of number size distribution of silver nanoparticles in antimicrobial consumer products. *J Anal At Spectrom* 30:1255–1265. <https://doi.org/10.1039/c4ja00410h>
- Chang Y-N, Zhang M, Xia L, et al (2012) The Toxic Effects and Mechanisms of CuO and ZnO Nanoparticles. *Materials (Basel)* 5:2850–2871. <https://doi.org/10.3390/ma5122850>
- Chen S, Goode AE, Skepper JN, et al (2016) Avoiding artefacts during electron microscopy of silver nanomaterials exposed to biological environments. *J Microsc* 261:157–166. <https://doi.org/10.1111/jmi.12215>
- Cioffi N, Torsi L, Ditaranto N, et al (2005) Copper nanoparticle/polymer composites with antifungal and bacteriostatic properties. *Chem Mater* 17:5255–5262. <https://doi.org/10.1021/cm0505244>
- Clar JG, Li X, Impellitteri CA, et al (2016) Copper nanoparticle induced cytotoxicity to nitrifying bacteria in wastewater treatment: A mechanistic copper speciation study by X-ray absorption spectroscopy. *Environ Sci Technol* 50:9105–9113. <https://doi.org/10.1021/acs.est.6b01910>
- Cleveland D, Long SE, Pennington PL, et al (2012) Pilot estuarine mesocosm study on the environmental fate of Silver nanomaterials leached from consumer

- products. *Sci Total Environ* 421–422:267–272.
<https://doi.org/10.1016/j.scitotenv.2012.01.025>
- Contini C, Schneemilch M, Gaisford S, Quirke N (2018) Nanoparticle-membrane interactions. *J Exp Nanosci* 13:62–81.
<https://doi.org/10.1080/17458080.2017.1413253>
- Conway JR, Adeleye AS, Gardea-Torresdey J, Keller AA (2015) Aggregation, Dissolution, and Transformation of Copper Nanoparticles in Natural Waters. *Environ Sci Technol* 49:2749–2756. <https://doi.org/10.1021/es504918q>
- Costa-fernández JM, Menéndez-miranda M, Bouzas-ramos D, et al (2016) Trends in Analytical Chemistry Mass spectrometry for the characterization and quantification of engineered inorganic nanoparticles. *Trends Anal Chem* 84:139–148. <https://doi.org/10.1016/j.trac.2016.06.001>
- Database. NC for BIP Titanium dioxide | TiO₂ - PubChem.
<https://pubchem.ncbi.nlm.nih.gov/compound/Titanium-dioxide>. Accessed 19 Mar 2020a
- Database. NC for BIP Zinc oxide | ZnO - PubChem.
https://pubchem.ncbi.nlm.nih.gov/compound/zinc_oxide. Accessed 20 Mar 2020b
- Dhawan A, Sharma V (2010) Toxicity assessment of nanomaterials: Methods and challenges. *Anal. Bioanal. Chem.* 398:589–605
- Dien M A Cotta T W Jeffries BS (2003) MINI-REVIEW Bacteria engineered for fuel ethanol production: current status. *Appl Microbiol Biotechnol* 63:258–266.
<https://doi.org/10.1007/s00253-003-1444-y>
- Directorate-General for Research and Innovation (2013) Nanotechnology : the invisible giant tackling Europe’s future challenges
- Djurišić AB, Leung YH, Ng AMC, et al (2015) Toxicity of Metal Oxide Nanoparticles: Mechanisms, Characterization, and Avoiding Experimental Artefacts. *Small* 11:26–44. <https://doi.org/10.1002/sml.201303947>
- Docter D, Westmeier D, Markiewicz M, et al (2015) The nanoparticle biomolecule corona: lessons learned - challenge accepted? *Chem Soc Rev* 44:6094–6121.
<https://doi.org/10.1039/c5cs00217f>
- Donlan RM (2001) Biofilm Formation: A Clinically Relevant Microbiological

- Process. Clin Infect Dis 33:1387–1392. <https://doi.org/10.1086/322972>
- Durenkamp M, Pawlett M, Ritz K, et al (2016) Nanoparticles within WWTP sludges have minimal impact on leachate quality and soil microbial community structure and function. Environ Pollut 211:399–405. <https://doi.org/10.1016/j.envpol.2015.12.063>
- Eduok S, Hendry C, Ferguson R, et al (2015) Insights into the effect of mixed engineered nanoparticles on activated sludge performance. FEMS Microbiol Ecol 91:1–9. <https://doi.org/10.1093/femsec/fiv082>
- Fabrega J (2009) The impacts of silver nanoparticles on planktonic and biofilm bacteria
- Ferry JL, Craig P, Hexel C, et al (2009) Transfer of gold nanoparticles from the water column to the estuarine food web. Nat Nanotechnol. <https://doi.org/10.1038/NNANO.2009.157>
- Filipe V, Hawe A, Jiskoot W (2010) Critical evaluation of nanoparticle tracking analysis (NTA) by NanoSight for the measurement of nanoparticles and protein aggregates. Pharm Res 27:796–810. <https://doi.org/10.1007/s11095-010-0073-2>
- Francia V, Montizaan D, Salvati A, Ni * -A Salvati@rug (2020) Interactions at the cell membrane and pathways of internalization of nano-sized materials for nanomedicine. Beilstein J Nanotechnol 2020:338–353. <https://doi.org/10.3762/bjnano.11.25>
- Fujimori Y, Sato T, Hayata T, et al (2012) Novel antiviral characteristics of nanosized copper(i) iodide particles showing inactivation activity against 2009 pandemic H1N1 influenza virus. Appl Environ Microbiol 78:951–955. <https://doi.org/10.1128/AEM.06284-11>
- Gázquez MJ, Bolívar JP, Garcia-Tenorio R, Vaca F (2014) A Review of the Production Cycle of Titanium Dioxide Pigment. Mater Sci Appl 05:441–458. <https://doi.org/10.4236/msa.2014.57048>
- Gottschalk F, Scholz RW, Nowack B (2010) Probabilistic material flow modeling for assessing the environmental exposure to compounds: Methodology and an application to engineered nano-TiO₂ particles. Environ Model Softw 25:320–332. <https://doi.org/10.1016/j.envsoft.2009.08.011>
- Gottschalk F, Sonderer T, Scholz RW, Nowack B (2009) Modeled environmental

- concentrations of engineered nanomaterials (TiO₂, ZnO, Ag, CNT, fullerenes) for different regions. *Environ Sci Technol* 43:9216–9222.
<https://doi.org/10.1021/es9015553>
- Gottschalk F, Sun T, Nowack B (2013) Environmental concentrations of engineered nanomaterials: Review of modeling and analytical studies. *Environ Pollut* 181:287–300. <https://doi.org/10.1016/J.ENVPOL.2013.06.003>
- Grigore ME, Biscu ER, Holban AM, et al (2016) Methods of synthesis, properties and biomedical applications of CuO nanoparticles. *Pharmaceuticals* 9:1–14.
<https://doi.org/10.3390/ph9040075>
- Grillo R, Rosa AH, Fraceto LF (2015a) Engineered nanoparticles and organic matter: A review of the state-of-the-art. *Chemosphere* 119:608–619.
<https://doi.org/10.1016/j.chemosphere.2014.07.049>
- Grillo R, Rosa AH, Fraceto LF (2015b) Engineered nanoparticles and organic matter: A review of the state-of-the-art. *Chemosphere* 119:608–619.
<https://doi.org/10.1016/j.chemosphere.2014.07.049>
- Handy RD, Owen R, Valsami-Jones E (2008a) The ecotoxicology of nanoparticles and nanomaterials: Current status, knowledge gaps, challenges, and future needs. *Ecotoxicology* 17:315–325
- Handy RD, Von Der Kammer F, Lead JR, et al (2008b) The ecotoxicology and chemistry of manufactured nanoparticles. *Ecotoxicology* 17:287–314
- Hao L, Chen L, Hao J, Zhong N (2013) Bioaccumulation and sub-acute toxicity of zinc oxide nanoparticles in juvenile carp (*Cyprinus carpio*): A comparative study with its bulk counterparts. *Ecotoxicol Environ Saf* 91:52–60.
<https://doi.org/10.1016/j.ecoenv.2013.01.007>
- Harding T, Jungblut AD, Lovejoy C, Vincent WF (2011) Microbes in high arctic snow and implications for the cold biosphere. *Appl Environ Microbiol* 77:3234–3243. <https://doi.org/10.1128/AEM.02611-10>
- Hartmann NB, Skjolding LM, Foss S, et al (2014) Title: Environmental fate and behaviour of nanomaterials
- Hou J, You G, Xu Y, et al (2016) Impacts of CuO nanoparticles on nitrogen removal in sequencing batch biofilm reactors after short-term and long-term exposure and the functions of natural organic matter. *Environ Sci Pollut Res* 23:22116–

22125. <https://doi.org/10.1007/s11356-016-7281-1>

- Hsiao IL, Hsieh YK, Wang CF, et al (2015) Trojan-horse mechanism in the cellular uptake of silver nanoparticles verified by direct intra- and extracellular silver speciation analysis. *Environ Sci Technol* 49:3813–3821.
<https://doi.org/10.1021/es504705p>
- Huang Z, Zheng X, Yan D, et al (2008) Toxicological effect of ZnO nanoparticles based on bacteria. *Langmuir* 24:4140–4144. <https://doi.org/10.1021/la7035949>
- Huangfu X, Xu Y, Liu C, et al (2019) A review on the interactions between engineered nanoparticles with extracellular and intracellular polymeric substances from wastewater treatment aggregates. *Chemosphere* 219:766–783.
<https://doi.org/10.1016/j.chemosphere.2018.12.044>
- Ikuma K, Decho AW, Lau BLT (2015) When nanoparticles meet biofilms - Interactions guiding the environmental fate and accumulation of nanoparticles. *Front Microbiol* 6:1–6. <https://doi.org/10.3389/fmicb.2015.00591>
- Jadhav S, Gaikwad S, Nimse M, Rajbhoj A (2011) Copper Oxide Nanoparticles: Synthesis, Characterization and Their Antibacterial Activity. *J Clust Sci* 22:121–129. <https://doi.org/10.1007/s10876-011-0349-7>
- Jahan S, Yusoff I Bin, Alias YB, Bakar AFBA (2017) Reviews of the toxicity behavior of five potential engineered nanomaterials (ENMs) into the aquatic ecosystem. *Toxicol Reports* 4:211–220.
<https://doi.org/10.1016/j.toxrep.2017.04.001>
- Jefferson KK (2004) What drives bacteria to produce a biofilm? *FEMS Microbiol Lett* 236:163–173. <https://doi.org/10.1016/j.femsle.2004.06.005>
- Jiang J, Oberdörster G, Biswas P (2009) Characterization of size, surface charge, and agglomeration state of nanoparticle dispersions for toxicological studies. *J Nanoparticle Res* 11:77–89. <https://doi.org/10.1007/s11051-008-9446-4>
- Jo HJ, Choi JW, Lee SH, Hong SW (2012) Acute toxicity of Ag and CuO nanoparticle suspensions against *Daphnia magna*: The importance of their dissolved fraction varying with preparation methods. *J Hazard Mater* 227–228:301–308. <https://doi.org/10.1016/j.jhazmat.2012.05.066>
- Joo SH, Aggarwal S (2018) Factors impacting the interactions of engineered nanoparticles with bacterial cells and biofilms: Mechanistic insights and state of

- knowledge. *J Environ Manage* 225:62–74.
<https://doi.org/10.1016/j.jenvman.2018.07.084>
- Jose GP, Santra S, Mandal SK, Sengupta TK (2011) Singlet oxygen mediated DNA degradation by copper nanoparticles: Potential towards cytotoxic effect on cancer cells. *J Nanobiotechnology* 9:9. <https://doi.org/10.1186/1477-3155-9-9>
- Joseph V, Engelbrekt C, Zhang J, et al (2012) Characterizing the Kinetics of Nanoparticle-Catalyzed Reactions by Surface-Enhanced Raman Scattering. *Angew Chemie Int Ed* 51:7592–7596. <https://doi.org/10.1002/anie.201203526>
- Kiser MA, Westerhoff P, Benn T, et al (2009) Titanium nanomaterial removal and release from wastewater treatment plants. *Environ Sci Technol* 43:6757–6763. <https://doi.org/10.1021/es901102n>
- Kumar A, Alam A, Rani M, et al (2017) Biofilms: Survival and defense strategy for pathogens. *Int. J. Med. Microbiol.* 307:481–489
- Laborda F, Bolea E, Cepriá G, et al (2016) Detection, characterization and quantification of inorganic engineered nanomaterials: A review of techniques and methodological approaches for the analysis of complex samples. *Anal Chim Acta* 904:10–32. <https://doi.org/10.1016/j.aca.2015.11.008>
- Lamsal RP, Jerkiewicz G, Beauchemin D (2018) Improving accuracy in single particle inductively coupled plasma mass spectrometry based on conventional standard solution calibration. *Microchem J* 137:485–489. <https://doi.org/10.1016/j.microc.2017.12.015>
- Lead JR, Wilkinson KJ (2006) Aquatic colloids and nanoparticles: Current knowledge and future trends. *Environ. Chem.* 3:159–171
- Lee B, Duong CN, Cho J, et al (2012) Toxicity of Citrate-Capped Silver Nanoparticles in Common Carp (*Cyprinus carpio*). *J Biomed Biotechnol* 2012:262670. <https://doi.org/10.1155/2012/262670>
- Liang Z, Das A, Hu Z (2010) Bacterial response to a shock load of nanosilver in an activated sludge treatment system. *Water Res* 44:5432–5438. <https://doi.org/10.1016/j.watres.2010.06.060>
- Lin PC, Lin S, Wang PC, Sridhar R (2014) Techniques for physicochemical characterization of nanomaterials. *Biotechnol. Adv.*
- Linhua H, Wang Z, Baoshan X (2009) Effect of sub-acute exposure to TiO₂

- nanoparticles on oxidative stress and histopathological changes in Juvenile Carp (Cyprinus carpio). *J Environ Sci* 21:1459–1466. [https://doi.org/10.1016/S1001-0742\(08\)62440-7](https://doi.org/10.1016/S1001-0742(08)62440-7)
- Liu J, Fan D, Wang L, et al (2014) Effects of ZnO, CuO, Au, and TiO₂ nanoparticles on *Daphnia magna* and early life stages of zebrafish *danio rerio*. *Environ Prot Eng* 40:139–149. <https://doi.org/10.5277/epe140111>
- Liu L, Bilal M, Duan X, Iqbal HMN (2019) Mitigation of environmental pollution by genetically engineered bacteria — Current challenges and future perspectives. *Sci. Total Environ.* 667:444–454
- Lomer MCE, Thompson RPH, Commisso J, et al (2000) Determination of titanium dioxide in foods using inductively coupled plasma optical emission spectrometry. *Analyst* 125:2339–2343. <https://doi.org/10.1039/b006285p>
- Loosli F, Le Coustumer P, Stoll S (2015a) Impact of alginate concentration on the stability of agglomerates made of TiO₂ engineered nanoparticles: Water hardness and pH effects. *J Nanoparticle Res* 17:1–9. <https://doi.org/10.1007/s11051-015-2863-2>
- Loosli F, Omar FM, Carnal F, et al (2014) Manufactured nanoparticle behavior and transformations in aquatic systems. Importance of natural organic matter. *Chimia (Aarau)* 68:783–787. <https://doi.org/10.2533/chimia.2014.783>
- Loosli F, Vitorazi L, Berret JF, Stoll S (2015b) Towards a better understanding on agglomeration mechanisms and thermodynamic properties of TiO₂ nanoparticles interacting with natural organic matter. *Water Res* 80:139–148. <https://doi.org/10.1016/j.watres.2015.05.009>
- López-moreno ML, Cede Y, Bailón-ruiz SJ, et al (2018) Environmental behavior of coated NMs : Physicochemical aspects and plant interactions. 347:196–217. <https://doi.org/10.1016/j.jhazmat.2017.12.058>
- Lowry G V, Gregory KB, Apte SC, Lead JR (2012) Transformations of Nanomaterials in the Environment. <https://doi.org/10.1021/es300839e>
- Ma H, Williams PL, Diamond SA (2013a) Ecotoxicity of manufactured ZnO nanoparticles - A review. *Environ Pollut* 172:76–85. <https://doi.org/10.1016/j.envpol.2012.08.011>
- Ma R, Levard C, Michel FM, et al (2013b) Sulfidation mechanism for zinc oxide

- nanoparticles and the effect of sulfidation on their solubility. *Environ Sci Technol* 47:2527–2534. <https://doi.org/10.1021/es3035347>
- Malvern Panalytical Isoelectric point of nanomaterials. <https://www.materials-talks.com/blog/2017/07/27/isoelectric-points-of-nanomaterials-qa/>. Accessed 26 Mar 2020
- Manusadzianas L, Caillet C, Fachetti L, et al (2012) Toxicity of copper oxide nanoparticle suspensions to aquatic biota. *Environ Toxicol Chem* 31:108–114. <https://doi.org/10.1002/etc.715>
- Mavrocordatos D, Pronk W, Boller M (2004) Analysis of environmental particles by atomic force microscopy, scanning and transmission electron microscopy. *Water Sci Technol* 50:9–18. <https://doi.org/10.2166/wst.2004.0690>
- Mchale JM, Auroux A, Perrotta AJ, et al (1997) Surface Energies and Thermodynamic Phase Stability in Nanocrystalline Aluminas
- Mehrabi K, Gundlach-Graham A, Günther D, Gundlach-Graham A (2019) Single-particle ICP-TOFMS with online microdroplet calibration for the simultaneous quantification of diverse nanoparticles in complex matrices. *Environ Sci Nano* 6:3349–3358. <https://doi.org/10.1039/c9en00620f>
- Melegari SP, Perreault F, Costa RHR, et al (2013) Evaluation of toxicity and oxidative stress induced by copper oxide nanoparticles in the green alga *Chlamydomonas reinhardtii*. *Aquat Toxicol* 142–143:431–440. <https://doi.org/10.1016/j.aquatox.2013.09.015>
- Merino N, Aronson HS, Bojanova DP, et al (2019) Living at the extremes: Extremophiles and the limits of life in a planetary context. *Front Microbiol* 10:780. <https://doi.org/10.3389/fmicb.2019.00780>
- Metreveli G, Philippe A, Schaumann GE (2015) Disaggregation of silver nanoparticle homoaggregates in a river water matrix. *Sci Total Environ* 535:35–44. <https://doi.org/10.1016/j.scitotenv.2014.11.058>
- Miao A-J, Luo Z, Chen C-S, et al (2010) Intracellular Uptake: A Possible Mechanism for Silver Engineered Nanoparticle Toxicity to a Freshwater Alga *Ochromonas danica*. *PLoS One* 5:e15196. <https://doi.org/10.1371/journal.pone.0015196>
- Misra SK, Dybowska A, Berhanu D, et al (2012) Science of the Total Environment

- The complexity of nanoparticle dissolution and its importance in nanotoxicological studies. *Sci Total Environ* 438:225–232.
<https://doi.org/10.1016/j.scitotenv.2012.08.066>
- Mitra A, Mukhopadhyay S (2016) Biofilm mediated decontamination of pollutants from the environment. *AIMS Bioeng* 3:44–59.
<https://doi.org/10.3934/bioeng.2016.1.44>
- Montaño MD, Lowry G V., Von Der Kammer F, et al (2014) Current status and future direction for examining engineered nanoparticles in natural systems. *Environ Chem* 11:351–366. <https://doi.org/10.1071/EN14037>
- Moore MN (2006) Do nanoparticles present ecotoxicological risks for the health of the aquatic environment? *Environ Int* 32:967–976.
<https://doi.org/10.1016/j.envint.2006.06.014>
- Moriarty P (2001) Nanostructured materials. *Reports Prog Phys* 64:297.
<https://doi.org/10.1088/0034-4885/64/3/201>
- Mostowtt T, Munoz J, McCord B (2019) An evaluation of monovalent, divalent, and trivalent cations as aggregating agents for surface enhanced Raman spectroscopy (SERS) analysis of synthetic cannabinoids. *Analyst* 144:6404–6414. <https://doi.org/10.1039/c9an01309a>
- Mourdikoudis S, Pallares RM, Thanh NTK (2018) Characterization techniques for nanoparticles: Comparison and complementarity upon studying nanoparticle properties. *Nanoscale* 10:12871–12934
- Mueller NC, Nowack B (2008) Exposure modelling of engineered nanoparticles in the environment. *Environ Sci Technol* 42:44447–53.
<https://doi.org/10.1021/es7029637>
- Musee N (2011) Nanowastes and the environment: Potential new waste management paradigm. *Environ Int* 37:112–128. <https://doi.org/10.1016/j.envint.2010.08.005>
- Naasz S, Altenburger R, Kühnel D (2018) Environmental mixtures of nanomaterials and chemicals: The Trojan-horse phenomenon and its relevance for ecotoxicity. *Sci. Total Environ.* 635:1170–1181
- National Center for Biotechnology Information. PubChem Database Copper(II) oxide | CuO - PubChem.
<https://pubchem.ncbi.nlm.nih.gov/compound/14829#section=Computed->

Properties. Accessed 19 Mar 2020

- Nowack B (2017) Evaluation of environmental exposure models for engineered nanomaterials in a regulatory context. *NanoImpact* 8:38–47.
<https://doi.org/10.1016/j.impact.2017.06.005>
- Nowack B, Bucheli TD (2007) Occurrence, behavior and effects of nanoparticles in the environment. *Environ. Pollut.* 150:5–22
- Ostaszewska T, Śliwiński J, Kamaszewski M, et al (2018) Cytotoxicity of silver and copper nanoparticles on rainbow trout (*Oncorhynchus mykiss*) hepatocytes. *Environ Sci Pollut Res* 25:908–915. <https://doi.org/10.1007/s11356-017-0494-0>
- Pacchionia G, Ferrari AM, Bagus PS (1996) Cluster and band structure ab initio calculations on the adsorption of CO on acid sites of the TiO₂(110) surface. *Surf Sci* 350:159–175. [https://doi.org/10.1016/0039-6028\(95\)01057-2](https://doi.org/10.1016/0039-6028(95)01057-2)
- Park DM, Brewer A, Reed DW, et al (2017) Recovery of Rare Earth Elements from Low-Grade Feedstock Leachates Using Engineered Bacteria. *Environ Sci Technol* 51:13471–13480. <https://doi.org/10.1021/acs.est.7b02414>
- Peralta-Videa JR, Zhao L, Lopez-Moreno ML, et al (2011) Nanomaterials and the environment: A review for the biennium 2008-2010. *J. Hazard. Mater.* 186:1–15
- Peters RJB, van Bommel G, Milani NBL, et al (2018) Detection of nanoparticles in Dutch surface waters. *Sci Total Environ* 621:210–218.
<https://doi.org/10.1016/j.scitotenv.2017.11.238>
- Petrova OE, Sauer K (2016) Escaping the biofilm in more than one way: Desorption, detachment or dispersion. *Curr. Opin. Microbiol.* 30:67–78
- Peulen TO, Wilkinson KJ (2011) Diffusion of nanoparticles in a biofilm. *Environ Sci Technol* 45:3367–3373. <https://doi.org/10.1021/es103450g>
- Piñero-Lambea C, Ruano-Gallego D, Fernández LÁ (2015) Engineered bacteria as therapeutic agents. *Curr. Opin. Biotechnol.* 35:94–102
- Pino P Del, Pelaz B, Zhang Q, et al (2014) Protein corona formation around nanoparticles - From the past to the future. *Mater. Horizons* 1:301–313
- Polesel F, Farkas J, Kjos M, et al (2018) Occurrence, characterisation and fate of (nano)particulate Ti and Ag in two Norwegian wastewater treatment plants. *Water Res* 141:19–31. <https://doi.org/10.1016/j.watres.2018.04.065>
- Rabin N, Zheng Y, Opoku-Temeng C, et al (2015) Biofilm formation mechanisms

- and targets for developing antibiofilm agents. *Future Med Chem* 7:493–512.
<https://doi.org/10.4155/fmc.15.6>
- Ramyadevi J, Jeyasubramanian K, Marikani A, et al (2011) Copper nanoparticles synthesized by polyol process used to control hematophagous parasites. *Parasitol Res* 109:1403–1415. <https://doi.org/10.1007/s00436-011-2387-3>
- Redmile-Gordon M, Chen L (2017) Zinc toxicity stimulates microbial production of extracellular polymers in a copiotrophic acid soil. *Int Biodeterior Biodegrad* 119:413–418. <https://doi.org/10.1016/j.ibiod.2016.10.004>
- Ren G, Hu D, Cheng EWC, et al (2009) Characterisation of copper oxide nanoparticles for antimicrobial applications. *Int J Antimicrob Agents* 33:587–590. <https://doi.org/10.1016/j.ijantimicag.2008.12.004>
- Renzi M, Blašković A (2019) Ecotoxicity of nano-metal oxides: A case study on daphnia magna. *Ecotoxicology* 28:878–889. <https://doi.org/10.1007/s10646-019-02085-3>
- Roco MC (2003) Broader societal issues of nanotechnology. *J. Nanoparticle Res.* 5:181–189
- Rodriguez JA (2002) Orbital-band interactions and the reactivity of molecules on oxide surfaces: From explanations to predictions. *Theor. Chem. Acc.* 107:117–129
- Rodriguez JA, Chaturvedi S, Kuhn M, Hrbek J (1998) Reaction of H₂S and S₂ with metal/oxide surfaces: Band-gap size and chemical reactivity. *J Phys Chem B* 102:5511–5519. <https://doi.org/10.1021/jp9815208>
- Roeselers G, Loosdrecht MCMV, Muyzer G (2008) Phototrophic biofilms and their potential applications. *J. Appl. Phycol.* 20:227–235
- Sabella S, Carney RP, Brunetti V, et al (2014) A general mechanism for intracellular toxicity of metal-containing nanoparticles. *Nanoscale* 6:7052–7061.
<https://doi.org/10.1039/c4nr01234h>
- Salata O (2004) Applications of nanoparticles in biology and medicine. *J Nanobiotechnology* 2:3. <https://doi.org/10.1186/1477-3155-2-3>
- Saleh NB, Chambers B, Aich N, et al (2015) Mechanistic lessons learned from studies of planktonic bacteria with metallic nanomaterials: implications for interactions between nanomaterials and biofilm bacteria. *Front Microbiol* 6:677.

- <https://doi.org/10.3389/fmicb.2015.00677>
- Samsonov V, Bazulev A, Sdobnyakov N (2006) On applicability of Gibbs thermodynamics to nanoparticles. *Open Phys* 1:474–484.
<https://doi.org/10.2478/bf02475858>
- Santos CSC, Gabriel B, Blanchy M, et al (2015) Industrial Applications of Nanoparticles - A Prospective Overview. In: *Materials Today: Proceedings*. Elsevier Ltd, pp 456–465
- Savolainen K, Alenius H, Norppa H, et al (2010) Risk assessment of engineered nanomaterials and nanotechnologies-A review. *Toxicology* 269:92–104
- Schiavo S, Oliviero M, Miglietta M, et al (2016) Genotoxic and cytotoxic effects of ZnO nanoparticles for *Dunaliella tertiolecta* and comparison with SiO₂ and TiO₂ effects at population growth inhibition levels. *Sci Total Environ* 550:619–627. <https://doi.org/10.1016/j.scitotenv.2016.01.135>
- Schmidt J, Vogelsberger W (2006) Dissolution kinetics of titanium dioxide nanoparticles: The observation of an unusual kinetic size effect. *J Phys Chem B* 110:3955–3963. <https://doi.org/10.1021/jp0553611>
- Schrand AM, Rahman MF, Hussain SM, et al (2010) Metal-based nanoparticles and their toxicity assessment. *Wiley Interdiscip Rev Nanomedicine Nanobiotechnology* 2:544–568. <https://doi.org/10.1002/wnan.103>
- Siripattanakul-Ratpukdi S, Ploychankul C, Limpiyakorn T, et al (2014) Mitigation of nitrification inhibition by silver nanoparticles using cell entrapment technique. *J Nanoparticle Res* 16:. <https://doi.org/10.1007/s11051-013-2218-9>
- Srivastava V, Gusain D, Sharma YC (2015) Critical Review on the Toxicity of Some Widely Used Engineered Nanoparticles. *Ind Eng Chem Res* 54:6209–6233.
<https://doi.org/10.1021/acs.iecr.5b01610>
- Stark WJ, Stoessel PR, Wohlleben W, Hafner A (2015) Industrial applications of nanoparticles. *Chem Soc Rev* 44:5793–5805.
<https://doi.org/10.1039/c4cs00362d>
- Stewart PS, Costerton JW (2001) Antibiotic resistance of bacteria in biofilms. *Lancet* 358:135–138
- Sun H, Zhang X, Niu Q, et al (2007) Enhanced accumulation of arsenate in carp in the presence of titanium dioxide nanoparticles. *Water Air Soil Pollut* 178:245–

254. <https://doi.org/10.1007/s11270-006-9194-y>
- Suri S, Ruan G, Winter J, Schmidt CE (2013) Microparticles and Nanoparticles. In: Biomaterials Science: An Introduction to Materials: Third Edition. Elsevier Inc., pp 360–388
- Tang J, Wu Y, Esquivel-Elizondo S, et al (2018) How Microbial Aggregates Protect against Nanoparticle Toxicity. *Trends Biotechnol* 36:1171–1182. <https://doi.org/10.1016/j.tibtech.2018.06.009>
- Tao X, Fortner JD, Zhang B, et al (2009) Effects of aqueous stable fullerene nanocrystals (nC60) on *Daphnia magna*: Evaluation of sub-lethal reproductive responses and accumulation. *Chemosphere* 77:1482–1487. <https://doi.org/10.1016/j.chemosphere.2009.10.027>
- Theron J, Walker JA, Cloete TE (2008) Nanotechnology and water treatment: Applications and emerging opportunities. *Crit. Rev. Microbiol.* 34:43–69
- Tsoligkas AN, Winn M, Bowen J, et al (2011) Engineering Biofilms for Biocatalysis. *ChemBioChem* 12:1391–1395. <https://doi.org/10.1002/cbic.201100200>
- Vidojkovic S, Rodriguez-Santiago V, Fedkin M V., et al (2011) Electrophoretic mobility of magnetite particles in high temperature water. *Chem Eng Sci* 66:4029–4035. <https://doi.org/10.1016/j.ces.2011.05.021>
- Vimbela G V., Ngo SM, Fraze C, et al (2017) Antibacterial properties and toxicity from metallic nanomaterials. *Int. J. Nanomedicine* 12:3941–3965
- Wagner S, Gondikas A, Neubauer E, et al (2014) Spot the Difference: Engineered and Natural Nanoparticles in the Environment-Release, Behavior, and Fate. *Angew Chemie Int Ed* 53:n/a-n/a. <https://doi.org/10.1002/anie.201405050>
- Wang LS, Gupta A, Rotello VM (2016a) Nanomaterials for the Treatment of Bacterial Biofilms. *ACS Infect Dis* 2:3–4. <https://doi.org/10.1021/acsinfecdis.5b00116>
- Wang Y, Zhu X, Lao Y, et al (2016b) TiO₂ nanoparticles in the marine environment: Physical effects responsible for the toxicity on algae *Phaeodactylum tricorutum*. *Sci Total Environ* 565:818–826. <https://doi.org/10.1016/j.scitotenv.2016.03.164>
- Wang ZL (2004) Zinc oxide nanostructures: Growth, properties and applications. *J Phys Condens Matter* 16:829–858. <https://doi.org/10.1088/0953->

- Weir A, Westerhoff P, Fabricius L, et al (2012) Titanium dioxide nanoparticles in food and personal care products. *Environ Sci Technol* 46:2242–2250. <https://doi.org/10.1021/es204168d>
- Westerhoff P, Song G, Hristovski K, Kiser MA (2011) Occurrence and removal of titanium at full scale wastewater treatment plants: implications for TiO₂ nanomaterials. *J Environ Monit* 13:1195–1203. <https://doi.org/10.1039/c1em10017c>
- Wiesner MR, Lowry G V., Alvarez P, et al (2006) Assessing the risks of manufactured nanomaterials. *Environ. Sci. Technol.* 40:4336–4345
- Windler L, Lorenz C, Von Goetz N, et al (2012) Release of titanium dioxide from textiles during washing. *Environ Sci Technol* 46:8181–8188. <https://doi.org/10.1021/es301633b>
- Xiao Y, Vijver MG, Chen G, Peijnenburg WJGM (2015) Toxicity and accumulation of Cu and ZnO nanoparticles in daphnia magna. *Environ Sci Technol* 49:4657–4664. <https://doi.org/10.1021/acs.est.5b00538>
- Xiao Y, Wiesner MR (2013) Transport and retention of selected engineered nanoparticles by porous media in the presence of a biofilm. *Environ Sci Technol* 47:2246–2253. <https://doi.org/10.1021/es304501n>
- Zhang J, Guo W, Li Q, et al (2018) The effects and the potential mechanism of environmental transformation of metal nanoparticles on their toxicity in organisms. *Environ. Sci. Nano* 5:2482–2499
- Zhang L, Li J, Yang K, et al (2016) Physicochemical transformation and algal toxicity of engineered nanoparticles in surface water samples. *Environ Pollut* 211:132–140. <https://doi.org/10.1016/j.envpol.2015.12.041>
- Zhang M, Yang J, Cai Z, et al (2019) Detection of engineered nanoparticles in aquatic environments: Current status and challenges in enrichment, separation, and analysis. *Environ Sci Nano* 6:709–735. <https://doi.org/10.1039/c8en01086b>
- Zhao J, Wang Z, Liu X, et al (2011) Distribution of CuO nanoparticles in juvenile carp (*Cyprinus carpio*) and their potential toxicity. *J Hazard Mater* 197:304–310. <https://doi.org/10.1016/j.jhazmat.2011.09.094>
- Zhu X, Wang J, Zhang X, et al (2010) Trophic transfer of TiO₂ nanoparticles from

daphnia to zebrafish in a simplified freshwater food chain. *Chemosphere* 79:928–933. <https://doi.org/10.1016/j.chemosphere.2010.03.022>

Specific Programme “Cooperation”: Nanosciences, Nanotechnologies, Materials and new Production Technologies | Programme | FP7 | CORDIS | European Commission. <https://cordis.europa.eu/programme/id/FP7-NMP>. Accessed 19 Feb 2020a

About this Publication on Nanotechnologies.

https://ec.europa.eu/health/scientific_committees/opinions_layman/en/nanotechnologies/about-nanotechnologies.htm#7. Accessed 19 Feb 2020b

Welcome to The Nanodatabase. <http://nanodb.dk/en/>. Accessed 24 Mar 2020c

2 Materials and Methods

2.1 Introduction

This chapter describes the methods used to assess CuO, TiO₂ and ZnO behaviour and interaction in wastewater and their removal by biomass involved in conventional and emerging wastewater treatment.

The assessment of the NP removal by wastewater was performed with the use of two different bacterial community, one aerobic, conventional activated sludge biomass, and one anaerobic, called anaerobic granular sludge. These two biomasses are representative of conventional and emerging wastewater treatment technology.

To understand the fate and behaviour of CuO, TiO₂ and ZnO in wastewater, real biomass-free liquor was prepared by removing all the bacteria via filtration. The liquor obtained was representative of primary treated wastewater entering the secondary phase of a conventional WWTP, namely activated sludge treatment. These sets of experiments were designed to study the NP removal, without biomass, due to the water quality of the liquor. In addition, to further investigate the mechanisms involved in this removal process, CuO, TiO₂ and ZnO size distribution, Z-potential and dissolution in the liquor were evaluated.

NP and liquor characterization were performed with an array of techniques such as transmission electron microscopy (TEM), dynamic light scattering (DLS), ultrafiltration as well as a series of water quality analysis that include chemical oxygen demand (COD), total organic carbon (TOC), total suspended solid (TSS), total suspended solids (TDS), Electrical conductivity and pH.

A specific analytical method involving acid digestion (4% HNO₃ and 4% H₂SO₄) in 55 ml Teflon MARSXpress Vessels (CEM Corporation) inserted in a microwave assisted reaction system (MARS 5) and inductively coupled plasma – optical emission spectrometry (ICP-OES) analysis was developed and validated as key part of this work. Detailed procedures are discussed in chapter 3.

2.2 Biological experiments

2.2.1 Activated sludge collection and storage

Activated sludge was collected from a municipal sewage plant serving the urban area of Glasgow, UK. This conventional biological full-scale WWTP includes preliminary, primary and secondary treatments. The samples were taken from the aeration tank and brought back to the lab within one hour where they were aerated and equilibrated to room temperature of 22 ± 1 °C. The total volume of sample collected per collection was 5 L. Of this, 1 L was used for sample characterization which included measurement of:

Experiments were consistently performed with freshly harvested activated sludge biological samples within 24 hours from collection. Overnight storage was at time required and was done in a fridge at 4 °C. The following day, the samples were re-equilibrated to room temperature of 22 ± 1 °C for at least two hours. This was performed in a safety cabinet to prevent environmental cross-contamination and the sample were gently agitated with a magnetic stirrer. During preliminary experiments the two hours period was found to be the least waiting time for the samples to reach the desired 22 ± 1 °C. Achievement of the target temperature was confirmed by measuring the sample temperature prior to the beginning of the experiments.

2.2.2 Anaerobic granular sludge collection and storage

Samples of anaerobic granular sludge (AGS), with a diameter varying from 2 to 5 mm, were collected from a 485 m³ expanded granular sludge bed plant treating distillery wastewater in Edinburgh, UK.

All the biomass was collected in a single event where 20 L of anaerobic granular sludge were collected. The volume of original liquor was substituted with standard synthetic wastewater, prepared with peptone (160 mg), meat extract (110 mg), urea (30 mg), anhydrous dipotassium hydrogen phosphate (K_2HPO_4 , 28 mg), sodium chloride (NaCl, 7 mg), calcium chloride dehydrate ($CaCl_2 \cdot 2H_2O$, 4 mg) and magnesium sulphate heptahydrate ($Mg_2SO_4 \cdot 7H_2O$, 2 mg) dissolved in 1 L of tap water for a final expected dissolved organic content (DOC) of 100 mg/L and pH of 7.5 ± 0.5 (OECD 2001). Aliquots of AGS in synthetic wastewater (750 ml) were stored in

airtight bottles (1 L) at 4°C for maximum 6 weeks. The bottles were not full to prevent them from bursting due to gas production during the storage period and were flushed with nitrogen gas to remove the presence of oxygen and maintain an anaerobic environment.

The day prior to the experiments, 4 g of wet AGS were weighted and added in each 50 ml plastic tube. The biomass was then supplied with 27 ml of synthetic wastewater and allowed to reach room temperature overnight. All the vials were flushed with nitrogen gas after the addition of the biomass and synthetic wastewater to remove all the oxygen and maintain the anaerobic environment. After that each vials was capped and placed on a rotary shaker at 50 rpm maintain the mix gently agitated to keep AGS in suspension.

2.2.3 Samples characterization

Total suspended solid (TSS) was determined according to the standard methods (APHA/AWWA/WEF 2012), while chemical oxygen demand (COD) was measured with cuvette test (Hach, Manchester, UK). Electrical conductivity, temperature, pH and total dissolved solids were measured with a multi pH Meter (Mettler Toledo FE20, Switzerland). Elemental contents in activated sludge and biomass-free liquor were measured with ICP-OES. Similarly, Cu^{2+} , Ti^{4+} and Zn^{2+} were analyzed, and batches with background Cu^{2+} , Ti^{4+} and Zn^{2+} concentrations above 1% of the target experimental concentrations were not used. All the chemicals used were analytical grade.

2.2.4 Biological experiments execution

The following approach for test vial preparation was followed for all the experiments: 27 ml of biomass in liquor (for activated sludge experiments) or in synthetic wastewater (for AGS experiments) were spiked with 3 ml of NP suspension, creating a final volume of 30 ml. In single NP experiments all the 3 ml of NP suspension were collected from the same stock solution. The final target NP concentrations were 9, 90 and 180 mg/L per NP type.

In mixed NP systems, three separate stock solutions were prepared. Respectively 1 ml of each of the three NP suspensions was added to achieve a final volume of 30

ml and the desired concentration depending on the experimental design. Such experiments were run with all the three NPs spiked at the same concentration of 9, 90 and 180 mg/L per NP type (creating total NP concentrations of 27, 270 and 540 mg/L).

2.2.5 Nanoparticle removal by activated sludge experiments

The glass vials (experimental vessels) were first all filled with 27 ml of well agitated activated sludge. When all the vials received the activated sludge fraction, 3 ml of NP suspension(s) according to the type of experiment (single or mixture NP) were added and then agitated at 250 rpm on an orbital shaker to obtain a homogeneous distribution throughout the experiment. The final target NP concentrations were 9, 90 and 180 mg/L per NP type. Mixture NP experiments were conducted with all the three NPs spiked at the same concentration of 9, 90 and 180 mg/L per NP type (creating total NP concentrations of 27, 270 and 540 mg/L). The final TSS of activated sludge biomass was 2000 mg/L, representative of a conventionally operated activated sludge treatment.

Specific agitation times, similarly to Kiser *et al.*, 2010, varying from 5 to 180 min were applied. After agitation the vials were removed from the shaker and the biomass was allowed to settle by gravity for 20 min. Afterwards, 14 ml of supernatant (effluent) were carefully collected, to avoid extraction of biomass, and acidified with two drops of concentrated HNO₃ (69%).

2.2.6 Nanoparticle removal by anaerobic granular sludge biomass

The day prior to the experiments, 4 g of wet AGS were weighted and added in each 50 ml plastic tube. The biomass was then supplied with 27 ml of synthetic wastewater and allowed to reach room temperature overnight. All the vials were flushed with nitrogen gas after the addition of the biomass and synthetic wastewater to remove all the oxygen and maintain the anaerobic environment. After that each vial was capped and placed on a rotary shaker at 50 rpm maintain the mix gently agitated to keep AGS in suspension.

On the day of the experiment 3 ml of NP suspension were added for single NP removal studies (to reach final NP concentrations of 9, 90 and 180 mg/l). This produced a final total suspended solid (TSS) value equal to 14667 ± 333 mg/L in both

single and mixed NP systems, representative of a conventionally anaerobic granular sludge treatment. The experimental vessels containing biomass, synthetic wastewater and NPs were then agitated at 50 rpm on a rotary shaker to maintain the mix gently agitated to ensure the AGS remain in suspension throughout the duration of the experiment, yet intact. In mixed NP systems, three separate stock solutions were prepared as for single NP experiments. The experimental vessels containing 27 ml of synthetic wastewater, 4 g of wet AGS biomass were then spiked with 1 ml of each of the three NP suspensions to achieve a final volume of 30 ml. All the three NPs were added at the same concentration of 9, 90 and 180 mg/L per NP type (creating total NP concentrations of 27, 270 and 540 mg of NPs/L). The vials were quickly re-flushed with nitrogen gas, capped and re-placed on the rotary shaker. Specific agitation times varied from a minimum of 5 min to a maximum of 360 min. After agitation the vials were removed from the shaker and the biomass was allowed to settle by gravity for 20 min. Afterwards, 14 ml of supernatant (simulated effluent) were carefully collected, to avoid extraction of biomass, and acidified with two drops of concentrated HNO₃ (69%) and stored at 4 °C prior to NP quantification.

2.2.7 Experimental differences

The two types of biological experiments were overall prepared and executed in a overall very similar way, however they still present some differences.

The preparation method for activated sludge experiments included pipetting of well mixed sample collected from the WTW, whereas AGS biomass was added via a fix weight followed by addition of synthetic wastewater. This was done for practical reasons. Collecting a constant and similar sample of AGS biomass suspended in liquid would have been nearly impossible to achieve. AGS do not suffer if removed from suspension for a short period of time, whereas activated sludge would. This would inevitably add a significant impact on the vitality of the biomass.

The final TSS for activated sludge was 2000 mg/L, whereas for AGS experiments it was 14667 ± 333 mg/L. The difference arises from the way the two types of treatments are generally operated, and both these conditions are representative of the operational mode of the two wastewater treatments from where the samples were originally collected.

For the same reason, the two types of experiments had different duration. The aim of this PhD research was to assess the removal of NPs by the two types of biomasses used in conventional and emerging WTW technology on a worst-case scenario. This included extremely high concentrations of NPs and bottom limit for the hydraulic retention time (HRT), which for conventional WTW is 3 hours, whereas for AnWT is 6 hours.

In addition, AGS experiments were run in synthetic wastewater, where activated sludge ones were run in real wastewater liquor. This was done due to two reasons: difficulties in AGS samples collection. The plant was 90 min drive away and harvesting frequent samples would have proved hard to achieve. Moreover, that plant treats industrial wastewater (distillery wastewater), which is a much richer media in comparison to household sewage. By using synthetic wastewater, we were able to carry out a more representative assessment of an AGS based urban WTW. In addition the procedure used to prepare it (OECD 2001), produced a final synthetic wastewater representative of urban wastewater for the various water quality parameters of interest. But it also gave a slightly higher dissolved organic carbon content (91.4 ± 13.6 mg C/L) versus what was determined for the wastewater liquor we collected (7.71 ± 0.47 mg C/L) to minimize potential impact on the biology of the AGS biomass.

2.3 Biomass-free liquor NP removal experiments

Some experiments were undertaken in biomass-free liquor (i.e., the liquid fraction) and synthetic wastewater to determine non-biomass related NP removal processes. For tests carried out in biomass-free liquor, an aliquot of the well-mixed sampled activated sludge was filtered through glass microfiber filter (GF/F grade, Whatman Inc.) and then through a $0.45 \mu\text{m}$ acetate cellulose syringe filter (VWR international LLC) to obtain the biomass-free liquor. Such filters were selected instead of 2 nm filters. As the latter were subject to frequent blockages and ended up broken several times due to the abundant particulate present in the activated sludge samples. This practical reason, would have made experiment preparation extremely time consuming, but more importantly, increased dramatically the risk of microbial contamination of the biomass-free liquor. The liquor was then stored at 4°C for maximum 1 week.

Standard synthetic wastewater (OECD 2001) was prepared with peptone (160 mg), meat extract (110 mg), urea (30 mg), anhydrous dipotassium hydrogen phosphate (K_2HPO_4 , 28 mg), sodium chloride (NaCl, 7 mg), calcium chloride dehydrate ($CaCl_2 \cdot 2H_2O$, 4 mg) and magnesium sulphate heptahydrate ($Mg_2SO_4 \cdot 7H_2O$, 2 mg) dissolved in 1 L of tap water for a final expected dissolved organic content (DOC) of 100 mg/L and pH of 7.5 ± 0.5 (OECD 2001).

The two liquors were characterized as follows immediately after preparation: Chemical oxygen demand (COD) was measured with cuvette test (Hach, Manchester, UK). Electrical conductivity, temperature, pH and total dissolved solids were measured with a multi pH Meter (Mettler Toledo FE20, Switzerland). Elemental contents in activated sludge and biomass-free liquor were measured with ICP-OES. Similarly, Cu^{2+} , Ti^{4+} and Zn^{2+} were analyzed, and batches with background Cu^{2+} , Ti^{4+} and Zn^{2+} concentrations above 1% of the target experimental concentrations were not used. All the chemicals used were analytical grade.

The turbidity of the two solutions was visually checked daily as indicator of potential microbial growth. In addition, the water quality parameters determined immediately after preparation were re-tested after 2 and 5 days to determine potential change in the composition of the solutions as further indicator of microbiological contamination and were never stored for longer than 7 days. None of the solutions, either biomass-free liquor and synthetic wastewater, were even found developing turbidity or suffer change in water quality parameters within 7 days. During preliminary tests, we found that microbiological growth occurred in biomass-free liquor stored at room temperature after 26 days.

The NP removal by liquor only fraction (no sludge biomass present) experiments were conducted exactly as the test that investigated nanoparticle removal by activated sludge and anaerobic granular sludge experiments. In single NP type tests, the experimental vessels were first all filled with 27 ml of wastewater and then spiked with 3 ml of NP suspension. For mixture scenario, the 27 ml of liquor were spiked with 1 ml of the three separate NP stock suspensions. The final target NP concentrations were 9, 90 and 180 mg/L per NP type. Mixture NP experiments were conducted with all the three NPs spiked at the same concentration of 9, 90 and 180 mg/L per NP type (creating total NP concentrations of 27, 270 and 540 mg/L). Agitation time for biomass-free

liquor ranges from 5 to 180 min as per the activated sludge studies, whereas the contact time in synthetic wastewater ranged from 5 to 360 min as done for the AGS experiments. After agitation the vials were allowed to settle by gravity for 20 min. Afterwards, 14 ml of supernatant (simulated effluent) were carefully collected, to avoid extraction of biomass, and acidified with two drops of concentrated HNO₃ (69%) and stored at 4 °C prior to NP quantification.

2.4 Nanomaterials

TiO₂ nanopowder (anatase, particle size <25 nm, 99.7% purity, catalog number 637254) and ZnO suspension (20% wt in water, particle size <100 nm, catalog number 721077) were purchased from Sigma-Aldrich Corp, St. Louis, MO, USA. CuO nanopowder (particle size 30-50 nm, 99% purity, catalog number 44663) was obtained from Alfa Aesar (Heysham, Lancashire, UK).

2.5 Nanoparticle suspensions preparation

Freshly made suspensions were prepared before each experimental run. All the suspensions were prepared in ultrapure water with pH adjusted to 11 ± 1 with 0.1 M NaOH and sonicated for 15 minutes with an ultrasonic processor UP200St equipped with sonotrode S26d7 (Hielscher Ultrasonic GmbH, Teltow, Germany) with 70 W, amplitude 100% and frequency of 26 ± 1 kHz. NP suspensions were prepared at pH 11 ± 1 after assessment of Z-potential. At such pH all the nanomaterials had a Z-potential greater than -30 mV. This provides stability to the NP suspensions and hinders homoaggregation.

2.6 Nanoparticle characterization

2.6.1 Transmission electron microscopy

CuO, TiO₂ and ZnO primary size and elemental composition were studied via transmission electron microscopy (TEM). Samples were prepared by dispersing suspensions of 5000 mg/L in ultrapure water with pH adjusted to 11 ± 1 with 0.1 M NaOH and sonicating for 15 minutes, following by dropping a single drop onto a holey carbon film on a 200-mesh copper grid (Agar Scientific Ltd, Stansted, UK) and allowing it to dry. The size, shape and chemical composition of each nanoparticle type

was characterized with scanning transmission electron microscopy using a JEOL ARM200F (JEOL UK, Welwyn Garden City, UK) operated at 200 kV, and with a condenser aperture set to give a beam convergence angle of 29 mrad and gun lens setting to give a probe current of ~400 pA. Imaging was performed using high angle annular dark field mode, whilst elemental composition was studied using electron energy loss spectroscopy (EELS) with a Gatan GIF Quantum ER spectrometer (Gatan Inc., Pleasanton, CA) using a camera length and aperture combination that gives an acceptance angle of 36 mrad. The data was quantified using standard routines with Gatan Digital Micrograph (Gatan Inc., Pleasanton, CA). Comparisons to standard spectra from the EELS database (<https://eelsdb.eu/>) (Ewels et al. 2016) were used, where appropriate. Size distributions were measured using manual measurement of the length, l , and width, w , of > 200 nanoparticles in each sample using Digital Micrograph, followed by the determination of an average diameter (as $d = \sqrt{wl}$) and an average aspect ratio ($a = l/w$) for each system. The TEM relies on a high voltage electron beam emitted by an electron gun fitted with a tungsten filaments cathode as an electron source. The acceleration of the electron beam (40 -100 kV) is directed by electrostatic and electromagnetic lenses and guided towards the specimen in observation. When the electron beam hit the specimen a fraction of them will be scattered, and relative to the density of the sample. The electrons that go through the specimen (unscattered electrons) will hit a fluorescent viewing screen, coated with either phosphor or zinc sulphide. An image is produced, and the different darkness relates to the sample density and scattered electrons.

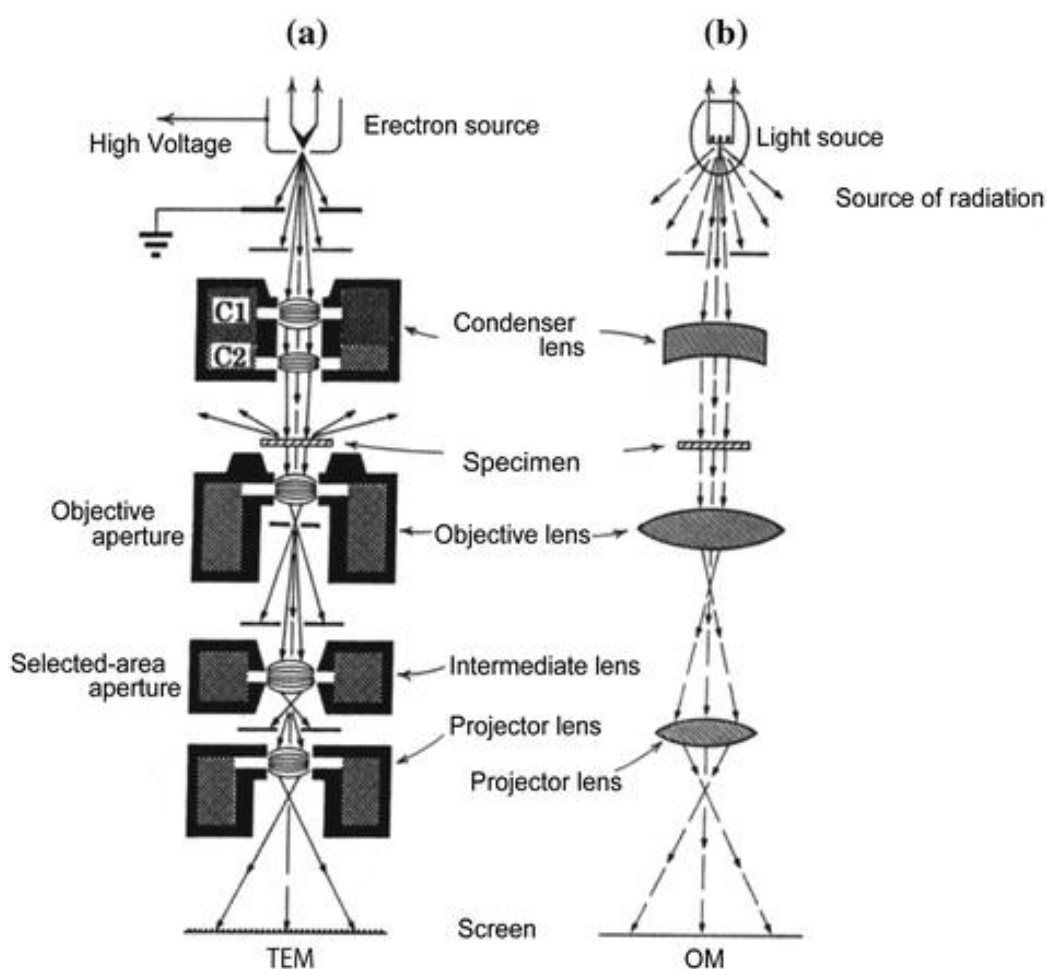


Fig. 2.1 Representation of a transmission electron microscopy (TEM) (Tanaka 2017)

The greatest challenge we encountered while doing TEM analysis of CuO, TiO₂ and ZnO suspensions was to find the concentrations that would give the best quality images. A set of NP suspensions at various concentrations (100, 1000, 3000, 5000 and 10.000 mg/L) was used during the preliminary investigations. As result of this work the 5000 mg/L stock solution was chosen as target concentration for TEM assessment. Suspensions at lower concentrations made identification of enough specimens (> 200) too difficult and time consuming. At higher concentrations (10.000 mg/L), nanoparticles were clustered and overlapping making identification of each NP unreliable as well the measurement of length (*l*) and width (*w*). The intermediate (5000 mg/L) concentration provided with a good density to easily observe the >200 nanoparticles required as well as accurately determine the physical dimensions of the observed specimens.

2.6.2 Dynamic light scattering

Dynamic light scattering (DLS), also known as photon correlation spectroscopy (PCS), is a widely used technique to characterize NP in suspensions. The two parameters that are studied to provide such determination are: size distribution in the form of hydrodynamic diameter (h_D) and particle charge (Z-potential) (Nobmann et al. 2007). The diffusion coefficient, and hence the hydrodynamic diameter calculated from it, depends on the size and shape of macromolecules (Stetefeld et al. 2016). When particles are hit by a monochromatic beam of laser light, the intensity of the scattered light varies at a rate that is dependent upon the diffusion coefficient (hydrodynamic diameter) (Ortega and García de la Torre 2007) of the particles (Stetefeld et al. 2016).

Zeta potential is a measure of the electric potential at the share plane which separates the stern and diffuse layer (Williams 2016). At this point the electric potential begins to decrease exponentially away from the NP surface (Fig. 2.2). This controls particle mobility and thus influence zeta potential of the particle (Vidojkovic et al. 2011).

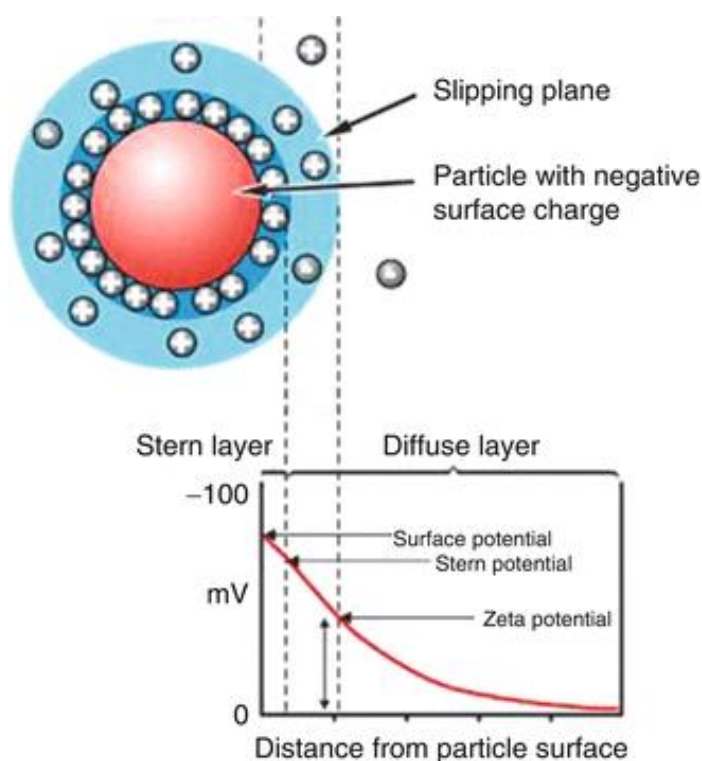


Fig. 2.2 Illustration of the electrical double layer (EDL) of a negatively charged nanoparticle. The EDL includes the stern layer as well the diffuse layer. The graph shows the Z-potentials (vertical axis) relative to the two layers and slipping planes as a function of the distance from the particle surface. Picture taken from (Williams 2016).

The charge at the slipping plane is highly dependent on the ionic strength and type of ions in suspension and size and shape of particle. Z-potential measures the magnitude of the repulsion between particles (Michael Schurr and Bloomfield 1977). Particles with a high Z-potential (either positive or negative, i.e $< -30\text{mV}$ and $> +30\text{mV}$) will repel each other. Hence, a high Z-potential will stabilize small particles and thus remain in suspension. For low Z-potential ($> -30\text{mV}$ and $< +30\text{mV}$) attraction due to van der Waals and other forces exceeds repulsion and will tend to aggregate (O'Brien and White 1978).

In practice, the zeta-potential is determined by measuring particle motion under an electric field. This is achieved through measurements of electrophoretic mobility via standard laser-velocimetry techniques (Lowry et al. 2016). This is then used to calculate the Z-potential via Henry's equation:

$$U_E = 2\varepsilon\zeta f(ka)/3\eta^{-1}$$

Where:

ε : Dielectric constant

ζ : Zeta potential

$f(ka)$: Henry's function

η : viscosity

In this work, the stability of CuO, TiO₂ and ZnO suspensions (100 mg/L) were studied by assessing the hydrodynamic diameter (h_D) and Z-potential as function of pH in ultrapure water and biomass free liquor at 25 °C by dynamic light scattering (DLS) with Zetasizer Nano ZSP (Malvern, UK) equipped with He-Ne laser 633nm light source and detection angle of 175° (back scatter). The pH of ultrapure water and biomass-free liquor were adjusted to a range varying from 3 to 12 with 0.1 M KOH and 0.1 M HCl prior to sonication. The NPs were then sonicated for 15 minutes and then agitated at 250 rpm for 30 minutes. Samples of properly mixed suspensions were collected with 2 ml syringes and immediately transferred in folded capillary zeta cells. For Z-potential evaluation, the Smoluchowski approximation model was used as most

often used for nanoparticles in aqueous media (Lowry et al. 2016). All the measurement of polydispersity index (PdI), an index used to estimate the average uniformity of nanoparticle suspensions, were below 0.76.

A limitation of this technique relates to the mode of data acquisition. Particle size distribution is based on the intensity of reflected light, which relates to the size of the particle. Thus, polydispersed solutions cannot be accurately measured with this technique. Hence it is necessary to ensure that NPs are properly dispersed to avoid the occurrence of false and polydispersed readings. We tested a range of NP concentrations, respectively 1, 10, 100, 1000, 3000, 5000 and 10.000 mg/L. A series of NP suspensions were tested, on which hydrodynamic diameter and Z-potential were measured. Determination of Z-potential was successful throughout the whole range of concentrations tested, whereas hydrodynamic diameter measurement were automatically rejected by the instrument software due to polydispersity index (>0.76) and identification of NP aggregation at concentration of 5000 and 10.000 mg/L. On the other end of the range tested, respectively 1 and 10 mg/L the measurement did not pass the software self-quality checks due to insufficient light being reflected by the NP present in the sample. This was frequently identified for 1 mg/L whereas it only occurred a few times for the 10 mg/L samples. However, given the constant and goodness and great similarity in the results of hydrodynamic diameter and Z-potential from the measurement at 100, 1000 and 3000 mg/L, the first one, 100 mg/L, was chosen as reference concentration to assess the stability of CuO, TiO₂ and ZnO suspensions.

2.6.3 Inductively coupled plasma – optical emission spectrometry

All the metal analysis performed in this work were carried out with an ICP-OES, iCAP 6200, Thermo Fisher scientific equipped with a quartz torch and glass spray mixing chamber (Standard glass cyclonic spray chamber), a ceramic nebulizer (PEEK Mira Mist Nebulizer).

NP quantification was done by measuring Cu²⁺, Ti⁴⁺ and Zn²⁺ as proxy and then the NP concentration was calculated. For such analysis, samples were acid digested (4% HNO₃ and 4% H₂SO₄) in 55 ml Teflon MARSXpress Vessels (CEM Corporation) inserted in a microwave assisted reaction system (MARS 5).

Samples of biomass free-liquor and synthetic wastewater were tested to identify the background levels of elements (Cu^{2+} , Ti^{4+} , Zn^{2+} , Al^{3+} , Ca^{2+} , Fe^{3+} , K^{4+} , Mg^{2+} and Na^+) with the purpose of characterizing the liquid media in which biomass-free NP removal experiments were run. These samples were acidified with a few drops of concentrated nitric acid (HNO_3).

Detailed procedures of the sample preparation, method development and validation for acid digestion and ICP-OES are thoroughly discussed in chapter 3.

2.6.4 Ultrafiltration

The dissolution of three nanomaterials under investigation in this work was assessed through the adoption of ultrafiltration and ICP-OES analysis.

It has been widely reported that either CuO and ZnO undergo dissolution in in many water matrices (Reed et al. 2012, Li et al. 2013) as well as wastewater (Lombi et al. 2012).. Contrarily, TiO_2 is a much more stable nanomaterial which is not subject to dissolution in water (Nohynek et al. 2007), and for this reason it was used to validate the ultrafiltration technique. For the validation purpose, three independent TiO_2 suspensions at concentration of 1, 10 and 100 mg/L were prepared. From these, three samples of 30 ml were collected from each stock suspension for a total of 9 samples. These were placed on an orbital shaker at 250 rpm for 24 hours (4 times the maximum length of contact time of the NP removal experiments). After this, the samples were centrifuged at 11,000x g for 30 min and then 9 ml of the supernatant were withdrawn and filtered using 0.2 μm acetate cellulose syringe filter (VWR international LLC). The filtrate then was treated as a NP sample and went through acid digestion (4% HNO_3 and 4% H_2SO_4) in 55 ml Teflon MARSXpress Vessels (CEM Corporation) inserted in a microwave assisted reaction system (MARS 5 and then analyzed with ICP-OES.

All the analysis of Ti^{4+} in the supernatant of the TiO_2 samples that went through the ultracentrifugation and acid digestion showed results below the *MQL*. The lack of titanium detection proves the goodness of the applied method. By nature, TiO_2 does not dissolve, hence the totality of the nanomaterial is expected to be in the form of suspended nanoparticles, which are subject to sedimentation at the centrifugal force applied here. On the contrary, free ions are not as they re dissolved elements. The non-

detectable concentrations of Ti^{4+} even after acid digestion (4% HNO_3 and 4% H_2SO_4) confirms that all the nanoparticles in the samples were centrifuged out of suspensions. Hence, this validates the goodness of the method to remove all the NPs from suspension, leaving only free ions in the supernatant originated from NP dissolution.

CuO and ZnO dissolution in biomass free-liquor was determined over a period of 3 hours in both single NP and mixtures systems. The same experimental set-up adopted to assess the NP removal was used, with the only difference that no sedimentation time was applied. The samples were centrifuged at 11,000x g for 30 min and then 9 ml of the supernatant were withdrawn and filtered using 0.2 μm acetate cellulose syringe filter (VWR international LLC) and the filtrate acidified with 2 drops of concentrated HNO_3 (69%) and then analyzed with ICP-OES.

2.7 Cleaning and sterilization

All the reusable glass and plasticware used in the experiments were firstly soaked in 10 folds diluted commercial bleach for at least 24 hours. Thereafter all the items were rinsed with water multiple times until bubbles disappeared. This was followed by a soaking period of at least 12 hours in 10% nitric acid (HNO_3) solution. Afterwards all the glass and plasticware were rinsed at least 5 times with deionized water.

2.8 Bibliography

- APHA/AWWA/WEF (2012) Standard Methods for the Examination of Water and Wastewater. Stand Methods 541. [https://doi.org/ISBN 9780875532356](https://doi.org/ISBN%209780875532356)
- Ewels P, Sikora T, Serin V, et al (2016) A Complete Overhaul of the Electron Energy-Loss Spectroscopy and X-Ray Absorption Spectroscopy Database : eelsdb . eu. 717–724. <https://doi.org/10.1017/S1431927616000179>
- Kiser MA, Ryu H, Jang H, et al (2010) Biosorption of nanoparticles to heterotrophic wastewater biomass. *Water Res* 44:4105–4114. <https://doi.org/10.1016/j.watres.2010.05.036>
- Li M, Lin D, Zhu L (2013) Effects of water chemistry on the dissolution of ZnO nanoparticles and their toxicity to *Escherichia coli*. *Environ Pollut* 173:97–102. <https://doi.org/10.1016/j.envpol.2012.10.026>
- Lombi E, Donner E, Tavakkoli E, et al (2012) Fate of zinc oxide nanoparticles during anaerobic digestion of wastewater and post-treatment processing of sewage sludge. *Environ Sci Technol* 46:9089–9096. <https://doi.org/10.1021/es301487s>
- Lowry G V., Hill RJ, Harper S, et al (2016) Guidance to improve the scientific value of zeta-potential measurements in nanoEHS. *Environ Sci Nano* 3:953–965. <https://doi.org/10.1039/C6EN00136J>
- Michael Schurr J, Bloomfield V (1977) Dynamic light scattering of biopolymers and biocolloid. *Crit Rev Biochem Mol Biol* 4:371–431. <https://doi.org/10.3109/10409237709105461>
- Nobbmann U, Connah M, Fish B, et al (2007) Dynamic light scattering as a relative tool for assessing the molecular integrity and stability of monoclonal antibodies. *Biotechnol Genet Eng Rev* 24:117–128. <https://doi.org/10.1080/02648725.2007.10648095>
- Nohynek GJ, Lademann J, Ribaud C, Roberts MS (2007) Grey Goo on the skin? Nanotechnology, cosmetic and sunscreen safety. *Crit. Rev. Toxicol.* 37
- O'Brien RW, White LR (1978) Electrophoretic mobility of a spherical colloidal particle. *J Chem Soc Faraday Trans 2 Mol Chem Phys* 74:1607–1626. <https://doi.org/10.1039/F29787401607>
- OECD (2001) Simulation Test - Aerobic Sewage Treatment: 303A: Activated Sludge

Units. OECD

- Ortega A, García de la Torre J (2007) Equivalent radii and ratios of radii from solution properties as indicators of macromolecular conformation, shape, and flexibility. *Biomacromolecules* 8:2464–2475.
<https://doi.org/10.1021/BM700473F>
- Reed RB, Ladner DA, Higgins CP, et al (2012) Solubility of nano-zinc oxide in environmentally and biologically important matrices. *Environ Toxicol Chem* 31:93–99. <https://doi.org/10.3346/jkms.2015.30.10.1496>
- Stetefeld J, McKenna SA, Patel TR (2016) Dynamic light scattering: a practical guide and applications in biomedical sciences. *Biophys Rev* 8:409.
<https://doi.org/10.1007/S12551-016-0218-6>
- Tanaka N (2017) Structure and Imaging of a Transmission Electron Microscope (TEM). *Electron Nano-Imaging* 17–28. https://doi.org/10.1007/978-4-431-56502-4_2
- Vidojkovic S, Rodriguez-Santiago V, Fedkin M V., et al (2011) Electrophoretic mobility of magnetite particles in high temperature water. *Chem Eng Sci* 66:4029–4035. <https://doi.org/10.1016/j.ces.2011.05.021>
- Williams PM (2016) Zeta Potential. *Encycl Membr* 2063–2064.
https://doi.org/10.1007/978-3-662-44324-8_612

Chapter 3

Assessment of the suitability of sample processing methods for quantification of NPs in wastewater samples

3.1 Summary

Copper oxide (CuO), titanium dioxide (TiO₂) and zinc oxide (ZnO) are among the most widely used nanoparticles (NPs) in commercially available products as well as in industrial applications. This leads to growing CuO, TiO₂ and ZnO mixture concentrations discharged into sewage network that eventually reach wastewater treatment plants. Hence, NPs have the potential to affect the environment but our understanding of the impact of a mixed NP system is still limited. To support research into the evaluation of NP mixture effects, it is imperative to develop robust, cost-effective and easy to use analytical methods to quantify NP mixtures in biological and environmental samples. Problematically, established standard methods for analysis of NP mixtures from such systems do not currently exist. Some attempts have been made, however the relative goodness of different methods have yet to be evaluated. This because such determination procedures involve the use of hydrofluoric acid (HF) or require complicated and time-consuming method development. This makes these analytical methods hard to be standardized and transferred to different scenarios. In this study we provide a detailed development and validation of a single analytical method to simultaneously quantify CuO, TiO₂ and ZnO in aqueous matrices without using HF and compared with other recovery methods. Microwave assisted acid digestion paired with inductively coupled plasma - optical emission spectrometry (ICP-OES) analysis is a combination of techniques that has the potential to quantify metal at ppb levels. Method quantification limit (*MQL*) were 0.005-0.01 ppm depending on the NP type. NPs samples with concentrations varying from 0.4 to 100 ppm, dispersed in ultrapure water and synthetic wastewater and digested in concentrated H₂SO₄ and HNO₃ showed trueness (expressed as metal recovery %) varying from 87.07 to 112.98 %. Precision (reported as relative standard deviation (RSD %)) varied from 0.79 to 15.84%. The results obtained highlight the robustness of this analytical method throughout a wide concentration range. The environmental matrix (synthetic wastewater) and the H₂SO₄ - HNO₃ mix used for the digestion did not have a negative impact on the determination of CuO, TiO₂ and ZnO mixture content.

3.2 Introduction

The growing and widespread utilization of nanomaterials is posing a greater risk due to the introduction of NPs in environmental and biological systems. Nanotechnology is a recent subject and has attracted attention for research and development in the last decades. However, parallel to its application, a greater compelling interest has drifted towards understanding the environmental impact of NPs. This encompasses the identification of NP presence and concentration in commercial products, their potential environmental release and consequent fate as well as NP effects on the exposed biosphere (Moore 2006). To develop understanding of NP behaviors in environmental systems requires the development of analytical techniques that can fit the purpose to provide adequate information through robust samples analysis (Mueller and Nowack 2008). Throughout the years more and more advanced analytical equipment and techniques have been adopted for qualitative and quantitative measurements of NPs. These include electron microscopy (EM) energy-dispersive X-ray spectroscopy (EDX), dynamic light scattering (DLS), gravimetric analysis, laser diffraction, field flow fractionation (FFF) and nanoparticles tracking analysis (NTA) (Quadros et al. 2013; Reed et al. 2014; Cascio et al. 2015; Mackevica et al. 2017; Rogers et al. 2018). These are examples of a combined approach where different techniques are used together to obtain proper NP determination. Inductively coupled plasma - optical emission spectrometry (ICP-OES) and inductively coupled plasma - mass spectrometry (ICP-MS) paired with acid digestion have gained major importance in NP detection and measurement. However, analysis of NP mixture with ICP-MS and ICP-OES have only recently been attempted. Furthermore, a standard method is currently lacking due to the complexity of NPs as analyte as well as because of the variety of different NP types. Nanomaterials have different chemical behavior and dissolve in different acids. For example, TiO_2 would only dissolve in either hydrofluoric acid (HF) or H_2SO_4 . CuO and ZnO are very prone to dissolution when in contact with inorganic acids, as well as AgNPs. However, AgNPs dissolve in HCl but this would lead to the formation of insoluble Ag-Cl compounds that would alter the analytical determination (Poitras et al. 2016). Therefore, the identification of the most appropriate acid mix for sample preparation depends on the NP type(s). This causes

difficulties in adopting analytical methods developed for a specific NP type to simultaneously determine more NP classes.

Research on environmental fate and behavior of NP mixtures has attracted far less attention than it should, given the fact that the most realistic condition under which NPs would be present in natural environment is as mixtures rather than a single NP type pollution. NP mixtures effects have focused on ecotoxicological studies including on single-strain bacteria (Yu et al. 2016), microbial community (Tong et al. 2015), microalgae (Liu et al. 2018), plants (Joško et al. 2017), invertebrates (Lu et al. 2017) and vertebrates (Hua et al. 2016). In contrast, there is a paucity in environmental research on NP mixture transport and fate in environmental and relevant engineered systems. Eduok et al. 2015 evaluated the biological effects and bulk removal of an AgNP, TiO₂ and ZnO mixture in a simulated WWTP. NP quantification was provided via acid digestion (in nitric acid, hydrogen peroxide and hydrofluoric acid) followed by ICP-AES measurement. HF is highly hazardous and not permitted in many laboratories. Furthermore, when using HF for elemental quantification via ICP-OES or ICP-AES, the analytical procedure needs to include a further step to neutralize HF with a basic compound to avoid deterioration of the instruments. This increases the time for sample preparation, costs and the volumes of chemicals required. In another work, the stability of co-existing TiO₂ and ZnO in natural waster was assessed to provide insights into aggregation and sedimentation of NPs in a natural aquatic system (Fang et al. 2017). In this case, the concentrations of the two nanomaterials were determined via ICP-AES after digestion in sulphuric acid and ammonium sulphate (inorganic salt). The addition of a specific amount of solid salt to each vessel makes the sample preparation much longer and the analytical method can hardly be considered suitable for large batches of samples. In neither of these two cases the analytical method development and validation were the aim of the work and such details were not reported. Consequently, the suitability of these methods for accurately revealing NP concentrations has not been assessed.

Inductively coupled plasma - optical emission spectrometry (ICP-OES) paired with acid digestion is considered a promising analytical technique that can be used to develop and validate a robust and reliable method to quantify metal-based nanoparticles. It provides specificity on elemental identification and exhibits limit of

detection (LoD) in the range of $\mu\text{g/L}$ which would meet the current and future predicted environmental concentration (PEC) of NPs in aquatic system as well as sewerage and WWTPs (Mueller and Nowack 2008, Gottschalk et al. 2009). It can exploit an acid mix of $\text{H}_2\text{SO}_4 - \text{HNO}_3$ which has the potential to dissolve most metallic NPs and yet being less hazardous of HF. It requires shorter and easier sample preparation than methods involving HF and inorganic salts, making it well suited for large batches of samples. However, a detailed protocol on an analytical method for quantification of CuO, TiO_2 and ZnO mixture via a single $\text{H}_2\text{SO}_4 - \text{HNO}_3$ acid digestion followed by ICP-OES measurement has not yet been investigated

In this work, we present the adaptation and validation of a single standard analytical procedure, currently used to quantify titanium (Ti), to simultaneously determine the total concentration of triple mixtures of suspended CuO, TiO_2 and ZnO nanoparticles in water and wastewater under laboratory conditions. The aim of this study was to assess whether an $\text{H}_2\text{SO}_4 - \text{HNO}_3$ acid mixture coupled with a microwave assisted reaction system aided digestion procedure may be capable of digesting metal-oxide NPs and therefore provide dissolved metal ions (the analytes) as a result. This was also compared against a $\text{HNO}_3 - \text{HCl}$ (reverse aqua-regia) approach, commonly used for digesting metals. The produced analytes (Cu^{2+} , Ti^{4+} and Zn^{2+}), are measured via ICP-OES and hence used as a proxy to provide total NP quantification. The suitability of ICP-OES measurements of these analytes (Cu^{2+} , Ti^{4+} and Zn^{2+}) in the digested solution was then assessed, and whether the results were an accurate portrayal of the known NP concentration. The scope was to provide a detailed protocol, alternative to the use of HF, which due to its hazardous nature is not widely applicable in many laboratories. This method is often used due to the chemical nature of TiO_2 , which gives this NP the properties of high stability and resistance to dissolution in water matrices as well as in most of the acids. TiO_2 indeed only, slowly, dissolves in HF or H_2SO_4 (Lomer et al. 2000).

The feasibility of this analytical method has been evaluated through assessment of linearity, precision, trueness, method detection limit (*MDL*), method quantification limit (*SQL*) and metal recoveries via acid digestion based on certified reference material (CRM). The method proposed here aims to be a single rapid and effective analytical method to perform quantification of NP mixture in environmental matrices

under laboratory conditions. This method has also the potential to be applicable to a broader range of metal-based NP mixtures and a variety of environmental matrices.

3.3 Materials and Methods

3.3.1 Preliminary investigations

The proposed analytical method relies on the identification of a suitable acid mixture and digestion protocol capable of efficiently breaking NPs down to provide metal ions to be measured as a proxy for NP quantification. TiO_2 is well known to be the hardest NP to digest in acid among those studied in this work. A preliminary investigation was carried out to assess and compare the feasibility of a modified 3030 G standard method for Ti (APHA/AWWA/WEF 2012) which used H_2SO_4 and HNO_3 for acid digestion. This method was used to quantify TiO_2 but details on the analytical method goodness were not provided (Kiser et al. 2009). This standard method involves hotplate digestion, which lasts six hours, it requires bigger acid and sample volumes and it is not recommended from a health and safety point of view. Such method requires a total 30 ml of concentrated acid per sample to boil in a glass jar heated by a hotplate. This would lead to the production of vapors and gases over the course of the heating period. The assessment of the applicability of the method needs to include the fact that multiple samples can be run on the same hotplate, hence the volume of generated gases would be greater. This requires a suitable fume cupboard as containment measure. In addition this method would have no way to find out whether the vessels have reached a suitable temperature to be handled by the analyst once the digestion is complete. Hence to be fully certain of this, it is likely that the vessels containing the acid digested samples would be left for several hours if not overnight before being transferred and diluted down with water in volumetric flasks. We adapted this standard procedure to a microwave assisted reaction system (MARS 5), equipped with 40 x 55 ml Teflon MARSXpress Vessels (CEM Corporation). This is a safer alternative, requires shorter time and smaller chemical volumes. The protection of health and safety of the analyst using this modified protocol is highly enhanced in comparison to the starting protocol. The MARS system requires less than a third of acids (4 vs 30 ml). It provides an enclosed environment with a dedicated sealed route to vent of the vapors should they escape the sealed tubes. In addition, these vessels are made of Teflon, which contrariety to glass made sample vessels have way thinner chances to break down causing spills that can cause harm to the analyst or to other equipment. However, in conjunction with the array of health and safety advantages,

such analytical protocol needs to satisfy its fitness to determine the analytes of interest. This was assessed through the testing of the protocols reported in tab. 3.1. In addition, we tested the goodness of the $\text{H}_2\text{SO}_4 - \text{HNO}_3$ acid mixture against an acid mixture (reverse aqua regia) of $\text{HNO}_3 - \text{HCl}$ (3:1). Reverse aqua regia digestion was chosen as comparison method due to its wide utilization in sample preparation for metal determination (Wang et al. 2016).

A series of TiO_2 suspensions at concentration of 100 mg/L were prepared as discussed (see chapter 4). Acid digestion of samples from TiO_2 suspensions were performed following four different acid digestion protocols (table 3.1) to determine Ti^{4+} recovery.

In addition, the same calibration standards used in the linearity experiments and containing Cu^{2+} , Ti^{4+} and Zn^{2+} , were treated as real samples and run through the digestion protocol to mimic what happens to NPs during the analytical protocol. The concentrations of the analytes were then measured to evaluate whether the acid digestion procedure could influence the goodness of the ICP-OES measurement of the analytes and therefore induce imprecise and or inaccurate quantification.

Table 3.1 TiO₂ microwave and hotplate assisted acid digestion procedures. Our method (first column) was developed based on the instrument properties. The same protocol was used for comparison with the reverse aqua regia digestion (second column). Third column shows 3030 G standard method for titanium (APHA/AWWA/WEF 2012) used by Kiser et al. (2009) and the fourth column shows the comparison hotplate digestion with reverse aqua regia.

	H₂SO₄-HNO₃ microwave digestion	3 HNO₃- 1 HCl, microwave digestion	H₂SO₄-HNO₃ hotplate digestion	3 HNO₃-1 HCl hotplate digestion
Step 1	Add 2 ml of both H ₂ SO ₄ and HNO ₃	Add 1 ml of HCl and 3 ml of HNO ₃	Add 10 ml of HNO ₃	Add 22.5 ml of HNO ₃ and 7.5 ml of HCl
Step 2	Ramp to 190 °C, 15 min	Ramp to 190 °C, 15 min	Heat at 120 °C, 1 hour	Heat at 120 °C, 1 hour
Step 3	Hold at 190 °C, 15 min	Hold at 190 °C, 15 min	Cool to 30 °C, 45 min	Cool to 30 °C, 45 min
Step 4	Ramp to 200 °C, 15 min	Ramp to 200 °C, 15 min	Add 20 ml of H ₂ SO ₄	Heat at 120 °C, 2 hours
Step 5	Hold at 200 °C, 30 min	Hold at 200 °C, 30 min	Heat at 120 °C, 2 hours	Cool to 30 °C, 1 hour
Step 6	Cool to 30 °C, 1 hour	Cool to 30 °C, 1 hour	Cool to 30 °C, 1 hour	

3.3.2 Instrumentations and analytical procedure

Sample digestion was performed in 55 ml Teflon MARSXpress Vessels (CEM Corporation) inserted in a microwave assisted reaction system (MARS 5). Inductively coupled plasma - optical emission spectroscopy measurements were performed with a ICP-OES, iCAP 6200, Thermo Fisher scientific equipped with a quartz torch and glass spray mixing chamber (Standard glass cyclonic spray chamber), a ceramic nebulizer (PEEK Mira Mist Nebulizer) and an auto sampler (ASX-520 AUTOSAMPLER). A solution of Yttrium (Y³⁺) at concentration of 5 ppm, prepared in 1 % HNO₃, from a certified standard was used as internal standard (IS) to eliminate problems that may arise such as temperature changes, power fluctuations and differences in solution parameters among others. Such situations have the capacity to influence the instrument performances and therefore affect the quality of the analysis. Digests were analyzed in triplicates and accepted if the IS relative standard deviation (RSD %) was below 5 %. Matrix matching quality controls (QC) containing Cu²⁺, Ti⁴⁺ and Zn²⁺ from certified standards (dissolved metals, not NPs) at known concentrations were run every 10-15

samples to monitor the consistency with the measurements. Analytes carry over effect was assessed by running two blank samples (matrix matching acid mix) after the highest standard of the calibration curve was analyzed and prior to begin the analysis of the real samples. The settings of the instruments and the analysis conditions are reported in table 3.2.

Table 3.2 ICP-OES method parameters

RF power	1150 W
Auxiliary gas flow rate	0.5 l/min
Nebulizer gas flow rate	0.5 l/min
Flush pump rate	100 rpm
Analysis pump rate	50 rpm
Sample flush time	30 s
Repeat per sample	3
Elements wavelength (nm)	Cu 224.7 Cu 324.7 Ti 308.8 Ti 323.9 Zn 202.5 Zn 206.2

The choice of the instrument and technique, ICP-OES, iCAP 6200, Thermo Fisher scientific was done in accordance with the following points:

- Analytes' concentration. ICP-OES provides a *LoQ* in the region of 1 to 10 $\mu\text{g/L}$, whereas the *LoQ* for ICP-MS based analysis is generally 1000 times lower. The *LoQ* of this analytical method for the analytes of interest was assessed satisfactory during the process of method validation.
- The reported removal rate for NPs by activated sludge has been reported up to 99 % in previously published reports. The lowest concentration used in this work is 9 mg/L. If we apply the 99% removal rate as “worst case scenario”, the amount of NPs left unremoved in the settled wastewater (fraction collected and analyzed in this work) would be equal to 90 $\mu\text{g/L}$, which is well within the linear range of ICP-OES (nominal *LoQ* = 10 $\mu\text{g/L}$).

3.3.3 Calibration and linear correlation

In this work we refer to nominal concentration as the theoretical concentration of testing substance calculated according to the preparation of the analyzed solution (ion

form, dilution of element standards) or suspension (nanoparticulate form, dispersion of a weighted amount of nanoparticle powder in a measured volume).

The linearity of the correlation between the analytes' concentrations (independent variable) and signal intensity (dependent variable) was assessed to identify the linear range of the analytical method for Cu^{2+} , Ti^{4+} and Zn^{2+} . A set of one blank (no analytes) and standards (six) with analytes' concentrations varying from 0.01 to 50 ppm were prepared in matrix matching solution (4% HNO_3 and 4% H_2SO_4) from certified standards of Cu^{2+} , Ti^{4+} and Zn^{2+} at 1000 ppm in 1% HNO_3 . Visual evaluation, correlation coefficient (r^2) and Lack of Fit (LoF) statistical test were used to assess the linearity of the signal as well as the linear range.

3.3.4 Method detection limit (*MDL*) and Method Quantification limit (*MQL*)

All instrumentation and analytical methods have an inherent minimum level below which they no longer function reliably. Analytical determination may become challenging at the extremities of the linear range. At high analytical level, underestimation may occur. At very low concentrations instead, analytical quantification is challenged by the possibility to encounter false positive or false negative situations and miss positive samples. For such purpose, it has been recommended that two different analytical levels are marked down prior to commence the process of analytical quantification. Method detection limit (*MDL*), is defined as that concentration level at which the analytical method provides 99% of certainty of "seeing" the analyte although its concentration can only be broadly estimated. Method Quantification limit (*MQL*) is instead the lowest amount of an analyte that can be precisely and accurately determined via the chosen analytical method. Based on preliminary investigation and data history review, *MDL* and *MQL* are key parameters affecting the choice of an analytical method that fits the purpose over another.

Two different approaches have been adopted to determine *MDL* and *MQL* for this analytical method according to the guidelines set by United States Environmental Protection Agency (USEPA) (CFC 1986) (https://www.epa.gov/sites/production/files/2016-12/documents/mdl-procedure_rev2_12-13-2016.pdf). One method estimates MDL_b and MQL_b based on multiple analysis of method blanks, while the other relies on analysis of spiked samples

and provides estimation of MDL_s and MQL_s . A series of at least 7 independent method blanks was analyzed over the course of at least three separate days and MDL_b was calculated based on the equation 1

$$MDL_b = \bar{X} + \sigma_b \cdot t_{(n-1, 1-\infty=0.99)} \quad (\text{eq. 1})$$

where \bar{X} is the mean of the method blank results, σ_b the standard deviation of the method blank sample analysis and $t_{(n-1, 1-\infty=0.99)}$ is the Student's t-value appropriate for the single-tailed 99th percentile t statistic and a standard deviation estimate with n-1 degrees of freedom. For MQL_b estimation, equation 2 was used.

$$MQL_b = \bar{X} + \sigma_b \cdot 10 \quad (\text{eq. 2})$$

This method was compared with an alternative procedure that relies on analysis of spiked samples at low analytes' concentration. Several independent matrix matching solutions containing Cu^{2+} , Ti^{4+} and Zn^{2+} were prepared at concentration of 0.005 and 0.01 ppm, analyzed and then the MDL_s was calculated according to equation 3

$$MDL_s = \sigma_s \cdot t_{(n-1, 1-\infty=0.99)} \quad (\text{eq. 3})$$

where σ_s is the standard deviation of the spiked samples analysis and $t_{(n-1, 1-\infty=0.99)}$ is the Student's t-value appropriate for the single-tailed 99th percentile t statistic and a standard deviation estimate with n-1 degrees of freedom. MQL_s , was then calculated as follow (eq. 4).

$$MQL_s = \sigma_s \cdot 10 \quad (\text{eq. 4})$$

In addition, a third method to estimate MDL and MQL was also applied. This procedure is often used in industrial applications and it is based on the analysis of method blanks, and then the calculated standard deviation is multiplied by a factor 3 for MDL_i and by

a factor 10 for MQL_i . This procedure is a simplified version, directly derived from the blanks method to determine MDL_b and MQL_b from USEPA guidelines

The estimated MDL and MQL were then verified by measuring samples prepared from certified Cu^{2+} , Ti^{4+} and Zn^{2+} standards at concentrations in the range of the calculated MDL and MQL .

In addition, the same calibration standards used in the linearity experiments and containing Cu^{2+} , Ti^{4+} and Zn^{2+} , were treated as real samples and run through the digestion protocol to mimic what happens to NPs during the analytical protocol. The concentrations of the analytes were then measured to evaluate whether the acid digestion procedure could influence the goodness of the ICP-OES measurement of the analytes and therefore induce imprecise and or inaccurate quantification.

3.3.5 Precision and trueness evaluation

A set of CuO , TiO_2 and ZnO NP mixture suspensions were prepared and processed through the whole analytical procedure. Precision was evaluated through calculation of the relative standard deviation (RSD %). While trueness was evaluated through assessment of bias. Four different set of experiments were run and as follows:

- CuO , TiO_2 and ZnO NPs from Sigma Aldrich. Suspensions prepared in ultrapure water.
- CuO , TiO_2 and ZnO NPs from Sigma Aldrich. Suspensions prepared in synthetic wastewater.
- CuO and ZnO NPs from Sigma Aldrich, TiO_2 NP standard reference material (SRM) (NIST1898) from National Institute of Standards and Technology prepared in ultrapure water.
- CuO and ZnO NP from Sigma Aldrich, TiO_2 NP standard reference material (SRM) (NIST1898) from National Institute of Standards and Technology prepared in synthetic wastewater.

The synthetic wastewater used was prepared by following a standard protocol (OECD, 2001), . Cu^{2+} , Ti^{4+} and Zn^{2+} background levels were determined prior to the execution of the tests as well as on the same day of the experiments.

3.4 Results and discussion

3.4.1 Linearity and linear range

Prior to working with NPs, the linearity of the independent variable (concentrations of the analytes) and the dependent variable (the signal intensity) for the dissolved metal ions Cu^{2+} , Ti^{4+} and Zn^{2+} was assessed by analyzing standards solutions, containing the analytes of interest, at known concentrations from 0.01 to 50 ppm (Fig 3.1).

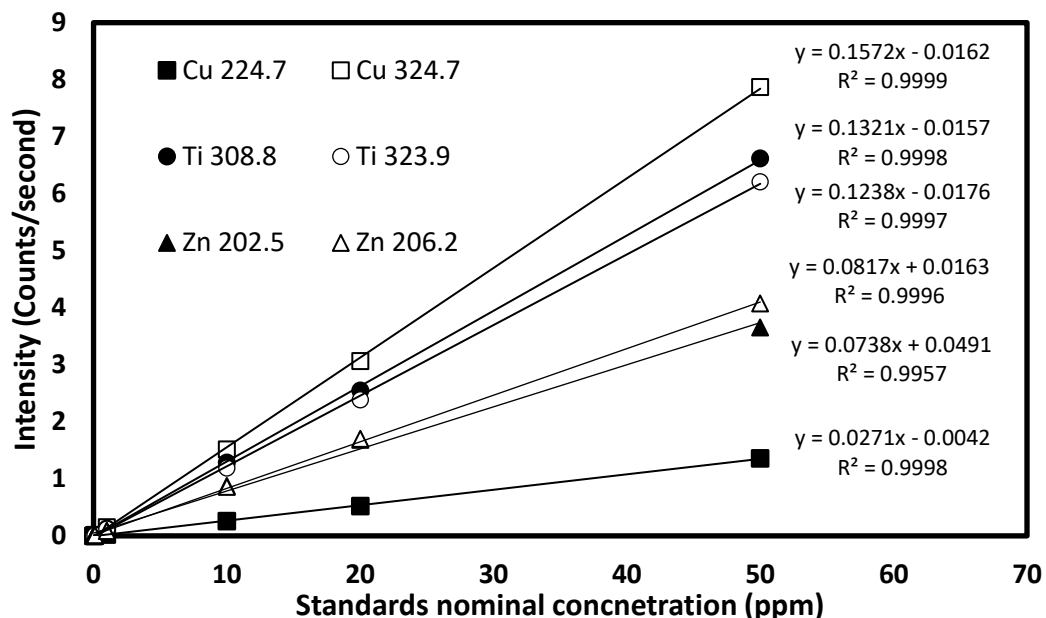


Fig. 3.1 Linear range of signal intensity and analytes' concentration for Cu^{2+} , Ti^{4+} and Zn^{2+} in 4% HNO_3 and 4% H_2SO_4 . Results are shown as average \pm standard deviation ($n=3$). All standard deviations smaller than the marker size (6), highest standard deviation value was 0.11 counts/second.

The standard solutions were prepared in a matrix of 4% HNO_3 and 4% H_2SO_4 , by dilution of certified standards. For each element, two different wavelengths were chosen according to the suggestion given by the instrument software as the most commonly used. The settings of the instrument were also maintained as suggested by the manufacturer. This because ICP-OES is a well-established routine method to measure trace elements in diverse sample ranges and matrices. For this reason, the evaluation of linearity of the analytes of interests in the range of concentrations was assessed via visual evaluation and supported by lack of Fit test. Statistical tests are used to confirm the goodness of fit of the linear regression model obtained by the calibration for the analytes of interest. This test compares the deviation of the points from the line caused by random scatter of the points of replicate measurements (mean

sum of squares of random error (MSS_{err}) with deviation of the points from the line caused by mismatch of the calibration model (mean sum of squares due to lack of fit MSS_{LOF}), obtained according to eq. 5

$$F_{calculated} = \frac{MSS_{LOF}}{MSS_{err}} = \frac{\sum(\bar{y}_i - \hat{y}_i)^2 / (n-2)}{\sum(y_i - \hat{y}_i)^2 / n(p-1)} \quad (\text{eq. 5})$$

where \bar{y}_i = the average value of experimental signal from replicate measurements at concentration level i ; \hat{y}_i = the signal value at concentration level i calculated using the calibration function; y_i = the experimental signal value at concentration level i ; n = number of concentration levels; p = number of replicate measurements at one concentration level. When $F_{calculated} < F_{tabulated}$ then the model can be considered fit for the data.

The simultaneous quantification of Cu^{2+} , Ti^{4+} and Zn^{2+} via ICP-OES show a linear range within the concentration tested (0.01 – 50 ppm) and all the values for R-square (r^2) are extremely close to 1 (Fig 3.1). However, r^2 provides an estimation of the relationship between the behavior of a dependent variable based on an independent variable and it does not provide indication on the goodness of fit of the generated regression model. A further control on the goodness of the measurement method was run by performing a lack of fit test. This statistical tool was adopted to test the null hypothesis for no lack of fit of the regression model, and such hypothesis was accepted and therefore deemed as valid when $F_{calculated} < F_{tabulated}$. For all the six tested wavelengths the null hypothesis was accepted (i.e. F_{calc} was always $< F_{tab}$; Table 3.3), and therefore, simultaneous analysis of Cu^{2+} , Ti^{4+} and Zn^{2+} via ICP-OES in the range of 0.01 to 50 ppm can be performed via a linear regression model created from element concentration (independent variable) and signal intensity (dependent variable).

Table 3.3 F tabulated and calculated to evaluate linearity of the signal intensity vs analytes concentration.

	Cu 224.7	Cu 324.7	Ti 308.8	Ti 323.9	Zn 202.5	Zn 206.5
F_{tab}	3.8853	3.8853	3.8853	3.8853	3.8853	3.8853
F_{calc}	0.2835	0.0035	0.0029	0.0036	0.0753	0.0154

Despite ICP-OES being a well-established analytical technique to selectively quantify multiple elements at once, the process of analytical method development and validation needs to begin to confirm the goodness of the regression model to apply in the analytical quantification. It has been reported that high concentrations of H₂SO₄ can have a negative impact on the measurements of elements. When measuring titanium, it was found that H₂SO₄ have a strong effect on the emission intensity, and as result with a matrix of 10% H₂SO₄ the linear range for titanium was up to 5 ppm (Lomer et al. 2000). The signal emission suppression effect was found dependent on H₂SO₄ concentration, with greater measurement errors at higher acid concentrations. However, in our case, the linearity of the emission for Ti⁴⁺ as well as Cu²⁺ and Zn²⁺ is much wider (0.01 – 50 ppm), and this could be explained with the lower final H₂SO₄ concentration (4%) we adopted. The data obtained confirm the feasibility of ICP-OES to simultaneously quantify Cu²⁺, Ti⁴⁺ and Zn²⁺ in a range that spreads from 0.01 to 50 ppm which has been identified as the linear range of the analytes concentrations – signal intensity relationship.

3.4.2 Limit of detection and limit of quantification evaluation

Method detection limit found following the method blanks (*MDL_b*), the simplified USEPA procedure (*MDL_i*) and from spiked samples (*MDL_s*) for Cu²⁺, Ti⁴⁺ and Zn²⁺ varied from 0.0004 to 0.015 ppm. *SQL* values varied from 0.0013 to 0.051 ppm (Table 3.4).

Table 3.4 Method Detection Limit (MDL) and Method Quantification Limit (MQL), reported in mg/L, for ICP-OES analysis of Cu²⁺, Ti⁴⁺ and Zn²⁺

Element wavelength	Blank method USEPA		Spiked sample 0.0005 ppm		Spiked sample 0.001 ppm		Routine blank method	
	<i>MDL_b</i>	<i>MQL_b</i>	<i>MDL_s</i>	<i>MQL_s</i>	<i>MDL_s</i>	<i>MQL_s</i>	<i>MDL_i</i>	<i>MQL_i</i>
Cu 224.7	0.005	0.016	0.0005	0.0017	0.0005	0.0016	0.004	0.014
Cu 324.7	0.008	0.023	0.0006	0.0018	0.0009	0.0028	0.006	0.020
Ti 308.8	0.009	0.028	0.0004	0.0013	0.0009	0.0029	0.008	0.026
Ti 323.9	0.010	0.029	0.0010	0.0031	0.0016	0.0050	0.008	0.027
Zn 202.5	0.014	0.051	0.0011	0.0036	0.0013	0.0042	0.015	0.051
Zn 206.2	0.014	0.051	0.0011	0.0036	0.0012	0.0038	0.015	0.050

The analytical method had greatest sensitivity for Cu²⁺ which constantly had the lowest *MDL* and *MQL*, whereas Zn²⁺ had the highest. However, the four different procedures used showed a discrepancy, with *MDL_b*, *MQL_b*, *MDL_s* and *MQL_s* generally 10 times higher than *MDL_s* and *MQL_s*. Therefore, samples containing Cu²⁺, Ti⁴⁺ and Zn²⁺ at concentrations of 0.005 and 0.01 ppm were measured to confirm the trueness of the quantification at these levels expressed as relative bias and precision expressed as relative standard deviation (RSD%) (Table 3.5).

Table 3.5 Confirmation and evaluation of ICP-OES analysis precision (RSD %) and trueness (bias %) of MDL with Cu²⁺, Ti⁴⁺ and Zn²⁺ standards in 4% H₂SO₄ and 4% HNO₃.

		Standard 0.005 ppm	Standard 0.01 ppm
Cu 224.7	Measured (ppm)	0.0048 ± 0.00017	0.00999 ± 0.00016
	RSD %	3.61	1.58
	Bias %	4.86	0.14
Cu 324.7	Measured (ppm)	0.0043 ± 0.00018	0.00987 ± 0.00028
	RSD %	4.26	2.85
	Bias %	14.86	1.29
Ti 308.8	Measured (ppm)	0.0052 ± 0.00013	0.01010 ± 0.00029
	RSD %	2.59	2.91
	Bias %	3.71	1
Ti 323.9	Measured (ppm)	0.0050 ± 0.00031	0.01017 ± 0.0005
	RSD %	6.33	4.87
	Bias %	0.57	1.71
Zn 202.5	Measured (ppm)	0.0041 ± 0.00036	0.01110 ± 0.00042
	RSD %	8.68	3.79
	Bias %	18	11
Zn 206.2	Measured (ppm)	0.0037 ± 0.00036	0.00997 ± 0.00038
	RSD %	9.71	3.82
	Bias %	26.86	0.29

These data confirm that ICP-OES analysis can quantify Cu²⁺, Ti⁴⁺ and Zn²⁺ in HNO₃ and H₂SO₄ matrix at concentrations of a few ppb, with generally better performances when measuring 0.01 ppm than 0.005 ppm. The assessment of precision and trueness of the multiple analysis of samples at known concentrations showed that quantification of Ti⁴⁺ is satisfactory at concentration of 0.005 ppm for both the wavelength used and this value was therefore set as Ti MQL. The same value of MQL was applied for quantification of Cu²⁺ when using the wavelength 224.7 nm given the

high goodness of analysis at 0.005 ppm. Contrarily, high bias was observed at the same concentration when the 324.7 nm wavelength was used. However, both wavelengths can properly measure Cu^{2+} at concentration of 0.01 ppm. Therefore, it appears that the wavelength 224.7 is more sensitive than the 324.7 nm wavelength, and therefore the latter was given a higher MQL of 0.01 ppm.

Zn^{2+} quantification was not satisfactory at 0.005 ppm. The measured values were 0.0041 ± 0.00036 for the 202.5 nm wavelength while 0.0037 ± 0.00036 for the 206.2 nm with relative bias varying from 18 to 26.86 % (Table 3.5). This shows a significant offset of the analysis in comparison to the concentration of the prepared standard. Hence, Zn^{2+} quantification at 0.005 ppm cannot be considered acceptable, although *MDL* and *MQL* calculated via the spiked samples were in the region of 0.0011 to 0.0042 ppm. *MDL* and *MQL* obtained via USEPA method usually provided higher values, both above 0.01 ppm. However, Zn^{2+} quantification at 0.01 ppm with the 206.2 nm wavelength yield good RSD% (3.82) and relative bias (0.29 %), meaning that quantification at this concentration is reliable and therefore 0.01 ppm was applied as MQL for Zn^{2+} . Contrarily when using the 202.5 nm wavelength the measured value was 0.0111 ± 0.00042 ppm with a RSD % of 3.79 but a bias of 11%. This suggests that the trueness of Zn^{2+} quantification at either 0.005 and 0.01 ppm cannot be considered acceptable and therefore the 206.2 nm wavelength should be used.

Different MDL were applied to different wavelength according to the assessed sensitivity. The assigned MDL were used as an indication, however the majority of the samples we run analyzed with this analytical method had concentration much greater than the set MDL. In addition, every sample was analyzed for both the wavelengths and the choice of the best one was based on the assessment of the analytical quality control samples. We consider the choice of following this procedure on a daily basis as a good practice that would provide the best quality results. Indeed the procedure of identifying the wavelength better performing among those already confirmed to work well for the analytes of interest allow the analyst to account for variation of the analysis due to differences arising from the instrument. Indeed the instrument used in this work is a common instrument used by a whole department. This means the possibility of multiple different set-up used for the same instrument as well as a variety of operators which can have an impact of the daily performances of the instrument. Picking the best

performing wavelength based on the analyte recovery of a set of multiple analytical quality controls of a known concentrations run at regular interval during the determination of real samples, is an objective way to account for instrument variation in performances and provides a means to gather the best quality and most robust data from the analytical method used.

3.4.3 Acid mixture and NP digestion protocol identification

Note that for the remainder of this chapter all TiO_2 , CuO and ZnO nanoparticles are simply referred to as TiO_2 , CuO and ZnO.

A suitable acid mixture and a microwave assisted reaction system digestion protocol for TiO_2 quantification were determined via preparation of nanoparticles suspensions (100 mg/L) which were then processed as described in tab. 3.2. The results of titanium recovery from acid digested TiO_2 suspensions are shown in Fig. 3.2.

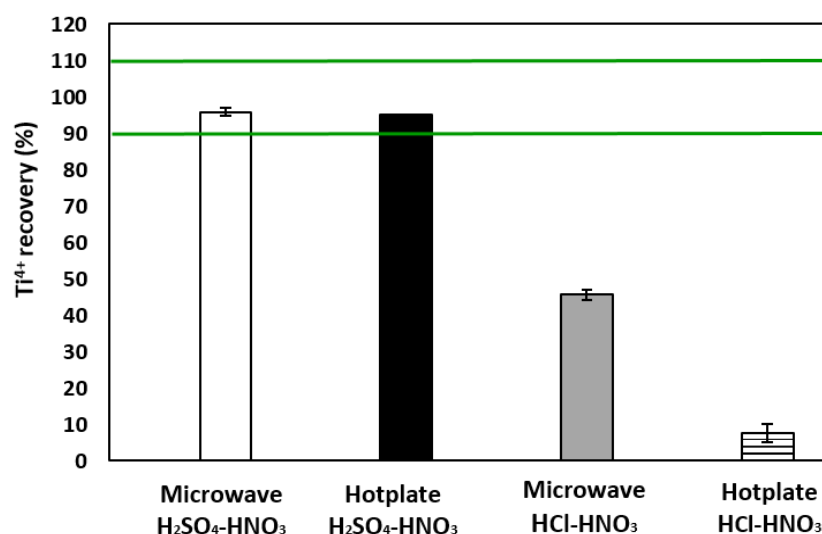


Fig. 3.2 Ti^{4+} recovery from suspensions of TiO_2 (100 mg/L) digested with different procedures and acid mixtures. The green lines (90 and 110 %) show the accepted value for metal recovery evaluation with ICP-OES (U.S. Environmental Protection Agency 1987). Results are shown as average \pm standard deviation (n=5).

When the digestion is carried out in HNO_3 and H_2SO_4 , the metal recovery was between 90 % and 110 % which falls within the range accepted by USEPA (U.S. Environmental Protection Agency 1987), regardless of the equipment used to perform the acid digestion (Fig. 3.2). On the contrary, when the carried out in $\text{HNO}_3 - \text{HCl}$

mixture, the acid digestion did not yield an acceptable metal recovery and therefore further application of this method should be discouraged for such purpose.

These preliminary data confirm the applicability of the standard method 3030 G (APHA/AWWA/WEF 2012) that involves an acid digestion on a hotplate with a HNO_3 - H_2SO_4 mixture. This standard method can achieve a suitable metal recovery from TiO_2 as nanoparticles. However, such procedure comes with multiple downsides: low number of samples processed simultaneously, high production of hazardous fumes, longer technical time and requires bigger volumes of acids. Therefore, we determined the applicability of a safer, cheaper and faster procedure to perform NP acid digestion in a microwave assisted reaction system. Such procedure is safer, faster, allows a greater number of samples to be processed at the same time and requires small volumes of acids, which concentration has been shown to have a detrimental effect on element quantification with ICP-OES (Lomer et al. 2000).

The effectiveness of the HNO_3 - H_2SO_4 digestion procedure in microwave assisted reaction system was also tested on suspensions of CuO and ZnO (100 mg/L). This was done to initially determine whether a single analytical method could be used to simultaneously quantify CuO , TiO_2 and ZnO . The results of metal recovery (Fig. 3.3) demonstrate that this procedure can achieve satisfactory results in digesting single NPs types.

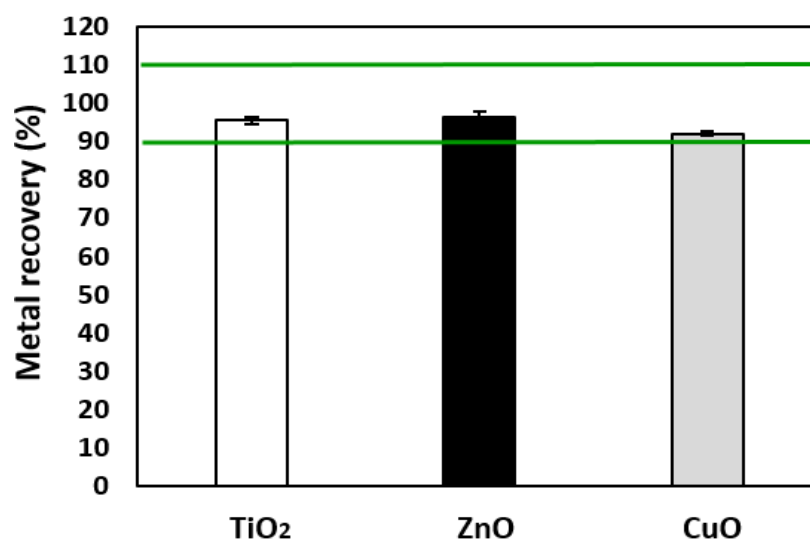
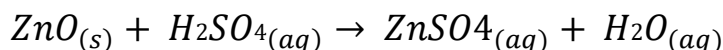
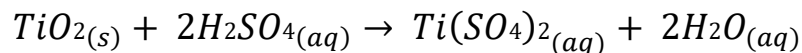
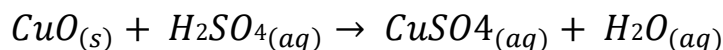


Fig. 3.3 Metal recovery from suspensions of single CuO , TiO_2 and ZnO (100 mg/L) digested in HNO_3 - H_2SO_4 through microwave assisted reaction system and ICP-OES analysis. The green lines (90 and 110 %) show the accepted value for metal recovery evaluation with ICP-OES (U.S. Environmental Protection Agency 1987). Results are shown as average \pm standard deviation (n=5).

Acid digestion of CuO, TiO₂ and ZnO in HNO₃ - H₂SO₄ mainly happens through the reactions reported below.



HNO₃ has lower reactivity in comparison to H₂SO₄ and it is added to ensure that the soluble products remain in solution, thus preventing analytes precipitation that would bias the measurement. Undesired reactions may happen during the acid digestion, for example silver (Ag) quantification in HCl digestion or in chlorine (Cl) rich matrices, can lead to the formation and precipitation of AgCl products that would make the measurements inaccurate and imprecise (Poitras et al. 2016). Therefore, we investigated whether the acid digestion procedure could have any negative effects on the availability and speciation of analytes of interests Cu²⁺, Ti⁴⁺ and Zn²⁺. Certified standards at known concentrations were treated as real samples, thus acid digested following the protocol used for NP quantification. The presence of insoluble precipitated compounds was visually evaluated by leaving the samples to rest in volumetric flasks and then Cu²⁺, Ti⁴⁺ and Zn²⁺ concentrations were determined via ICP-OES. The results reported in Fig. 3.4 show that the measured values were in strong agreement with the nominal values throughout the complete tested concentration range (0.01 – 50 ppm).

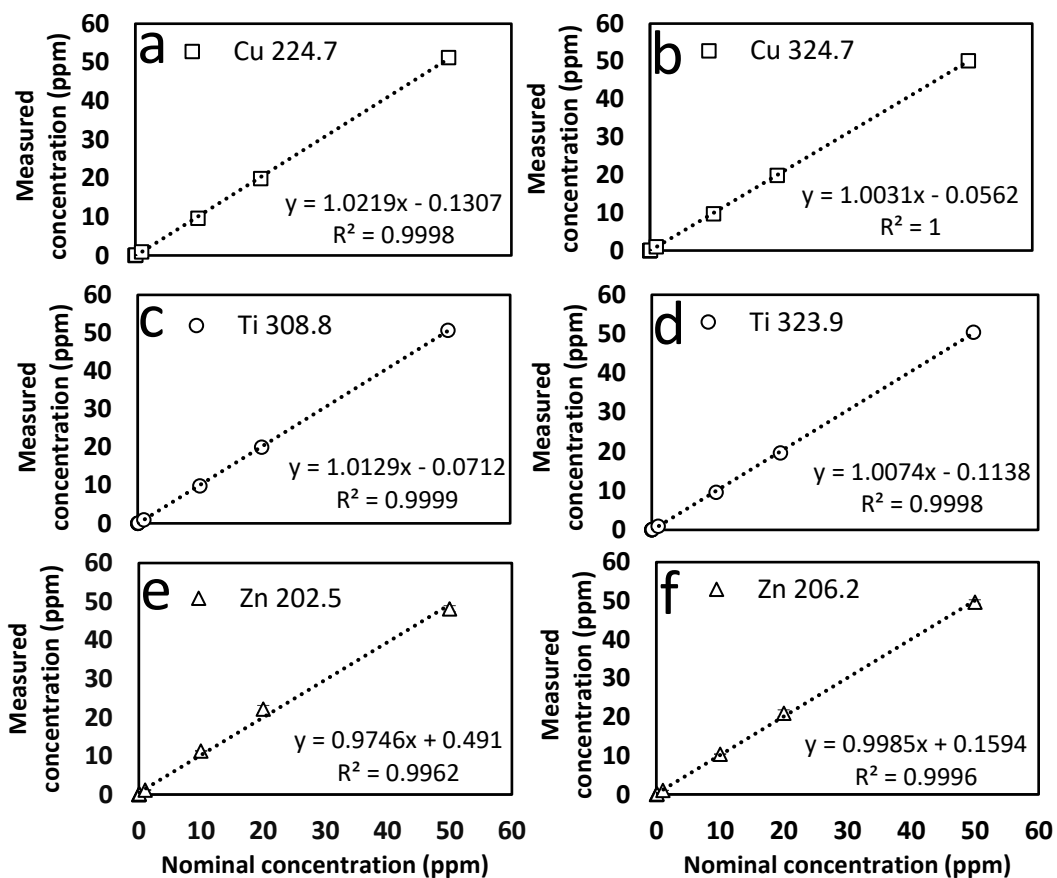


Fig. 3.4 Measured versus nominal concentrations of Cu²⁺, Ti⁴⁺ and Zn²⁺ determined after acid digestion procedure. Panel **a** and **b** refer to Cu²⁺, **c** and **d** to Ti⁴⁺ while Zn²⁺ is shown in panels **e** and **f**. Every point is shown as average \pm standard deviation ($n=3$). Error bars only visible for Zn²⁺ tests. In panels **a,b,c** and **d**, standard deviations are covered by the markers (size used is 5) and did not exceed the value of 0.77 mg/l for Cu²⁺ and 0.59 mg/L for Ti⁴⁺.

These findings confirm the goodness of the HNO₃ - H₂SO₄ digestion procedure coupled with ICP-OES measurement to determine Cu²⁺, Ti⁴⁺ and Zn²⁺ from the relative acid digested oxide-based NPs. Satisfactory metal recovery and no undesired effects on the availability, and therefore determination of the analytes of interests through the analytical process, open to the possibility to establish a single analytical procedure to simultaneously quantify CuO, TiO₂ and ZnO mixtures.

3.4.4 Determination and evaluation of analytical trueness and precision

The goodness of simultaneous quantification of CuO, TiO₂ and ZnO mixtures via HNO₃ - H₂SO₄ digestion and ICP-OES measurement was assessed through a range of NP concentration from 0.4 to 100 mg/L. Precision (reported as RSD%) and trueness (metal recovery %) are reported in Table 3.5, 3.6, 3.7, and 3.8.

Table 3.3 Summary of the analytical method trueness (metal recovery) and precision (RSD %) for Cu²⁺, Ti⁴⁺ and Zn²⁺ in ultrapure water (n=5). All nanoparticles purchased from Sigma Aldrich.

Cu ²⁺	Concentration (mg/L)	0.38	3.83	5.96	24.13	46.17	59.60	95.86
	Average recovery (%)	106.49	90.08	87.07	92.29	92.43	92.11	93.90
	RSD (%)	1.60	1.01	1.27	2.11	1.19	2.25	1.62
Ti ⁴⁺	Concentration (mg/L)	0.39	3.87	5.99	24.57	46.51	59.93	96.85
	Average recovery (%)	162.62	88.66	114.70	91.07	90.66	91.26	90.29
	RSD (%)	15.84	3.80	3.21	3.17	2.59	2.64	0.90
Zn ²⁺	Concentration (mg/L)	0.38	3.82	5.96	23.62	46.44	59.61	95.60
	Average recovery (%)	99.72	99.28	89.90	94.74	94.66	93.31	96.35
	RSD (%)	8.77	1.68	1.58	0.94	0.81	2.98	1.75

Table 3.4 Summary of the analytical method trueness (metal recovery) and precision (RSD %) for Cu²⁺, Ti⁴⁺ and Zn²⁺ in synthetic wastewater (n=5). All nanoparticles purchased from Sigma Aldrich.

Cu ²⁺	Concentration (mg/L)	0.40	4.01	6.33	25.40	47.29	59.90	100.34
	Average recovery (%)	100.62	93.04	92.86	97.67	95.58	97.63	89.89
	RSD (%)	6.13	0.79	1.15	0.90	2.25	3.66	2.44
Ti ⁴⁺	Concentration (mg/L)	0.39	3.89	5.99	24.69	46.15	59.90	97.33
	Average recovery (%)	94.82	112.98	102.97	100.31	96.49	91.88	92.47
	RSD (%)	10.89	3.12	5.16	2.26	2.44	3.59	2.51
Zn ²⁺	Concentration (mg/L)	0.38	3.82	5.94	24.58	47.72	59.90	95.59
	Average recovery (%)	100.51	100.49	98.90	100.66	100.42	96.86	95.53
	RSD (%)	2.98	0.92	1.82	0.89	2.49	3.89	2.24

Table 3.5 Summary of the analytical method trueness (metal recovery) and precision (RSD %) for Cu^{2+} , Ti^{4+} and Zn^{2+} in ultrapure water (n=5). TiO_2 certified reference material purchased from NIST. CuO and ZnO purchased from Sigma Aldrich.

Cu^{2+}	Concentration (mg/L)	0.40	4.22	6.20	25.63	47.51	59.76	99.70
	Average recovery (%)	95.81	94.28	94.47	95.17	97.00	95.74	95.23
	RSD (%)	2.79	4.90	1.77	3.32	3.82	3.08	2.63
Ti^{4+}	Concentration (mg/L)	0.41	3.97	5.91	24.26	46.27	59.81	98.12
	Average recovery (%)	94.95	100.48	97.43	101.28	94.56	96.32	96.37
	RSD (%)	3.99	4.01	1.72	5.42	1.93	2.61	3.12
Zn^{2+}	Concentration (mg/L)	0.38	3.88	5.82	24.88	47.19	59.63	97.18
	Average recovery (%)	98.42	92.36	97.78	97.80	98.66	97.91	97.57
	RSD (%)	4.11	3.08	1.98	1.64	2.37	1.39	2.13

Table 3.6 Summary of the analytical method trueness (metal recovery) and precision (RSD %) for Cu^{2+} , Ti^{4+} and Zn^{2+} in synthetic wastewater (n=5). TiO_2 certified reference material purchased from NIST. CuO and ZnO purchased from Sigma Aldrich.

Cu^{2+}	Concentration (mg/L)	0.40	3.94	6.11	25.87	46.93	60.30	100.89
	Average recovery (%)	106.12	97.70	96.66	95.43	98.86	93.26	95.14
	RSD (%)	0.88	2.74	3.37	1.23	1.18	2.49	2.85
Ti^{4+}	Concentration (mg/L)	0.40	4.03	6.21	24.92	45.88	60.07	96.91
	Average recovery (%)	101.59	107.15	97.22	98.98	97.58	97.61	95.12
	RSD (%)	2.17	2.88	3.44	1.15	3.24	2.89	1.69
Zn^{2+}	Concentration (mg/L)	0.37	3.71	5.73	25.07	47.19	59.77	95.13
	Average recovery (%)	107.71	100.49	100.84	94.28	101.92	101.15	96.42
	RSD (%)	2.35	3.80	1.08	2.18	1.40	2.26	0.81

Metal recovery for all the three NP types varied from 87.07 to 162.62 % (Tables 3.5 to 3.8). However, despite a few cases, metal recovery was mostly calculated between 90 and 110 %, which is the accepted range for analytes recovery by USEPA. In addition, most of the cases in which metal recovery did not fall within the accepted range was at low concentrations and this therefore could be attributed to the complexity of preparing sampling with multiple NPs, balance sensitivity limitation and the difficulties with working with such low weight of nanopowder. The preparation

of the NP standard at the lowest concentration was attempted multiple time. In addition, the preparation of the standards at known concentrations for analytical method validation must be carried out independently for every solution. This means that the preparation of the low-level standards could not have been done via dilution, leaving manual preparation as the only option in spite of the difficult in the preparation process. These tests were carried out in ultrapure water and synthetic wastewater. The background level of Cu^{2+} , Ti^{4+} and Zn^{2+} were measured prior to and on the same day of the experiments. The concentrations of these elements in either matrix have always been below the MDL. Contrarily, Cu^{2+} , Ti^{4+} and Zn^{2+} concentrations in real wastewater were extremely variable and very often above MDL.

In addition, the linear range of the analytes of interest was previously determined until the concentration of 50 ppm (fig. 3.1 and tab 3.3), whereas here we also tested higher concentrations to unveil acid digestion performances. When samples had concentrations which exceeding the determined limit of the linear range they were diluted accordingly.

Overall, the measured concentrations of Cu^{2+} , Ti^{4+} and Zn^{2+} after acid digestion of sample containing the relative NPs were in strong agreement with their nominal concentrations as shown in fig 3.5, 3.6 and 3.7.

CuO and ZnO are known to easily dissolve in strong acids such as HNO_3 and H_2SO_4 , and our results corroborate this (table 3.5, 3.6, 3.7 and 3.8). In all the four experimental setup, the purchased CuO and ZnO were commonly used NPs. Regardless of the matrix in which they are suspended in, whether that is water (tab 3.5 and 3.7) or synthetic wastewater (tab 3.6 and 3.8), the acid mixture we adopted provides excellent digestion efficiency. This, added with the high ICP-OES sensitivity and lack of detrimental effects on the availability of Cu^{2+} and Zn^{2+} , indicates that the proposed analytical method can be adopted to quantify mixtures of CuO and ZnO .

Among the ones investigated in this study, TiO_2 is the nanomaterial least prone to dissolve in aqueous matrices and acids. It is considered insoluble and would only slowly dissolve in HF or H_2SO_4 (Wamer et al. 1997). Hence, the assessment of the goodness of the analytical method for TiO_2 required a further step to prove its suitability. The method validation was divided into two categories according to the NP type. The whole method was proved against commonly used TiO_2 (tab 3.5 and 3.6)

(purchased from Sigma Aldrich and used in the following experimental chapters) as well as TiO₂ as certified reference material (CRM) from National Institute of Standards and Technology (NIST) (tab 3.7 and 3.8). This was used in order to demonstrate reliability of the metal recovery of the proposed analytical method.

Tab. 3.6 and 3.7 and Fig. 3.6a and 3.6b, show the performances of TiO₂ determination, with the nanomaterial purchased as regular NP. The outcome obtained from tests with conventional TiO₂ show satisfactory results in both ultrapure water and synthetic sewage with RSD % greater than 5 % only found at concentration of 0.39 mg/L in ultrapure water. However, the average metal recovery for that treatment was 162.62 %. The high RSD % and metal recovery could be attributed to the difficulty of preparing such a low concentration suspension from powder.

As reported in Table 3.8 and 3.9, very similar metal recovery and RSD % are observed from digestion of TiO₂ as certified reference material (CRM) from National Institute of Standards and Technology (NIST). Furthermore, the measured values were also in strong agreement with the nominal concentrations adopted in the tests (Fig. 3.6c and 3.6d). Paired with the relative metal recoveries (Table 3.8 and 3.9) confirm that the analytical method owns the properties of precision (low RSD %) and trueness (analyte recovery from a certified reference material). This provides great value to this analytical method to ensure goodness and robustness of the analysis and quality assurance. In addition, we have proven the ability of a simple, rapid and less hazardous analytical method to simultaneously quantify CuO, TiO₂ and ZnO with a single procedure without the need to use HF.

This method has been shown to be applicable in water and wastewater matrices, and its application could easily be expanded to other aqueous environmental sample matrices such as ecotoxicological and growth media for either algae, bacteria and aquatic organisms. The synthetic wastewater we used was prepared by following a standard OECD protocol. It has a high dissolved organic matter content as well as intense ionic strength. These two factors are well known to have the possibility to alter the goodness of analytical measurements; however, this was not the case for this method as we observed similar and equally good results in digestion of NP in either ultrapure water and synthetic wastewater. This is likely due to strength of the acid mixture in conjunction with the MARS digestion system. This sample preparation

process allows the “consumption” of the organic matter which present in the wastewater. In addition the acid mix aids to maintain all the ions in solution which prevents measurement error due to precipitation. This makes MARS acid digested wastewater sample highly similar to ultrapure water-based samples which further can explain the similarity in robust analytical results in the method validation.

This work provides for the first time strong evidences of the suitability of a quick and less hazardous method to simultaneously quantify CuO, TiO₂ and ZnO without using HF. It is however important to highlight that the method proposed here is adequate for NP analysis in controlled conditions such as laboratory experiments. Under this setting, background level of the ions of interest (in this case Cu²⁺, Ti⁴⁺ and Zn²⁺) can be determined prior to performing this method. In addition, under controlled conditions, it can be assumed that 100% of the NPs are added by the users, and if in any doubt, the target NP concentrations can be decided to make the environmental NP background irrelevant. Hence, the main limitation of such method is the fact that it can not be applied on its own to determine NP concentrations in environmental sample. However, this is a gap that can be closed by the implementation of different analytical techniques, such as TEM, DLS, FFF and ultrafiltration, in conjunction to our method. This array of analysis can give a suitable characterization and quantification of NPs in environmental samples.

It is also important to highlight that from this work further analytical methods can easily be developed and expanded to other less common NP types such as AgNP, AuNP, CeNP, MnNP among others, as well as to different aqueous and solids matrices.

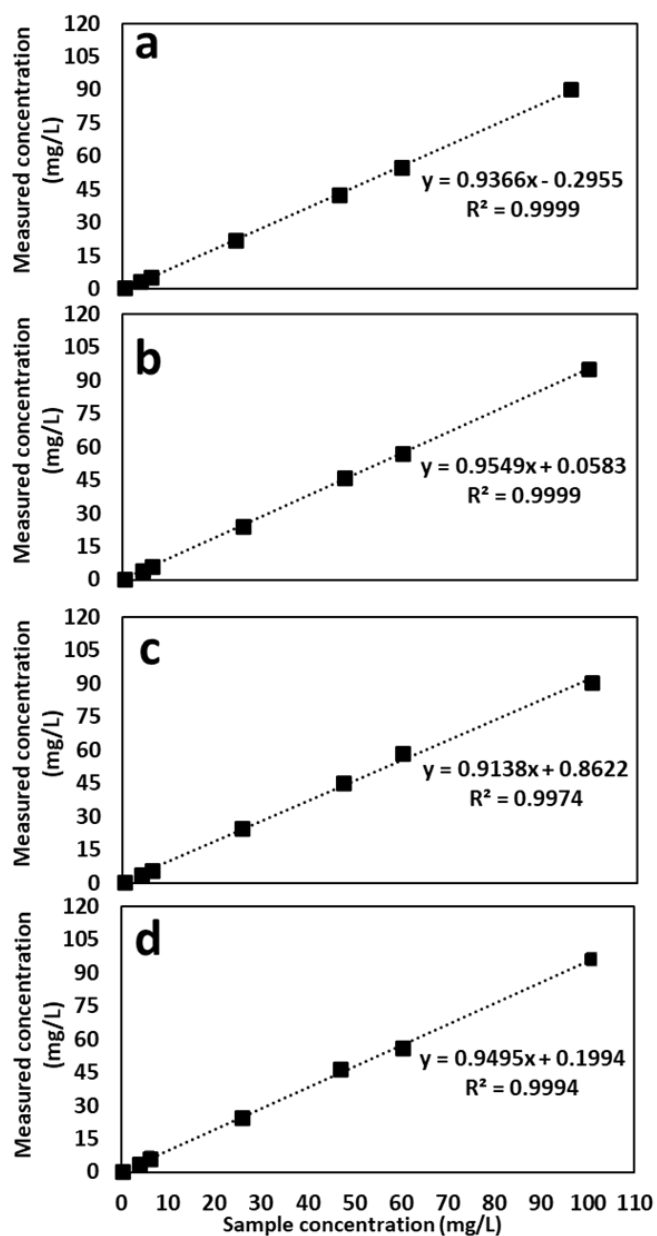


Fig. 3.5 Measured concentration of Cu^{2+} determined with ICP-OES after HNO_3 - H_2SO_4 digestion of samples containing CuO , TiO_2 and ZnO . Cu^{2+} quantification happened simultaneously to Ti^{4+} and Zn^{2+} determination (results shown in Fig. 3.6 and Fig. 3.7) Panel **a** refers to suspensions prepared in water and commercial TiO_2 . Panel **b** refers to suspensions prepared in synthetic wastewater and commercial TiO_2 . Panel **c** refers to suspensions prepared in water and certified reference material for TiO_2 . Panel **d** refers to certified reference TiO_2 suspensions prepared in synthetic wastewater. Every point is shown as average \pm standard deviation ($n=5$). Where not visible, standard deviations covered by markers (size 6).

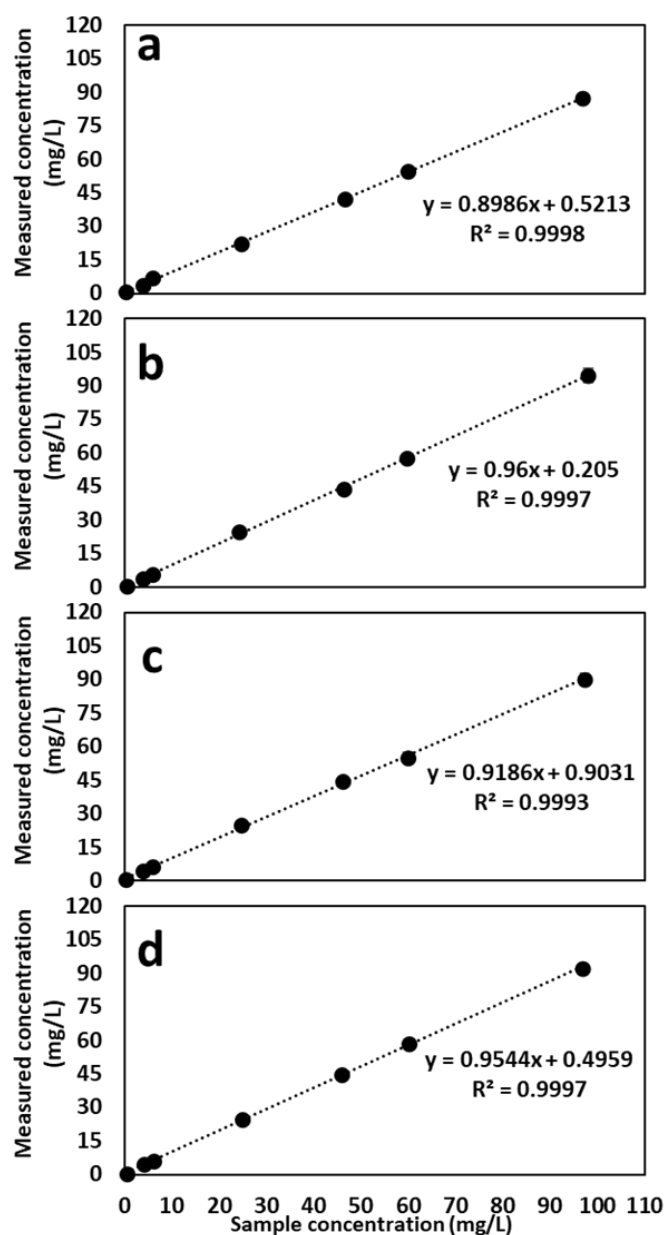


Fig. 3.6 Measured versus nominal concentration of Ti^{4+} determined with ICP-OES after HNO_3 - H_2SO_4 digestion of samples containing CuO , TiO_2 and ZnO . Ti^{4+} quantification happened simultaneously to Cu^{2+} and Zn^{2+} determination (results shown in Fig. 3.5 and Fig. 3.7) Panel **a** refers to suspensions prepared in water and commercial TiO_2 . Panel **b** refers to suspensions prepared in synthetic wastewater and commercial TiO_2 . Panel **c** refers to suspensions prepared in water and certified reference material for TiO_2 . Panel **d** refers to certified reference TiO_2 suspensions prepared in synthetic wastewater. Every point is shown as average \pm standard deviation ($n=5$). Where not visible, standard deviations covered by markers (size 6).

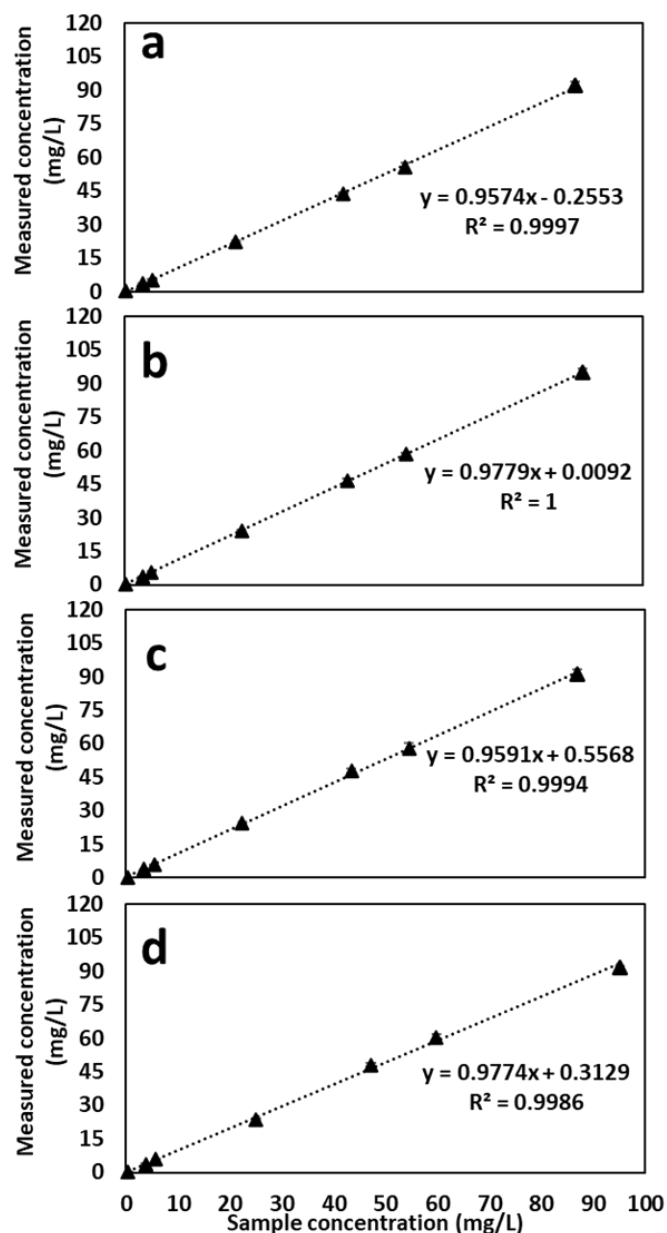


Fig. 3.7 Measured versus nominal concentration of Zn²⁺ determined with ICP-OES after HNO₃ - H₂SO₄ digestion of samples containing CuO, TiO₂ and ZnO. Zn²⁺ quantification happened simultaneously to Cu²⁺ and Ti⁴⁺ determination (results shown in Fig. 3.5 and Fig. 3.6) Panel **a** refers to suspensions prepared in water and commercial TiO₂. Panel **b** refers to suspensions prepared in synthetic wastewater and commercial TiO₂. Panel **c** refers to suspensions prepared in water and certified reference material for TiO₂. Panel **d** refers to certified reference TiO₂ suspensions prepared in synthetic wastewater. Every point is shown as average ± standard deviation (n=5). Where not visible, standard deviations covered by markers (size 6).

3.5 Conclusions, advantages and limitations of the analytical method

The aim of this study was to develop and validate a single analytical method to quantify mixtures of CuO, TiO₂ and ZnO. A microwave assisted HNO₃ - H₂SO₄ digestion paired with ICP-OES analysis was demonstrated to be a robust, precise and accurate procedure to determine the concentrations of CuO, TiO₂ and ZnO mixtures in synthetic wastewater and ultrapure water. The method quantification limits (*MQL*) were found ranging between 0.005 and 0.01 ppm and the metal recoveries met the accepted USEPA standards (90 – 110 %) for a concentrations range varying from 0.40 to 100 ppm irrespective of the NP type. The presence of dissolved organic matter and high ionic strength, a common cause of analytical issues, in the synthetic wastewater did not cause any problem in the quantification of the analytes of interests, hence confirming the robustness of the analytical method. This is suggested to be due to the strength of the MARS aided HNO₃ - H₂SO₄ digestion.

The presented method has been developed from the 3030 G standard method for Ti (APHA/AWWA/WEF 2012). In comparison to such method, the microwave assisted HNO₃ - H₂SO₄ digestion paired with ICP-OES analysis is greatly faster, less hazardous and requires smaller sample size and acids' volumes. In addition, it does not need the highly dangerous and often in many laboratories not permitted HF, hence improving the workplace safety for analysts.

Only recently, ICP-MS techniques have seen a sharp improvement leading to the development of single-particle inductively coupled plasma time-of-flight mass spectrometry (sp-ICP-TOFMS) capable of providing either qualitative and quantitative analysis of NPs (Mehrabi et al. 2019). Therefore, such instruments and the required method development are still uncommon, expensive and time demanding. Contrarily, ICP-OES and microwave assisted acid digestion are routinely used and are still considered reliable method to quantify NPs in controlled environment experimental scenarios. Given the semi-qualitative nature of the analysis (it can discern the type of metal, but lacks in identification of whether the metal is in NP form or dissolved ion) these techniques cannot be used alone to provide NP determination in real environment samples. However, this obstacle can be overcome with the incorporation of other qualitative analysis such as TEM-EDS or EELS, DLS and sequential filtration and ultrafiltration to evaluate the chemical signature, particle distribution and isolate the

dissolved fraction from the colloidal in real environmental samples (Polesel et al. 2018).

Overall, this work provides first evidence of a single analytical method to determine the content of mixtures of three of the most common and widely used NPs such as CuO, TiO₂ and ZnO in aqueous matrices. This method has the potential, through further method development, to be applied to a huge range of different NP mixtures in a variety of environmental matrices, aqueous as well as solid ones, like soil and sludge.

3.6 Bibliography

- APHA/AWWA/WEF (2012) Standard Methods for the Examination of Water and Wastewater. Stand Methods 541. [https://doi.org/ISBN 9780875532356](https://doi.org/ISBN%209780875532356)
- Cascio C, Geiss O, Franchini F, et al (2015) Detection, quantification and derivation of number size distribution of silver nanoparticles in antimicrobial consumer products. *J Anal At Spectrom* 30:1255–1265. <https://doi.org/10.1039/c4ja00410h>
- CFC (1986) Definition and Procedure for the Determination of the Method Detection Limit—Revision 1.11. Code Fed Regul Title 40, Part 136, Append B
- Eduok S, Hendry C, Ferguson R, et al (2015) Insights into the effect of mixed engineered nanoparticles on activated sludge performance. *FEMS Microbiol Ecol* 91:1–9. <https://doi.org/10.1093/femsec/fiv082>
- Fang J, Shijirbaatar A, Lin D hui, et al (2017) Stability of co-existing ZnO and TiO₂nanomaterials in natural water: Aggregation and sedimentation mechanisms. *Chemosphere* 184:1125–1133. <https://doi.org/10.1016/j.chemosphere.2017.06.097>
- Gottschalk F, Sondere T, Schols R, Nowack B (2009) Modeled Environmental Concentrations of Engineered Nanomaterials for Different Regions. *Environ Sci Technol* 43:9216–9222. <https://doi.org/10.1021/es9015553>
- Hua J, Peijnenburg WJGM, Vijver MG (2016) TiO₂ nanoparticles reduce the effects of ZnO nanoparticles and Zn ions on zebrafish embryos (*Danio rerio*). *NanoImpact* 2:45–53. <https://doi.org/10.1016/j.impact.2016.06.005>
- Joško I, Oleszczuk P, Skwarek E (2017) Toxicity of combined mixtures of nanoparticles to plants. *J Hazard Mater* 331:200–209. <https://doi.org/10.1016/j.jhazmat.2017.02.028>
- Kiser MA, Westerhoff P, Benn T, et al (2009) Titanium nanomaterial removal and release from wastewater treatment plants. *Environ Sci Technol* 43:6757–6763. <https://doi.org/10.1021/es901102n>
- Liu Y, Wang S, Wang Z, et al (2018) Tio₂, sio₂ and zro₂ nanoparticles synergistically provoke cellular oxidative damage in freshwater microalgae. *Nanomaterials* 8:. <https://doi.org/10.3390/nano8020095>
- Lomer MCE, Thompson RPH, Commisso J, et al (2000a) Determination of titanium

- dioxide in foods using inductively coupled plasma optical emission spectrometry. *Analyst* 125:2339–2343. <https://doi.org/10.1039/b006285p>
- Lomer MCE, Thompson RPH, Commisso J, et al (2000b) Determination of titanium dioxide in foods using inductively coupled plasma optical emission spectrometry. *Analyst* 125:2339–2343. <https://doi.org/10.1039/b006285p>
- Lu G, Yang H, Xia J, et al (2017) Toxicity of Cu and Cr Nanoparticles to *Daphnia magna*. *Water Air Soil Pollut* 228:. <https://doi.org/10.1007/s11270-016-3206-3>
- Mackevica A, Olsson ME, Hansen SF (2017) The release of silver nanoparticles from commercial toothbrushes. *J Hazard Mater* 322:270–275. <https://doi.org/10.1016/j.jhazmat.2016.03.067>
- Mehrabi K, Gundlach-Graham A, Günther D, Gundlach-Graham A (2019) Single-particle ICP-TOFMS with online microdroplet calibration for the simultaneous quantification of diverse nanoparticles in complex matrices. *Environ Sci Nano* 6:3349–3358. <https://doi.org/10.1039/c9en00620f>
- Moore MN (2006) Do nanoparticles present ecotoxicological risks for the health of the aquatic environment? *Environ Int* 32:967–976. <https://doi.org/10.1016/j.envint.2006.06.014>
- Mueller NC, Nowack B (2008) Exposure modelling of engineered nanoparticles in the environment. *Environ Sci Technol* 42:44447–53. <https://doi.org/10.1021/es7029637>
- OECD (2001) Simulation Test - Aerobic Sewage Treatment: 303A: Activated Sludge Units. OECD
- Poitras EP, Levine MA, Harrington JM, et al (2016) Coupled Plasma Mass Spectrometry. 163:184–192. <https://doi.org/10.1007/s12011-014-0141-2>.Development
- Polesel F, Farkas J, Kjos M, et al (2018) Occurrence, characterisation and fate of (nano)particulate Ti and Ag in two Norwegian wastewater treatment plants. *Water Res* 141:19–31. <https://doi.org/10.1016/j.watres.2018.04.065>
- Quadros ME, Pierson R, Tolve NS, et al (2013) Release of silver from nanotechnology-based consumer products for children. *Environ Sci Technol* 47:8894–8901. <https://doi.org/10.1021/es4015844>
- Reed RB, Faust JJ, Yang Y, et al (2014) Characterization of nanomaterials in metal

colloid-containing dietary supplement drinks and assessment of their potential interactions after ingestion. *ACS Sustain Chem Eng* 2:1616–1624.

<https://doi.org/10.1021/sc500108m>

Rogers KR, Navratilova J, Stefaniak A, et al (2018) Characterization of engineered nanoparticles in commercially available spray disinfectant products advertised to contain colloidal silver. *Sci Total Environ* 619–620:1375–1384.

<https://doi.org/10.1016/j.scitotenv.2017.11.195>

Tong T, Wilke CM, Wu J, et al (2015) Combined Toxicity of Nano-ZnO and Nano-TiO₂: From Single- to Multinanomaterial Systems. *Environ Sci Technol* 49:8113–8123. <https://doi.org/10.1021/acs.est.5b02148>

U.S. Environmental Protection Agency (1987) An Interlaboratory study of inductively coupled plasma atomic emission spectroscopy method 6010 and digestion method 3050

Wamer WG, Yin JJ, Wei RR (1997) Oxidative damage to nucleic acids photosensitized by titanium dioxide. *Free Radic Biol Med* 23:851–858.

[https://doi.org/10.1016/S0891-5849\(97\)00068-3](https://doi.org/10.1016/S0891-5849(97)00068-3)

Wang Y, Baker LA, Helmeczi E, Brindle ID (2016) Rapid high-performance sample digestion of base metal ores using high-intensity infrared radiation with determination by nitrogen-based microwave plasma optical spectrometry. *Anal Chem Res* 7:17–22. <https://doi.org/10.1016/j.ancr.2016.02.002>

Yu R, Wu J, Liu M, et al (2016) Toxicity of binary mixtures of metal oxide nanoparticles to *Nitrosomonas europaea*. *Chemosphere* 153:187–197.

<https://doi.org/10.1016/j.chemosphere.2016.03.065>

Chapter 4

Insights into the removal mechanisms of nanoparticles and nanoparticle mixtures by activated sludge biomass

4.1 Summary

Wastewater treatment plants are an important barrier in the prevention of nanoparticle (NP) release into the environment. This study shows that the currently operated activated sludge technology copes efficiently with different loading scenarios of some of the most commonly used NPs. We investigated how activated sludge biomass could remove high concentrations of CuO, TiO₂ and ZnO NPs, in systems containing either one NP type or a mixture; the association between NPs and activated sludge biomass happens quickly and stabilizes within 30-90 minutes. The removal of single type NPs exceeds 90% irrespective of concentrations and types. Similarly, the biomass could retain over 90% of the total CuO, TiO₂ and ZnO as a mixture of NPs at 9 and 90 mg/L, while less (around 75%) was retained at 180 mg/L. The impact of the activated sludge liquor (i.e., liquid with biomass removed) on CuO, TiO₂ and ZnO removal and behaviour was assessed. NP removal varied from 19 to 48% in single NP systems and 58 and 90% in mixture experiments. The z-potential and Z-hydrodynamic diameters were also analysed to study the NP stability. In biomass-free liquor, CuO, TiO₂ and ZnO may be partially stabilized by the dissolved organic matter fraction as shown by the lack of aggregation and the absence of a point of zero charge, which was only observed in ultrapure water. However, despite stabilization, some aggregation in liquor does occur, which leads to partial CuO, TiO₂ and ZnO removal by sedimentation. Nevertheless, efficient NP removal relies on the presence of biomass to prevent NPs entering receiving water bodies.

4.2 Introduction

The increased exploitation of nanotechnology in the last decades has resulted in a significant number of nanoparticulate products currently available on the market. Nanoparticles (NPs) are utilized across a wide range of sectors including pharmaceutical, cosmetic, chemical, textile and food industries (Vance et al. 2015). The actual widespread use of nano-based products has led to the inevitable consequences of different NPs being released into sewer networks from urban and industrial effluents (Benn and Westerhoff 2008, Farkas et al. 2011, Mackevica et al. 2017). Once in the wastewater stream, NPs are transported through the sewerage network with no or minimal loss (Kaegi et al. 2013) and eventually enter wastewater treatment plants (WWTPs) (Kiser et al. 2009). Significantly, it has been shown that NPs pass through the preliminary and primary treatment stages of WWTPs with little removal (Hou et al. 2012), thus reaching the activated sludge treatment stage. Hence, the WWTPs' role, and especially by activated sludge treatment, is crucial in preventing NPs from being released into receiving water bodies. It is therefore imperative to investigate the mechanisms involved in the removal process of single NP types and their mixtures by activated sludge biomass.

Most of the studies on the removal of nanomaterials in WWTPs have so far addressed single NP conditions. However, the co-occurrence of different NPs is the most likely scenario due to the widespread array of nano-based products currently available (Yu et al. 2016). There is uncertainty regarding the possible interactions that the simultaneous presence of more NP types in WWTP would cause (Eduok et al. 2015). Joško et al. (2017) reported controversial results when comparing the stability of an array of binary mixtures of CuO, ZnO, TiO₂, Cr₂O₃ and Fe₂O₃ versus individually spiked NPs. After 30 min and after 3 days, some of the tested combined NPs showed increased aggregation levels in respect to single NPs, while other combinations had the opposite behaviour. However, the majority of the combinations tested showed a wider particle size distribution after 3 days than after 30 min, which suggests that different NP types aggregate over time and that this therefore impacts their environmental fate and behaviour in terms of solubility, absorption and aggregation. In contrast, Fang et al. (2017), conducted a study on the stability of co-existing TiO₂ and ZnO dispersed in natural water collected from a Chinese canal. The results showed

that when combined, nanomaterials compete to interact with natural colloids and dissolved organic matter. This leads to hindrance on NP collision, which results in diminished aggregation. However, the authors also mentioned that homo-aggregation, hetero-aggregation between NPs and colloids, TiO₂ and ZnO and hetero-aggregation were all contributing to NP removal. However, this is still controversial as increased size distribution of coexisting TiO₂ and ZnO has been reported, although both the nanomaterials were negatively charged in aqueous suspensions. In spite of the electrostatic repulsion, combined TiO₂ and ZnO formed larger aggregates with respect to single NPs due to an increased frequency of collisions (Tong et al. 2014). It is therefore necessary to further develop our understanding of how co-existing nanomaterials would influence their environmental fate, behavior and removal efficiency during wastewater treatment. The effect induced on aggregation and sedimentation by high concentrations may be particularly relevant in case of triple NP-type mixtures spiked at high dosages, like presented in this study.

In light of this, the assessment of whether the available technologies can cope with current and future NP loading scenarios still requires elucidation, especially with regards to NP mixtures. To date, few have studied the interactions between different classes of NPs in WWTP. This relatively new field of NP research has so far focused on ecotoxicological assessment and bulk removal amounts. It has been reported that an pilot-scale activated-sludge system operating for 315 days could efficiently remove mixtures of Ag⁰, TiO₂ and ZnO, loaded at concentrations varying between 11 and 124 mg/kg of biomass (Eduok et al. 2015). Moreover, from the comparison between activated sludge biomass affinity for mixture of NPs and the equivalent salts, the authors reported NP sorption on biomass to be at least two times higher than the respective salts. Overall, the removal rate of NPs was high for the whole duration of the long term experiment, and no differences were noted in comparison with other studies assessing the removal of singly added Ag⁰, TiO₂ (Kiser et al. 2010) and ZnO (Cháuque et al. 2014). In comparison, Yang et al. (2015) demonstrated that a continuously operated activated-sludge sequencing batch reactor (SBR) could remove over the 95% of the added nC60, but the addition of AgNP (2 mg/L) led to SBR disruption and caused short-term fall in nC60 and COD removal efficiency; the system recovered to its performances prior to AgNP “pulse” in 4 days. Although the overall

bioreactors functionality was stable for the majority of the duration of the experiments, the authors recognized that the NP removal could be greatly impacted by short-term, “pulse” inputs from different NPs. Pulse events are significant as WWTPs often experience damaging and challenging pulses of contaminants, for example, during unregulated release events. Therefore, exploration of the ability of a WWT plant to remove a specific pollutant should consider higher-than-expected concentrations.

While previous studies have focused on ecotoxicology and bulk removal quantities, to date, very little has been done to explore the mechanisms and removal profile of NP mixtures by activated sludge biomass. Moreover, previous research have adopted NP concentrations, in the range of $\mu\text{g/L}$ to mg/L , based on the predicted environmental concentrations (PEC) of nanomaterials (Mueller and Nowack 2008, Gottschalk et al. 2009). However, as consequence of the continual rise in nanomaterial production and the potential for high concentration pulses to pass through WWTPs, efficiency, mechanisms and removal profile at concentration exceeding current PEC should be explored.

The objectives of this study were to evaluate the profile and mechanisms of the short-term removal of CuO, TiO₂ and ZnO either singularly or as mixtures by activated sludge biomass and biomass-free liquor collected from a real WWTP. The aim of this work was to provide an initial assessment on the capacity of activated sludge treatment to efficiently remove NP mixture at concentrations level that could occur either in the future or during pulse events. Additionally, CuO, TiO₂ and ZnO Z-average diameter and zeta potential in biomass-free liquor were studied to help understand the role of aggregation as a removal mechanism.

4.3 Materials and Methods

4.3.1 Activated sludge collection and biomass free liquor preparation

Activated sludge was collected from a municipal sewage plant serving the urban area of Glasgow, UK. This conventional biological full-scale WWTP includes preliminary, primary and secondary treatments. The samples were taken from the aeration tank and brought back to the lab within one hour where they were aerated and equilibrated to room temperature of 22 ± 1 °C.

Some experiments were undertaken in biomass-free liquor (i.e., the liquid fraction) to determine non-biomass related NP removal processes. For this, an aliquot of the well-mixed sampled activated sludge was filtered through glass microfiber filter (GF/F grade, Whatman Inc.) and then through a 0.45 μm acetate cellulose syringe filter (VWR international LLC) to obtain the biomass-free liquor.

4.3.2 Nanoparticle removal by activated sludge biomass and in biomass-free liquor

Nanoparticle removal batch tests with activated sludge biomass (TSS = 2000 mg/L) and biomass-free liquor were performed in a series of glass vials. In single NPs experiments, the nanomaterials were added to achieve final concentrations of 9, 90 and 180 mg/L of CuO, TiO₂ and ZnO, while only 9 and 180 mg/L were tested in the biomass-free liquor experiments. Similarly, mixtures experiments were run with all the three NPs spiked at the same concentration of 9, 90 and 180 mg/L per NP type (creating total NP concentrations of 27, 270 and 540 mg/L). All the three levels of CuO, TiO₂ and ZnO mixtures were tested in either activated sludge biomass tests and in biomass-free liquor.

In the single NP experiments, 27 ml of wastewater (with or without biomass) were spiked with 3 ml of NP suspension, creating a final volume of 30 ml. In mixed NP systems, three separate stock solutions were prepared as for single NP experiments. Then 27 ml of either activated sludge or biomass-free liquor were spiked with 1 ml of each NP suspension to achieve a final volume of 30 ml. The glass vials were then agitated at 250 rpm on an orbital shaker to obtain a homogeneous distribution throughout the experiment. Specific agitation times, similarly to Kiser *et al.*, 2010, varying from 5 to 180 min were applied. After agitation the vials were removed from

the shaker and the biomass was allowed to settle by gravity for 20 min. Afterwards, 14 ml of supernatant (effluent) were carefully collected, to avoid extraction of biomass, and acidified with two drops of concentrated HNO₃ (69%).

4.3.3 Nanoparticle quantification

Acid digestion followed by analysis with inductively coupled plasma optical emission spectroscopy (ICP-OES, iCAP 6200, Thermo fisher scientific) was used to quantify Cu²⁺, Ti⁴⁺ and Zn²⁺ as proxy of CuO, TiO₂ and ZnO. Shortly, 6 ml of samples were transferred into 55 ml teflon MARSXpress Vessels (CEM Corporation) to which 2 ml of HNO₃ (69%) and 2 ml of H₂SO₄ (95%) were added. The samples were then put in microwave assisted reaction system (MARS 5) and processed with the following program: 15 min ramp to 190 °C, 15 min hold, 15 min ramp to 200 °C, 15 min hold followed by 60 min of cooling to room temperature. The digested samples were then transferred into 50 ml volumetric flasks and diluted with ultrapure water. Calibration curve was obtained with matrix matching (4% HNO₃ and 4% H₂SO₄) certified standards of Cu²⁺, Ti⁴⁺ and Zn²⁺ at concentrations of 0.2, 2, 10, and 20 ppm. Yttrium (Y³⁺) at concentration of 5 ppm was used as internal standard. Prior to the beginning of the experiments, spike and recovery of Cu²⁺, Ti⁴⁺ and Zn²⁺ from acid digestion of CuO, TiO₂ and ZnO were assessed. Samples containing known amount of NPs were digested and then the concentration of Cu²⁺, Ti⁴⁺ and Zn²⁺ were measured and the metal recovery was calculated.

4.3.4 Nanoparticle characterization, dissolution and stability in ultrapure water and biomass free liquor

TiO₂ nanopowder (anatase, particle size <25 nm, 99.7% purity, catalog number 637254) and ZnO suspension (20% wt in water, particle size <100 nm, catalog number 721077) were purchased from Sigma-Aldrich Corp, St. Louis, MO, USA. CuO nanopowder (particle size 30-50 nm, 99% purity, catalog number 44663) was obtained from Alfa Aesar (Heysham, Lancashire, UK). Freshly made suspensions were prepared before each experimental run. All the suspensions were prepared in ultrapure water with pH adjusted to 11 ± 1 with 0.1 M NaOH and sonicated for 15 minutes with an ultrasonic processor UP200St equipped with sonotrode S26d7 (Hielscher

Ultrasonic GmbH, Teltow, Germany) with 70 W, amplitude 100% and frequency of 26 ± 1 kHz.

Samples for transmission electron microscopy were prepared by dispersing suspensions of 5000 mg/L in ultrapure water with pH adjusted to 11 ± 1 with 0.1 M NaOH and sonicating for 15 minutes, following by dropping a single drop onto a holey carbon film on a 200 mesh copper grid (Agar Scientific Ltd, Stansted, UK) and allowing it to dry. The size, shape and chemical composition of each nanoparticle type was characterized with scanning transmission electron microscopy using a JEOL ARM200F (JEOL UK, Welwyn Garden City, UK) operated at 200 kV, and with a condenser aperture set to give a beam convergence angle of 29 mrad and gun lens setting to give a probe current of ~ 400 pA. Imaging was performed using high angle annular dark field mode, whilst elemental composition was studied using electron energy loss spectroscopy (EELS) with a Gatan GIF Quantum ER spectrometer (Gatan Inc., Pleasanton, CA) using a camera length and aperture combination that gives an acceptance angle of 36 mrad. The data was quantified using standard routines with Gatan Digital Micrograph (Gatan Inc., Pleasanton, CA). Comparisons to standard spectra from the EELS database (<https://eelsdb.eu>) (Ewels et al. 2016) were used, where appropriate. Size distributions were measured using manual measurement of the length, l , and width, w , of $> X$ nanoparticles in each sample using Digital Micrograph, followed by the determination of an average diameter (as $d = \sqrt{wl}$) and an average aspect ratio ($a = l/w$) for each system.

The stability of CuO, TiO₂ and ZnO suspensions (100 mg/L) were studied by assessing the hydrodynamic diameter (h_D) and Z-potential as function of pH in ultrapure water and biomass free liquor at 25 °C by dynamic light scattering (DLS) with Zetasizer Nano ZSP (Malvern, UK) equipped with He-Ne laser 633nm light source and detection angle of 175° (back scatter). The pH of ultrapure water and biomass-free liquor were adjusted to a range varying from 3 to 12 with 0.1 M KOH and 0.1 M HCl prior to sonication. The NPs were then sonicated for 15 minutes and then agitated at 250 rpm for 30 minutes. Samples of properly mixed suspensions were collected with 2 ml syringes and immediately transferred in folded capillary zeta cells. For Z-potential evaluation, the Smoluchowski approximation model was used. All the

measurement of polydispersity index (PdI), an index used to estimate the average uniformity of nanoparticle suspensions, were below 0.76.

CuO and ZnO dissolution in biomass free-liquor was determined over a period of 3 hours in both single NP and mixtures systems. The same experimental set-up adopted to assess the NP removal was used, with the only difference that no sedimentation time was applied. The samples were centrifuged at 11,000x g for 30 min and then 9 ml of the supernatant were withdrawn and filtered using 0.2 μm acetate cellulose syringe filter (VWR international LLC) and the filtrate acidified with 2 drops of concentrated HNO_3 (69%) and then analyzed with ICP-OES.

4.3.5 Analytical methods

Total suspended solid (TSS) was determined according to the standard methods (APHA/AWWA/WEF 2012), while chemical oxygen demand (COD) was measured with cuvette test (Hach, Manchester, UK). Electrical conductivity, pH and total dissolved solids were measured with a multi pH Meter (Mettler Toledo FE20, Switzerland). Elemental contents in activated sludge and biomass-free liquor were measured with ICP-OES. Similarly, Cu^{2+} , Ti^{4+} and Zn^{2+} were analyzed, and batches with background Cu^{2+} , Ti^{4+} and Zn^{2+} concentrations above 1% of the target experimental concentrations were not used. All the chemicals used were analytical grade.

4.4 Results and discussion

4.4.1 Nanoparticles characterization

Fig. 4.1 shows representative images nanoparticle clusters of the three represented in this work.

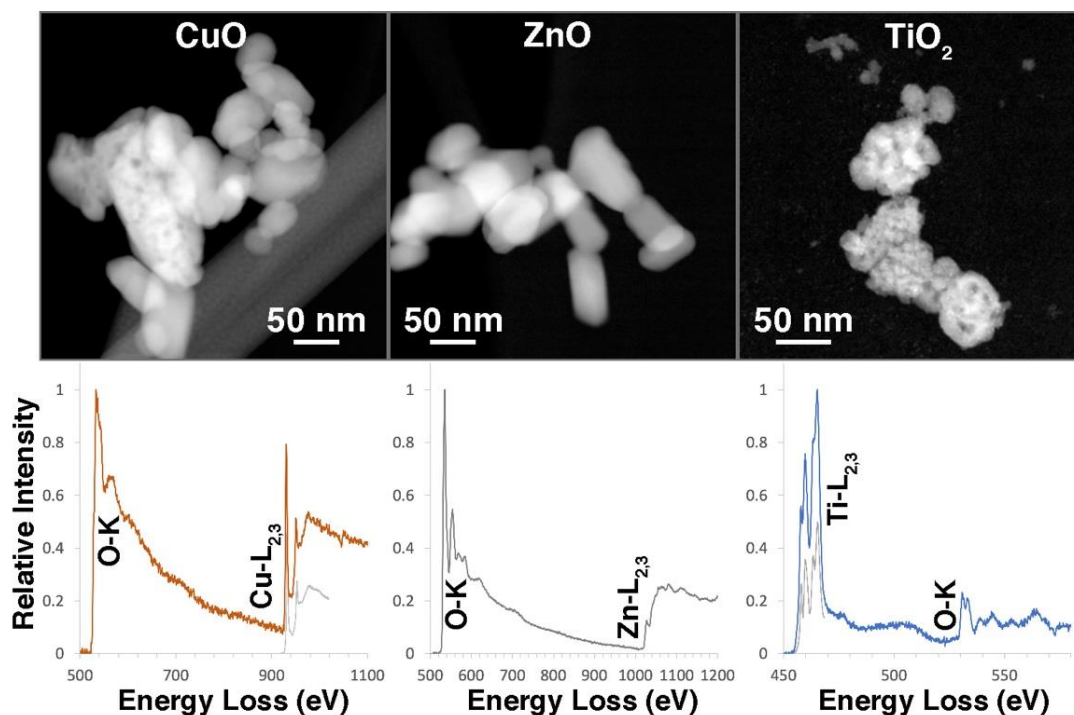


Fig. 4.1 High angle annular dark field scanning transmission electron microscopy images of the CuO, ZnO and TiO₂ nanoparticles, together with representative EELS spectra for each type of nanoparticle, with comparisons to standards for CuO (Ngantcha et al. 2005) and anatase TiO₂ (Bertoni et al. 2006), both in pale grey below the experimental spectrum.

Table 4.1 summaries the size distributions of nanoparticle sample images. CuO diameters were broadly distributed, 54.5 ± 26.1 nm (size distribution ranged from 30.7 to 147.1 nm); TiO₂ had a tighter distribution of 32.5 ± 5.3 nm (with sizes ranging from 22.1 to 51.4 nm), while ZnO nanoparticles had a fairly narrow diameter range of 50.3 ± 12.5 nm (ranging between 25.4 and 102.1 nm).

Table 4.1 Nanoparticle characterization in ultrapure water and biomass-free liquor. Primary size determined via transmission electron microscopy (TEM), hydrodynamic diameter and Z-potential via dynamic light scattering (DLS).

	Primary size (water, pH = 11 ± 1)	Hydrodynamic diameter (water, pH = 11 ± 1)	Z-potential (water, pH = 11 ± 1)	Hydrodynamic diameter (biomass-free liquor, pH = 7.1 ± 0.5)	Z-potential (biomass-free liquor, pH = 7.1 ± 0.5)
Units	nm	nm	mV	nm	mV
CuO	54.5 ± 26.1	251 ± 7.4	-44.9 ± 1.2	326.9 ± 13.8	-13.4 ± 0.7
TiO₂	32.5 ± 5.3	202.3 ± 35.3	-39.9 ± 1.3	325.3 ± 21.3	-15.2 ± 0.2
ZnO	50.3 ± 12.5	214.2 ± 4.5	-34.9 ± 0.3	302.7 ± 9.7	-20.4 ± 0.3

Electron energy loss spectroscopy (EELS) spectra for each type of nanoparticle matched expectations and are also shown in Fig. 4.1. CuO showed well defined white lines at the Cu-L_{2,3} edge, as expected for this oxide (Ngantcha et al. 2005). ZnO showed a weak white line at the L₃ edge and well-defined peaks on the O-K edge, which were very similar in shape to those from ZnO synthesized by colleagues in the School of Chemistry at the University of Glasgow (not shown; personal communication). TiO₂ showed a Ti-L_{2,3} edge, which matched well to the details of peak splitting expected for anatase as demonstrated by a standard spectrum for this phase, acquired at slightly higher energy resolution, and shown below the experimental spectrum (Ewels et al. 2016).

DLS analysis revealed a hydrodynamic diameter (h_D) of 251 ± 7.4 nm, 202.3 ± 35.3 nm and 214.2 ± 4.5 nm for CuO, TiO₂ and ZnO, respectively; and their respective Z-potential values were -44.9 ± 1.2 mV, -39.9 ± 1.3 mV and -34.9 ± 0.3 mV in ultrapure water at pH 11 ± 1 . A summary of NP characterization is provided in Table 4.1. When in biomass-free liquor, h_D were 326.9 ± 13.8 nm for CuO, 325.3 ± 21.3 nm for TiO₂ and 302.7 ± 9.7 nm for ZnO. The relative Z-potential measurements were -13.4 ± 0.7 mV, -15.2 ± 0.2 mV and -20.4 ± 0.3 mV. All three NPs showed an increase in h_D and reduced Z-potential in biomass-free liquor. This is likely to be due to interaction with the negatively charged dissolved organic matter (DOM). Such effect has previously been recorded. For example, the presence of alginate and Suwannee River humic acids in water increased TiO₂ stability. According to the authors, the adsorption of the organic compounds onto the NPs would provide them a negatively charged electrosteric repulsion (Loosli et al. 2013). In addition, Zhang et al. (2009) studied the effect of Suwannee River NOM as surrogate of real NOM, on the stability of ZnO, NiO, TiO₂, Fe₂O₃ and SiO₂. The authors concluded that the adsorption of organic molecules onto NPs may impart the surface charge and enhance their negative z-potential. This could be confirmed by replicating such studies in which the stability of NP suspension in ultrapure water against DOM-spiked water over a prolonged period of time. For future works, it would also be of great interest to assess whether the same effect occurs when NPs are present in mixture rather than as single NP type.

Overall, among the nanomaterials tested, ZnO suffered the smallest increase in h_D and the lowest Z-potential reduction. The data obtained by NP characterization in biomass-free liquor may suggest that ZnO could be least affected by aggregation.

4.4.2 Removal of singularly spiked CuO, TiO₂ and ZnO by activated sludge biomass

The physiochemical characterization of activated sludge and biomass-free liquor samples are presented in Table 4.2. On average, mixed liquor suspended solids (MLSS) samples had a pH of 7.1 ± 0.5 , total dissolved solids (TDS) of 320.1 ± 37.4 mg/L, conductivity of 593.6 ± 60.4 $\mu\text{S}/\text{cm}$, total suspended solids (TSS) of 2292.9 ± 136.7 mg/L and chemical oxygen demand (COD) of 101.7 ± 39.3 mg O₂/L.

Measurement of Cu²⁺, Ti⁴⁺ and Zn²⁺ concentrations activated sludge and biomass-free liquor ranged from a maximum average of 0.78 ± 0.55 mg/L to an average minimum of 0.05 ± 0.07 mg/L. Not surprisingly metal concentration were higher in the activated sludge in comparison to the liquid phase to remark the effectiveness of the activated sludge treatment. Interestingly, Ti⁴⁺ recorded the highest overall concentrations due to two independent samples that were measured > 2 mg Ti⁴⁺ /L in activated sludge and around 1 Ti⁴⁺ /L. These samples were re-analyzed and the results were confirmed. Cu²⁺, Ti⁴⁺ and Zn²⁺ background concentrations were always measured prior to the execution of the experiments, and that batch of samples would be rejected if above 1% of the target experimental concentrations.

Table 4.2 Activated sludge and biomass-free liquor characteristics

	Units	Activated sludge	Biomass-free liquor
pH		7.1 ± 0.5	7.0 ± 0.4
TDS	mg/L	320.1 ± 37.4	316.4 ± 35.3
Conductivity	µs/cm	593.6 ± 60.4	586.7 ± 56.1
TSS	mg/L	2292.9 ± 136.7	ND
COD	mg O ₂ /L	101.7 ± 39.3	91.1 ± 35.9
DOC	mg C/L	ND	7.71 ± 0.47
Cu	mg/L	0.13 ± 0.09	0.05 ± 0.07
Ti	mg/L	0.78 ± 0.55	0.31 ± 0.21
Zn	mg/L	0.21 ± 0.08	0.08 ± 0.06
Al	mg/L	ND	0.02 ± 0.01
Ca	mg/L	ND	30.45 ± 2.15
Fe	mg/L	ND	0.04 ± 0.02
K	mg/L	ND	11.81 ± 2.11
Mg	mg/L	ND	5.90 ± 0.61
Na	mg/L	ND	60.78 ± 4.24

*ND = Not determined

Overall, activated sludge biomass was capable of removing > 90% of NPs irrespective of starting concentrations (Fig. 4.2a, 4.2b, 4.2c). However, the removal profiles and amounts appear to depend on the NP type.

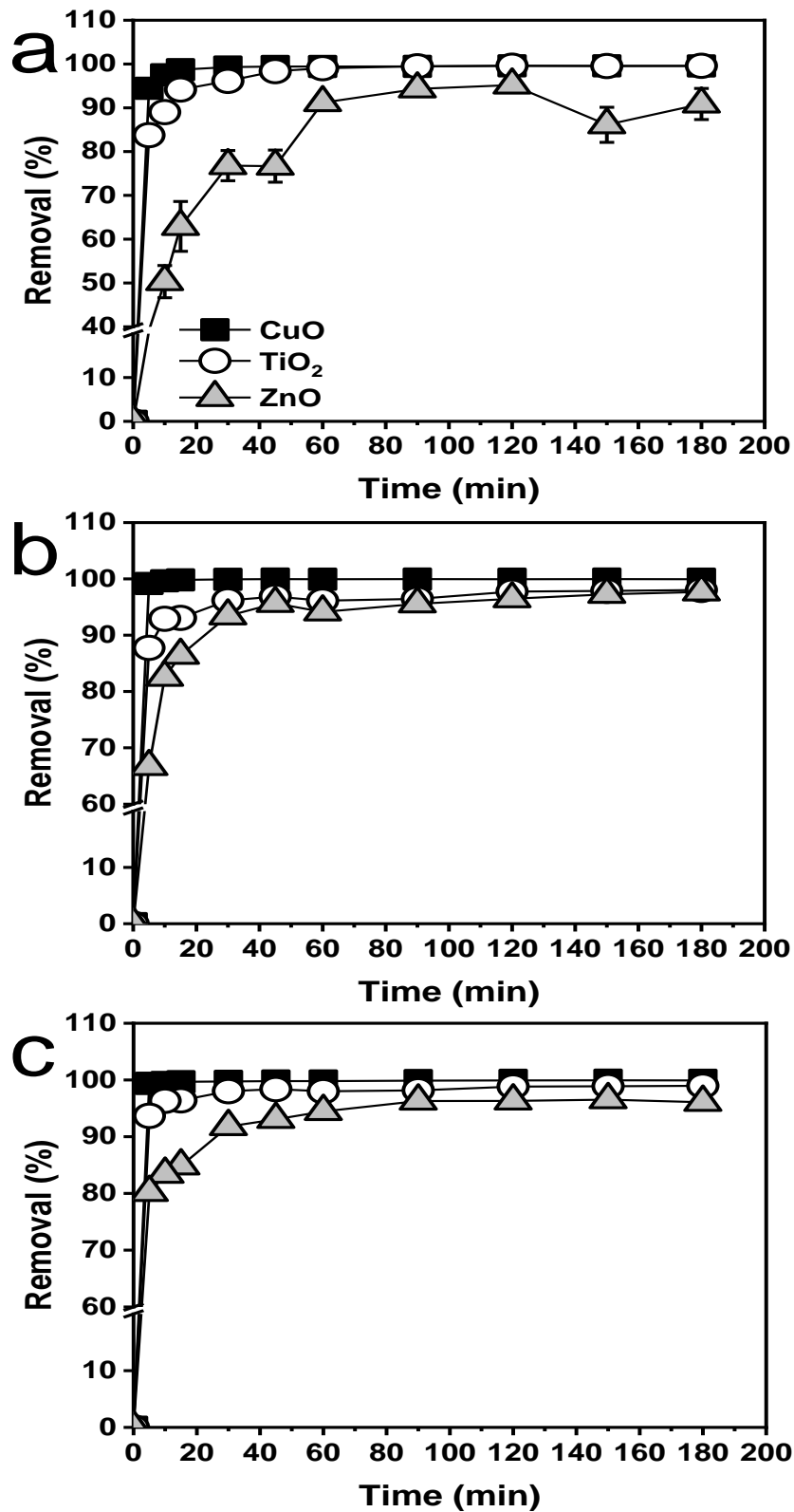


Fig. 4.2 Removal profile ($n=3 \pm$ standard deviation) of singularly spiked CuO, TiO₂ and ZnO reported as removal percent. Nanomaterials were spiked in presence of activated sludge biomass at concentrations of 9 mg/L (a), 90 mg/L (b) and 180 (c). Where not visible, standard deviations covered by markers (size 9).

The highest removal efficiency was CuO, as > 99.5% of the NP loads were removed by the activated sludge biomass. Similarly, the amount of TiO₂ removal was > 98% in all the experimental conditions. Slightly lower performances were observed for ZnO, as the quantities removed varied from 90.9 ± 3.5% at 9 mg/L loading, 97.7 ± 0.1% at 90 mg/L, and 96.1 ± 0.2% at 180 mg/L. These findings are in line with previous studies assessing the capacity of 3600 mg/L of activated sludge biomass to remove TiO₂ and ZnO at concentrations of 10 and 50 mg/L (Barton et al. 2014). Moreover, the same authors observed a similar pattern, with ZnO showing the lowest removal amount compared to TiO₂, and it increased at higher doses. Similarly, Park et al. (2013) found that in a similar system, operated for 25 hours with 3000 mg/L of mixed liquor suspended solids (MLSS), over 95% of TiO₂ spiked at 10 mg/L were removed in one hour. Our results are consistent with these findings, which showed rapid and effective removal of NPs by activated sludge biomass. Moreover, our work extended these findings by showing that activated sludge biomass can efficiently remove CuO, TiO₂ and ZnO NPs at higher concentrations of up to 180 mg/L within this timeframe, and the removal efficiency appears to be NP type dependent.

Although activated sludge biomass has great potential to efficiently remove high concentrations of NPs, its short-term efficiency may vary according to the type of nanomaterials. Over 94% of total CuO was removed in less than 10 minutes irrespective of the concentrations; the percent of removed TiO₂ exceeded 95% after 30 minutes at the concentrations of 9 and 90 mg/L; only 10 minutes were necessary to remove more than 95% at 180 mg/L. Although the overall removal performances of ZnO were still high, activated sludge could remove 94-95% of NPs in 90 minutes at all concentrations used here.

This could suggest that activated sludge biomass has a slightly lower affinity for ZnO in comparison to CuO and TiO₂. Alternatively, it is well known that ZnO is susceptible to dissolution in many water matrices (Reed et al. 2012, Li et al. 2013), as well as wastewater (Lombi et al. 2012). Therefore, CuO and ZnO dissolution at concentration of 9, 90 and 180 mg/L was assessed in biomass-free liquor. The concentration of released Zn²⁺ ions after 180 min varied from 0.42 ± 0.01 mg/L (9

mg/L ZnO level), 0.78 ± 0.01 (90 mg/L ZnO) and 0.79 ± 0.4 mg/L (180 mg/L ZnO). CuO dissolution ranged from 0.014 ± 0.001 to 0.008 ± 0.001 and 0.101 ± 0.004 mg Cu^{2+}/L (9, 90 and 180 mg/L, respectively) (Fig. 4.3).

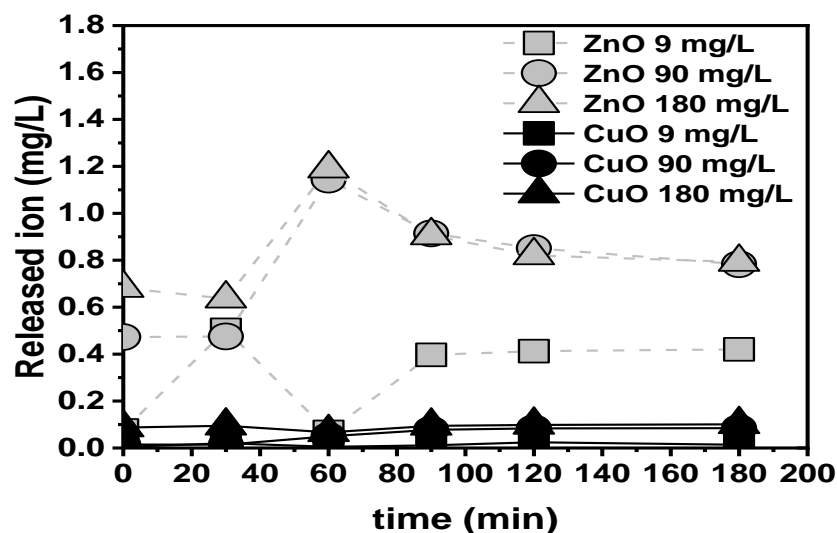


Fig. 4.3 Concentration of released Cu^{2+} and Zn^{2+} in single CuO and ZnO dissolution experiments in biomass-free liquor ($n=3 \pm$ standard deviation). Where not visible, standard deviations covered by markers (size 9).

ZnO dissolution was found roughly 10 times higher than CuO when comparing the equivalent spiking levels. However, the NP dissolution rate does not appear to be concentration dependent as the amount of released ions at the two highest concentrations are similar for both the nanomaterials. On the contrary it appears that the maximum dissolution rate for ZnO under these conditions is about $0.8 \text{ mg Zn}^{2+}/\text{L}$ and $0.1 \text{ mg Cu}^{2+}/\text{L}$ for CuO. These results are in agreement with what reported by Miao et al. (2015), who observed NOM dependent CuO dissolution in presence of alginate, BSA and EPS. The authors found that very little dissolution happens when organic compounds were added in concentration between 1 and 10 mg/L, and the measured DOC in the biomass-free liquor used in this work was $7.71 \pm 0.47 \text{ mg C/L}$. Hence, ZnO dissolution, which was roughly ten time higher than CuO dissolution, may also influence NP behaviour in wastewater in such way that could provoke differences in removal profile between ZnO and CuO and TiO_2 . Activated sludge efficiency in removing Zn^{2+} was proved to be lower in comparison to ZnO by Zhang et al. (2017),

who observed that Zn^{2+} removal by activated sludge was roughly 10% lower compared to the removal of ZnO NPs. According to the authors, this is ascribed to the difference in the removal process deriving from the lack of sedimentation of the Zn^{2+} ions; whilst aggregation driven, sedimentation is the main processes governing NP removal. Besides, in a media rich in dissolved organic matter (DOM), such as wastewater, the generated Zn^{2+} can associate with the present NOM. When metals-NOM complexation happens, ions became less available to activated sludge biomass, which leads to hindrance of cellular uptake (Sunda and Huntsman 1998). Therefore, the combination between the reduced sedimentation rate and the presence of Zn^{2+} -sequestering NOM complexes, triggered by ZnO dissolution could be factors that can help explain the observed difference between ZnO removal in comparison to CuO and TiO_2 found here.

4.4.3 Removal and behaviour of singularly spiked CuO, TiO_2 and ZnO in biomass-free liquor

At the concentration of 9 mg/L, the average removal percent in biomass-free liquor was $34.3 \pm 4.5\%$ for CuO, $34.4 \pm 4.6\%$ for TiO_2 and $19.6 \pm 9.5\%$ for ZnO (Fig. 4.4a). When spiked at 180 mg/L (Fig. 4.4b), the average percent of NP removed increased to $53.4 \pm 10.4\%$ for CuO, $90.0 \pm 6.5\%$ for TiO_2 and $48.5 \pm 7.2\%$ for ZnO.

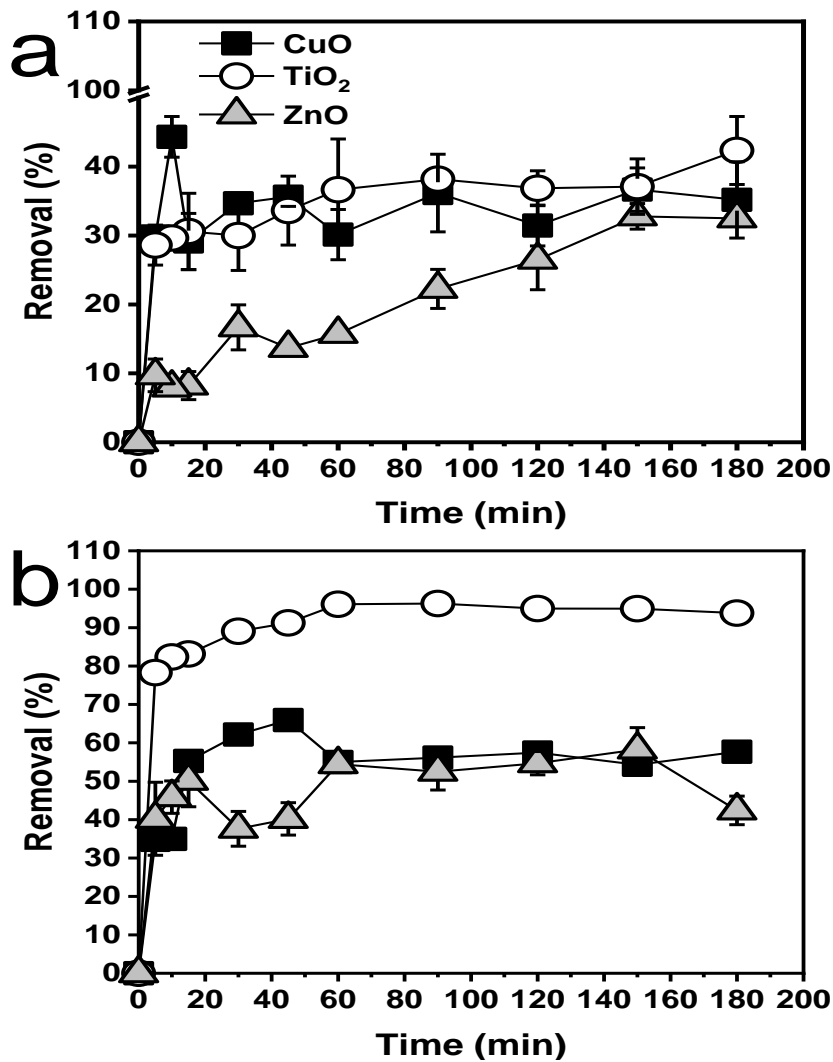


Fig. 4.4 Removal profile ($n=3 \pm$ standard deviation) of singularly spiked CuO, TiO₂ and ZnO reported as removal percent. Nanomaterials were spiked in biomass-free liquor at concentrations of 9 mg/L (a) and (b) and 180 mg/L. Where not visible, standard deviations covered by markers (size 9).

These results show that a fraction of NPs are removed from suspension in the absence of activated sludge. Partial removal of NPs in absence of biomass has been previously reported. In a study assessing the fate of CeO₂ in simulated wastewater treatment, the percent of NPs removed in filtered primarily-treated municipal wastewater was 45% after 24 hours (Gómez-Rivera et al. 2012). Further evidences of NP removal in absence of biomass can be found in the works of Conway et al. (2015) where aggregation of CuO at the concentration of 20 mg/L in a real WWTP effluent (not activated sludge liquor as used here) was shown to happen in one hour and Miao et al. (2016), who reported partial CuO removal (the removal percent were 18.1%,

21% and over 40% at concentrations of 1, 10 and 50 mg/L respectively) due to sedimentation in synthetic wastewater after 4 hours. Our work extends these findings by showing that a) aggregation occurs in liquor from a real activated sludge system, b) liquor-only aggregation occurs for TiO₂ and ZnO, as well as CuO, and c) liquor only aggregation occurs in higher concentrations up to at least 180 mg/l. Still, our results strengthen Conway and Miao's findings, by confirming their data for CuO and similar removal profiles were observed for TiO₂ and ZnO, and we further expanded the assessment to concentrations of 180 mg/L. Therefore, it appears that the removal in liquor-only systems is most likely due to sedimentation driven by aggregation of NPs. Hence, our findings suggest that CuO, TiO₂ and ZnO aggregation driven sedimentation are important processes through which NPs can be removed in WWTPs systems.

Aggregation is evidently an important part of the NP removal process and, therefore, likely to happen under a range of possible conditions; aggregate-driven sedimentation may be the primary NP removal mechanism in WWTPs (Miao et al. 2015). Therefore, it has the potential to sharply influence the environmental fate of nanomaterials and the removal performances throughout different stage of sewage treatment processes. However, water parameters affect NP behaviour. For instance, the presence of natural colloids (Quik et al. 2012) and electrolytes (Loosli et al. 2015) enhance NP aggregation. On the contrary, the sorption of NOM provides a steric repulsion, which stabilizes NPs and hinders aggregation (Grillo et al. 2015).

To explore the stabilizing effect of NOM, the stability of CuO, TiO₂ and ZnO dispersed in ultrapure water at concentration of 100 mg/L was investigated by measurements of Z-average hydrodynamic diameter (h_D) and z-potential as a function of pH. These data were then compared with measurements taken in biomass-free liquor. Firstly, the zeta potential (surface charge) in ultrapure water from pH 3 to 12 was measured and the point of zero charges (pzc) were pH=6 for CuO (Fig. 4.5a), 5.4 for TiO₂ (Fig. 4.6a), and 7.8 for ZnO (Fig. 4.7a). In ultrapure water, a peak in h_D for all the NPs was observed broadly around the pzc (Fig. 4.5b, 4.6b, 4.7b). This is due to the surface charge at pHs around the pzc being low and, therefore, the electrostatic repulsion between NPs is minimal. This leads to the observed increased NP size due to aggregation.

Following this, NPs were spiked in biomass-free liquor (with $\text{pH} = 7.1 \pm 0.5$). Z-potentials for CuO and TiO₂ were respectively -13.4 ± 0.8 and -15.2 ± 0.2 mV; the z-potential for ZnO was -20.4 ± 0.3 mV. Changes in NP z-potential in biomass-free liquor at different pH values (from 3.5 to 11.5) were then assessed, and the NP charge in biomass-free liquor was less affected by pH than when in ultrapure water, with values ranging between -10.6 and -28.6 mV (Fig. 4.5a, 4.6a, 4.7a). When measuring the h_D , NPs in filtered liquor remained at a similar size at all pHs and did not show a peak in size, thus again contrasting the results from ultrapure water. The h_D throughout the whole pH range tested for CuO was found to be 373.9 ± 67.6 nm, 329.1 ± 89.3 nm for TiO₂ and 323.8 ± 45.9 nm for ZnO (Fig. 4.5b, 4.6b, 4.7b). These hydrodynamic diameters are in agreement with previous works, where CuO h_D in WWTP effluent was measured at a single pH ($\text{pH} = 7.6$) 276 nm and showed slight aggregation to reach a h_D of 400 nm after one hour (Conway et al. 2015).

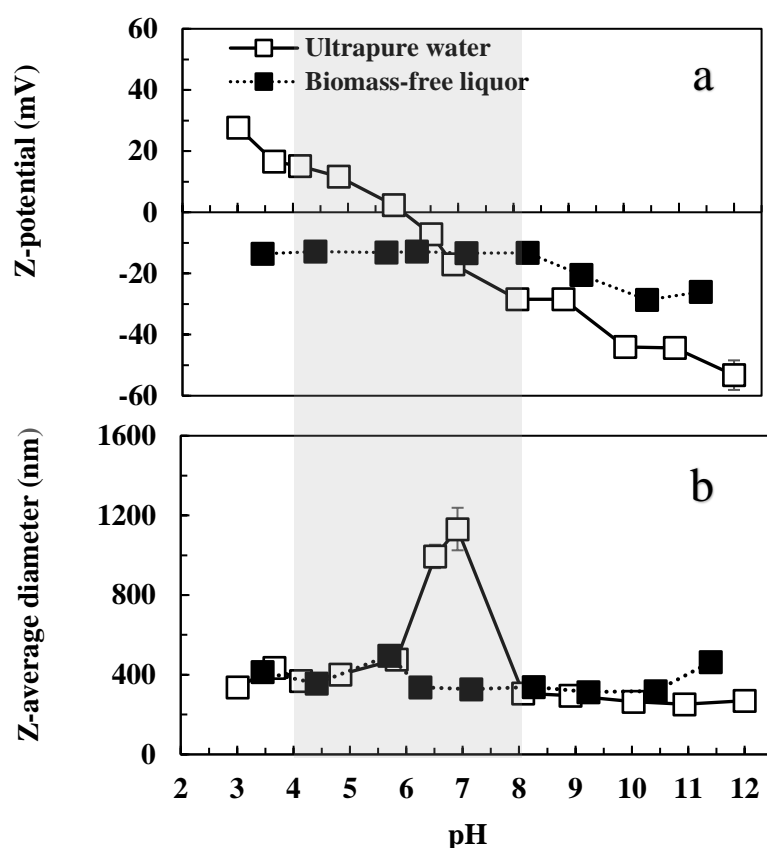


Fig. 4.5 Zeta potential (a) and Z-average diameter (b) of 100 mg/L CuO suspension as function of pH in ultrapure water and biomass-free liquor. The grey area ($\text{pzc} \pm 2$ unit) shows pH range where aggregation is expected to happen due to low zeta potential. Where not visible, standard deviations covered by markers (size 8).

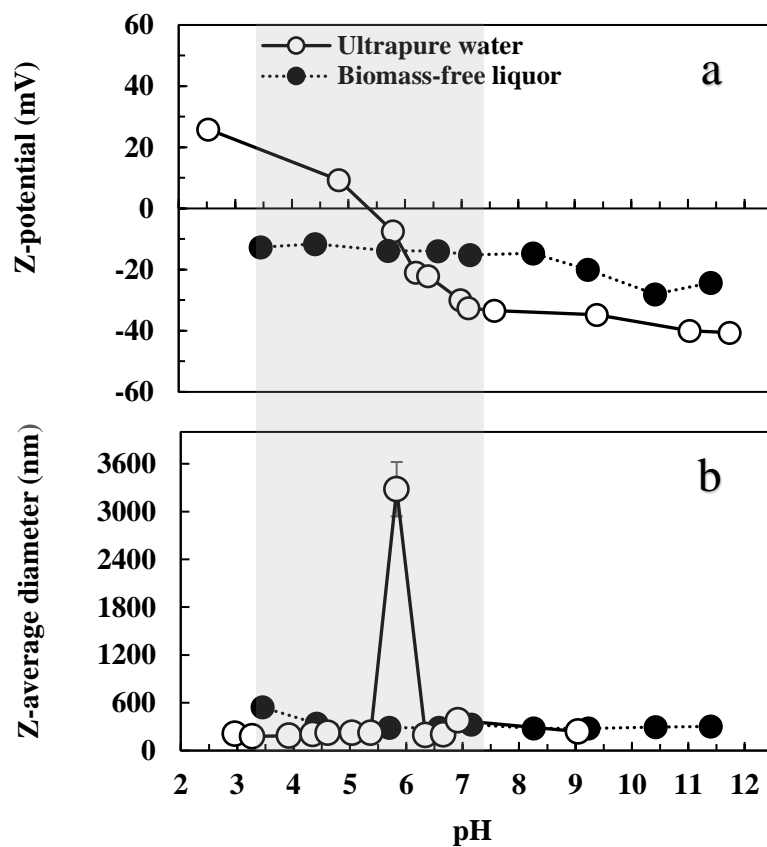


Fig. 4.6 Zeta potential (a) and Z-average diameter (b) of 100 mg/L TiO₂ suspension as function of pH in ultrapure water and biomass-free liquor. The grey area (pzc ± 2 unit) shows pH range where aggregation is expected to happen due to low zeta potential. Where not visible, standard deviations covered by markers (size 8).

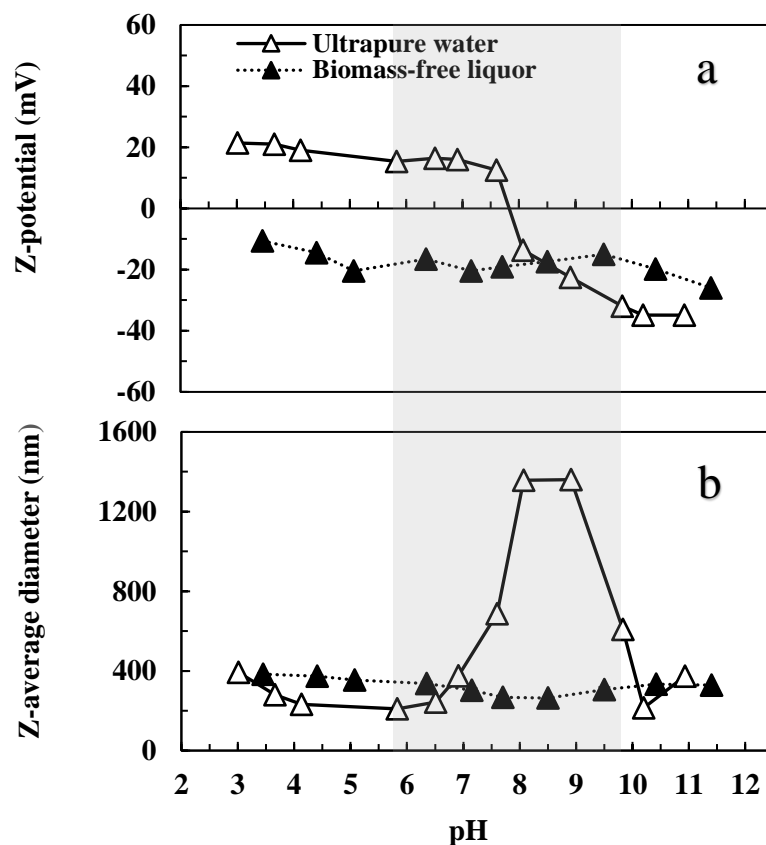


Fig. 4.7 Zeta potential (a) and Z-average diameter (b) of 100 mg/L ZnO suspension as function of pH in ultrapure water and biomass-free liquor. The grey area (pzc \pm 2 unit) shows pH range where aggregation is expected to happen due to low zeta potential. Where not visible, standard deviations covered by markers (size 8).

Similarly, TiO₂ and ZnO were observed in the dimensional range of 300 – 400 nm with zeta potential varying from -17.1 to -20.5 mV in 0.22 μ m biomass-free wastewater influent collected from two distinct WWTPs with pH ranging from 7.82 to 8.15 (Zhou et al. 2015). In addition, Zhang et al. (2009) studied the effect of Suwannee River NOM as surrogate of real NOM, on the stability of ZnO, NiO, TiO₂, Fe₂O₃ and SiO₂. The authors concluded that the adsorption of organic molecules onto NPs may impart the surface charge and enhance their negative z-potential. Another study investigating the effect of alginate and Suwannee River humic acids on TiO₂ stability found that the adsorption of the organic compounds onto the NPs would provide them a negatively charged electrosteric repulsion (Loosli et al. 2013). Furthermore, Keller et al. (2010) found that CeO₂, TiO₂ and ZnO spiked in different aqueous media were

negatively charged in presence of TOC and low ionic strength. Therefore, we suggest that the adsorption of the NOM fraction present in the biomass-free liquor may produce a negatively charged electrosteric barrier made of organic compounds that can partially enhance NP stability. Overall, aggregation driven sedimentation is an important process in NP removal in WWTP systems, but the presence of NOM may prevent it from being totally effective at removing NPs. Hence biomass is needed to remove the remainder of the NPs.

4.4.4 Removal of CuO, TiO₂ and ZnO mixtures by activated sludge biomass

To explore whether the co-occurrence of CuO, TiO₂ and ZnO could lead to different removal profiles and performances, activated sludge biomass was spiked with three CuO, TiO₂ and ZnO mixtures. The experiments were run with all the three NPs spiked at the same concentration of 9, 90 and 180 mg/L per NP type (creating total NP concentrations of 27, 270 and 540 mg/L), the three mixtures are called 9 mg/L, 90 mg/L and 180 mg/L. The cumulative removal of CuO, TiO₂ and ZnO mixtures at the 9 mg/L concentration in presence of activated sludge biomass (2000 mg/L TSS) was a quick and efficient process, which stabilized with greater than 95% removal after 30 minutes and reached a maximum value of $97.5 \pm 0.1\%$ at 180 min (Fig. 4.8a).

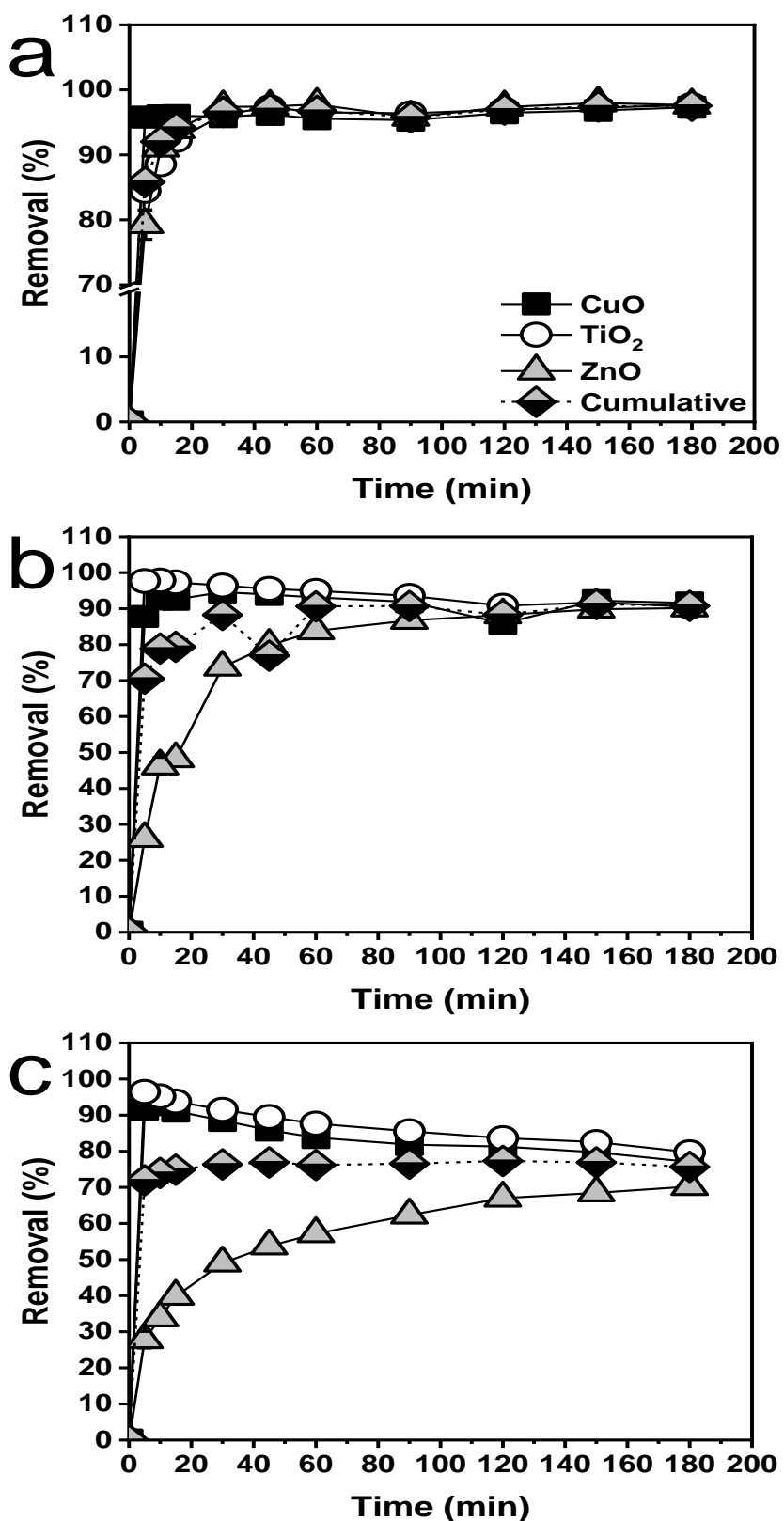


Fig. 4.8 Removal profile ($n=3 \pm$ standard deviation) of CuO, TiO₂ and ZnO mixtures reported as relative removal percent. Panels **a,b,c**, each nanoparticle type was spiked in presence of activated sludge biomass at concentrations of 9 mg/L (**a**), 90 mg/L (**b**) and 180 (**c**) for a final concentration of 27, 270 and 540 mg of NP/L. Where not visible, standard deviations covered by markers (size 9).

When the NP mixture were added at concentrations of 90 and 180 mg/L, the cumulative removal percent after 180 min decreased: $90.8 \pm 0.3\%$ at 90 mg/L mixture and $74.6 \pm 0.2\%$ at 180 mg/L (Fig 4.8b, 4.8c). Furthermore, a different pattern removal profile and efficacy of the three NPs was observed, where CuO and TiO₂ showed a similar profile that clearly differed from ZnO. The removal of CuO and TiO₂ at both 90 mg/L and 180 mg/L mixture experiments peaked within 30 minutes, varying between 92 % and 97%. This was then followed by a phase in which CuO and TiO₂ concentrations in the effluent increased until 180 min where almost 10% of the initial load was released back into suspension (Fig 4.8b, 4.8c). In contrast, the profile of ZnO removal when added in presence of CuO and TiO₂ resembled what was found during the experiments where ZnO was singularly spiked, although some differences in percent removal were also noticed. The ZnO removal was slower and less efficient in comparison to what observed for CuO and TiO₂, as well as to singularly spiked ZnO at 90 and 180 mg/L. Indeed, the activated sludge removal efficiency towards ZnO at 90 mg/L decreased from $97.7 \pm 0.1\%$ to $90.2 \pm 0.27\%$ and from $96.1 \pm 0.2\%$ to $70.2 \pm 0.2\%$ at 180 mg/L when NPs were added as mixtures. This could indicate that the activated sludge biomass has lower affinity for ZnO in comparison to CuO and TiO₂. Similarly, to what observed for singularly spiked NPs, it appears that activated sludge biomass has high efficiency in removing mixtures of CuO, TiO₂ and ZnO at 9 mg/L with overall removal rate greater than 97% for all the three tested nanomaterials after 180 min (Fig. 4.8a). However, when spiked as mixtures at 90 mg/L and 180 mg/L lower removal percent and different removal profiles were observed. The high concentrations tested may be the reason behind these differences.

The toxicity of CuO and ZnO NPs in activated sludge has been largely discussed (Ingle et al. 2014). The main effects reported are enhanced reactive oxygen species (ROS) development, increase in lactate dehydrogenase (LDH) release and extracellular polymeric substances (EPS) production (Wang et al. 2017, Zheng et al. 2011). Together with these physiological effects, activated sludge flocs can suffer morphological consequences. Increased EPS production was found upon exposure of activated sludge biomass to 1 mg/L ZnO to create a dense matrix to protect the cells (Puay et al. 2015). Furthermore, Geyik and Çeçen (2016) and Wang et al. (2016), who respectively exposed activated sludge biomass to AgNP and ZnO, stated that the

presence of NPs can lead to damages of the external matrix with further reduction of its integrity and possible detachment of components of the EPS matrix. Therefore, the exposure of activated sludge biomass to mixtures of CuO, TiO₂ and ZnO at concentrations of 90 and 180 mg/L may cause the structural damages to the flocs and therefore the external EPS matrix of the biomass would start to degrade and be released and exuded into the surrounding liquor. The detachment or exudation of organic molecules of the damaged EPS matrix to which NPs adhere can explain either the increasing concentration of CuO and TiO₂ in the simulated effluent and the lower removal rate for ZnO. The fraction of organic molecules detached from the biomass may act as a “carrier” and bring CuO and TiO₂ NPs back into the effluent. Furthermore, this release of organic matter may act as stabilizing agents for the nanoparticles, inhibiting their aggregation and sedimentation. Indeed, it has been shown that NP aggregation is a reversible process (Metreveli et al. 2015); the addition of NOM to aggregated NPs can induce disaggregation and restabilization. Moreover, these organic molecules could as well enhance ZnO stability and undergo complexation with Zn²⁺ ions and therefore reduce the overall ZnO removal rate.

4.4.5 Removal and behaviour of CuO, TiO₂ and ZnO mixtures in biomass-free liquor

The removal of co-occurring CuO, TiO₂ and ZnO in biomass-free liquor was assessed to investigate to which extent NP mixtures are affected by aggregation and sedimentation and how this impacts their removal and behaviour in wastewater. The quantification of the fraction of CuO, TiO₂ and ZnO found in the simulated effluent after settling in biomass-free liquor is shown in Fig. 4.9a, 4.9b, 4.9c. The cumulative removal of the NPs varied from 60.5 ± 1.0 % at 9 mg/L, to 58.1 ± 7.2 % at 90 mg/L and 84.5 ± 0.2 % at 180 mg/L.

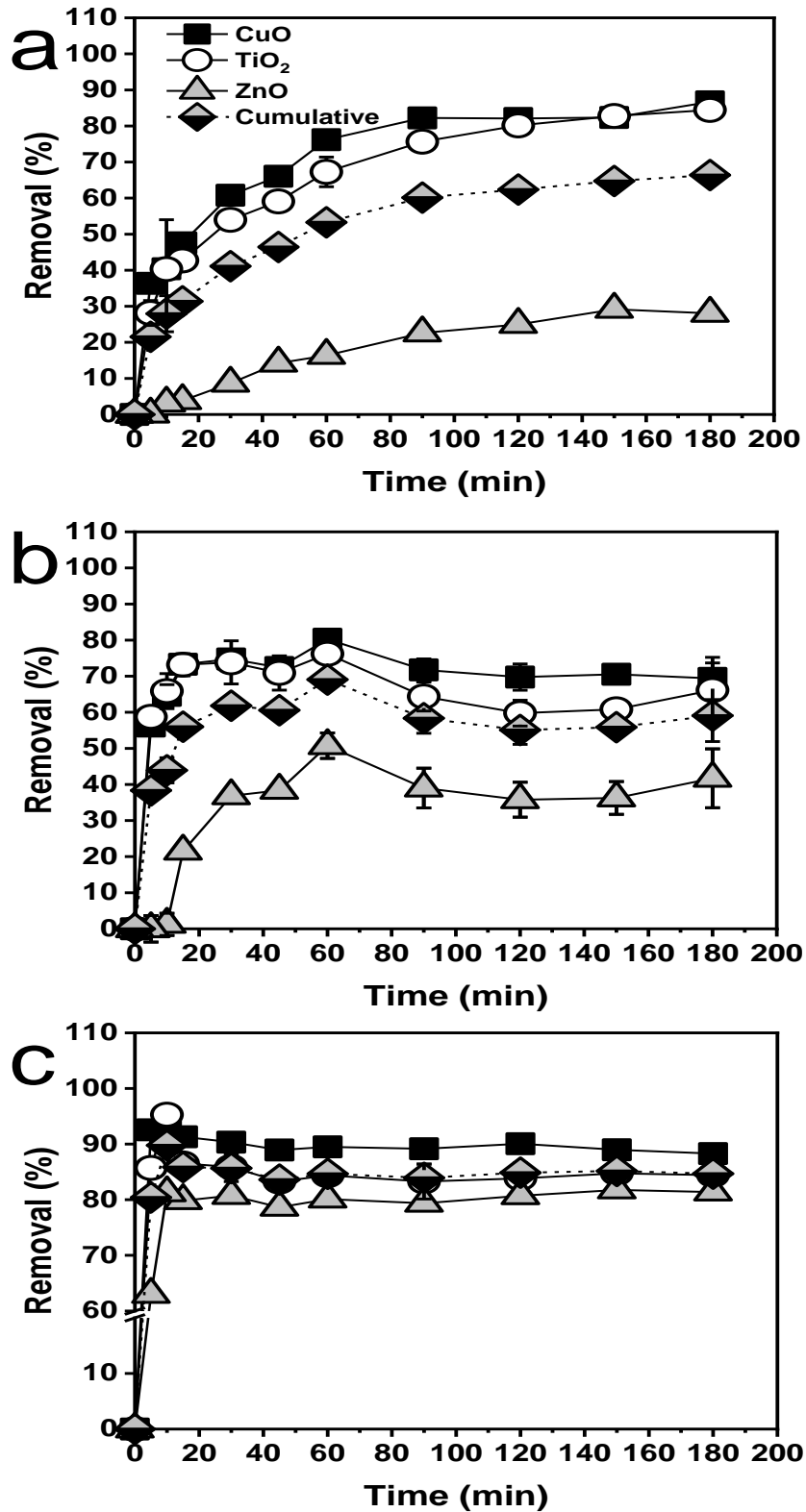


Fig. 4.9 Removal profile ($n=3 \pm$ standard deviation) of CuO, TiO₂ and ZnO mixtures reported as relative removal percent. Panels **a,b,c**, each nanoparticle type was spiked in biomass-free liquor at concentrations of 9 mg/L (**a**), 90 mg/L (**b**) and 180 (**c**) for a final concentration of 27, 270 and 540 mg of NP/L. Where not visible, standard deviations covered by markers (size 9).

These results indicate that a partial removal of co-occurring NPs may happen even in absence of biomass and despite the partial stabilizing effect of the NOM fraction in wastewater. Interestingly, at a concentration of 180 mg/L, the cumulative removal in biomass free liquor was roughly 10 % greater than what found at the same concentrations in presence of activated sludge biomass ($84.48 \pm 0.23\%$ vs $74.60 \pm 0.19\%$). This data may further highlight the magnitude of the negative impact coming from the exposure of such high NP concentrations on the floc integrity, meaning that the overall removal capacity of the biomass could be compromised. At the tested level of 9 mg/L mixture experiments, compared to CuO and TiO₂, ZnO appears to be the nanomaterial least susceptible to removal via aggregation driven sedimentation (only 28% ZnO removed in biomass free liquor compared to 87% and 84% for CuO and TiO₂ respectively). It appears that the aggregation driven sedimentation of CuO and TiO₂ are similar, while the impact of co-occurring NP on ZnO removal did not achieve the same magnitude observed for CuO and TiO₂ especially at 9 and 90 mg/L. In contrast, at 180 mg/L, the removal due to sedimentation of the three NPs was very similar, and this could be due to the very high concentrations tested. This could be explained by the difference of Z-potential in biomass free liquor. At unaltered pH = 7.1 ± 0.5 , CuO and TiO₂ Z-potentials were respectively -13.4 ± 0.8 mV and -15.2 ± 0.2 mV, while ZnO z-potential was -20.4 ± 0.3 mV (Fig. 4.5a, 4.6a, 4.7a). The lower Z-potential of CuO and TiO₂ may provide a weaker electrostatic repulsion that could only partially hinder homo-aggregation (CuO - CuO, TiO₂ - TiO₂, CuO - TiO₂), while the formation of aggregates with ZnO may be prevented to greater extents due to higher Z-potential. As results of this, CuO and TiO₂ may form larger aggregates and settle much quicker than ZnO. However, with increasing concentrations, the electrosteric repulsion is likely to be overcome by an increased frequency of collision (Tong et al. 2014) which would explain the increase in ZnO sedimentation at higher concentrations.

CuO, TiO₂ and ZnO dissolution was also investigated in mixed NP systems. The results shown in Fig 4.10 confirm that ZnO appears to be the NP type more susceptible to dissolution, in mixture systems; an observation also noted in single NP experiments.

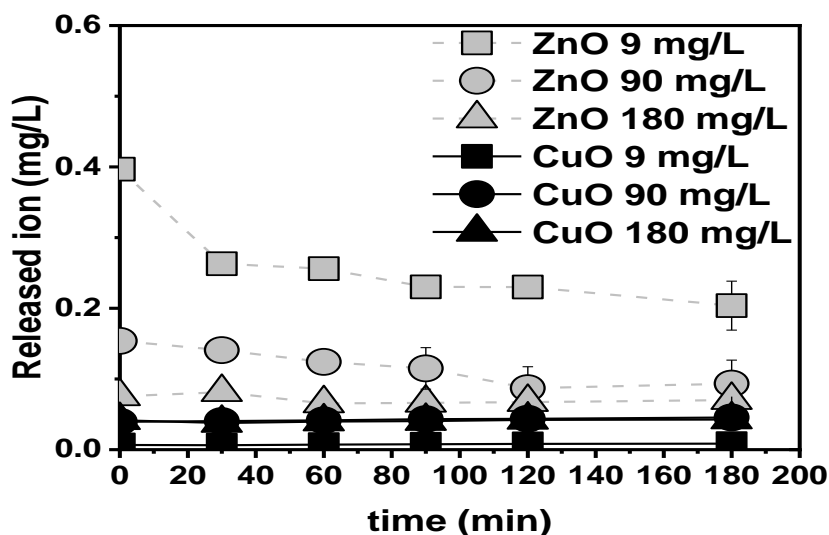


Fig. 4.10 Concentration of dissolved Cu^{2+} and Zn^{2+} in mixtures CuO, TiO_2 and ZnO dissolution experiments in biomass-free liquor ($n=3 \pm$ standard deviation). Where not visible, standard deviations covered by markers (size 9).

Surprisingly, the highest concentration of released Zn^{2+} ions was measured at the concentration of 9 mg/L. On average, during the 3 hours, the Zn^{2+} concentration was 0.26 ± 0.07 mg/L. However, a decrease in concentration from initial 0.40 ± 0.01 mg/L to a final 0.2 ± 0.03 was found. At higher dosages (90 and 180 mg/L) the average released Zn^{2+} were lower, at 0.12 ± 0.03 mg/L and 0.07 ± 0.01 mg/L respectively. On the contrary, CuO dissolution rate was always less than what was observed for ZnO, as Cu^{2+} concentration varied from 0.01 to 0.04 mg/L irrespective of the NP concentrations. It is interesting to note how CuO and ZnO dissolution rates in mixture systems are lower than what was observed in single NP experiments. This may be attributed to the co-existence of different nanomaterials. As well as the higher removal efficiency found in mixture experiments, co-occurring NPs at high concentrations tend to rapidly aggregate. The aggregation process may hinder or prevent dissolution due to reduced exposure of surfaces. Additionally, it has been reported that TiO_2 has great adsorption capacity for heavy metals (Ray and Shipley 2015). Therefore, the presence of TiO_2 could lead to adsorption of the released Zn^{2+} and Cu^{2+} ions onto it and this could lead to enhanced NP aggregation through buffering surface charge (Wang et al. 2011). This has previously been reported that in presence of divalent cations, including Zn^{2+} and Cu^{2+} NP aggregate (Zamborini et al. 2000). Therefore, CuO and ZnO dissolution in mixture systems was found lower in comparison to single NP

experiments. It is possible that at such concentrations, NP aggregation prevents or hinders dissolution. Alternatively, the lowered CuO and ZnO dissolution observed, may be partially explained by a triggering effect due to the dissolution process itself. When dissolution happens, ions are released and they can adsorb onto NP, such as TiO₂. When this happens, NP surface charge may be impaired and as a result, aggregation and therefore sedimentation increase.

4.5 Conclusions

This study aimed to assess whether activated sludge biomass may cope with single CuO, TiO₂, ZnO and their mixtures at high concentrations (9, 90 and 180 mg/L). The association between NPs and activated sludge biomass happens quickly, in the first minutes of contact time, and then stabilize within 30-90 minutes. Activated sludge biomass could yield removal efficiency greater than 90% of singularly spiked CuO, TiO₂ and ZnO irrespective of concentrations within a regular hydraulic retention time (180 min). Similarly, the cumulative removal of CuO, TiO₂ and ZnO mixture exceeded 90% at concentrations of 9 and 90 mg/L, however, the removal efficiency decreased to $74.6 \pm 0.2\%$ in mixture experiments of 180 mg/L. At such levels, ecotoxicological implications might begin to have a major impact. Indeed, after an initial phase in which the NP removal process occurred as for single NPs, we observed that a fraction of the previously removed NPs were found resuspended in the effluent.

We also demonstrated that the NP removal is promoted by aggregation driven sedimentation. In absence of biomass, the fraction of single CuO, TiO₂, ZnO removed during the settlement phase varied from 30 to 85% and it increased with NP concentrations. Aggregation driven sedimentation was found to be an important process in mixture system as well. The overall removal in liquor only experiments varied from 58 to 84%. This was observed despite the stabilizing effect played by organic matter fraction, which appeared to partially hinder CuO, TiO₂ and ZnO aggregation. In the biomass free liquor, NPs were negatively charged, regardless of the pH, and no point of zero charge and little aggregation was observed opposite to what found in ultrapure water. This is most likely due to adsorption of the dissolved organic matter present in the liquor. When this happens, NPs acquire an electrosteric barrier that can hinder aggregation.

Overall this study shows that the currently operated activated sludge technology can efficiently cope with current and possible future loading scenarios of some of the most commonly used NPs in commercially available products. The fate of NPs can be influenced by wastewater and liquor chemistry, and aggregation driven sedimentation can only induce a partial NP removal highlighting the importance and efficiency of the activated sludge treatment.

3.6 Bibliography

- APHA/AWWA/WEF (2012) Standard Methods for the Examination of Water and Wastewater. Stand Methods 541. [https://doi.org/ISBN 9780875532356](https://doi.org/ISBN%209780875532356)
- Barton LE, Therezien M, Auffan M, et al (2014) Theory and Methodology for Determining Nanoparticle Affinity for Heteroaggregation in Environmental Matrices Using Batch Measurements. *Environ Eng Sci* 31:421–427. <https://doi.org/10.1089/ees.2013.0472>
- Benn TM, Westerhoff P (2008) Nanoparticle Silver Released into Water from Commercially Available Sock Fabrics. 4133–4139. <https://doi.org/10.1021/es7032718>
- Chaúque EFC, Zvimba JN, Ngila JC, Musee N (2014) Stability studies of commercial ZnO engineered nanoparticles in domestic wastewater. *Phys Chem Earth* 67–69:140–144. <https://doi.org/10.1016/j.pce.2013.09.011>
- Conway JR, Adeleye AS, Gardea-Torresdey J, Keller AA (2015) Aggregation, Dissolution, and Transformation of Copper Nanoparticles in Natural Waters. *Environ Sci Technol* 49:2749–2756. <https://doi.org/10.1021/es504918q>
- Eduok S, Hendry C, Ferguson R, et al (2015) Insights into the effect of mixed engineered nanoparticles on activated sludge performance. *FEMS Microbiol Ecol* 91:1–9. <https://doi.org/10.1093/femsec/fiv082>
- Ewels P, Sikora T, Serin V, et al (2016) A Complete Overhaul of the Electron Energy-Loss Spectroscopy and X-Ray Absorption Spectroscopy Database : eelsdb . eu. 717–724. <https://doi.org/10.1017/S1431927616000179>
- Fang J, Shijirbaatar A, Lin D hui, et al (2017) Stability of co-existing ZnO and TiO₂nanomaterials in natural water: Aggregation and sedimentation mechanisms. *Chemosphere* 184:1125–1133. <https://doi.org/10.1016/j.chemosphere.2017.06.097>
- Farkas J, Peter H, Christian P, et al (2011) Characterization of the effluent from a nanosilver producing washing machine. *Environ Int* 37:1057–1062. <https://doi.org/10.1016/j.envint.2011.03.006>
- Geyik AG, Çeçen F (2016) Exposure of activated sludge to nanosilver and silver ion: Inhibitory effects and binding to the fractions of extracellular polymeric substances. *Bioresour Technol* 211:691–697.

<https://doi.org/10.1016/j.biortech.2016.03.157>

- Gómez-Rivera F, Field JA, Brown D, Sierra-Alvarez R (2012) Fate of cerium dioxide (CeO₂) nanoparticles in municipal wastewater during activated sludge treatment. *Bioresour Technol* 108:300–304. <https://doi.org/10.1016/j.biortech.2011.12.113>
- Gottschalk F, Sondere T, Schols R, Nowack B (2009) Modeled Environmental Concentrations of Engineered Nanomaterials for Different Regions. *Environ Sci Technol* 43:9216–9222. <https://doi.org/10.1021/es9015553>
- Grillo R, Rosa AH, Fraceto LF (2015) Engineered nanoparticles and organic matter: A review of the state-of-the-art. *Chemosphere* 119:608–619. <https://doi.org/10.1016/j.chemosphere.2014.07.049>
- Hou L, Li K, Ding Y, et al (2012) Removal of silver nanoparticles in simulated wastewater treatment processes and its impact on COD and NH₄ reduction. *Chemosphere* 87:248–252. <https://doi.org/10.1016/j.chemosphere.2011.12.042>
- Ingle AP, Duran N, Rai M (2014) Bioactivity, mechanism of action, and cytotoxicity of copper-based nanoparticles: A review. *Appl Microbiol Biotechnol* 98:1001–1009. <https://doi.org/10.1007/s00253-013-5422-8>
- Joško I, Oleszczuk P, Skwarek E (2017) Toxicity of combined mixtures of nanoparticles to plants. *J Hazard Mater* 331:200–209. <https://doi.org/10.1016/j.jhazmat.2017.02.028>
- Kaegi R, Voegelin A, Ort C, et al (2013) Fate and transformation of silver nanoparticles in urban wastewater systems. *Water Res* 47:3866–3877. <https://doi.org/10.1016/j.watres.2012.11.060>
- Keller AA, Wang H, Zhou D, Miller RJ (2010) Stability and Aggregation of Metal Oxide Nanoparticles in Natural Aqueous Matrices Stability and Aggregation of Metal Oxide Nanoparticles in Natural Aqueous Matrices. 44:1962–1967. <https://doi.org/10.1021/es902987d>
- Kiser MA, Ryu H, Jang H, et al (2010) Biosorption of nanoparticles to heterotrophic wastewater biomass. *Water Res* 44:4105–4114. <https://doi.org/10.1016/j.watres.2010.05.036>
- Kiser MA, Westerhoff P, Benn T, et al (2009) Titanium Nanomaterial Removal and Release from Wastewater Treatment Plants. *Environ Sci Technol* 43:6757–6763. <https://doi.org/10.1021/es901102n@proofing>

- Li M, Lin D, Zhu L (2013) Effects of water chemistry on the dissolution of ZnO nanoparticles and their toxicity to *Escherichia coli*. *Environ Pollut* 173:97–102. <https://doi.org/10.1016/j.envpol.2012.10.026>
- Lombi E, Donner E, Tavakkoli E, et al (2012) Fate of zinc oxide nanoparticles during anaerobic digestion of wastewater and post-treatment processing of sewage sludge. *Environ Sci Technol* 46:9089–9096. <https://doi.org/10.1021/es301487s>
- Loosli F, Coustumer P Le, Stoll S (2013) TiO₂ nanoparticles aggregation and disaggregation in presence of alginate and Suwannee River humic acids. pH and concentration effects on nanoparticle stability. *Water Res* 47:6052–6063. <https://doi.org/https://doi.org/10.1016/j.watres.2013.07.021>
- Loosli F, Vitorazi L, Berret JF, Stoll S (2015) Towards a better understanding on agglomeration mechanisms and thermodynamic properties of TiO₂ nanoparticles interacting with natural organic matter. *Water Res* 80:139–148. <https://doi.org/10.1016/j.watres.2015.05.009>
- Mackevica A, Olsson ME, Hansen SF (2017) The release of silver nanoparticles from commercial toothbrushes. *J Hazard Mater* 322:270–275. <https://doi.org/10.1016/j.jhazmat.2016.03.067>
- Metreveli G, Philippe A, Schaumann GE (2015) Disaggregation of silver nanoparticle homoaggregates in a river water matrix. *Sci Total Environ* 535:35–44. <https://doi.org/10.1016/j.scitotenv.2014.11.058>
- Miao L, Wang C, Hou J, et al (2015) Enhanced stability and dissolution of CuO nanoparticles by extracellular polymeric substances in aqueous environment. *J Nanoparticle Res* 17:. <https://doi.org/10.1007/s11051-015-3208-x>
- Miao L, Wang C, Hou J, et al (2016) Aggregation and removal of copper oxide (CuO) nanoparticles in wastewater environment and their effects on the microbial activities of wastewater biofilms. *Bioresour Technol* 216:537–544. <https://doi.org/10.1016/j.biortech.2016.05.082>
- Mueller NC, Nowack B (2008) Exposure modelling of engineered nanoparticles in the environment. *Environ Sci Technol* 42:44447–53. <https://doi.org/10.1021/es7029637>

- Ngantcha JP, Gerland M, Kihn Y, Rivière A (2005) Correlation between microstructure and mechanical spectroscopy of a Cu-Cu₂O alloy between 290 K and 873 K. *Eur Phys J Appl Phys*. <https://doi.org/10.1051/epjap:2004200>
- Park HJ, Kim HY, Cha S, et al (2013) Removal characteristics of engineered nanoparticles by activated sludge. *Chemosphere* 92:524–528. <https://doi.org/10.1016/j.chemosphere.2013.03.020>
- Puay NQ, Qiu G, Ting YP (2015) Effect of Zinc oxide nanoparticles on biological wastewater treatment in a sequencing batch reactor. *J Clean Prod* 88:139–145. <https://doi.org/10.1016/j.jclepro.2014.03.081>
- Quik JTK, Stuart MC, Wouterse M, et al (2012) Natural colloids are the dominant factor in the sedimentation of nanoparticles. *Environ Toxicol Chem* 31:1019–1022. <https://doi.org/10.1002/etc.1783>
- Ray PZ, Shipley HJ (2015) Inorganic nano-adsorbents for the removal of heavy metals and arsenic: A review. *RSC Adv* 5:29885–29907. <https://doi.org/10.1039/c5ra02714d>
- Reed RB, Ladner DA, Higgins CP, et al (2012) Solubility of nano-zinc oxide in environmentally and biologically important matrices. *Environ Toxicol Chem* 31:93–99. <https://doi.org/10.3346/jkms.2015.30.10.1496>
- Sunda WG, Huntsman SA (1998) Processes regulating cellular metal accumulation and physiological effects: Phytoplankton as model systems. *Sci Total Environ* 219:165–181. [https://doi.org/10.1016/S0048-9697\(98\)00226-5](https://doi.org/10.1016/S0048-9697(98)00226-5)
- Tong T, Fang K, Thomas SA, et al (2014) Chemical interactions between nano-ZnO and nano-TiO₂ in a natural aqueous medium. *Environ Sci Technol* 48:7924–7932. <https://doi.org/10.1021/es501168p>
- Vance ME, Kuiken T, Vejerano EP, et al (2015) Nanotechnology in the real world: Redeveloping the nanomaterial consumer products inventory. *Beilstein J Nanotechnol* 6:1769–1780. <https://doi.org/10.3762/bjnano.6.181>
- Wang D, Tejerina B, Lagzi I, et al (2011) Bridging interactions and selective nanoparticle aggregation mediated by monovalent cations. *ACS Nano* 5:530–536. <https://doi.org/10.1021/nn1025252>
- Wang S, Li Z, Gao M, et al (2017) Long-term effects of cupric oxide nanoparticles (CuO NPs) on the performance, microbial community and enzymatic activity of

- activated sludge in a sequencing batch reactor. *J Environ Manage* 187:330–339. <https://doi.org/10.1016/j.jenvman.2016.11.071>
- Wang ST, Wang WQ, Zhang ZR, You H (2016) The impact of zinc oxide nanoparticles on phosphorus removal and the microbial community in activated sludge in an SBR. *RSC Adv* 6:96706–96713. <https://doi.org/10.1039/c6ra19486a>
- Yang Y, Wang Y, Hristovski K, Westerhoff P (2015) Simultaneous removal of nanosilver and fullerene in sequencing batch reactors for biological wastewater treatment. *Chemosphere* 125:115–121. <https://doi.org/10.1016/j.chemosphere.2014.12.003>
- Yu R, Wu J, Liu M, et al (2016) Toxicity of binary mixtures of metal oxide nanoparticles to *Nitrosomonas europaea*. *Chemosphere* 153:187–197. <https://doi.org/10.1016/j.chemosphere.2016.03.065>
- Zamborini FP, Hicks JF, Murray RW (2000) Quantized double layer charging of nanoparticle films assembled using carboxylate/(Cu^{2+} or Zn^{2+})/carboxylate bridges [4]. *J Am Chem Soc* 122:4514–4515. <https://doi.org/10.1021/ja0006696>
- Zhang D, Trzcinski AP, Oh H-S, et al (2017) Comparison of the effects and distribution of zinc oxide nanoparticles and zinc ions in activated sludge reactors. *J Environ Sci Heal Part A* 52:1073–1081. <https://doi.org/10.1080/10934529.2017.1338896>
- Zhang Y, Chen Y, Westerhoff P, Crittenden J (2009) Impact of natural organic matter and divalent cations on the stability of aqueous nanoparticles. *Water Res* 43:4249–4257. <https://doi.org/10.1016/j.watres.2009.06.005>
- Zheng X, Wu R, Chen Y (2011) Effects of ZnO nanoparticles on wastewater biological nitrogen and phosphorus removal. *Environ Sci Technol* 45:2826–2832. <https://doi.org/10.1021/es2000744>
- Zhou X hong, Huang B cheng, Zhou T, et al (2015) Aggregation behavior of engineered nanoparticles and their impact on activated sludge in wastewater treatment. *Chemosphere* 119:568–576. <https://doi.org/10.1016/j.chemosphere.2014.07.037>

Chapter 5

CuO, TiO₂, ZnO nanoparticle removal by anaerobic granular sludge

5.1 Summary

Copper oxide (CuO), titanium dioxide (TiO₂) and zinc oxide (ZnO) have found a widespread array of applications in industrial and commercial processes and materials. The greater usage of nanoparticles (NPs) has hence caused the release of NPs into sewage networks to rapidly increase. Anaerobic wastewater treatment (AnWT) is one of the emerging processes used to treat sewage. It is finding greater applications due to its potential for reduced environmental footprint compared to aerobic treatment. In this work, we assessed the extent to which anaerobic granular sludge (AGS) could remove high concentration of single type and mixtures of CuO, TiO₂ and ZnO NPs. This was done under NP concentrations (9 to 180 mg/l single type and 27 to 540 mg/l mixed) that were much higher than have been previously explored for these systems, and thus examining potential future NP load scenarios, and those from possible unregulated release. The removal of single type NPs varied from 23 to 77 %, whilst when added as triple NP type mixtures, overall AGS could remove from 30 to 60 % of the NP input. The NPs removal due to aggregation driven sedimentation in pure synthetic wastewater was calculated from 13 to 26 % and varied in a concentration dependent manner (more were removed at higher concentrations). This indicates that while the granules play an important role in NP removal, likely by attachment to their surfaces, aggregation driven sedimentation of NPs is also an important removal process in anaerobic systems.

5.2 Introduction

Although it has been suggested that Sumerians used anaerobic remediation of wastes 5000 years ago (Deublein and Steinhauser 2010), anaerobic wastewater treatment (AnWT) has gained greater interest as well as reputation since the early 20th century (Klinkner 2014). This secondary biological wastewater treatment is a biochemical process in which microorganisms embedded in biofilms called granules degrade organic material under anaerobic conditions through a well-known process called anaerobic digestion (Botheju et al. 2010). In addition to reducing the pollution load from the sewage, during the AnWT process, biogas, a gaseous mixture composed of methane and carbon dioxide, is produced. Biogas can be used for generation of heat and electricity, hence making such a process more environmentally sustainable (Velasco et al. 2018). Besides the generation of a sub product which can be used as fuel, anaerobic treatment technologies have other advantages over conventional aerobic sewage treatments. These include no requirement for aeration, smaller volumes of waste sludge produced that needs further treatment, minor spaces are needed and greater ability to treat strong wastewater and higher resistance to adverse conditions (Lettinga 1995; Holmes and Smith 2016; Poh et al. 2016). Hence, the growing interest for AnWT in the treatment of organic matter rich urban and industrial sewage (Shi et al. 2017). Over 2200 working AnWT plants were installed by 2006 (Van Lier et al. 2008) and anaerobic technology based facilities are still being built with the increase of the relative available interest and knowledge.

An increasing range of nanoparticles (NPs) and NP containing products are commercially available on the market (Gottschalk et al. 2009). The release of NPs into the sewage network during the production, usage or disposal is well established (Gottschalk and Nowack 2011; Weir et al. 2012; Mackevica et al. 2017) with concentrations varying from 1µg/L to 10 mg/L (Kiser et al. 2009). In parallel, the growing utilization of anaerobic processes to handle sewage enhances the likelihood of NPs reaching AnWT plants. Therefore, the presence of NPs may impair the performances of AnWT process (Li et al. 2015).

To date, there are scarce studies that have focused on evaluating the impact of different NP types on the performances of anaerobic granular sludge (AGS). For example, anaerobic sludge exposed to up to 2000 mg/L of TiO₂ showed increased

production of extracellular polymeric substances (EPS) and methane with an average NP removal of 92 %. This could be due the nanomaterial's insoluble nature and the formation of aggregates by TiO₂. The NPs – biomass surface association can provide the anaerobic granules with extra electrons to use in methane production. The authors also suggest that the aggregated status and hence larger size of the NPs can hinder the possibility of TiO₂ moving into the inner part of the granules. Due to the interaction with NPs, granules responded with increased production of polysaccharides to thicken the external fraction of the granules, as a defensive measure, which is where the majority of the NPs were observed (Cervantes-Avilés et al. 2018). In another study, an AGS treatment operated for 90 days and fed with CuO, TiO₂ and ZnO, singularly spiked, at concentration of 5 mg/L, produced an effluent with the nanomaterial concentrations varying from 0.8 to 0.3 mg/L. The calculated removal efficiency fluctuated from 80 to 95 % with the highest removal found for CuO and the lowest for ZnO. CuO and ZnO were also found to have greater toxicity on AGS in comparison to TiO₂. The authors explained that this could be attributed to the different properties of the nanomaterials as CuO and ZnO dissolution releases Cu²⁺ and Zn²⁺, whereas TiO₂ dissolution does not occur (Li et al. 2017). (Li et al. 2017). FeNP were also found highly adsorbed onto AGS surfaces showing high removal efficiency. This NPs – microorganism interaction also stimulated methane production which was enhanced in comparison to the control AGS group (He et al. 2017). The importance of time dependent association between CuO and AGS was also mentioned by Otero-González et al. (2014). An AGS bioreactor operated over the course of 107 days treating synthetic sewage with an average CuO concentration of 1.39 mg/L yielded a NP removal of 77 % with an average effluent CuO concentration of 0.32 mg/L. The removal efficiency was found affected by the hydraulic retention time (HRT) which declined from 80 % to 66 % when shortening the HRT from 12 to 6 hours. The shorter contact time may reduce the binding of NPs to extracellular polymers or microbe surfaces, reduce entrapment into flocs, and limit active cellular uptake and diffusion into biofilms (Westerhoff et al. 2013). In another study, ceria nanoparticles (CeO₂) were found toxic towards the more external bacteria of AGS granules, which further led to decreased acidification rate but no or minimal effect on methanogenesis (methanogenesis is carried out by microorganisms located in the inner part of the

granule). Due to the dense structure of the granules, CeO₂ could hardly penetrate the granules after combining with their external membrane. Hence, the superficial NP – AGS interactions have a critical role in the development of NP toxicity and fate (Ma et al. 2013).

These studies suggest that the timescale of the NPs – AGS association plays a key role in the removal profile of nanomaterials and their effects on the treatment process. However, to date, a detailed time-sensitive study on the removal profile of NPs by AGS has not yet been provided. In addition, as per the majority of the removal studies, only the single NP scenario has been examined, clearly defining some key gaps that can unveil important insight to better understand NPs – AGS interactions and AnWT performances.

The aim of this study was to assess the capacity and the time sensitivity of the AGS process to remove CuO, TiO₂ and ZnO. Three different NPs levels, 9, 90 and 180 mg/L were tested to assess a broad spectrum of concentrations. These cover current environmentally relevant NPs loading scenarios as well as future and extreme conditions, such as highly urbanized and polluted areas as well as illegal discharges. Therefore, they cover higher concentrations than previously examined by others. Moreover, the examination of mixed CuO, TiO₂ and ZnO in AGS systems has not been examined before. Additionally, we also investigated the time dependent removal profile of triple CuO, TiO₂ and ZnO mixtures. The NP removal via aggregation driven sedimentation in synthetic wastewater only systems (no biomass) was also quantified to evaluate the matrix effect on NP fate.

5.3 Materials and methods

5.3.1 Biomass collection and storage

Samples of anaerobic granular sludge (AGS), with a diameter varying from 2 to 5 mm, were collected from a 485 m³ expanded granular sludge bed plant treating distillery wastewater in Edinburgh, UK. The granules were rinsed several times with ultrapure water to remove any impurities. The volume of original liquor was substituted with standard synthetic wastewater, prepared with peptone (160 mg), meat extract (110 mg), urea (30 mg), anhydrous dipotassium hydrogen phosphate (K₂HPO₄, 28 mg), sodium chloride (NaCl, 7 mg), calcium chloride dehydrate (CaCl₂·2H₂O, 4 mg) and magnesium sulphate heptahydrate (Mg₂SO₄·7H₂O, 2 mg) dissolved in 1 L of tap water for a final expected dissolved organic content (DOC) of 100 mg/L and pH of 7.5 ± 0.5 (OECD 2001). Aliquots of AGS were stored in airtight bottles at 4°C for maximum 6 weeks.

5.3.2 Nanoparticle preparation

Commercially available TiO₂ nanopowder (anatase, particle size <25 nm, 99.7% purity, catalog number 637254) and ZnO (particle size <100 nm, catalog number 721077) were purchased from Sigma-Aldrich Corp, St. Louis, MO, USA. CuO nanopowder (particle size 30-50 nm, 99% purity, catalog number 44663) was obtained from Alfa Aesar (Heysham, Lancashire, UK). Freshly made suspensions were prepared before each experimental run. All the suspensions were prepared in ultrapure water with pH adjusted to 11 ± 1 with 0.1 M NaOH (to prevent aggregation) and sonicated for 15 minutes with an ultrasonic processor UP200St equipped with sonotrode S26d7 (Hielscher Ultrasonic GmbH, Teltow, Germany) with 70 W, amplitude 100% and frequency of 26 ± 1 kHz. NP suspensions in ultrapure water with pH adjusted to 11 ± 1 were characterized prior to the beginning of the tests. For characterization purposes, particle size distribution and elemental composition, were determined through transmission electron microscopy (TEM) and electron energy loss spectroscopy (EELS) (see chapter 2). Dynamic light scattering was used for hydrodynamic diameter (h_D) and Z-potential evaluation (see chapter 2).

5.3.3 Nanoparticle quantification

Acid digestion followed by analysis with inductively coupled plasma optical emission spectroscopy (ICP-OES, iCAP 6200, Thermo fisher scientific) was used to quantify Cu^{2+} , Ti^{4+} and Zn^{2+} as a proxy for CuO, TiO_2 and ZnO. Samples were acidified with HNO_3 (69%) immediately after collection and kept at 4°C for preservation purpose. Afterwards, 6 ml of well mixed samples were transferred into 55 ml teflon MARSXpress Vessels (CEM Corporation) to which 2 ml of HNO_3 (69%) and 2 ml of H_2SO_4 (95%) were added. The samples were then put in a microwave assisted reaction system (MARS 5) and the Cu^{2+} , Ti^{4+} and Zn^{2+} concentrations were determined via ICP-OES. For full protocol details, see chapter. 2.

5.3.4 Nanoparticle removal by anaerobic granular sludge biomass

Nanoparticle removal batch tests with activated sludge biomass were run as a function of NP concentration (9, 90 and 180 mg/L) and type (CuO, TiO_2 and ZnO). The amount of biomass remained constant in all the experiments, equal to 4 g of wet AGS were weighted and added in each 50 ml plastic tube. The biomass was then supplied with 27 ml of synthetic wastewater and allowed to reach room temperature overnight. On the day of the experiment 3 ml of NP suspension were added for single NP removal studies (to reach final NP concentrations of 9, 90 and 180 mg/l). This produced a final total suspended solid (TSS) value equal to 14667 ± 333 mg/L in both single and mixed NP systems. The experimental vessels containing biomass, synthetic wastewater and NPs were then agitated at 50 rpm on a rotary shaker to maintain the mix gently agitated to ensure the AGS remain in suspension throughout the duration of the experiment, yet intact. In mixed NP systems, three separate stock solutions were prepared as for single NP experiments. The experimental vessels containing 27 ml of synthetic wastewater, 4 g of wet AGS biomass were then spiked with 1 ml of each of the three NP suspensions to achieve a final volume of 30 ml. All the three NPs were added at the same concentration of 9, 90 and 180 mg/L per NP type (creating total NP concentrations of 27, 270 and 540 mg of NPs/L). Specific agitation times varied from a minimum of 5 min to a maximum of 360 min. After agitation the vials were removed from the shaker and the biomass was allowed to settle by gravity for 20 min. Afterwards, 14 ml of supernatant (simulated effluent) were carefully collected, to

avoid extraction of biomass, and acidified with two drops of concentrated HNO₃ (69%) and stored at 4 °C prior to NP quantification.

5.3.5 Analytical methods

The standard synthetic wastewater was characterized following the same procedure as for the biomass-free liquor (see chapter 3.3.5). Total suspended solids (TSS) was determined according to the standard methods (APHA/AWWA/WEF 2012), while chemical oxygen demand (COD) was measured with cuvette test (Hach, Manchester, UK). Electrical conductivity, pH and total dissolved solids were measured with a multi pH Meter (Mettler Toledo FE20, Switzerland). Cu²⁺, Ti⁴⁺ and Zn²⁺ background levels as well as Al, Ca, Fe, K and Mg concentrations in synthetic wastewater were determined via ICP-OES. All the chemicals used were analytical grade.

5.4 Results and discussion

5.4.1 Removal of singularly spiked CuO, TiO₂ and ZnO by anaerobic granules sludge

The removal profile of some of the most common nanomaterials found in commercial products, CuO, TiO₂ and ZnO by AGS over the course of 6 hours was tested as a function of nanoparticle type and time. Overall, among all the concentrations (9, 90 and 180 mg/L) and NP types tested, AGS could remove between 23 and 77 % of the singularly spiked CuO, TiO₂ and ZnO in synthetic wastewater within 360 min (Fig. 5.1a, 5.1b, 5.1c).

At concentration of 9 mg/L, AGS had greater efficiency in removing ZnO, measured to 68.5 ± 1.5 %. CuO removal reached a level of 58.2 ± 1.3 % while the lowest removal was towards TiO₂, as AGS could remove 31.5 ± 1.3 % (Fig. 5.1a).

At the second concentration level tested (90 mg/L) (Fig. 5.1b), the greatest NP removal was observed for CuO, (77.2 ± 2.4 %). The removal efficiency was slightly lower towards TiO₂ as 57.6 ± 1.6 % of the nanomaterial were removed, whereas the 34.4 ± 1.4 % of removal for ZnO, was the lowest observed among the three NP types spiked at 90 mg/L.

A very similar pattern was observed with single CuO, TiO₂ and ZnO spiked at 180 mg/L, where the calculated removal efficiency was respectively 76.3 ± 1.2 % for CuO, 57.5 ± 2.4 % for TiO₂ and 23 ± 5.1 % for ZnO (Fig. 5.1c).

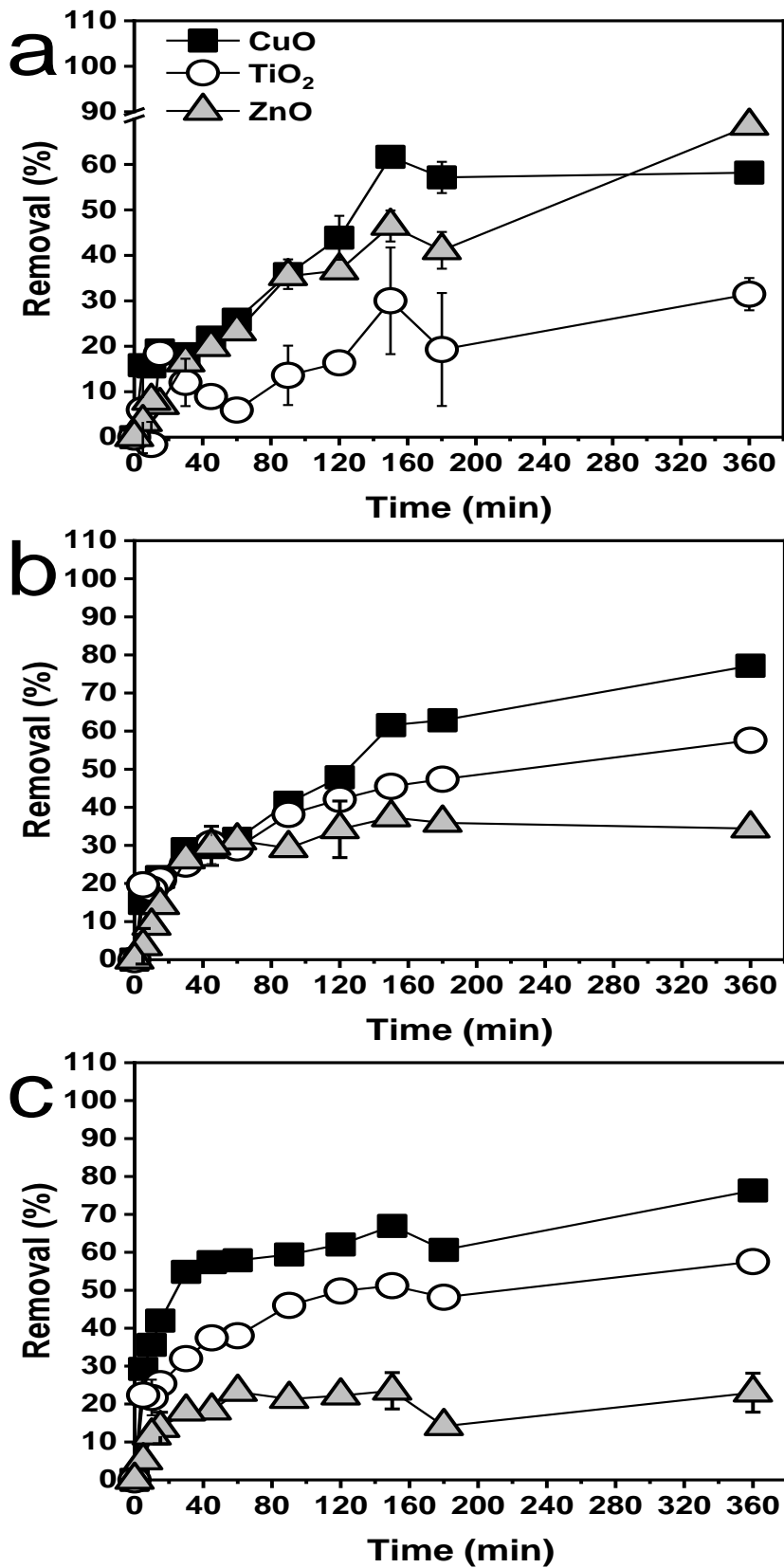


Fig. 5.1 Removal profile ($n=3 \pm$ standard deviation) of singularly spiked CuO, TiO₂ and ZnO reported as removal percent. Nanomaterials were spiked in presence of anaerobic granular sludge (AGS) at concentrations of 9 mg/L (a), 90 mg/L (b) and 180 mg/L(c).

These findings suggest that AGS have the potential to remove nanoparticles from wastewater. This corroborates what was reported for AGS treating synthetic sewage containing CuO, TiO₂ and ZnO at concentration of 5 mg/L during a long-term exposure experiment. The biomass had greater affinity, hence better removal efficiency for respectively CuO, TiO₂ and ZnO with the percentage of NPs retained in the system on average above 80% (Li et al. 2017). The higher removal efficiency compared to this study could be explained by the lower concentration tested by Li et al (2017) and by the prolonged experimental time they adopted. Advancing on this, results in the current study reported here indicate NPs present at a much greater concentration can be removed by AGS. While overall percentage removal was lower, due to the higher concentrations, the actual amount on NPs removed (expressed as measured concentration in mg/L) was greater as presented in Table 5.1. This can be seen when comparing the removal of CuO and TiO₂ at the two highest levels tested. The removal efficiencies (%) do not differ when increasing the spiking level. The removal percent of CuO did not show a clear increase as it went from 77.2 ± 2.4 % at 90 mg/L to 76.3 ± 1.2 % at 180 mg/L. Similarly, what found for TiO₂ is a removal efficiency of 57.6 ± 1.6 % (at 90 mg/L) and 57.5 ± 2.4 % at 180 mg/L. When assessing the removal efficiency this does not show sign of variation and the performances of the treatment appear as the same. By evaluating the concentrations of NPs removed (Table 5.1), it is instead clear that the AGS spiked at level of 180 mg/L could remove twice as much CuO and TiO₂ in comparison to the amount of NPs removed at 90 mg/L. For CuO the final fraction removed went from roughly 60 to 120 mg/L whereas the concentration of TiO₂ removed increased from 45.4 ± 1.2 to 92.6 ± 3.9 mg/L (Table 5.1). In the same table 5.1 resuming the results as well the following tables and plots there are sporadic elevated standard deviations and error bars. This is attributed to the nature of the microorganisms used in this work. AGS were added into the experimental vessels through weighing the target amount (4 g). However, this practice could easily be subject to imperfection that could cause greater variance in the results. This was not observed in the activated sludge experiments. The preparation of that experimental setup offered fewer chances of errors during preparation as activated sludge was simply pipetted from an adequately stirred pool solution into the experimental vessels.

Table 5.1 Resume of concentration and the relative removal efficiency (n=3 ± standard deviation) of CuO, TiO₂ and ZnO removed by anaerobic granular sludge (AGS) in the single NP systems.

9 mg/L		Concentration of NP removed (mg/L)			NP removal efficiency (%)		
Time (min)	CuO	TiO ₂	ZnO	CuO	TiO ₂	ZnO	
5	1.4 ± 0.2	0.3 ± 0.5	0.3 ± 0.2	15.8 ± 2.6	6 ± 9.5	3.3 ± 1.7	
10	1.3 ± 0.2	-0.1 ± 0.8	0.7 ± 0.1	15.5 ± 1.9	-1.6 ± 14.1	8 ± 0.8	
15	1.7 ± 0.1	1.1 ± 1.3	0.7 ± 0.2	19.1 ± 1.1	18.4 ± 22.5	7 ± 1.7	
30	1.6 ± 0.1	0.7 ± 1.9	1.5 ± 0.2	18.2 ± 1.2	12 ± 32.1	16.4 ± 2.5	
45	1.9 ± 0.1	0.5 ± 1.1	1.8 ± 0.2	21.9 ± 1.4	9 ± 18.7	19.8 ± 1.8	
60	2.2 ± 0.1	0.3 ± 0.8	2.2 ± 0.2	25.8 ± 0.8	6 ± 13.6	23.3 ± 2.2	
90	3.1 ± 0.3	0.8 ± 1	3.3 ± 0.3	35.9 ± 3.3	13.6 ± 17.3	35.4 ± 3.2	
120	3.8 ± 0.4	0.9 ± 1.2	3.4 ± 0.1	43.9 ± 4.8	16.4 ± 21.2	36.7 ± 1.2	
150	5.4 ± 0.2	1.7 ± 3.5	4.3 ± 0.3	61.7 ± 2.3	30 ± 60.3	46.5 ± 3.4	
180	5 ± 0.3	1.1 ± 0.7	3.8 ± 0.4	57.1 ± 3.4	19.3 ± 12.4	41.1 ± 4	
360	5 ± 0.1	1.8 ± 0.2	6.3 ± 0.1	58.2 ± 1.3	31.5 ± 3.5	68.5 ± 1.5	
90 mg/L		Concentration of NP removed (mg/L)			NP removal efficiency (%)		
Time (min)	CuO	TiO ₂	ZnO	CuO	TiO ₂	ZnO	
5	13 ± 1.3	15.5 ± 0.6	3 ± 4	14.9 ± 1.5	19.7 ± 0.7	3.5 ± 4.7	
10	15.9 ± 2.3	14.6 ± 1.9	7.5 ± 2.6	18.2 ± 2.6	18.5 ± 2.4	8.9 ± 3	
15	18.9 ± 1.2	16.4 ± 2.2	12.1 ± 1.9	21.7 ± 1.3	20.9 ± 2.8	14.3 ± 2.2	
30	25.3 ± 0.8	19.8 ± 1.5	22.3 ± 1.6	29 ± 0.9	25.1 ± 1.9	26.3 ± 1.9	
45	25.8 ± 3.8	24 ± 1.8	25.3 ± 4.4	29.6 ± 4.3	30.5 ± 2.3	29.9 ± 5.1	
60	27.7 ± 2.1	23.1 ± 2	26.5 ± 2.1	31.7 ± 2.4	29.3 ± 2.5	31.3 ± 2.5	
90	36 ± 1.2	30.1 ± 1.9	24.8 ± 0.9	41.2 ± 1.4	38.1 ± 2.4	29.2 ± 1	
120	41.8 ± 1.5	33.2 ± 0.9	29 ± 6.3	47.9 ± 1.7	42.1 ± 1.1	34.2 ± 7.4	
150	53.8 ± 2	35.9 ± 1.3	31.6 ± 0.5	61.6 ± 2.3	45.5 ± 1.6	37.3 ± 0.5	
180	54.9 ± 0.6	37.4 ± 1.2	30.4 ± 0.8	62.8 ± 0.7	47.4 ± 1.5	35.9 ± 0.9	
360	67.4 ± 2.1	45.4 ± 1.2	29.1 ± 1.2	77.2 ± 2.4	57.6 ± 1.6	34.4 ± 1.4	
180 mg/L		Concentration of NP removed (mg/L)			NP removal efficiency (%)		
Time (min)	CuO	TiO ₂	ZnO	CuO	TiO ₂	ZnO	
5	46 ± 4.9	36 ± 0.5	8.5 ± 3.2	29.3 ± 3.1	22.4 ± 0.3	5.1 ± 1.9	
10	56 ± 4.3	35 ± 7.6	19.3 ± 3	35.6 ± 2.8	21.7 ± 4.7	11.7 ± 1.8	
15	66.1 ± 2.7	40.8 ± 4.3	22.6 ± 6.9	42 ± 1.7	25.4 ± 2.7	13.7 ± 4.2	
30	86.3 ± 2.2	51.5 ± 4.6	29.7 ± 3	54.8 ± 1.4	32 ± 2.8	18 ± 1.8	
45	90.3 ± 3.3	60.2 ± 2.8	30.2 ± 1.6	57.4 ± 2.1	37.4 ± 1.7	18.3 ± 0.9	
60	91.1 ± 1.7	61.2 ± 2.6	38.4 ± 4.7	57.9 ± 1.1	38 ± 1.6	23.2 ± 2.8	
90	93.5 ± 1.4	74 ± 2.8	35.3 ± 0.8	59.4 ± 0.9	46 ± 1.8	21.3 ± 0.5	
120	97.6 ± 1.1	80.2 ± 6.3	36.8 ± 3.2	62.1 ± 0.7	49.8 ± 3.9	22.2 ± 1.9	
150	105.3 ± 1	82.4 ± 3.2	38.9 ± 7.9	66.9 ± 0.7	51.2 ± 2	23.5 ± 4.8	
180	95.4 ± 0.9	77.5 ± 4.4	23.4 ± 1.8	60.6 ± 0.5	48.2 ± 2.7	14.2 ± 1.1	
360	120 ± 1.9	92.6 ± 3.9	38 ± 8.5	76.3 ± 1.2	57.5 ± 2.4	23 ± 5.1	

It is also very interesting to note the influence that the NPs – AGS contact time has on the removal efficiency. We assessed the nanomaterial – biomass interaction for 6 hours to deliberately focus on the time-dependent NP removal profile. Six hours is considered a bottom limit for the hydraulic retention time (HRT) in AnWT (Otero-González et al. 2014) and we wanted to investigate the extreme case scenarios of very

short HRT with high NP concentrations needed to be handled by the wastewater treatment. It has been reported that reduction in HRT from 12 to 6 hours led to decreased CuO removal by AGS (Otero-González et al. 2014). NP removal is likely, at least in part, to occur via attachment onto the external membranes. The attachment of NPs onto the external membrane of AGS has been microscopically observed and also the amount of NP adhered to the granules was proven to be NP concentration dependent (Cervantes-Avilés et al. 2018). Our data suggest that time is an important factor in controlling the fate and partitioning of NPs entering an AnWT and hence affecting whether nanoparticles are removed from the liquor or released in environment. As shown in (Fig. 5.1a, 5.1b, 5.1c), the association between singularly spiked NPs and AGS seems to be a time-dependent process with a rapid binding of a portion of the NPs in the first 30 minutes. This first stage of NPs – granules interaction is highly likely to occur on the granules surface and be driven by electrostatic and van der Waals forces. The removal profile then shows a more gradual phase of removal that reaches a steady state between 150 and 180 min. This secondary and slower phase might be driven by a different interaction mechanism. Overtime, the majority of the free surface sites can be saturated and blocked by the association with nanomaterials. In this secondary and steady paced phase, the removal of NPs is likely to occur via an alternative and slower route such as diffusion or active uptake into the granules. For example, the biosorption of AgNP, SiO₂ and TiO₂ onto activated sludge was found to follow a similar profile. An initial rapid association occurred in the early contact phase which then stabilized within 60 min and remained steady to above 90 % (Park et al. 2013).

The total amount of ZnO removed were respectively 6.3 ± 0.1 , 29.1 ± 1.2 and 38 ± 8.5 mg/L. In comparison to CuO and TiO₂, ZnO removal at the concentration of 9 mg/L was found the greatest both as concentration of removed NPs and removal efficiency. However, with the increase of the added NPs, ZnO removal did not follow the profile observed for the other two nanomaterials. Proof of this is provided by the concentrations of ZnO removed at the three levels assessed. ZnO removal still appears concentration dependent as the amount of NPs removed increases at higher concentrations, but this does not occur as sharply as for CuO and TiO₂. This seems to suggest that the AGS driven removal mechanism may differ according to the nature of

the NPs. It is well known that zinc effect on biota is concentration dependent. Indeed, zinc is an essential trace element for bacterial growth, but at higher concentrations, it becomes toxic and has even antimicrobial properties. Bio-methanogenesis is a complicated process through which AGS symbiotic bacteria produce methane from more complicated organic matter species. The efficiency of such process is dependent on the presence and concentration of conductive materials. NPs such as iron oxide nanoparticles (IONPs) (He et al. 2017) and graphene (Tian et al. 2017) added at mg/L levels have been found to enhance gas production in anaerobic systems. It is suggested that NPs can act as primary electron donors or have an electron shuttles function, which promotes the electron transfer process and enhance bio-gas production (Zhang et al. 2014; Colunga et al. 2015). Zinc is not specifically recognised for contribution in electron transfer process that occurs in Bio-gas production, however, is an essential trace element for bacterial use. In light of the previously mentioned evidences of positive impact of NPs on microorganisms metabolism, we formulated the hypothesis that AGS could actively internalize ZnO for metabolic purposes at lower, non-toxic, environmental concentrations while reducing or minimizing the higher uptake at higher, potentially toxic, concentrations tested in this work. However, active adsorption is not the only mechanisms through which AGS can remove NPs. Electrostatic and van der Waals forces also play a key role especially in the first and rapid association phase with the AGS external membrane. In addition, aggregation can influence NP removal as well. As seen in chapter 3, ZnO in a biomass free liquor collected from the aeration basin of secondary treatment in a municipal sewage plant, showed the highest z-potential (greatest electrostatic repulsion) and was found to be the nanomaterial least susceptible to aggregation in comparison to CuO and TiO₂. This would explain the reduction in percentage ZnO removal at increased concentrations.

Copper is also an element needed by microorganism but at significantly lower concentrations than zinc while no biological function is recognised for titanium. The removal profile of CuO and TiO₂ at higher concentrations could confirm that AGS do not or very minimally actively uptake these nanomaterials, and that their removal occurs via pathways that differ from ZnO's. However, the removal efficiency for these two NPs was in most of the cases higher than what found for ZnO. This could be due to other AGS – NPs interactions and influence of aggregation driven sedimentation

and may suggest a weaker AGS surface affinity for ZnO. An interesting way to initiate investigate this in further details could be through the assessment of the aggregation-driven sedimentation removal in biomass-free media of double NP type mixtures.

Overall, our results are in line with previous data on the capacity of AGS to remove singularly spiked CuO, TiO₂ and ZnO. Despite the removal efficiency we observed (23 – 77 %) was to some extent lower to what previously reported for commonly used NPs (80 – 90 %), this is possibly due to the higher concentrations we tested. These data corroborate that AGS have the potential to satisfactory remove NPs from wastewater at environmental concentrations. The treatment performances (removal efficiency) as well as the amount of NPs removed from the influent stream at the lowest environmentally relevant concentration suggest this. Furthermore, our results at higher concentrations (90 and 180 mg/L) tested for three different NP types, also provide new insights into the AGS mediated removal of NPs and expand the range of concentrations at which AGS efficiency has been tested. This provides data on the evaluation of simulated extreme event scenarios as well as illegal discharge situations. This work also sheds light on the relevance of the AGS – NPs association, which has been found to happen in a time and NP type and concentration dependent manner. In addition, the AGS - NP sorption is slower in comparison to what observed in the interaction with aerobic activated sludge (see chapter 3).

5.4.2 Removal of CuO, TiO₂ and ZnO nanoparticle mixtures by anaerobic granules sludge

The AGS mediated removal profile of triple NPs (CuO, TiO₂ and ZnO) mixtures at concentration of 9 mg/L (total of 27 mg NP/L), 90 mg/L (total of 270 mg/L) and 180 mg/L (total concentration of 540 mg/L) was evaluated similarly to the single NP scenario and are shown in (Fig. 5.2, 5.3, 5.4).

When spiked at 9 mg/L, the NP mixture cumulative removal (Fig. 5.2d) by AGS after 360 min was found 64.8 ± 0.7 % with ZnO as the nanomaterial with the highest removal percentage (87.7 ± 0.4 %) (Fig. 5.2c). This was nearly 30% more than the final removal of CuO and TiO₂, which were very similar, and were respectively 52.4 ± 1.1 % and 49.1 ± 2.7 % (Fig. 5.2a, Fig. 5.2b).

When added at the highest concentration tested (180 mg/L each), the cumulative AGS removal efficiency was 50.9 ± 0.8 %. AGS showed highest efficacy in removing TiO_2 (62.1 ± 1.2 %) while CuO and ZnO were similarly removed as much as 45.3 ± 1.3 % and 47.9 ± 0.8 % (Fig. 5.4a, Fig. 5.4b, Fig. 5.4c, Fig. 5.4d).

The simultaneous co-presence of CuO, TiO_2 and ZnO in urban sewage is a highly likely scenarios with a greater environmental relevance in comparison to single NP pollution conditions. It has been shown that NP mixtures may have different environmental behaviour and toxicity in comparison to the single NPs (Eduok et al. 2015; Yu et al. 2016; Fang et al. 2017). However, the level of understanding of how the presence of NPs as a mixture may alter and impact the interaction with microorganisms employed in secondary treatments is still low. Especially the NP mixtures – AGS interactions and hence the removal performances are still scarcely documented.

As found for the single NP scenario, the AGS mediated removal efficiency of CuO and TiO_2 did not show such a degree of variation with the increase of concentration and ranged between 35 and 65 %. On the other hand, the removal of ZnO showed the highest removal efficiency, which exceeded 80 %, at 9 mg/L. The calculated efficiency however decreased to roughly 20 % and 50 % at the concentrations of 90 and 180 mg/L respectively. It is interesting to note how ZnO removal profiles follow a very similar pattern in both single and mixture scenarios. This may further confirm the nanomaterial type dependent nature of the NPs – AGS association. The biosorption of CuO and TiO_2 may be determined and primarily driven by electrostatic and van der Waals forces as well as aggregation at higher concentrations. The removal of ZnO instead at 9 mg/L, does not show an immediate interaction with the granules but instead occurs at a slower but steady pace. This could be the evidence of active transport and diffusion thorough the external AGS membrane. This could be triggered by AGS biomass actively internalizing ZnO for metabolic purposes at lower, non-toxic, environmental concentrations. Such hypothesis would be worth further investigating in future work. Such attempt could provide a more detailed understanding of the nature of the AGS-ZnO interactions. Experiments designed for this purpose could also be a good platform to research the metabolic use of Zinc and

understand whether AGS and other microorganism uptake ZnO and other nanoparticles as ion source.

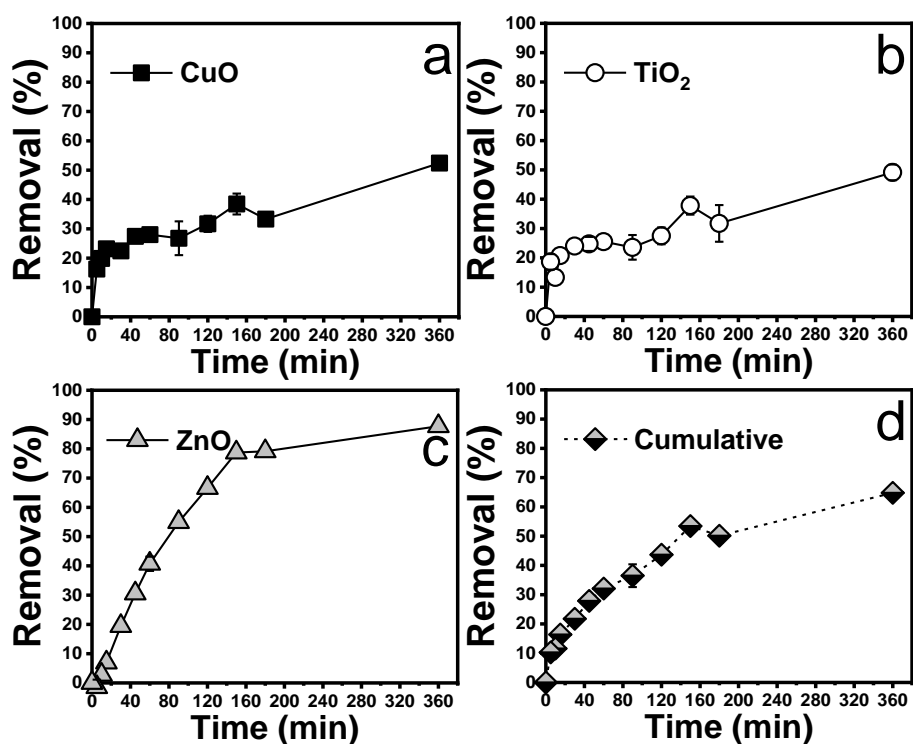


Fig. 5.2 Removal profile ($n=3 \pm$ standard deviation) of CuO (a), TiO₂ (b), ZnO (c) mixtures and cumulative (d) reported as relative removal percent. Each nanoparticle type was spiked in presence of anaerobic granular sludge (AGS) at concentration of 9 mg/L for a final concentration of 27 mg of NP/L. Removal of each NP type was reported in a separate panel for visual clarity.

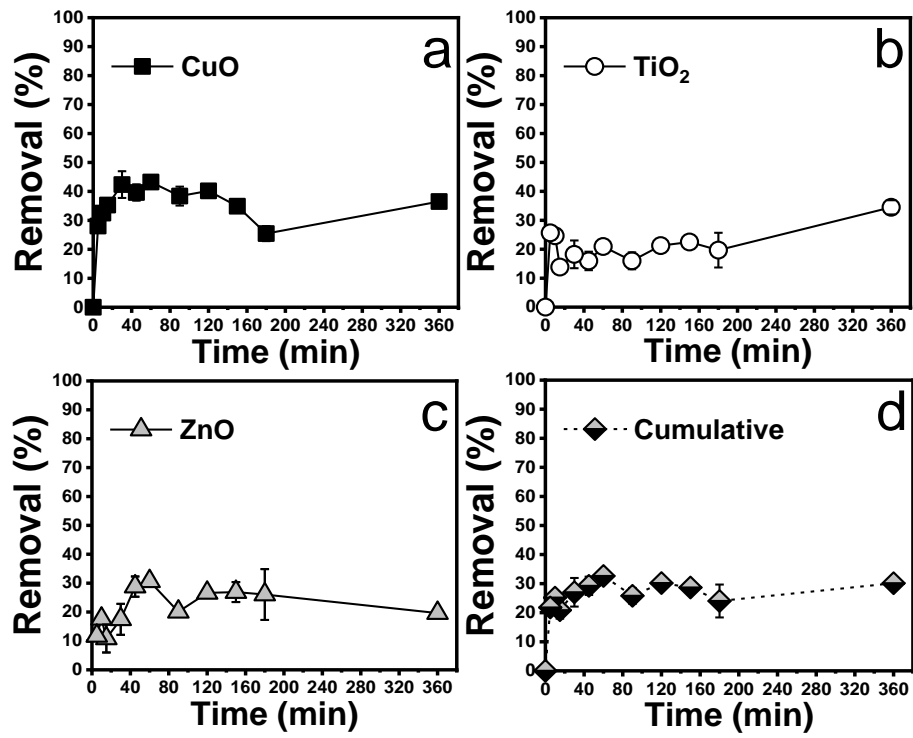


Fig. 5.3 Removal profile ($n=3 \pm$ standard deviation) of CuO (a), TiO₂ (b), ZnO (c) mixtures and cumulative (d) reported as relative removal percent. Each nanoparticle type was spiked in presence of anaerobic granular sludge (AGS) at concentration of 90 mg/L for a final concentration of 270 mg of NP/L. Removal of each NP type was reported in a separate panel for visual clarity.

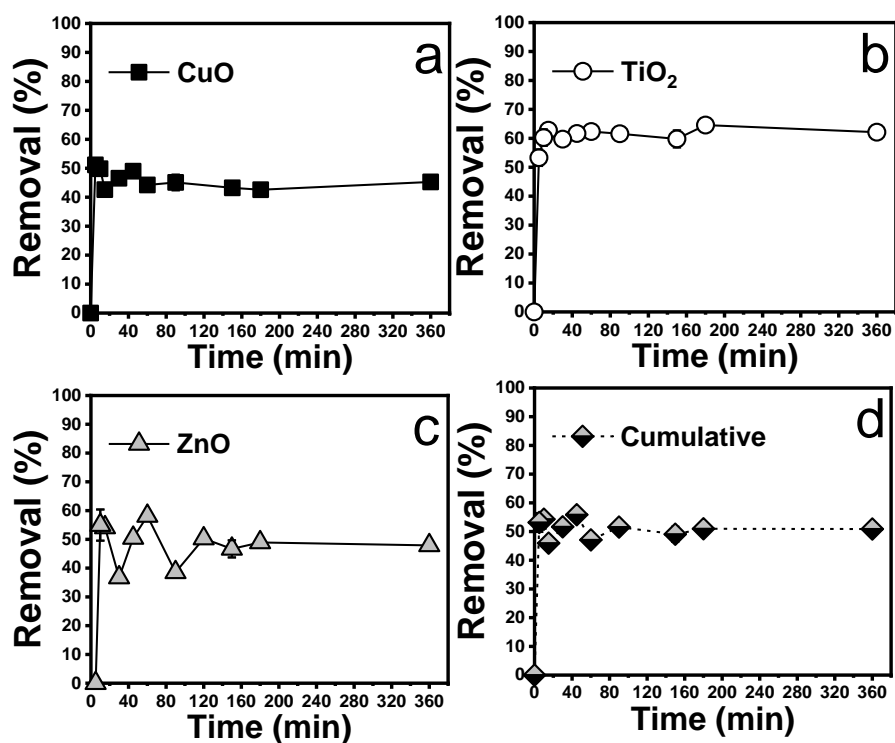


Fig. 5.4 Removal profile ($n=3 \pm$ standard deviation) of CuO (a), TiO₂ (b), ZnO (c) mixtures and cumulative (d) reported as relative removal percent. Each nanoparticle type was spiked in presence of anaerobic granular sludge (AGS) at concentration of 180 mg/L for a final concentration of 540 mg of NP/L. Removal of each NP type was reported in a separate panel for visual clarity.

The cumulative removal also shows a time dependent removal profile. At the lowest experimental total concentration (27 mg/L), the AGS – NPs system seem to reach an equilibrium after 150 min. When increasing the total concentrations, the time needed to reach a steady state diminishes as shown in Fig. 5.3d and 5.4d. At higher concentrations, the steady state appears to occur at an earlier point. Especially at the level of 180 mg/L CuO and TiO₂ stabilize immediately whereas ZnO fluctuate around the value at which then stabilizes around 50 % in 60 min. This is most likely due to the higher total amount of NPs the AGS were in contact with, accounting for 270 and 540 mg/L respectively. At such exposure levels, the occurrence and impact of NP aggregation increases with consequences on NP behaviour and removal. At such high concentrations, the NP – NP collision frequency increases. Despite NPs being negatively charged in environmental matrices (Keller et al. 2010; Loosli et al. 2013; Loosli et al. 2015) the high amount of NPs leads to increased aggregation and hence removal due to settlement. Hence the influence of the enhanced aggregation driven

sedimentation at high concentrations could be such to reduce the time needed for the systems to reach a steady state.

The AGS morphology may also account as a significant factor in the observed NP removal profile and efficiency. In comparison to flocculent biofilm, AGS have smaller specific surface (Gu et al. 2014). In addition, the adsorption of NPs onto biosolids has been shown to occur onto specific sites with high affinity of the external membrane. The biomass (sorber) has a certain sorption capacity which is determined by the specific surface and the properties of the sorber itself and by the properties and concentration of sorbate (NPs) (Kiser et al. 2010). A smaller specific surface also leads to a lower number of specific sites for the NPs – AGS biosorption (Ma et al. 2013).

The cumulative concentration of NPs removed was 16 ± 0.2 mg/L at 9 mg/L, which then increased to 69.6 ± 4.5 and 260.2 ± 4.1 mg/L at the spiking levels of respectively 90 and 180 mg/L (Table 5.2). The cumulative removal efficiency by spiking level were 64.8 ± 0.7 , 30.1 ± 1.9 and 50.9 ± 0.8 %. As discussed later in section 4.4.3, the aggregation driven sedimentation removal in synthetic wastewater seems to be NP concentration dependent (i.e. greater removal efficiency at higher concentrations). However, the NP removal in presence of AGS does not follow the same pattern, with the highest cumulative removal efficiency found at 9 mg/L when the aggregation in wastewater only system was observed at its minimum. This indicates that other process, and not aggregation, are playing a key role at this low 9 mg/l concentration in the AGS system. Given the removal profile (very quick and stabilizes at 30-45 minutes of NPs – AGS contact time) and the features of toxicity for copper and no biological effect for titanium, it appears that the removal of CuO and TiO₂ are driven by Electrostatic and van der Waals forces, with no or minimal active uptake by the biomass. With regards to ZnO, the specific removal profile (which occurs at a slower but steady pace) when added at low concentration such as 9 mg/L, it is hypothesised that AGS could actively adsorb Zn²⁺ for metabolic purposes. At higher concentrations, when zinc begins to be toxic and display antimicrobial properties, the active uptake will diminish and eventually cease. At the higher spiking levels then, greater amount of NPs on the system lead to increased removal via aggregation driven sedimentation which stabilises the systems at an early stage.

Table 5.2 Resume of concentration and the relative removal efficiency ($n=3 \pm$ standard deviation) of CuO, TiO₂ and ZnO removed by anaerobic granular sludge (AGS) in mixture experiments. Concentration 1 (9 mg/L * NP type equal to total concentration of 27 mg/L), concentration 2 (90 mg/L * NP type equal to total concentration of 270 mg/L), concentration 3 (180 mg/L * NP type equal to total concentration of 540 mg/L).

9 mg/l	Concentration of NP removed (mg/L)				NP removal efficiency (%)			
Time (min)	CuO	TiO ₂	ZnO	Cumulative	CuO	TiO ₂	ZnO	Cumulative
5	1.3 ± 0.2	1.6 ± 0.2	-0.1 ± 0.2	2.8 ± 0.6	16.3 ± 2	18.6 ± 2.6	-1.4 ± 2.6	10.3 ± 2.4
10	1.6 ± 0	1.2 ± 0.1	0.2 ± 0.1	3 ± 0.2	19.9 ± 0.6	13.3 ± 1.4	2.8 ± 1.2	11.6 ± 0.6
15	1.8 ± 0.1	1.8 ± 0.2	0.6 ± 0.1	4.2 ± 0.1	23.2 ± 1.6	20.8 ± 1.9	7 ± 1.6	16.4 ± 0.7
30	1.8 ± 0	2.1 ± 0	1.7 ± 0.2	5.5 ± 0.2	22.5 ± 0.2	24 ± 0.5	19.4 ± 1.7	21.8 ± 0.8
45	2.2 ± 0.1	2.1 ± 0.2	2.7 ± 0.1	7 ± 0.4	27.4 ± 1.8	24.8 ± 2.4	30.6 ± 1	27.9 ± 1.5
60	2.2 ± 0.1	2.2 ± 0.1	3.5 ± 0.2	8 ± 0.2	28 ± 1.5	25.5 ± 1.1	40.7 ± 2.4	32.1 ± 0.8
90	2.1 ± 0.5	2 ± 0.4	4.8 ± 0.2	8.9 ± 1	26.8 ± 5.8	23.6 ± 4.2	54.9 ± 2.2	36.5 ± 3.9
120	2.5 ± 0.2	2.4 ± 0.2	5.8 ± 0.1	10.7 ± 0.4	31.7 ± 2.8	27.5 ± 2.9	66.6 ± 0.7	43.7 ± 1.5
150	3.1 ± 0.3	3.3 ± 0.3	6.8 ± 0	13.2 ± 0.6	38.4 ± 3.6	37.8 ± 3.1	78.7 ± 0.3	53.4 ± 2.1
180	2.7 ± 0.2	2.7 ± 0.5	6.9 ± 0	12.3 ± 0.7	33.3 ± 2	31.7 ± 6.2	79.1 ± 0.1	50.1 ± 2.4
360	4.2 ± 0.1	4.2 ± 0.2	7.6 ± 0	16 ± 0.2	52.4 ± 1	49.1 ± 2.7	87.7 ± 0.4	64.8 ± 0.7
90 mg/l	Concentration of NP removed (mg/L)				NP removal efficiency (%)			
Time (min)	CuO	TiO ₂	ZnO	Cumulative	CuO	TiO ₂	ZnO	Cumulative
5	21.9 ± 0.4	20.1 ± 1	8.4 ± 0.7	50.4 ± 1.8	28.1 ± 0.5	25.7 ± 1.3	11.7 ± 1	21.8 ± 0.8
10	25.4 ± 1.2	19.3 ± 1.3	12.6 ± 0.9	57.3 ± 2.7	32.5 ± 1.5	24.6 ± 1.7	17.7 ± 1.3	25.2 ± 1.2
15	27.6 ± 1.4	10.8 ± 1.7	7.8 ± 3.5	46.2 ± 6.5	35.3 ± 1.8	13.8 ± 2.2	10.9 ± 4.8	20.9 ± 2.9
30	33.1 ± 3.6	14.3 ± 3.8	12.5 ± 3.8	59.9 ± 11.2	42.4 ± 4.6	18.2 ± 4.8	17.5 ± 5.4	27 ± 4.9
45	31 ± 2.2	12.5 ± 2.5	20.6 ± 2.5	64 ± 7.2	39.6 ± 2.8	16 ± 3.2	28.8 ± 3.5	29.2 ± 3.1
60	33.8 ± 1.6	16.4 ± 1.2	21.9 ± 1.5	72.1 ± 4.3	43.3 ± 2.1	20.9 ± 1.6	30.6 ± 2.1	32.6 ± 1.9
90	30 ± 2.6	12.5 ± 2.3	14.3 ± 1.5	56.9 ± 6.3	38.4 ± 3.3	16 ± 2.9	20.1 ± 2.1	25.8 ± 2.7
120	31.4 ± 1.1	16.6 ± 0.5	19 ± 1.2	67.1 ± 2.6	40.2 ± 1.4	21.2 ± 0.7	26.6 ± 1.8	30.2 ± 1.2
150	27.3 ± 0.8	17.6 ± 0.7	19.2 ± 2.5	64.1 ± 4	34.9 ± 1	22.5 ± 1	26.9 ± 3.5	28.7 ± 1.8
180	19.9 ± 2	15.4 ± 4.7	18.6 ± 6.3	53.9 ± 13	25.4 ± 2.6	19.7 ± 6	26.1 ± 8.8	24 ± 5.7
360	28.6 ± 1.4	27 ± 1.9	14 ± 1.2	69.6 ± 4.5	36.5 ± 1.7	34.5 ± 2.4	19.6 ± 1.7	30.1 ± 1.9
180 mg/l	Concentration of NP removed (mg/L)				NP removal efficiency (%)			

Time (min)	CuO	TiO ₂	ZnO	Cumulative	CuO	TiO ₂	ZnO	Cumulative
5	83.3 ± 3.5	89.9 ± 4.8	93.8 ± 9.3	267 ± 16.5	51.2 ± 2.1	53.3 ± 2.9	55 ± 5.4	53.2 ± 3.3
10	81.1 ± 1.6	101.6 ± 4.9	92.4 ± 1.3	275.1 ± 5.5	49.8 ± 1	60.2 ± 2.9	54.1 ± 0.7	54.3 ± 0.9
15	69.4 ± 1.2	105.9 ± 3.8	62.7 ± 1.3	238 ± 5.2	42.6 ± 0.8	62.8 ± 2.2	36.7 ± 0.8	46 ± 0.9
30	75.8 ± 2.4	100.7 ± 3.7	86.2 ± 1.2	262.7 ± 1.2	46.6 ± 1.5	59.7 ± 2.2	50.5 ± 0.7	51.6 ± 0.3
45	79.8 ± 3.4	104 ± 1.1	99.2 ± 3.2	282.9 ± 7.3	49 ± 2.1	61.7 ± 0.6	58.1 ± 1.9	55.9 ± 1.6
60	72 ± 0.7	105.1 ± 2.7	65.7 ± 2.5	242.9 ± 4.5	44.2 ± 0.4	62.3 ± 1.6	38.5 ± 1.4	47.1 ± 0.9
90	73.4 ± 4.5	103.8 ± 1.3	85.8 ± 2	263.1 ± 6.6	45.1 ± 2.8	61.6 ± 0.8	50.3 ± 1.1	51.5 ± 1.4
120	97.3 ± 56.8	122.7 ± 40.1	101.9 ± 59.5	321.9 ± 156	59.7 ± 34.9	72.7 ± 23.8	59.7 ± 34.9	45 ± 0.9
150	70.4 ± 3.8	100.8 ± 5.1	79.7 ± 5.1	250.9 ± 13.5	43.2 ± 2.3	59.8 ± 3	46.7 ± 3	49.1 ± 2.7
180	69.3 ± 2.6	108.9 ± 2.9	83.5 ± 2.7	261.7 ± 7.7	42.6 ± 1.6	64.6 ± 1.7	48.9 ± 1.6	51 ± 1.5
360	73.7 ± 2.3	104.8 ± 2	81.7 ± 1.4	260.2 ± 4.1	45.3 ± 1.4	62.1 ± 1.2	47.9 ± 0.8	50.9 ± 0.8

This work investigated for the first time the fate of triple NPs (CuO, TiO₂ and ZnO) mixtures in AnWT. Our results show that AGS can partially remove triple NPs mixtures composed of some of the most used and widely present nanomaterials in daily consumer products. This investigation covered an environmental likely NP concentration of 9 mg/L, as well as above the expected NP levels in WWTP scenarios (90 and 180 mg/L) to simulate extreme conditions. Under normal circumstances, AGS can remove from 30 to 50 % of the cumulative CuO, TiO₂ and ZnO load. We also observed that AGS mediated cumulative NP removal happens in concentration and time dependent manner. In addition, the morphology and biology of the granules appears to be an important factor in the treatment efficiency.

5.4.3 Removal of CuO, TiO₂ and ZnO nanoparticle mixtures in synthetic wastewater (without anaerobic granules)

The removal of co-occurring triple NPs (CuO, TiO₂ and ZnO) mixtures in synthetic wastewater only systems (no biomass) was also assessed. The aim of these experiments was to evaluate to which extent NP mixtures are affected by aggregation and sedimentation and how this impacts their removal and behaviour in wastewater. This therefore reveals removal mechanisms that are not directly related to the granules. These experiments involved the suspension of the anaerobic granules in synthetic wastewater with the same composition as reported in the previous work in this chapter. The quantification of the fraction of CuO, TiO₂ and ZnO found in the simulated effluent after settling in synthetic wastewater is shown in Fig. 5.5 (9 mg/L, total conc. of 27 mg/L), 5.6 (90 mg/L, total conc. of 270 mg/L) and 5.7 (180 mg/L total conc. of 540 mg/L).

At the lowest concentration tested, all the three nanomaterials showed a relatively similar removal efficiency due to aggregation driven sedimentation. This reached a steady state for CuO (Fig. 5.5a) and TiO₂ (Fig. 5.5b) around 15 % in roughly 30 min. Whereas up to 150 min were needed for the ZnO removal to stabilize (Fig. 5.5c) at a slightly lower removal efficiency (13 %). The cumulative removal stabilized at around 13 % within 60 min (Fig. 5.5b).

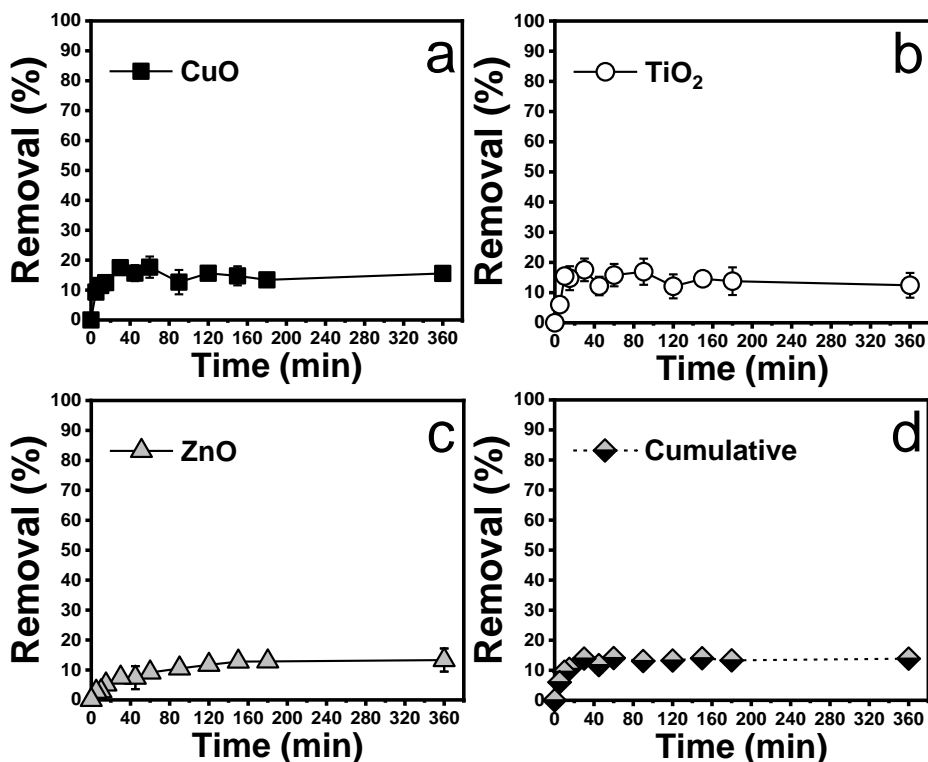


Fig. 5.5 Removal profile ($n=3 \pm$ standard deviation) of CuO (a), TiO₂ (b), ZnO (c) mixtures and cumulative (d) reported as relative removal percent. Each nanoparticle type was spiked in synthetic wastewater at concentration of 9 mg/L for a final concentration of 27 mg of NP/L. Removal of each NP type was reported in a separate panel for visual clarity.

At the concentration of 90 mg/L, both the cumulative and the NP type specific removal of CuO, TiO₂ and ZnO mixture increased in comparison to what observed at the concentration of 9 mg/L. Once stabilized, after 60 min, the cumulative removal was found calculated around 20 % (Fig. 5.6d) which accounted for a total amount of NPs removed equal to 37.5 ± 9.7 mg/l, roughly 7 % higher than the lower concentration (9 mg/L) where a total of 3.5 ± 0.2 mg/L were removed from the synthetic wastewater. The CuO and TiO₂ removal profile, efficiency (Fig. 5.6a and 5.6b) and concentration (Table 5.3) were similar. The aggregation driven sedimentation removal of ZnO instead showed the lowest value, (14%) as well as the smallest increase (1%) with the concentration rise (Fig. 5.6c) with only 8.9 ± 2.9 mg/L removed. This could be another proof suggesting that ZnO is the nanomaterial least susceptible to aggregation and sedimentation in synthetic wastewater among those investigated in this work. This

further confirms our findings in the assessment of NP removal in biomass-free liquor from a secondary treatment of a municipal WWTP (see sections 3.4.3 and 3.4.5).

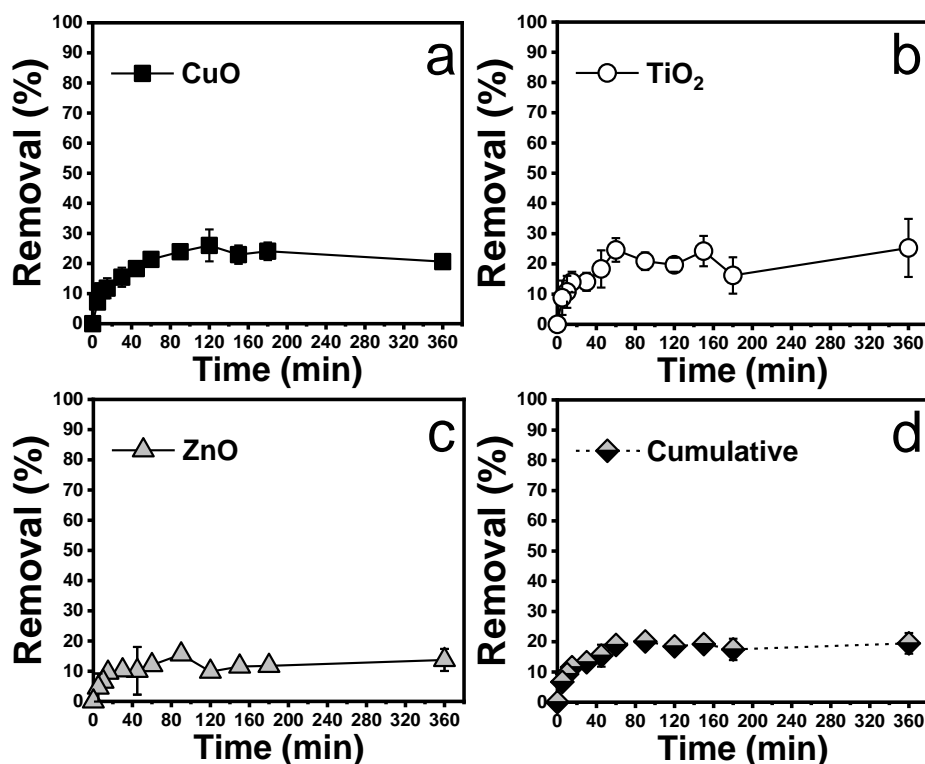


Fig. 5.6 Removal profile ($n=3 \pm$ standard deviation) of CuO (a), TiO₂ (b), ZnO (c) mixtures and cumulative (d) reported as relative removal percent. Each nanoparticle type was spiked in synthetic wastewater at concentration of 90 mg/L for a final concentration of 270 mg of NP/L. Removal of each NP type was reported in a separate panel for visual clarity.

When added at 180 mg/L for a total concentration of 540 mg NP/L, the removal of all the nanomaterials increased again and reduced the variability between the NP types as about 30% of CuO (Fig. 5.7a), and 25 % of TiO₂ and ZnO (Fig. 5.7b and Fig. 5.7c) were removed in synthetic wastewater with no AGS biomass added. The cumulative removal stabilized in 30 min to a level of 26 % (Fig. 5.7d).

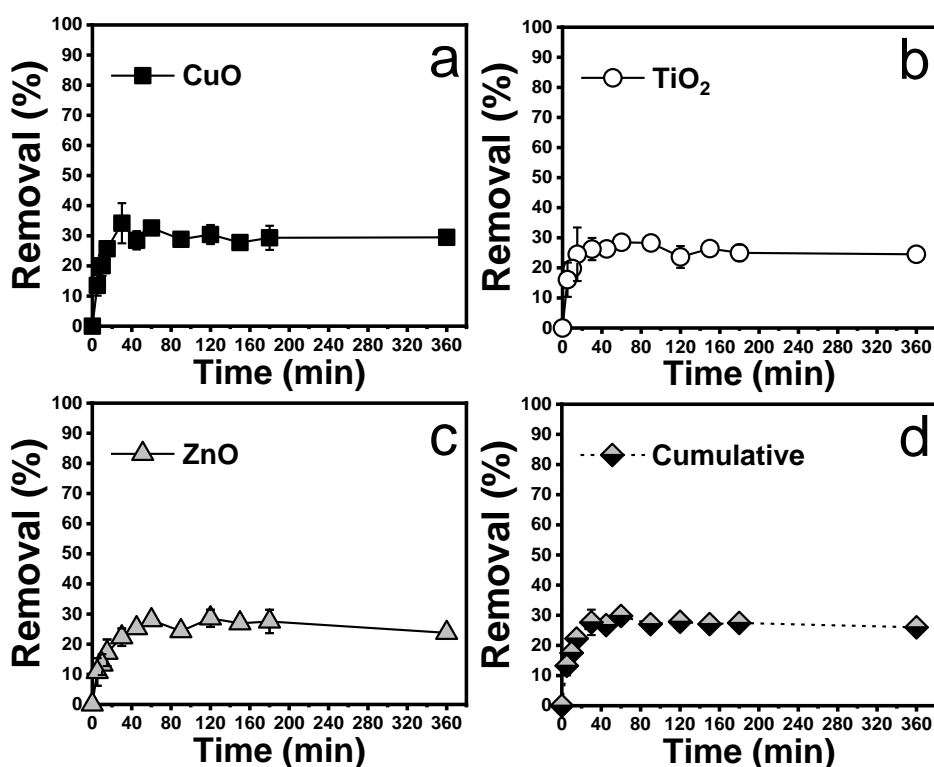


Fig. 5.7 Removal profile ($n=3 \pm$ standard deviation) of CuO (a), TiO₂ (b), ZnO (c) mixtures and cumulative (d) reported as relative removal percent. Each nanoparticle type was spiked in synthetic wastewater at concentration of 180 mg/L for a final concentration of 540 mg of NP/L. Removal of each NP type was reported in a separate panel for visual clarity.

These results indicate that a partial removal of co-occurring NPs may happen even in absence of AGS biomass in synthetic wastewater and at high total NP concentrations up to at least 540 mg/l. This also highlights the importance of the environmental matrix on the fate and impact of nanomaterials. It appears that the removal of co-existing CuO, TiO₂ and ZnO due to aggregation driven sedimentation is dependent on the NP concentration as well as the nature of the liquor in which NP are dispersed. This works indeed finds that single type and NP mixtures are partially removed in liquor only systems (without biomass present), however the amount of NPs removed depends on the nanomaterial types as well the water quality parameters of the liquid in which NPs are suspended.

The percent of cumulative NP removed when no AGS biomass is present showed an increase at higher input concentrations which went from 13.9 % (27 mg NP/L), to 19.5 % (270 mg NP/L) and yet increased to 26 % at the final level tested (540 mg NP/L). This is equivalent to respectively 3.5 ± 0.2 , 37.5 ± 9.7 and 132 ± 8.3 mg/L of

total NPs removed in the systems tested. These data suggest that the removal via aggregation driven sedimentation occurs in a NP inflow concentration dependent manner. This trend is similar to what found when evaluating the removal profile of CuO, TiO₂ and ZnO in biomass free liquor collected from the aeration basin of secondary treatment in a municipal sewage plant (see paragraph 3.4.5). In that case the NP removal increased at higher concentrations, which went from 60 % at 9 mg/L to 85 % at 180 mg/L. Hence the NP concentration appears to be one of the key factors governing the aggregation and sedimentation of NPs.

Table 5.3 Resume of concentration and the relative removal efficiency (n=3 ± standard deviation) of CuO, TiO₂ and ZnO mixtures removed in synthetic wastewater experiments. Concentration 1 (9 mg/L * NP type equal to total concentration of 27 mg/L), concentration 2 (90 mg/L * NP type equal to total concentration of 270 mg/L), concentration 3 (180 mg/L * NP type equal to total concentration of 540 mg/L).

9 mg/l		Concentration of NP removed (mg/L)				NP removal efficiency (%)			
Time (min)	CuO	TiO ₂	ZnO	Cumulative	CuO	TiO ₂	ZnO	Cumulative	
5	0.8 ± 0.1	0.5 ± 0.1	0.2 ± 0.1	1.5 ± 0.1	9.3 ± 1.7	6 ± 1.1	2.7 ± 1	6 ± 0.5	
10	1 ± 0.2	1.3 ± 0.2	0.2 ± 0.1	2.5 ± 0.3	11.5 ± 1.9	15.5 ± 2.5	2.9 ± 1.2	9.5 ± 1	
15	1 ± 0.1	1.3 ± 0.3	0.4 ± 0.1	2.7 ± 0.5	12.5 ± 0.8	14.8 ± 3.9	5.2 ± 1.5	10.5 ± 1.7	
30	1.5 ± 0.1	1.5 ± 0.3	0.6 ± 0.1	3.6 ± 0.3	17.5 ± 1.7	17.5 ± 3.7	7.5 ± 1.4	13.9 ± 0.8	
45	1.3 ± 0.2	1 ± 0.3	0.6 ± 0.3	3 ± 0.6	15.6 ± 2.7	12.2 ± 3.1	7.4 ± 3.8	11.7 ± 2.5	
60	1.5 ± 0.3	1.4 ± 0.3	0.8 ± 0.2	3.6 ± 0.1	17.7 ± 3.5	15.8 ± 3.7	9.1 ± 2	14.1 ± 0.6	
90	1.1 ± 0.3	1.4 ± 0.4	0.9 ± 0.1	3.4 ± 0.6	12.6 ± 4.1	16.9 ± 4.3	10.5 ± 1.4	13.1 ± 2.2	
120	1.3 ± 0.1	1 ± 0.3	1 ± 0.1	3.3 ± 0.5	15.6 ± 1.4	12.1 ± 4	11.7 ± 1.8	13.2 ± 2	
150	1.2 ± 0.3	1.2 ± 0.1	1.1 ± 0.1	3.5 ± 0.3	14.7 ± 3.2	14.6 ± 1.1	12.8 ± 1.1	14 ± 1.4	
180	1.1 ± 0.2	1.2 ± 0.4	1.1 ± 0.1	3.4 ± 0.5	13.4 ± 2	13.8 ± 4.6	12.8 ± 0.7	13.3 ± 1.9	
360	1.3 ± 0.2	1.1 ± 0.4	1.1 ± 0.3	3.5 ± 0.2	15.6 ± 2.3	12.4 ± 4.1	13.3 ± 3.9	13.9 ± 0.6	
90 mg/l		Concentration of NP removed (mg/L)				NP removal efficiency (%)			
Time (min)	CuO	TiO ₂	ZnO	Cumulative	CuO	TiO ₂	ZnO	Cumulative	
5	1.9 ± 1.8	1.8 ± 4.8	1.5 ± 3.7	5.2 ± 2.4	7.2 ± 2.1	8.8 ± 5.7	4.6 ± 4.6	6.7 ± 1.2	
10	5 ± 0.9	3.4 ± 4.4	3.1 ± 1.9	11.5 ± 2.8	10.9 ± 1	10.7 ± 5.3	6.5 ± 2.3	9.3 ± 0.9	
15	5.7 ± 2.7	6.1 ± 2.9	5.5 ± 2.4	17.3 ± 4.5	11.8 ± 3.3	14 ± 3.4	9.5 ± 3	11.6 ± 1.7	
30	8.7 ± 2.6	6.2 ± 2.5	6.1 ± 1.8	21 ± 2.2	15.4 ± 3.2	14.1 ± 3	10.3 ± 2.2	13.2 ± 0.8	
45	11 ± 2.2	9.8 ± 5.2	6 ± 6.3	26.8 ± 9.5	18.3 ± 2.7	18.3 ± 6.2	10.1 ± 7.9	15.4 ± 3.6	
60	13.6 ± 2	15.1 ± 3.3	7.5 ± 1.6	36.1 ± 4.9	21.4 ± 2.5	24.6 ± 3.9	12 ± 2	18.9 ± 1.8	
90	15.6 ± 1.8	11.9 ± 2.4	10.4 ± 1.6	37.9 ± 0.5	23.9 ± 2.2	20.9 ± 2.9	15.6 ± 2	20.1 ± 0.3	
120	17.4 ± 4.4	10.9 ± 1.9	5.8 ± 2.1	34.1 ± 7.2	26 ± 5.3	19.7 ± 2.3	9.8 ± 2.6	18.5 ± 3	
150	14.9 ± 2.5	14.7 ± 4.2	7.1 ± 1.5	36.7 ± 3.7	23 ± 3.1	24.2 ± 5	11.5 ± 1.9	19.2 ± 1.5	
180	15.8 ± 2.4	8 ± 5	7.3 ± 1.9	31.1 ± 9.2	24.1 ± 2.9	16.2 ± 6	11.8 ± 2.3	17.5 ± 3.5	
360	12.9 ± 0.8	15.6 ± 8.1	8.9 ± 2.9	37.5 ± 9.7	20.6 ± 1	25.3 ± 9.6	13.7 ± 3.6	19.5 ± 3.4	

180 mg/l	Concentration of NP removed (mg/L)				NP removal efficiency (%)			
Time (min)	CuO	TiO ₂	ZnO	Cumulative	CuO	TiO ₂	ZnO	Cumulative
5	22.5 ± 5.6	28.2 ± 10	18.1 ± 7.7	68.8 ± 16.3	13.5 ± 3.4	16.1 ± 5.7	10.8 ± 4.6	13.2 ± 3.2
10	33.4 ± 5.6	34.8 ± 3.6	22.2 ± 5.8	90.4 ± 5.3	20.1 ± 3.4	19.8 ± 2.1	13.2 ± 3.5	17.5 ± 1
15	42.8 ± 2.5	43.1 ± 15.6	28.7 ± 7.4	114.6 ± 12.5	25.7 ± 1.5	24.5 ± 8.9	17.2 ± 4.4	22.3 ± 2
30	56.9 ± 11.1	46.1 ± 6.5	37.3 ± 4.9	140.4 ± 21.2	34.2 ± 6.7	26.2 ± 3.7	22.3 ± 2.9	27.7 ± 4.2
45	47.5 ± 5.1	46.2 ± 4.1	42.4 ± 2.5	136.1 ± 6.8	28.5 ± 3	26.3 ± 2.3	25.3 ± 1.5	26.7 ± 1.2
60	54.3 ± 3.7	50.1 ± 1	46.9 ± 3.8	151.2 ± 7.5	32.6 ± 2.2	28.5 ± 0.6	28 ± 2.3	29.8 ± 1.6
90	48 ± 4	49.7 ± 4.1	40.8 ± 4.3	138.5 ± 4.6	28.8 ± 2.4	28.3 ± 2.3	24.3 ± 2.6	27.1 ± 0.8
120	50.7 ± 5.3	41.5 ± 6.4	47.9 ± 4.8	140 ± 5.9	30.4 ± 3.2	23.6 ± 3.6	28.6 ± 2.9	27.8 ± 1.4
150	46.2 ± 4.2	46.4 ± 3.9	45.1 ± 3.1	137.8 ± 4.5	27.8 ± 2.5	26.4 ± 2.2	26.9 ± 1.8	27.1 ± 0.9
180	48.9 ± 6.7	43.9 ± 4.8	46.1 ± 6.5	138.9 ± 7.7	29.3 ± 4	25 ± 2.7	27.5 ± 3.9	27.5 ± 1.5
360	49.1 ± 2.9	43.1 ± 4.1	39.8 ± 3.5	132 ± 8.3	29.5 ± 1.7	24.5 ± 2.3	23.8 ± 2.1	26 ± 1.6

The physiochemical characterization of the OECD standard synthetic wastewater (OECD 2001) is presented in Table 5.4. On average, the samples had a pH of 7.4 ± 0.2 , total dissolved solids (TDS) of 237.5 ± 21.9 mg/L, conductivity of 326.1 ± 22.4 μ s/cm, chemical oxygen demand (COD) of 94.4 ± 7.4 mg O₂/L and dissolved organic carbon equal to 91.4 ± 13.6 mg C/L.

Table 5.4 Comparison of synthetic wastewater and biomass-free liquor characteristics and the respective cumulative removal (%) of CuO, TiO₂ and ZnO mixtures. Concentration 1 (9 mg/L * NP type equal to total concentration of 27 mg/L), concentration 2 (90 mg/L * NP type equal to total concentration of 270 mg/L), and 3 (180 mg/L * NP type equal to total concentration of 540 mg/L).

	Units	Synthetic wastewater	Biomass-free liquor
pH		7.4 ± 0.2	7.0 ± 0.4
TDS	mg/L	237.5 ± 21.9	316.4 ± 35.3
Conductivity	μ s/cm	326.1 ± 22.4	586.7 ± 56.1
COD	mg O ₂ /L	94.4 ± 7.4	91.1 ± 35.9
DOC	mg C/L	91.4 ± 13.6	7.71 ± 0.47
Cu	mg/L	LOQ	0.05 ± 0.07
Ti	mg/L	LOQ	0.31 ± 0.21
Zn	mg/L	LOQ	0.08 ± 0.06
Al	mg/L	0.82 ± 0.12	0.02 ± 0.01
Ca	mg/L	9.21 ± 0.77	30.45 ± 2.15
Fe	mg/L	1.93 ± 0.38	0.04 ± 0.02
K	mg/L	18.41 ± 2.61	11.81 ± 2.11
Mg	mg/L	2.17 ± 0.25	5.90 ± 0.61
Na	mg/L	9.82 ± 0.72	60.78 ± 4.24
<hr/>			
Mixture 9 mg/L		13.9 ± 0.6	60.5 ± 1.0
Mixture 90 mg/L		19.5 ± 3.4	58.1 ± 7.2
Mixture 180 mg/L		26 ± 1.6	84.5 ± 0.2

The nature and characteristics of the liquid matrix in which NPs are suspended are also known for having a great impact capable of controlling NP mobility, bioavailability and toxicity in wastewater plants as well as in other environmental

compartments (Garner and Keller 2014). It is well known that the increase in ionic strength, (higher monovalent and divalent cations concentration), can affect NP stability. Under such conditions, the presence of electrolyte ions causes the decrease in the thickness of the electrical double layer and a consequent reduction in the repulsive electrostatic interactions among NPs (Liu et al. 2013).

Similar but opposite influence is due to dissolved organic matter (DOM). It has been shown that NPs in environmental matrix containing negatively charged DOM acquire a negative charge due to the DOM – NP association (Diegoli et al. 2008). This leads to the formation of an organic capping surrounding NPs which can create an electrostatic repulsion hindering NP aggregation (Zhang et al. 2009; Keller et al. 2010; Loosli et al. 2013; Zhou et al. 2015). However, with increasing NP concentrations, the electrostatic repulsion is likely to be overcome by a higher frequency of NP – NP collisions (Tong et al. 2014) which would explain the observed increased CuO, TiO₂ and ZnO sedimentation at higher concentrations.

The synthetic wastewater used here had a much higher concentration of DOM in comparison to the concentrations of the measured monovalent and bivalent cations. The sum of the measured cations was equal to 42.36 mg/L (the calculated total molarity is 1.74 mM) while the amount of DOM was 91.4 ± 13.6 mg C/L. Baalousha et al. (2013), reported that divalent cations are much more effective than monovalent cations in triggering NP aggregation. This is suggested to take place via reduction of repulsive electrostatic forces (this can happen at as low as 1.5 mM of Ca²⁺, the cation with the greatest impact on NPs stability). Contrarily to this, monovalent cations had no or minimal destabilizing effects, only chloride ions specifically induced aggregation and destabilization of AgNPs. This is the result of AgNP dissolution that leads to the following formation of insoluble AgCl. However, the sum molarity of the two most abundant divalent cations in our system (Ca²⁺ and Mg²⁺) was lower than 0.5 mM. Interestingly, Wang et al. (2014), evaluated how salinity and DOC combine to control the stability of AgNP-citrate, AgNP-PVP and TiO₂NPs. The results showed that all the nanomaterials taken into account were negatively affected by interacting with cations, which enhance aggregation, whilst DOM prevents it. However, when combining the two factors, the results showed that DOM could hinder NP aggregation at low salinity (below 5 ppt) but this stabilizing effect reduced at higher salinity (30

ppm). It is important to note that the work from Wang et al. (2014) investigated a maximum of 10.5 mg DOC/L. Our experimental conditions had a similar level of total cations around 40 mg/L but a much higher DOC value (> 90 mg C/L). We therefore suggest that CuO, TiO₂ and ZnO suspended in synthetic wastewater are greatly subject to a more prominent stabilization effect related to high presence of DOC. This is well known to act as capping agent that can hinder NP - NP aggregation by creating an electrosteric barrier. The relatively high level of cations, but even greater presence of organic matter can explain the partial/minimal NP removal via sedimentation the overall result is the stabilization of the nanomaterials due to the prominent DOC induced effects. Such combination is likely to be the reason that more NPs were not removed via aggregation driven sedimentation. A further point to reinforce this hypothesis comes from the comparison of the liquor composition and CuO, TiO₂ and ZnO removal reported in Tab. 5.4. This tables reports the water quality characteristics of the two media and show the removal percent of the triple NP mixture experiments without biomass present.

The comparison of these results shows a greater NP removal in biomass free liquor collected from a conventional wastewater treatment plant, where under these experimental conditions between 58 and 85 % of the added nanomaterials were removed. When spiked in synthetic wastewater, the NP removal was calculated between 13 and 27.5 %. This difference in results seems to indicate a great effect on NP environmental fate and behavior deriving from the liquid composition. Indeed, the secondary liquor had a much higher cations content, especially the concentration of the divalent cations Ca²⁺ and Mg²⁺ were respectively three and two times higher than what measured in synthetic wastewater. The latter however had greater presence of DOC which was roughly 10 times more abundant in synthetic wastewater. As previously mentioned, dissolved organic matter can stabilize NPs whereas the presence of cations would enhance aggregation. Another interesting point comes from the comparison of COD. The results among the two media are similar, but the DOC content in real secondary liquor is much lower. This could mean that a big portion of the COD could be under the form of small colloidal particles that would not be filtered out in the biomass removal process. This seems to be confirmed by the higher values of TDS and conductivity in the liquor. The presence of colloidal forms is another factor

that can negatively impact the stability of NPs in suspension causing sedimentation (Quik et al. 2012).

Overall, the results obtained by spiking CuO, TiO₂ and ZnO in synthetic wastewater, confirm once again how greatly the environmental matrix can affect and control NP mobility, bioavailability, behaviour and fate in environmental matrices. It once more suggests that the composition of the liquor itself may be the key factor, as it may modify the environmental fate of nanomaterials. Wastewater is a great example of a highly and unpredictable liquid matrix whose composition can be highly variable in time and space and hence hard to predict and standardize. The great difference in composition and effects on NPs fate ascertained when using real wastewater and synthetic sewage is strong evidence in support of this hypothesis. In addition, this work shows that even in the AGS mediated removal of CuO, TiO₂ and ZnO mixtures, aggregation driven sedimentation is responsible for almost 50 % of the NP removal observed at 9, 90 and 180 mg/L. Besides, concentration is a key factor, as the NP removal via aggregation appear to be dependent on the inlet CuO, TiO₂ and ZnO level.

5.5 Conclusions

This study aimed to assess to which extent anaerobic granular sludge could cope with single CuO, TiO₂, ZnO and their triple NPs mixtures. The assessment was carried out at concentrations of 9, 90 and 180 mg/L to evaluate likely and above predicted NP environmental concentrations. The NPs – AGS biomass association appears to be NP type and concentration dependent. We observed a high removal efficiency towards ZnO at low concentration which then significantly falls at higher concentrations. A more constant removal was instead measured for CuO, TiO₂. Time is also a key factor governing The NPs – AGS biomass association, as the biosorption does not happen quickly as for activated sludge, especially at low concentrations. The removal via aggregation driven sedimentation increased with the rise in NP concentration, with 13 to 26 % of the NPs load removed in absence of AGS. This confirmed once more how significantly the fate of NP in AnWT and environment can be influenced by the matrix in which NPs are present. Hence, for a more appropriate NP assessment and more detailed understanding of NP behaviour the evaluation of the environmental conditions should be an essential factor to be considered.

5.6 Bibliography

- APHA/AWWA/WEF (2012) Standard Methods for the Examination of Water and Wastewater. Stand Methods 541. [https://doi.org/ISBN 9780875532356](https://doi.org/ISBN%209780875532356)
- Baalousha M, Nur Y, Römer I, et al (2013) Science of the Total Environment Effect of monovalent and divalent cations , anions and fulvic acid on aggregation of citrate-coated silver nanoparticles. *Sci Total Environ* 454–455:119–131. <https://doi.org/10.1016/j.scitotenv.2013.02.093>
- Botheju D, Lie B, Bakke R (2010) Oxygen effects in anaerobic digestion - II. Model Identif Control 31:55–65. <https://doi.org/10.4173/mic.2010.2.2>
- Cervantes-Avilés P, Ida J, Toda T, Cuevas-Rodríguez G (2018) Effects and fate of TiO₂ nanoparticles in the anaerobic treatment of wastewater and waste sludge. *J Environ Manage* 222:227–233. <https://doi.org/10.1016/j.jenvman.2018.05.074>
- Colunga A, Rangel-Mendez JR, Celis LB, Cervantes FJ (2015) Graphene oxide as electron shuttle for increased redox conversion of contaminants under methanogenic and sulfate-reducing conditions. *Bioresour Technol* 175:309–314. <https://doi.org/10.1016/j.biortech.2014.10.101>
- Deublein D, Steinhauser A (2010) Biogas from Waste and Renewable Resources: An Introduction, Second Edition
- Diegoli S, Manciualea AL, Begum S, et al (2008) Interaction between manufactured gold nanoparticles and naturally occurring organic macromolecules. *Sci Total Environ* 402:51–61. <https://doi.org/10.1016/j.scitotenv.2008.04.023>
- Eduok S, Hendry C, Ferguson R, et al (2015) Insights into the effect of mixed engineered nanoparticles on activated sludge performance. *FEMS Microbiol Ecol* 91:1–9. <https://doi.org/10.1093/femsec/fiv082>
- Fang J, Shijirbaatar A, Lin D hui, et al (2017) Stability of co-existing ZnO and TiO₂nanomaterials in natural water: Aggregation and sedimentation mechanisms. *Chemosphere* 184:1125–1133. <https://doi.org/10.1016/j.chemosphere.2017.06.097>
- Garner KL, Keller AA (2014) Emerging patterns for engineered nanomaterials in the environment: A review of fate and toxicity studies. *J Nanoparticle Res* 16:. <https://doi.org/10.1007/s11051-014-2503-2>
- Gottschalk F, Nowack B (2011) The release of engineered nanomaterials to the

- environment. *J Environ Monit* 13:1145. <https://doi.org/10.1039/c0em00547a>
- Gottschalk F, Sondere T, Schols R, Nowack B (2009) Modeled Environmental Concentrations of Engineered Nanomaterials for Different Regions. *Environ Sci Technol* 43:9216–9222. <https://doi.org/10.1021/es9015553>
- Gu L, Li Q, Quan X, et al (2014) Comparison of nanosilver removal by flocculent and granular sludge and short- and long-term inhibition impacts. *Water Res* 58:62–70. <https://doi.org/10.1016/j.watres.2014.03.028>
- He CS, He PP, Yang HY, et al (2017) Impact of zero-valent iron nanoparticles on the activity of anaerobic granular sludge: From macroscopic to microcosmic investigation. *Water Res* 127:32–40. <https://doi.org/10.1016/j.watres.2017.09.061>
- Holmes DE, Smith JA (2016) Biologically Produced Methane as a Renewable Energy Source. *Adv Appl Microbiol* 97:1–61. <https://doi.org/10.1016/bs.aambs.2016.09.001>
- Keller AA, Wang H, Zhou D, Miller RJ (2010) Stability and Aggregation of Metal Oxide Nanoparticles in Natural Aqueous Matrices Stability and Aggregation of Metal Oxide Nanoparticles in Natural Aqueous Matrices. 44:1962–1967. <https://doi.org/10.1021/es902987d>
- Kiser MA, Ryu H, Jang H, et al (2010) Biosorption of nanoparticles to heterotrophic wastewater biomass. *Water Res* 44:4105–4114. <https://doi.org/10.1016/j.watres.2010.05.036>
- Kiser MA, Westerhoff P, Benn T, et al (2009) Titanium Nanomaterial Removal and Release from Wastewater Treatment Plants. *Environ Sci Technol* 43:6757–6763. <https://doi.org/10.1021/es901102n@proofing>
- Klinkner BA (2014) Anaerobic Digestion as a Renewable Energy Source and Waste Management Technology: What Must be Done for This Technology to Realize Success in the United States? *UMass Law Rev* 9:68–95
- Lettinga G (1995) Anaerobic digestion and wastewater treatment systems. *Antonie Van Leeuwenhoek* 67:3–28. <https://doi.org/10.1007/BF00872193>
- Li H, Cui F, Liu Z, Li D (2017) Bioresource Technology Transport, fate, and long-term impacts of metal oxide nanoparticles on the stability of an anaerobic methanogenic system with anaerobic granular sludge. *Bioresour Technol*

- 234:448–455. <https://doi.org/10.1016/j.biortech.2017.03.027>
- Li LL, Tong ZH, Fang CY, et al (2015) Response of anaerobic granular sludge to single-wall carbon nanotube exposure. *Water Res* 70:1–8.
<https://doi.org/10.1016/j.watres.2014.11.042>
- Liu W, Sun W, Borthwick AGL, Ni J (2013) Comparison on aggregation and sedimentation of titanium dioxide, titanate nanotubes and titanate nanotubes-TiO₂: Influence of pH, ionic strength and natural organic matter. *Colloids Surfaces A Physicochem Eng Asp* 434:319–328.
<https://doi.org/10.1016/j.colsurfa.2013.05.010>
- Loosli F, Coustumer P Le, Stoll S (2013) TiO₂ nanoparticles aggregation and disaggregation in presence of alginate and Suwannee River humic acids. pH and concentration effects on nanoparticle stability. *Water Res* 47:6052–6063.
<https://doi.org/https://doi.org/10.1016/j.watres.2013.07.021>
- Loosli F, Vitorazi L, Berret JF, Stoll S (2015) Towards a better understanding on agglomeration mechanisms and thermodynamic properties of TiO₂ nanoparticles interacting with natural organic matter. *Water Res* 80:139–148.
<https://doi.org/10.1016/j.watres.2015.05.009>
- Ma J, Quan X, Si X, Wu Y (2013) Responses of anaerobic granule and flocculent sludge to ceria nanoparticles and toxic mechanisms. *Bioresour Technol* 149:346–352. <https://doi.org/10.1016/j.biortech.2013.09.080>
- Mackevica A, Olsson ME, Hansen SF (2017) The release of silver nanoparticles from commercial toothbrushes. *J Hazard Mater* 322:270–275.
<https://doi.org/10.1016/j.jhazmat.2016.03.067>
- OECD (2001) Simulation Test - Aerobic Sewage Treatment: 303A: Activated Sludge Units. OECD
- Otero-González L, Field JA, Sierra-Alvarez R (2014) Inhibition of anaerobic wastewater treatment after long-term exposure to low levels of CuO nanoparticles. *Water Res* 58:160–168.
<https://doi.org/10.1016/j.watres.2014.03.067>
- Park HJ, Kim HY, Cha S, et al (2013) Removal characteristics of engineered nanoparticles by activated sludge. *Chemosphere* 92:524–528.
<https://doi.org/10.1016/j.chemosphere.2013.03.020>

- Poh PE, Gouwanda D, Mohan Y, et al (2016) Optimization of Wastewater Anaerobic Digestion Using Mechanistic and Meta-heuristic Methods: Current Limitations and Future Opportunities. *Water Conserv Sci Eng* 1:1–20.
<https://doi.org/10.1007/s41101-016-0001-3>
- Quik JTK, Stuart MC, Wouterse M, et al (2012) Natural colloids are the dominant factor in the sedimentation of nanoparticles. *Environ Toxicol Chem* 31:1019–1022. <https://doi.org/10.1002/etc.1783>
- Shi X, Leong KY, Ng HY (2017) Anaerobic treatment of pharmaceutical wastewater: A critical review. *Bioresour Technol* 245:1238–1244.
<https://doi.org/10.1016/j.biortech.2017.08.150>
- Tian T, Qiao S, Li X, et al (2017) Nano-graphene induced positive effects on methanogenesis in anaerobic digestion. *Bioresour Technol* 224:41–47.
<https://doi.org/10.1016/j.biortech.2016.10.058>
- Tong T, Fang K, Thomas SA, et al (2014) Chemical interactions between nano-ZnO and nano-TiO₂ in a natural aqueous medium. *Environ Sci Technol* 48:7924–7932. <https://doi.org/10.1021/es501168p>
- Van Lier JB, Mahmoud N, Zeeman G (2008) Anaerobic Wastewater Treatment
- Velasco P, Jegatheesan V, Othman M (2018) Recovery of dissolved methane from anaerobic membrane bioreactor using degassing membrane contactors. *Front Environ Sci* 6:1–6. <https://doi.org/10.3389/fenvs.2018.00151>
- Wang H, Burgess RM, Cantwell MG, et al (2014) Stability and aggregation of silver and titanium dioxide nanoparticles in seawater: Role of salinity and dissolved organic carbon. *Environ Toxicol Chem* 33:1023–1029.
<https://doi.org/10.1002/etc.2529>
- Weir A, Westerhoff P, Fabricius L, et al (2012) Titanium dioxide nanoparticles in food and personal care products. *Environ Sci Technol* 46:2242–2250.
<https://doi.org/10.1021/es204168d>
- Westerhoff PK, Kiser A, Hristovski K (2013) Nanomaterial removal and transformation during biological wastewater treatment. *Environ. Eng. Sci.* 30:109–117
- Yu R, Wu J, Liu M, et al (2016) Toxicity of binary mixtures of metal oxide nanoparticles to *Nitrosomonas europaea*. *Chemosphere* 153:187–197.

<https://doi.org/10.1016/j.chemosphere.2016.03.065>

Zhang HK, Lu H, Wang J, et al (2014) Cr(VI) reduction and Cr(III) immobilization by acinetobacter sp. HK-1 with the assistance of a novel quinone/graphene oxide composite. *Environ Sci Technol* 48:12876–12885.

<https://doi.org/10.1021/es5039084>

Zhang Y, Chen Y, Westerhoff P, Crittenden J (2009) Impact of natural organic matter and divalent cations on the stability of aqueous nanoparticles. *Water Res* 43:4249–4257. <https://doi.org/10.1016/j.watres.2009.06.005>

Zhou X hong, Huang B cheng, Zhou T, et al (2015) Aggregation behavior of engineered nanoparticles and their impact on activated sludge in wastewater treatment. *Chemosphere* 119:568–576.

<https://doi.org/10.1016/j.chemosphere.2014.07.037>

6 Conclusions

6.1 Summary

The aim of this PhD was to assess whether conventional and emerging secondary biological treatments can remove single and NP mixtures from wastewater and hence prevent their release and reduce their potential to cause harm in receiving water bodies.

Recently, research has focused on the hazard and risk deriving from exposure to nanoparticles. A growing body of evidence indicate that NPs have the potential to exhibit toxicity to aquatic organisms and may be accumulated and concentrated throughout the food web.

Direct consequence of the nanomaterials market expansion is the growing release of nanoparticles in wastewater. With regards to this, wastewater treatment plants play a key role in protecting the environment by removing the pollution load and hence returning treated sewage that would not causa harm to the receiving water bodies. However, wastewater treatment plants were not designed or developed to remove emerging contaminants such as nanoparticles. Therefore, understanding whether wastewater treatment plants can remove nanoparticles from the incoming sewage stream and prevent nano particulate pollution is essential to enable a sustainable development of nanotechnology industry, while also protecting the environment und living organisms.

This assessment was carried out in this PhD research thesis by an initial development and validation of a suitable sample processing protocol paired with analysis method, capable to accurately and precisely quantify single and triple mixtures of nano sized copper oxide (CuO), titanium dioxide (TiO₂) and zinc oxide (ZnO).

Following this initial step, the removal of CuO, TiO₂ and ZnO by real activated sludge collected from a municipal wastewater treatment plant was investigated. In addition, the effects of real sewage entering a secondary treatment was studied in order to assess the stability and hence the environmental fate of nanoparticle suspensions. Moreover, the removal capability of an emerging wastewater biological treatment, anaerobic granulated sludge, was determined. This work has specifically focused on a range of NP concentrations as well as mixture systems that encompasses current,

future and extreme scenarios that wastewater treatment plants are likely to face already now and in the future.

This chapter presents a summary of the main funding from each research chapter and highlights potential future work in this research field.

6.2 Assessment of the suitability of sample processing methods and analytical method for NP quantification in wastewater samples

A wide array of sample processing methods and analytical techniques are currently available to quantify nanoparticles. Yet, a single accepted and standardized procedure is still lacking. In addition, simultaneous quantification of different NP types is a topic of growing interest. Yet again, quantification of NP mixtures is still a completely emerging branch which has received minimal research attention. In recent years, inductively coupled plasma - optical emission spectrometry (ICP-OES) paired with acid digestion have gained major importance in NP detection and measurement. Here we address this technological gap by developing and validating a single sample processing method and an analytical protocol. The goodness of a single H_2SO_4 – HNO_3 acid digestion followed by ICP-OES measurement has here been proven. This method showed great success in providing accurate and precise measurements of single CuO, TiO_2 and ZnO as well as their triple mixtures. It was hypothesized that the H_2SO_4 – HNO_3 acid mix could obviate the use of the far more hazardous hydrofluoric acid (HF) and simultaneously dissolve the nanoparticulate form. The success of this stage of the sample process would create an aqueous solution containing the relative analytes of interest (Cu^{2+} , Ti^{4+} and Zn^{2+}) that would then be quantified via ICP-OES analysis.

First, the reliability of the acid digestion process was evaluated and compared in relation to digestion method and acid mixtures. The results show that H_2SO_4 – HNO_3 acid mix provide satisfactory metal recovery for all the NP types tested. Irrespectively of the digestion method, both microwave and hotplate assisted digestions gave metal recovery values within the USEPA accepted range. On the contrary, reverse aqua regia of (HNO_3 – HCl (3:1)) digestion did not offer satisfactory metal recovery. This implies that the choice of an acid mixture tailored to the NP types of interest is essential to obtain reliable NP quantification.

Once the identification of a suitable acid mixtures, we assessed whether the analytical procedure could affect the availability of the produced analytes of interests. It is well known that acids can react with other substances to create insoluble undesired compounds such as in the case of silver nanoparticles dissolved in hydrochloric acid (HCl). In this eventuality, the analytical method would no longer be accurate, hence not reliable. This was evaluated by processing and analyzing standard solutions containing the dissolved cations after undergoing the whole analytical procedures. The results of these tests showed no evidence of undesired effects on the analytes. Therefore, satisfactory metal recovery and no undesired effects on the availability, and therefore determination of the analytes of interests through the analytical process, open to the possibility to establish a single analytical procedure to simultaneously quantify CuO, TiO₂ and ZnO mixtures.

The method Limit of detection (*MDL*) and limit of quantification (*MQL*) were also evaluated following different procedures and were calculated in the region between 0.005 and 0.01 ppm. These results show that this analytical method can quantify extremely low levels of CuO, TiO₂ and ZnO which in many natural matrices and personal products would easily be present at concentrations higher than these method limits.

Finally, the goodness of this single sample processing method for and analytical method for NP quantification was tested over a concentration range up to 100 ppm. This was done to evaluate method trueness (metal recovery) and precision (relative standard deviation, RSD %). These tests confirmed the goodness of the procedure for all the analytes of interest throughout the concentration range in both water and wastewater.

The results presented in this chapter indicate that a single H₂SO₄ – HNO₃ acid digestion followed by ICP-OES measurement can successfully be used to quantify single and triple mixtures of nano-sized CuO, TiO₂ and ZnO in aqueous samples. Including the H₂SO₄ – HNO₃ acid digestion has the potential to make this method a widely applied technique. This could be valuable for determining many other NP types and could be applicable to a wide variety of sample matrices including the majority of common aqueous and many solid samples too.

6.3 Nanoparticle removal by activated sludge biomass

The development and validation of a suitable analytical method enables us to explore the fate of CuO, TiO₂ and ZnO in biological secondary treatment conventionally used in wastewater treatment plants.

Activated sludge biomass is an engineered microbial population that exploits the dissolved carbon, nitrogen and phosphorus-based compounds present in sewage to fuel its metabolism. Through this, these pollutants are removed from wastewater and their contamination of the receiving water bodies is prevented.

Activated sludge has an history of over a century of utilization to safeguard the natural environment, but it has not originally been developed nor adapted to deal and cope with the presence of NPs. The presence of such emerging contaminants at rapidly increasing concentrations in sewage is now giving rise to a serious concern for the environment und living creatures that has so far only been marginally investigated.

In response to this, the removal ability of real activated sludge biomass collected from a conventional wastewater treatment plant was studied. The results of such investigation show that the association between the biomass and NPs happens very quickly and occurs in the first minutes of contact time. The association than follows a profile which generally stabilizes within 120 minutes. The overall performances in terms of NP removal, always exceeding 90 %, irrespectively of the NP type (CuO, TiO₂ and ZnO) and concentration (9, 90 and 180 mg/L) in single NP type system.

Following the successful evaluation single NP removal by activated sludge, a further assessment involving triple NP mixture was carried out. This section of the current work was designed to further enhance the environmental relevance of the assessment and more importantly to investigate one of the current main gaps in the environmental assessment of nanoparticles: their fate and behaviour in mixture systems. Very remarkably, activated sludge was capable to remove over 90 % of the spiked NPs at levels of 9 and 90 mg/L (respectively cumulative NP spiking concentrations were 27 and 270 mg/L). However, at the highest level of 180 mg/L per NP type (total concentration of 540 mg/L), activated sludge-led cumulative removal exceeded 95 %, but this initial phase was followed by a second profile during which we measured an increase in NP detected unremoved. This could suggest that at such concentration, activated sludge biomass begins to be subjected to structural damages

due to the presence of NPs. This can lead to degradation of the external membrane as well as the intentional release of extracellular polymeric substances as a defense mechanism which would re-suspend a portion of the previously immobilized NPs. The observation of this fall in the treatment performances could set an initial set-point for wastewater companies to monitor, manage, maintain and optimize treatment performances standards against the presence of NPs in the incoming sewage stream.

This possible first detection of a threshold NP concentration was reinforced by the results obtained through the investigation on the effect of the liquid matrix on NP stability and hence fate in wastewater treatment plants. This part of the work was done to attempt to close a gap on the influence of the liquor fraction on NP behaviour and removal. Components present in water such as cations, organic matter, solids and pH can induce changes on NP stability via electrostatic and electrostatic interactions. However, the impact of secondary liquor (sewage treated through preliminary and primary treatments) has not been evaluated yet. Most studies have either focused on other aqueous matrices such as lake and river water or used synthetic wastewater. In the present study, real secondary liquor was collected and when added in it, NPs showed a constant negative charge irrespectively of the pH (varying from 3 to 10) with no or minimal sign of aggregation. These findings differ from what observed in ultrapure water, where the surface charge and hence size distribution of the NP suspension were found pH dependent. The presence of dissolved organic matter seems to be the reason behind these results. Organic molecules can interact with NPs which then gain an organic and negatively charged coating which enhances the with electrosteric repulsion and hence stabilizes them which ultimately is observed as reduction in size distribution.

This investigation was further expanded by assessing the removal of NPs in liquor only systems (no biomass present) to study to which extent CuO, TiO₂ and ZnO were removed by aggregation driven sedimentation. The results showed that NPs are removed to certain extent even when biomass is not present. However, the observed results were interestingly lower to the expectations. The presence of cations and neutral pH would suggest high removal due to the reduction of electrostatic forces which would make NPs more neutral and hence more subject to aggregation. However, the presence of dissolved organic matter seems to be the reason hindering this process.

The results presented here indicate that activated sludge is a highly efficient treatment that achieves high removal of some of the most commonly used NPs in both single and triple NP mixture scenarios. This treatment process is highly efficient within its conventional operational parameters such as retention time, mix liquor suspended solids, pH and DO. Furthermore, the application of activated sludge is shown to be essential to achieve such performances due to the limited removal of NPs in absence of biomass caused by the stabilizing effect apported by the chemical nature of wastewater. This treatment has shown great and consistent efficiency throughout a wide range of concentrations. However, a fall in performances was observed at the highest mixture level tested. This could indicate a threshold concentration after which treatment performances may be impaired.

6.4 Nanoparticle removal by anaerobic granular sludge

Following the assessment of CuO, TiO₂ and ZnO by activated sludge, a similar approach was used to test the removal performances of anaerobic granular sludge. This was done to expand the investigation to an emerging secondary biological treatment which has attracted growing attention in recent years.

Anaerobic granule sludge-based treatment has a variety of advantages in comparison to conventional biological treatments. These include no need to supply oxygen and no or minimal production of waste sludge, hence lower operational costs. In addition, anaerobic sludge produces biogas which can be used as fuel for combined heat and power engines to produce energy making such process more sustainable.

Overall, the removal performances were lower in comparison to what observed in activated sludge experiments. The time dependent removal profile also appears to differ as the granules – NPs association happens in a slower manner during the initial phase to then stabilize overtime. Among the three NP types tested, ZnO was the nanomaterial most greatly removed. In addition, no fall in removal performances was observed, confirming that anaerobic granules are much more resistant to the exposure to contaminants. This can be attributed to the different structure between the two types of biomass. The thicker granules of the anaerobic granules make them more resistant to the harmful effects of contaminants, however the smaller specific surface makes them less efficient absorber.

The removal of CuO, TiO₂ and ZnO when no biomass is present (in this case synthetic wastewater) was also lower in this set of tests. This can confirm our previous findings, suggesting that the presence of organic matter plays a key role in stabilizing NPs. Indeed, the synthetic wastewater used here had a higher amount of dissolved organic carbon compounds which decreased the quantity of NPs removed via aggregation driven sedimentation.

These findings suggest that anaerobic granules sludge-based treatments can partially remove single type and triple NP mixtures at environmental and extremely high concentrations. This treatment may be further developed and optimized to achieve greater performances.

6.5 Comparison between activated and anaerobic granular sludge treatments performances

Biological wastewater treatments are based on a simple principle: the complex microbial community utilizes the nutrient (carbon, nitrogen and phosphorous based compounds) to produce new biomass. Through this process, the pollutant load is retained in the system and its discharge in the environment is prevented. This further avoids pollution events in the receiving water bodies.

Aerobic activated and anaerobic granular sludges operate under different conditions, but ultimately, provide the same result of reducing the pollution load from sewage. Engineered application of activated sludge has occurred for over a century with countless treatment plants currently operated around the globe. Anaerobic granular sludge-based sewage treatment plants have instead been developed in the last decades. Hence anaerobic granular sludge is often considered as an improved and more advanced treatment. This reputation is due to three main features that make this treatment more environmentally sustainable. These are: a) lower costs and lower energy consumption as no oxygen needs to be supplied; b) smaller volumes of waste sludge produced that needs to undergo further treatment and simultaneous production of biogas which can be used to fuel combined heat and power (CHP) engines; c) the granular structure provides greater resistance to harsh or rapidly changing environmental conditions which makes such treatment more stable and easier to be operated.

Neither of these biological secondary treatments have originally been designed to remove nanoparticles. As an emerging contaminant, the presence of nanoparticles in sewage now poses a new challenge for wastewater treatment plants.

In this work we specifically challenged both treatments with single and triple NP type mixtures. The treatment performances, in term of nanoparticle removal, were studied at concentrations that resemble current environmental conditions (9 mg/L) and span up to severe high concentrations (90 and 180 mg/L) that could occur in extreme events.

When it comes to the solely nanoparticle removal, activated sludge displays the best performances. The treatment was shown capable of removing over 90 % CuO, TiO₂ and ZnO regardless of type and concentration in single NP systems. Similar results were observed for the 9 mg/L mixture system, however the cumulative removal efficiency fell to around 75% at the highest NP level.

Lower performances were instead observed for anaerobic granular sludge. In single NP system, the percent of CuO, TiO₂ and ZnO removed varied from 30 to 70 %. A similar range of removal, from 30 to 56 %, of the added nanoparticles were removed when present as triple nanoparticle type mixture. Similarly, the cumulative removal percent in mixture systems varied from 30.1 ± 1.9 at 90 mg/l to 64.8 ± 0.7 at 9 mg/L.

Interestingly, the results of NP removal when in biomass-free systems show quite a broad range in biomass free liquor, with the lowest being 31 % up to a maximum of 93 %. Contrary to this, the removal of NP mixtures in synthetic wastewater showed a much more homogeneous removal with a max and minimum removal percent of respectively 29 and 12 %. A comprehensive results overview is reported in Table 6.1. This includes the amount of NPs removed, the removal percent for biotic experiments (where either activated sludge or anaerobic granular sludge biomass was used) as well as abiotic experiment where the NP removal was assessed in biomass-free liquor or synthetic wastewater. In addition, the concentrations of removed nanoparticles was normalized against the weight of biomass added int the experiments and reported as mg of nanoparticles removed by 1 gram of biomass.

Table 6.1 Resume of all the CuO, TiO₂ and ZnO removal experiments. Activated sludge and biomass free-liquor experiments duration was 180 min. Anaerobic granular sludge (AGS) and synthetic wastewater tests were run for 360 min. All the results are reported as (n=3 ± standard deviation). (-) Experiments not run.

		Activated sludge biomass			Anaerobic granular sludge biomass			Biomass-free liquor		Synthetic wastewater	
		Final NP removed (mg/L)	Final NP removal (%)	mg NP Removed / g biomass	Final NP removed (mg/L)	Final NP removal (%)	mg NP removed/ g biomass	Final NP removed (mg/L)	Final NP removal (%)	Final NP removed (mg/L)	Final NP removal (%)
9 mg/l Single NP	CuO	9.1 ± 0.1	99.6 ± 0.1	4.5 ± 0.2	5 ± 0.1	58.2 ± 1.3	0.04 ± 0.01	3.2 ± 0.5	35.2 ± 5.5	-	-
	TiO ₂	8.9 ± 0.1	99.6 ± 0.2	4.5 ± 0.2	1.8 ± 0.2	31.5 ± 3.5	0.02 ± 0.01	3.8 ± 0.5	42.3 ± 4.9	-	-
	ZnO	8.5 ± 0.3	90.9 ± 3.5	4.2 ± 0.3	6.3 ± 0.1	68.5 ± 1.5	0.05 ± 0.01	4 ± 0.1	32.5 ± 0.5	-	-
90 mg/l Single NP	CuO	89.1 ± 0.2	99.9 ± 0.1	44.5 ± 0.3	67.4 ± 2.1	77.2 ± 2.4	0.52 ± 0.08	-	-	-	-
	TiO ₂	87.9 ± 0.2	98 ± 0.6	44 ± 0.2	45.4 ± 1.2	57.6 ± 1.6	0.34 ± 0.07	-	-	-	-
	ZnO	86.9 ± 0.2	97.7 ± 0.1	43.5 ± 0.9	29.1 ± 1.2	34.4 ± 1.4	0.22 ± 0.05	-	-	-	-
180 mg/l Single NP	CuO	174.3 ± 0.1	99.9 ± 0.1	87.2 ± 0.2	120 ± 1.9	76.3 ± 1.2	0.94 ± 0.11	101.3 ± 0.3	57.7 ± 0.2	-	-
	TiO ₂	176.1 ± 0.1	99 ± 0.6	86.1 ± 1.9	92.6 ± 3.2	57.5 ± 2.4	0.72 ± 0.09	162 ± 2.1	93.8 ± 1.5	-	-
	ZnO	172.1 ± 0.2	96.1 ± 0.2	88.1 ± 1.4	38 ± 8.5	23 ± 5.1	0.31 ± 0.04	73.6 ± 6.5	42.4 ± 3.8	-	-
9 mg/l Mixture	CuO	8.1 ± 0.1	97.3 ± 0.1	4 ± 0.3	4.2 ± 0.1	52.4 ± 1	0.03 ± 0.01	6.7 ± 0.1	86.7 ± 0.1	1.3 ± 0.2	15.6 ± 2.3
	TiO ₂	7.9 ± 0.1	97.7 ± 0.2	4 ± 0.1	4.2 ± 0.2	49.1 ± 2.7	0.03 ± 0.01	6.9 ± 0.1	84.4 ± 0.1	1.1 ± 0.4	12.4 ± 4.1
	ZnO	10.9 ± 0.1	97.6 ± 0.2	5.5 ± 1	7.6 ± 0.1	87.7 ± 0.4	0.06 ± 0.01	3 ± 0.2	28.1 ± 0.2	1.1 ± 0.3	13.3 ± 3.9
	Cumulative	27 ± 0.1	97.5 ± 0.1	13.5 ± 1.4	16 ± 0.2	64.8 ± 0.7	0.12 ± 0.03	16.5 ± 0.2	60.5 ± 1.0	3.5 ± 0.2	13.9 ± 0.6
90 mg/l Mixture	CuO	77.2 ± 0.2	91.6 ± 0.3	38.6 ± 0.9	28.6 ± 1.4	36.5 ± 1.7	0.21 ± 0.05	58.7 ± 4.8	69.4 ± 5.4	12.9 ± 0.8	20.6 ± 1
	TiO ₂	67.1 ± 0.2	90.6 ± 0.2	33.6 ± 2.6	27 ± 1.9	34.5 ± 2.4	0.2 ± 0.04	57 ± 5.8	66.1 ± 6.4	15.6 ± 8.1	25.3 ± 9.6
	ZnO	82.3 ± 0.4	90.2 ± 0.3	41.1 ± 2.3	14 ± 1.2	19.6 ± 1.7	0.11 ± 0.03	50.8 ± 6.9	41.7 ± 7.7	8.9 ± 2.9	13.7 ± 3.6
	Cumulative	226.6 ± 0.6	90.8 ± 0.3	113.3 ± 1.8	69.6 ± 4.5	30.1 ± 1.9	0.52 ± 0.08	166.6 ± 5.1	58.1 ± 7.2	37.5 ± 9.7	19.5 ± 3.4
180 mg/l Mixture	CuO	135.3 ± 0.4	77 ± 0.3	67.6 ± 0.6	73.7 ± 2.3	45.3 ± 1.4	0.55 ± 0.09	84.5 ± 0.6	88.3 ± 0.7	49.1 ± 2.9	29.5 ± 1.7
	TiO ₂	129.9 ± 0.4	79.7 ± 0.3	65 ± 2.4	104.8 ± 2.0	62.1 ± 1.2	0.79 ± 0.09	161.9 ± 0.2	84.4 ± 0.4	43.1 ± 4.1	24.5 ± 2.3
	ZnO	168.8 ± 0.6	70. ± 0.2	84.4 ± 1.7	81.7 ± 1.4	47.9 ± 0.8	0.61 ± 0.08	127.9 ± 0.7	81.4 ± 0.9	39.8 ± 3.5	23.8 ± 2.1
	Cumulative	434.1 ± 1.4	74.6 ± 0.2	217 ± 4.1	260.2 ± 4.1	50.9 ± 0.8	1.95 ± 0.12	374.2 ± 0.4	84.5 ± 0.2	132 ± 8.3	26 ± 1.6

These data indicate that CuO, TiO₂ and ZnO can be removed from wastewater by the two biomass types (aerobic and anaerobic) used in these experiments. The experimental conditions adopted resemble fully operational WTWPs. Hence, the great majority of NPs entering a conventional sewage plant would be removed and retained by the biomass in the secondary treatment. This ultimately means that if not specifically designed for this purpose, conventional and new generation WTWPs would prevent massive release of NPs in receiving water bodies through treated effluent. The results are encouraging as the NP concentrations tested included current as well as future and extreme case scenarios that urban/industrial WTWPs could experience at present or in the future. Nevertheless, it is worth to go into further details in an attempt to shed more lights on the mechanisms and differences reported among the two different treatment types.

Overall the results indicate that activated sludge treatment is capable of removing a greater quantity, hence greater removal percent, of CuO, TiO₂ and ZnO than AGS. For example, at 9 mg/L in single NP experiments, at the end of the 180 minutes of contact time, activated sludge could remove 9.1 ± 0.1 , 8.9 ± 0.1 and 8.5 ± 0.3 mg/L of respectively CuO, TiO₂ and ZnO. These correspond to removal percent of 99.6 ± 0.1 , 99.6 ± 0.2 and 90.9 ± 3.5 %. When the same experiments were run with AGS biomass instead, the concentrations of NP removed were 5 ± 0.1 , 1.8 ± 0.2 and 6.3 ± 0.1 mg/L. The calculated removal percentages are: 58.2 ± 1.3 for CuO, 31.5 ± 3.5 for TiO₂ and 68.5 ± 1.5 % for ZnO. In addition, the amount of NP (mg) removed per gram of biomass for activated sludge vary between 4.2 ± 0.2 mg ZnO/g biomass up to 4.2 ± 0.2 mg /g biomass for CuO and TiO₂. Much lower values were found for AGS. These were roughly 100 times lower with the highest removal of 0.05 ± 0.01 mg ZnO/g biomass and the lowest for TiO₂ calculated as 0.02 ± 0.01 mg/g AGS biomass.

Similar results were identified when testing the second highest NP concentration in single NP system experiments as well. The CuO, TiO₂ and ZnO removal by activated sludge was in the narrow 97 – 99 % region with around 86 – 89 mg/L removed by the biomass regardless of the NP type. In contrast, AGS removal percent varied from a minimum of 34.4 ± 1.4 % for ZnO to a maximum of 77.2 ± 2.4 % for CuO. In general the biomass could only remove a maximum of 67.4 ± 2.1 mg/L of

CuO as maximum. A very similar pattern was observed for experiments run at target concentration of 180 mg/L.

Generally, activated sludge is more efficient in removing NP mixture than AGS biomass. This is evidenced by the data of NP removed (mg/L), removal percent (%) and NP removed/1 g of biomass. This difference was commonly found to be in the range of 20 – 40 % less NP removed regardless of type and concentrations. If we then consider the amount of NPs (mg) removed per single gram of biomass, the difference in removal performance is exacerbated where over 260 mg of cumulative CuO, TiO₂ and ZnO are removed by 1 gram of activated sludge in the 180 mg/L mixture experiments (540 mg/L was the total NP concentration added in the experiment). On the contrary a gram of AGS could only remove 1.95 ± 0.12 mg of cumulative CuO, TiO₂ and ZnO. Both these two values are the highest level of total removed NPs across all the experiments. The main different feature among the two biomass is the surface/volume ratio among the two, with activated sludge having by far the highest among the two. This opens to a further consideration regarding the mechanism(s) involved in the NP removal by wastewater treating biomass. Overall the physical structure of these two types of microbial population appears to be the key reason behind the differences in NP removal we observed. Activated sludge is flocs structured which usually do not exceed 2 mm, while anaerobic granules can easily exceed 10 mm. Activated sludge are not very thick but have an enormous specific surface. This is clearly highlighted by the greater capacity of activated sludge to remove NPs when considered normalized against 1 gram of biomass. The variety of NPs – biomass contacts have been shown to occur via different types of interactions. However, the predominant way through which biomass can remove NPs is believed to be through association via chemical, physical or biological mechanisms primarily on specific sites of the EPS structure. Due to its greater surface/volume, activated sludge is in possession of a much greater number of specific sites where NPs – Biomass association can take place in comparison to AGS. The granules have got a greater volume, dimension, thickness and density, but because of their physical structure, the locations where interactions with NPs can occur are fewer than those of activated sludge biomass. In conclusion, for this purpose, activated sludge, as identified by the

results in table 6.1, is a more efficient type of biomass in removing NPs from wastewater than AGS biomass.

However, as reported above, this work found out that 1 gram of activated sludge biomass was capable to remove over 217 mg of CuO, TiO₂ and ZnO. This was observed at the highest exposure level where each NPs was spiked at 180 mg/L for a total CuO, TiO₂ and ZnO concentration of 540 mg/L. Hence, it could be assumed that the same amount of biomass could easily remove the majority of CuO, TiO₂ and ZnO mixture at 90 mg/L total concentration of 270 (mg/L) and all the other concentrations tested (27 mg/L as mixture at 9 mg/L) and all the single NP experiments at all the concentrations as all these are below the total over 217 mg of CuO, TiO₂ and ZnO removed at the highest level. Parallely to this, we noted that the amount of NPs removed via aggregation driven sedimentation also increased at higher concentrations. This highlights that this is also another mechanism which has great potential to influence the environmental faith and hence release of NPs that enter a WWTP. In particular this seems to be primary affected by two factors. The first one is the NP concentration. As expected, the higher the concentration, the higher the chances of NPs colliding with each other and hence forming bigger NP aggregates which would be more susceptible to sedimentation. This is well shown in Fig. 61 where the amount of NPs removed where no biomass was added was studied in function of spiking concentration of CuO, TiO₂ and ZnO as well as their mixture (cumulative concentrations). As shown in the graph, the amount of NPs removed via sedimentation increases proportionally to the spiking concentration.

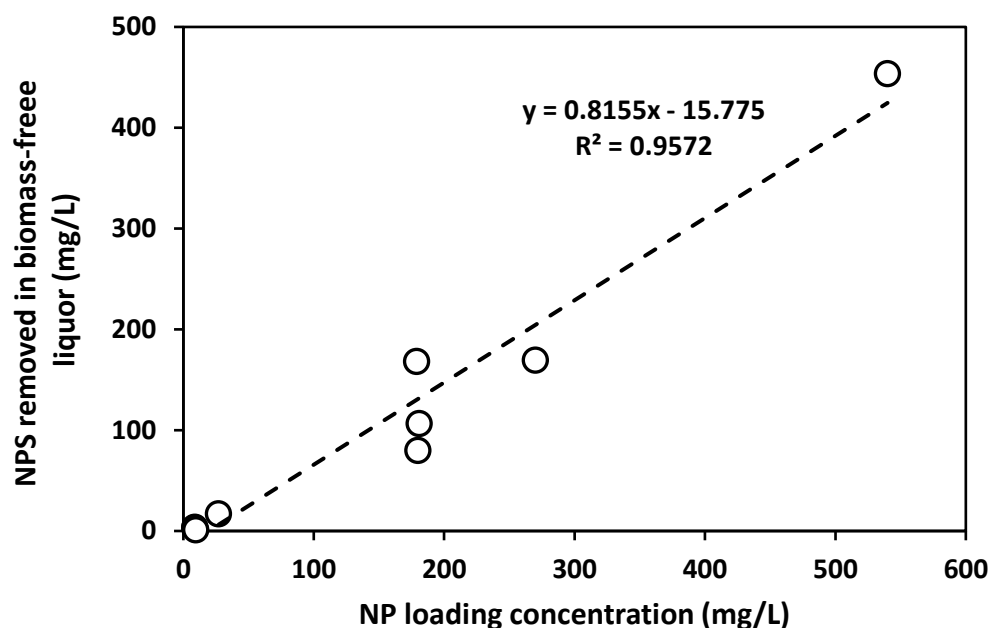


Fig. 6.1 Assessment of the amount of CuO, TiO₂ and ZnO and their mixture (in mg/L) removed by aggregation driven sedimentation when no biomass was added as function of the spiking concentration. Note that mixture experiments are reported as cumulative concentration (27 mg/L, 270 and 540 mg/L).

These findings are in line with what expected for substances that are found suspended in water. NPs can interact with other (nano)particles, and when these get to the vicinity of another, if the electrosteric forces between them are not enough to provide repulsion, then the NP – NP interaction can occur. This can lead to aggregation, which can then be classified as homo aggregation if it happens between particles of the same type, or hetero if it occurs between NPs of different nature. In this work we demonstrated that NP removal via aggregation driven sedimentation takes place in primary treated wastewater that would enter a secondary treatment stage. In addition, the aggregation driven sedimentation-based NP removal seems to happen in a concentration dependent manner. Hence, higher the amount of NPs, greater the self-removal due to aggregation and sedimentation. Evidence of this can also be found when comparing the individual removal of CuO, TiO₂ and ZnO between single and mixture experiments. For example the amount of NP removed in single NP tests at 9 mg/L were respectively 3.2 ± 0.5 , 3.8 ± 0.5 and 4 ± 0.1 mg/L. When spiked as mixture, always at the level of 9 mg/L, the amount of CuO and TiO₂ increased to 6.7 ± 0.1 and 6.9 ± 0.1 mg/L, whereas ZnO removed decreased to 3 ± 0.2 mg/L. At the highest spiking level (180 mg/L), the amount of ZnO removed in mixture system was over 50

mg/L higher (127.9 ± 0.7 mg/L) than what measured in single NP system (73.6 ± 6.5 mg/L). CuO experienced a slight reduction in removal when present in mixture, and fell of roughly 15 mg/L from 101.3 ± 0.3 mg/L to 84.5 ± 0.6 mg/L. The concentration of TiO₂ removed was the highest in both experiments. In fact, almost the totality of TiO₂ (over 85 % of removal efficiency in both experiments). Even when no biomass was present in the system, 162 ± 2.1 mg/L were removed in single NP experiments, while 161.9 ± 0.2 mg/L were removed in mixture tests. Interestingly, CuO, TiO₂ and ZnO could be removed via aggregation driven sedimentation in synthetic wastewater when no biomass was added too. However, in these experiments the amounts of removed NPs were drastically reduced in comparison to the biomass-free liquor. At 9 mg/L all the three NP types saw a removal between 1.1 and 1.3 mg/L and a cumulative of 3.5 mg/L. This is roughly 5 times less NPs removed than in biomass free liquor. At 90 mg/L the lowest amount of NPs removed occurred for ZnO where 8.9 ± 2.9 mg/L were removed, whereas the maximum was recorded at 15.6 ± 8.1 mg/L for TiO₂ and a cumulative removal of 37.5 ± 9.7 mg/L. These numbers are roughly 5 times lower than biomass-free removal experiments too. Similar numbers were found for the highest concentration tested (180 mg/L) with a cumulative removal of 132 ± 8.3 mg/L. This is about 3 times less than the cumulative removal of CuO, TiO₂ and ZnO mixture at 180 mg/L in biomass free liquor. The results of this experiment show a smaller difference in comparison to the biomass free liquor experiments than what found for 9 and 90 mg/L experiments. In fact, the total concentration of CuO was 49.1 ± 2.9 mg/L and it is only 2 times less than the equivalent in biomass-free liquor. In addition the concentration of ZnO removed (39.8 ± 3.5 mg/L) was just 3 times lower, and it was 4 times lower for TiO₂. This suggest once again that the self-removal of NPs via aggregation driven sedimentation is highly dependent of the NP concentration, and the higher the level of NPs present in a liquid, the higher the self-removal. However, these data also highlight the importance of the liquid in which NPs are present. As just reported, the amount of NPs removed highly differ based on the liquid used, with biomass-free liquor having a much greater impact on the removal of CuO, TiO₂ and ZnO via aggregation driven sedimentation. To further assess this, it is important to evaluate the two different liquids. The physiochemical characterization of the OECD

standard synthetic wastewater and biomass free liquor is reported in table 6.2 (reported form chapter 5).

Table 6.2 Comparison of synthetic wastewater and biomass-free liquor. Table reported from chapter 5 (Table 5.4)

	Units	Synthetic wastewater	Biomass-free liquor
pH		7.4 ± 0.2	7.0 ± 0.4
TDS	mg/L	237.5 ± 21.9	316.4 ± 35.3
Conductivity	µs/cm	326.1 ± 22.4	586.7 ± 56.1
COD	mg O ₂ /L	94.4 ± 7.4	91.1 ± 35.9
DOC	mg C/L	91.4 ± 13.6	7.71 ± 0.47
Cu	mg/L	LOQ	0.05 ± 0.07
Ti	mg/L	LOQ	0.31 ± 0.21
Zn	mg/L	LOQ	0.08 ± 0.06
Al	mg/L	0.82 ± 0.12	0.02 ± 0.01
Ca	mg/L	9.21 ± 0.77	30.45 ± 2.15
Fe	mg/L	1.93 ± 0.38	0.04 ± 0.02
K	mg/L	18.41 ± 2.61	11.81 ± 2.11
Mg	mg/L	2.17 ± 0.25	5.90 ± 0.61
Na	mg/L	9.82 ± 0.72	60.78 ± 4.24

These two liquors could at first seem quite similar. However, this characterization shows a few parameters that are likely to have a great impact on NP behaviour and self-removal as well. Indeed, the secondary wastewater liquor shows a much higher cations content, especially the concentration of the divalent cations Ca²⁺ and Mg²⁺ were respectively three and two times higher than what measured in synthetic wastewater. The latter however had greater presence of DOC which was roughly 10 times more abundant in synthetic wastewater. Dissolved organic matter can stabilize NPs whereas the presence of cations would enhance aggregation. Another interesting point comes from the comparison of COD. The results among the two media are similar, but the DOC content in real secondary liquor is much lower. This could mean that a big portion of the COD could be under the form of small colloidal particles that would not be filtered out in the biomass removal process. This seems to be confirmed

by the higher values of TDS and conductivity in the liquor. The presence of colloidal forms is another factor that can negatively impact the stability of NPs in suspension causing sedimentation. The combination of these parameters is likely to be the explanation on why a much greater amount of CuO, TiO₂ and ZnO were removed in biomass-free liquor rather than in the synthetic wastewater.

Another indication of the effect of the liquor on NP behavior and removal could be found in the evaluation of hydrodynamic diameter (h_D) and Z-potential in biomass-free liquor (table 6.3, taken from chapter 4, table 4.1). In this instance, when in biomass-free liquor, ZnO had the lowest hydrodynamic diameter (302.7 ± 9.7 nm) and more importantly the highest Z-potential (-20.4 ± 0.3 mV) among the NPs tested. Higher Z-potential means higher electrostatic repulsion, hence lower aggregation, which can ultimately result in lower self-removal due to aggregation driven sedimentation. This can be seen by comparing the amount of NPs removed when no biomass was added. ZnO is the nanomaterial least removal in most of the experiments run in either biomass-free liquor or synthetic wastewater. The only two cases are at 9 mg/L, single NP, in biomass-free liquor where the amount of NPs removed were all very similar though, ranging between 3.2 and 4 mg/L. The other case is at 180 mg/L mixture in biomass-free liquor where ZnO had roughly 15 mg/L removed more than CuO. Further research is certainly needed on this topic, however these evidences strongly support the findings of ZnO being the NPs least affected by aggregation driven sedimentation. In addition, a key role is played by the composition of the liquid NPs are suspended in.

Table 6.3 Nanoparticle characterization in ultrapure water and biomass-free liquor. Primary size determined via transmission electron microscopy (TEM), hydrodynamic diameter and Z-potential via dynamic light scattering (DLS).

	Primary size (water, pH = 11 ± 1)	Hydrodynamic diameter (water, pH = 11 ± 1)	Z-potential (water, pH = 11 ± 1)	Hydrodynamic diameter (biomass-free liquor, pH = 7.1 ± 0.5)	Z-potential (biomass-free liquor, pH = 7.1 ± 0.5)
Units	nm	nm	mV	nm	mV
CuO	54.5 ± 26.1	251 ± 7.4	-44.9 ± 1.2	326.9 ± 13.8	-13.4 ± 0.7
TiO₂	32.5 ± 5.3	202.3 ± 35.3	-39.9 ± 1.3	325.3 ± 21.3	-15.2 ± 0.2
ZnO	50.3 ± 12.5	214.2 ± 4.5	-34.9 ± 0.3	302.7 ± 9.7	-20.4 ± 0.3

Overall, this work tries to offer an overview of CuO, TiO₂ and ZnO removal in wastewater liquor and by two biomass types (aerobic and anaerobic). The series of experiments discussed in this work provide a series of findings and suggestions regarding the NP removal mechanisms. The majority of NPs entering a biological secondary treatment in a sewage plant would not pass through and hence be released in the environment. The NP removal is driven by two main factors: interactions with the biomass and aggregation driven sedimentation.

This confirms how the structural features of granular sludges equip them with great capacity to deal with stress caused by adverse environmental conditions. One example of this is pollution and presence of chemicals such as nanoparticles studied in this work. On the contrary, granular sludge is thicker and therefore much more structurally resistant. However, their architecture provides them much smaller specific surface in comparison to activated sludge. As NPs – bacteria interactions initially occur on the external membrane, the biofilm with the greater surface would yield the better NP capture efficiency. However, overtime, NPs can trigger adverse reactions to organisms, bacteria included, mainly through oxidative stress. The reduction in performances seems to be NP concentration dependent and this could indicate a threshold concentration after which activated sludge treatment would no longer provide an effective wastewater treatment. Contrary to activated sludge results, when pushing the limit of the added nanoparticles in triple mixture, there were no indications suggesting a reduction in performances due to the high amount of nanoparticles the granules were exposed to. This angle was not considered in this work, nevertheless it would be of great interest to further investigate the eco-toxicological side of the wastewater biomass exposure to NPs. Suggestions for future works and studies are reported in the following sections. When this happens, a biofilm with a looser structure such as activated sludge would be much more subject to suffer negative effects which can result in loss of structural integrity, metabolism distribution and ultimately death. In this context, a thicker structure such as the one of anaerobic granular sludge provides greater resistance to the damages produced by the presence of nanoparticles. The amount of microorganisms in this type of biofilm structure is enormously greater than what found in activated sludge flocs. Due to such spatial organization, only the

more external microorganisms would suffer damages from the presence of nanoparticles. The more external layers of the granules host principally carbonaceous bacteria which are the most resistant among the bacteria present in this consortium. Methanogen and nitrifying bacteria sit in the more internal and more protected area of the granules and tightly embedded in polysaccharides. On the contrary, despite the presence of polysaccharides and other extracellular polymeric substances, the protection that the flocculent structure can provide cannot achieve the level of granular sludge due to the looser structure.

Taken this into account, activated sludge is the most efficient secondary biological treatment in removing nanoparticles. Activated sludge can remove greater number of different nanoparticles in a shorter period of time.

However, nanoparticles are not yet a class of contaminants that is regulated by laws. This means that wastewater companies are not legally required yet to monitor and ensure removal or reduction of NP concentration below a certain value (discharge consent) set by environmental agency and law.

One of the main issues across wastewater companies is the aging of assets. In the upcoming years, it is expected that tighter discharge consents will be introduced, and companies will need to undergo a significative campaign to renew, upgrade and improve existing treatment plants or build new ones. The main driver leading this renovation campaign is sustainability. Water and wastewater companies in UK have committed to achieve net zero carbon by 2030 to protect the environment. Anaerobic biological wastewater treatments are increasingly gaining more and more consideration given its successful application in the private industrial sector. The possibility to pair such treatments with facilities fueled by biogas to produce cleaner energy, makes anaerobic treatment tremendously more environmentally sustainable. On the contrary, aerobic treatments present a greater energy demand to supply oxygen, need expensive engineering system to recirculate portion of the sludge, whereas the wasted biomass needs to be pumped or tankered to treatment centers where the biogas yield from such feed is not competitive if compared to regular food waste.

From the results presented in this work it seems that anaerobic granules are less efficient in removing nanoparticles in comparison to activated sludge treatment. The key factor appears to be the smaller specific surface, that anaerobic granules have,

which allows fewer nanoparticle – bacteria interactions. However, we suggest that this limiting factor could be overcome with the increase of anaerobic granules biomass used to treat wastewater. This adjustment could guarantee improved performances in removing nanoparticles as well as other contaminants hence meeting even more stringent environmental discharge consents. In addition, this would increase the carbon footprint of anaerobic treatment as the granules do not need oxygen or addition of other chemicals to function.

6.6 Future work

The research presented here demonstrates that aerobic activated and anaerobic granular sludge based secondary biological treatment can remove single as well as mixtures of nanoparticles from wastewater. To ensure the safe development of the nanotechnology industry, the nanoparticle removal study presented in this thesis must be further explored. Future work should include: 1) the standardization of an analytical method capable of provide qualitative and quantitative results for multiple nanomaterials in environmental samples. This will provide more accurate and detailed assessment of the nanoparticle occurrence in wastewater. Of particular interest would be a study focusing on daily, seasonal, and aerial variation of concentration and type of nanomaterials. This would provide the basis to understand and plan the design of the future wastewater treatment plants; 2) an assessment of the removal performances of other common and emerging types of nanomaterials, such as silver and gold nanoparticles, quantum dots, and carbon-based nanomaterials among others with focus on single type and, more importantly, mixture scenarios. The understanding of how a variety of environmental factors affect NP removal by biomass or in liquid matrices is still limited. For example very little has been done in the investigation of the effect of the presence of metals towards NP removal. It is known that NPs are used to removed heavy metals from contaminated lands/waters bodies. This would cause reduction in Z-potential, hence increased aggregation driven sedimentation. It is also unknown whether this could increase or reduce NP and heavy metal toxicity towards biofilms and aquatic organisms; Besides, further experiments could be designed to study in more details the mechanisms behind NP mixture interactions. For example double NP types mixture experiments to understand the extent of the attraction – repulsion

forces between NPs in environmental matrices. For example dual NPs mixture experiments could be designed to ascertain the extents of the repulsion- attraction with ZnO which was found the nanomaterial with the highest Zeta-potential and hence least removed by aggregation driven sedimentation. On a similar train of thoughts, the hypothesis of cations and organic matter affecting NP Zeta-potential and hence size distribution and ultimately aggregation driven sedimentation could be investigated by slightly modifying the liquid media. Starting from synthetic wastewater, several variation of the same recipe could be designed to study how different variables impact NP behaviour and removal. For example divalent cations could be completely removed, or the amount of dissolved organic matter could be increased or reduced if not omitted at all. Another interesting set of experiments could include studying the removal of NPs as a function of biomass, hence using a single concentration and evaluate how the NP removal varies when different amount of biomass are added. 3) it has been suggested that the presence of nanoparticles may increase biogas production. This research stream is still at a very early stage, however it would be relevant for both anaerobic and aerobic treatments. Anaerobic granules naturally produce biogas, while activated sludge is disposed in sludge treatment centers. Elucidating whether the presence of nanomaterial can increase the biogas production could have a great impact on further understanding how sustainable these treatments really are. In addition, this work, as well as others before, report than the great majority of NPs are removed via secondary biological treatments. These findings therefore shift the attention on the environmental fate of NPs towards different human made processes such as sludge digestion as well activated sludge recirculation. In fact, activated sludge is constantly recirculated or wasted. A good part of the biomass is reintroduced at the head of the secondary treatment once sedimentation has occurred to maintain achieve the desired MLSS value. However, not all of it can be recirculated, as the increase in MLSS due to the consumption of the organic pollution, a fraction of activated sludge needs to be wasted to counterbalance the increase in biomass. The fraction that is wasted, is usually treated in sludge centers where anaerobic digestion occurs. As result of this product, biogas and fertilizer are produced. In light of the results reported in this work, NPs would be present in both sludge streams. NPs would be present in the fraction of sludge that is retained within the WWTPs. Hence overtime,

this biomass would be potentially enriched in NPs due to the constant exposure to the incoming stream of sewage containing NPs. Further investigating this process would be of great interest, with a specific angle towards possible fall in performances overtime. As mentioned before, also the sludge that would be wasted and further treated would contain a fraction of NPs. Understanding the possible effects of their presence and more importantly, the physio-chemical changes that can occur to NPs while undergoing anaerobic digestion is yet a gap to be filled, as well as evaluating the fate of NPs once land applied when the fertilizer. With the increase in NP concentration in sludge, it will be essential to evaluate nanoparticle concentration, chemical speciation and how nanomaterial partition in this final product; 4) in this work we specifically focused on aerobic activated and anaerobic granular sludge treatments as most representative scenarios of current and future wastewater treatment plants. However, these are not the only biological wastewater technologies available. Other biological wastewater treatments include submerged aerated filters (SAF) units, aerobic granules, substrate attached growth biofilm processes and algae-based wastewater treatments. These types of technologies have so far found less application. Not surprisingly, this presents a research gap that, when filled, would enable water and wastewater industries to design the most sustainable and efficient treatments of the future.